Nina Sejkora, BSc

Interaction of the Jovian Magnetosphere with the Galilean Moons
–
Focusing on Europa and Ganymede

MASTER'S THESIS

to achieve the university degree of

Diplom-Ingenieurin

Master's degree programme: Space Sciences and Earth from Space

submitted to

Graz University of Technology

Supervisor

Univ.-Prof. Dr. Helmut O. Rucker

Institute of Physics

Faculty of Natural Sciences
Karl-Franzens University Graz

Graz, May 2018

AFFIDAVIT

I declare that I have authored this thesis independently, that I have not used other than the declared sources/resources, and that I have explicitly indicated all material which has been quoted either literally or by content from the sources used. The text document uploaded to TUGRAZonline is identical to the present master‘s thesis.

Date

Signature

Abstract

There are several models for the Jovian magnetic field existent in the literature. Until the most recent ones making use of Juno measurements, they all rely on data from a few flybys, and some on additional constraints, like the Io footprint. All these models attempt to describe Jupiter's field in various detail. When applying them for modeling efforts, each of them leads to different results. However, a quantification of those differences is often difficult.

It is the aim of this thesis to develop a metric to enable a quantitative comparison between Jovian magnetic field models. The metric evaluates the deviations between satellite footprints calculated with the magnetic field model under consideration and observed auroral footprints. In preparation of this task, first the mathematical basics of the description of planetary magnetic fields are reviewed. Secondly, the theory for the interaction mechanism between the magnetosphere and the moons orbiting within it is presented. It is this interaction between the rapidly rotating planet, its magnetic field, the corotating plasma and the Galilean satellites, which leads to the formation of auroral satellite footprints in Jupiter's ionosphere. Lastly, the developed metric is described and applied to different magnetic field models.

The resulting metric quantifies the applicability of a magnetic field model for the magnetic mapping of Europa and Ganymede footprints. It clearly indicates non-causalities inherent in the model. The metric's main limitation is the availability of observational data: observations of the Europa footprint are sparse, the data does not cover the entire longitudinal range, and is inhomogeneous between Northern and Southern hemisphere. The metric has been applied fully to the two magnetic field models VIP4 and VIPAL, and in a shortened manner to JRM09 (Juno Reference Model through perijove 9). In the analysis VIP4 showed major non-causalities in the Northern hemisphere. VIPAL and JRM09 are similar, especially in the North. Both offer improvements compared to VIP4. In the Southern hemisphere, the results for all three models are qualitatively alike. In the observational range none of them offers significant improvements compared to the others.

Zusammenfassung

In der Literatur sind etliche Modelle für Jupiters Magnetfeld verfügbar. Bis auf die neuesten, welche die Messungen der Raumsonde Juno nutzen, basieren sie alle auf Daten von wenigen Vorbeiflügen und teilweise zusätzlichen Nebenbedingungen, wie zum Beispiel dem Io-Fußpunkt. Alle diese Modelle versuchen Jupiters Feld in unterschiedlichem Detailgrad darzustellen. Wenn zur Modellierung herangezogen, liefern sie verschiedene Ergebnisse. Oft ist eine Quantifizierung dieser Unterschiede jedoch schwierig.

Das Ziel dieser Arbeit ist es, eine quantitative Metrik für den Vergleich von Jupitermagnetfeldmodellen zu entwickeln. Diese Metrik untersucht die Abweichung zwischen Satellitenfußpunkten, welche mit einem bestimmten Magnetfeldmodell berechnet wurden, und den beobachteten Polarlichtfußpunkten. Vorbereitend, werden zuerst die mathematischen Grundlagen der Beschreibung von planetaren Magnetfeldern wiedergegeben. Anschließend wird die Theorie zur Wechselwirkung der Magnetosphäre mit den darin umlaufenden Monden präsentiert. Es ist diese Wechselwirkung zwischen dem schnell rotierenden Planeten, seinem Magnetfeld, dem mitrotierenden Plasma und den Galileischen Monden, welche zur Entstehung der Polarlichtfußpunkte in Jupiters Ionosphäre führt. Zuletzt wird die entwickelte Metrik beschrieben und auf verschiedene Magnetfeldmodelle angewandt.

Die erhaltene Metrik quantifiziert die Eignung eines Magnetfeldmodells für die Anwendung zur magnetischen Abbildung von Europas und Ganymedes Fußpunkten. Sie zeigt dem Modell inhärente Nichtkausalitäten deutlich auf. Die größte Einschränkung der Metrik ist die Verfügbarkeit von Beobachtungsdaten: Beobachtungen von Europas Fußpunkt sind spärlich; außerdem deckten die Daten nicht den gesamten Längenbereich ab und sind ungleichmäßig zwischen Nord- und Südhalbkugel verteilt. Die Metrik wurde in ihrer Gesamtheit auf die Modelle VIP4 und VIPAL angewandt und in einer gekürzten Fassung auf JRM09 (Juno Referenzmodell bis einschließlich Perijovum 9). Die Analyse von VIP4 zeigte starke Nichtkausalitäten in der nördlichen Hemisphäre. VIPAL und JRM09 ähneln sich, besonders im Norden. Beide bieten Verbesserungen zu VIP4. In der südlichen Hemisphäre sind alle drei Modelle qualitativ ähnlich. Im beobachteten Bereich bietet keines signifikante Verbesserungen im Vergleich zu den anderen.

Acknowledgements

The development of this thesis was partially supported by the funding from the foundation Dr. Anton Oelzelt-Newin from the Austian Academy of Sciences (ÖAW). These fundings enabled the participation at two scientific conferences (the EPSC 2017 in Riga, and the EGU General Assembly 2018 in Vienna), and a scientific visit to the Space sciences, Technologies and Astrophysics Research Institute at the University of Liège. I want to express my gratitude for the help I received there. In particular I want to offer my special thanks to Bertrand Bonfond and Denis Grodent for the assistance in improving my calculations, and the valuable input which formed the basis for the development of the comparison metric described in here.

I also want to thank my supervisor Prof. Rucker for his continued feedback on my work and for making it possible for me to receive the funding mentioned above. I believe his eye for detail hardly missed a single typing error – and it also helped to greatly improve my graphics and figures.

Finally, I wish to thank my family and friends for the many ways in which they supported me in my studies. They often lent me an open ear, and sometimes it was their comment which helped me find the mistake I had missed.

Contents

Chapter 1

Introduction

The first evidence that Jupiter may posses a strong magnetic field was found in the radio, when Burke and Franklin (1955) attributed the occurrence of a variable radio source to the planet Jupiter. When Pioneer 10 reached Jupiter, the magnetic field could finally be characterized in-situ (Smith et al. 1974). But even before these in-situ measurements, the magnetic field had already been studied in detail, using ground-based radio data. These data also showed the first indications of the interaction of satellites with the Jovian magnetosphere – Bigg (1964) showed the influence Io has on Jupiter's decametric radio emissions. Until today, many more observations of features triggered by the satellite's interaction with the magnetosphere have been performed. Amongst others, which will be of special concern in the following, are the auroral footprints on Jupiter caused by the moons Io, Europa and Ganymede. The properties of these features and the processes forming them are explained in Chapter 3.

Based on the data acquired by Pioneer 10 and later spacecraft, and in some cases also other constraints, e.g. based on the satellite interaction, various magnetic field models have been developed for Jupiter. They usually offer a description of the field with spherical harmonics. The basics of this method, and including also the treatment of potential external sources, are provided in Chapter 2. All the various models which have been put forward over time aim to describe the field in different levels of detail, i.e. include contributions up to a different degree and order. When using different models for the representation of processes, they lead to different results. However, to quantify those differences, and especially to determine which solution is the "better " one, is not trivial. Not knowing the "real" global magnetic field structure, one may rely on proxies and compare the predictions of models to those. This is the main idea of Chapter 4: to develop a metric quantifying the suitability of the model for the mapping of satellite footprints (especially those of Europa and Ganymede). This metric shall be understood to be a general statement of, "model A is better than model B". It can only evaluate their usefulness for mapping the Europan and Ganymedean footprints. Other applications (e.g. at other radial distances), may have different requirements, and thus one model may be more or less useful in one regime or the other. In Chapter 4, the metric is applied to two selected models, VIP4 (Connerney et al. 1998) and VIPAL (Hess et al. 2011).

For the recently published JRM09 model (Connerney et al. 2018), which is based on measurements taken by the Juno spacecraft, a minimal analysis, to compare it to the other two models, has been performed as well. The conclusion in Chapter 5 gives an assessment of the quality of the metric and summarizes the results obtained by applying it to the three models.

Chapter 2

Mathematical Description of the Jovian Magnetic Field

A major, if not the main, ingredient governing the interactions in Jupiter's magnetosphere, is obviously the planets strong magnetic field. It is carving out the gigantic magnetosphere itself, within which the moons orbit; it is, together with the planet's fast rotation, causing the plasma to corotate until far out, which triggers the interaction with the Galilean satellites leading to auroral footprints (see Chapter 3). To be able to describe all these processes, a model of the magnetic field is needed. For the representation of the internal field of a magnetized planetary body, the use of spherical harmonics is widespread. This method is explained in Sections 2.1 and 2.2. The description there is mainly based on Merrill et al. (1998), unless specified otherwise. A useful tool, especially for the visual depiction of magnetic fields is the concept of magnetic field lines, which is introduced in Section 2.3. In the Jovian magnetosphere, there exists one complication when attempting to understand its structure. Beyond a few Jovian radii away from Jupiter, the local magnetic field is not only governed by sources in Jupiter's interior, but by a circumplanetary current sheet. A simple model approximatively describing its contribution is presented in Section 2.4.

2.0 Comments on the Use of "Magnetic Field" and "Magnetic Induction"

A precise terminology has to distinguish between the magnetic field $\mathbf{H}$ and the magnetic induction $\mathbf{B}$. Their exact relationship is given below, i.a. equations (2.1) et seq. Here it is only important to note that in the vacuum of space, they follow the straightforward relation

$$\mathbf{B} = \mu_0 \mathbf{H}.$$

For this reason, in literature the terms "magnetic induction" and "magnetic field" are often used interchangeably. Most importantly, $\mathbf{B}$ is usually referred to as "magnetic field". The use of the actual magnetic field $\mathbf{H}$ is rare. In the present thesis, the

Sections 2.1 and 2.2 apply the precise terminology distinguishing between field and induction. Afterwards, the widespread terminology, calling **B** the magnetic field, is adopted.

2.1 Description of a Planetary Magnetic Field with Spherical Harmonics

The description starts with the Maxwell equations for the magnetic field

$$\nabla \times \mathbf{H} = \mathbf{j} + \frac{\partial \mathbf{D}}{\partial t} \tag{2.1}$$

$$\nabla \cdot \mathbf{B} = 0. \tag{2.2}$$

The items in the above equations are defined as follows:

H	...	magnetic field
B	...	magnetic induction $\mathbf{B} = \mu_0(\mathbf{H} + \mathbf{M})$
		M ... magnetization
		$\mu_0 = 4\pi \cdot 10^{-7}$ N/A^2 ... vacuum permeability
j	...	electric current density
D	...	electric displacement current density

If one assumes an electromagnetic vacuum outside of the planet, the current densities **j** and $\frac{\partial \mathbf{D}}{\partial t}$ are zero. Therefore the rotation of **H** vanishes, which means that **H** is a conservative vector field. Such a field can be described by the gradient of a scalar potential ψ_H

$$\mathbf{H} = -\nabla \psi_{\mathrm{H}}.$$

Above the planet's surface, one can also assume the magnetization to vanish, so, the magnetic induction reduces to $\mathbf{B} = \mu_0 \mathbf{H}$. In that case the statement above is also true for the magnetic induction if multiplied by μ_0

$$\mathbf{B} = -\mu_0 \nabla \psi_{\mathrm{H}} = -\nabla \psi, \tag{2.3}$$

with $\psi = \mu_0 \psi_{\mathrm{H}}$ being the scalar potential of the magnetic induction. By combining equations (2.2) and (2.3) one obtains the Laplace equation for the magnetic potential

$$\Delta \psi = 0 \qquad \text{with} \qquad \Delta = \nabla^2.$$

In the context of planetary magnetic fields it is obvious to use spherical coordinates, in which case the Laplace equation reads as

$$\frac{1}{r}\frac{\partial^2}{\partial r^2}(r\psi) + \frac{1}{r^2 \sin\vartheta}\frac{\partial}{\partial \vartheta}\left(\sin\vartheta \frac{\partial \psi}{\partial \vartheta}\right) + \frac{1}{r^2 \sin^2\vartheta}\frac{\partial^2 \psi}{\partial \varphi^2} = 0.$$

For the exact definition of the coordinate system used, the reader is referred to Figure 2.1(a). The equation above can be solved by the separation of variables, i.e. with the ansatz

$$\psi(r, \vartheta, \varphi) = \frac{U(r)}{r} P(\vartheta) Q(\varphi).$$

Inserting this into the Laplace equation the general solution for the potential ψ

$$\psi(r,\vartheta,\varphi) = \sum_{l=0}^{\infty}\sum_{m=0}^{l}\left[A_{l,m}\, r^{l} + B_{l,m}\, r^{-(l+1)}\right] Y_l^m(\vartheta,\varphi) \tag{2.4}$$

is obtained. The constants $A_{l,m}$ and $B_{l,m}$ specify the contributions to the potential of external and internal sources respectively. This is obvious from the fact that if there are no external sources, the potential must vanish at infinity, i.e. $A_{l,m} \overset{!}{=} 0$. On the other hand, if there are no internal sources, the potential must not diverge towards the center, i.e. $B_{l,m} \overset{!}{=} 0$. The functions $Y_l^m(\vartheta,\varphi)$ are the surface harmonics of degree l and order m, defined by

$$Y_l^m(\vartheta,\varphi) = \left[\frac{(2l+1)(l-m)!}{4\pi(l+m)!}\right]^{1/2} P_{l,m}(\cos\vartheta)\, e^{im\varphi}.$$

Here $P_{l,m}$ are the associated Legendre functions, given by

$$P_{l,m}(\chi) = \frac{1}{2^l l!}(1-\chi^2)^{m/2}\,\frac{\mathrm{d}^{l+m}}{\mathrm{d}\chi^{l+m}}(\chi^2-1)^l,$$

where $\chi = \cos\vartheta$. In Geophysics the use of the partially normalized Schmidt functions instead of the associated Legendre functions is common. The Schmidt functions are defined as

$$P_l^m = \begin{cases} P_{l,m} & \text{for } m = 0 \\ \left[\frac{2(l-m)!}{(l+m)!}\right]^{1/2} P_{l,m} & \text{for } m > 0. \end{cases}$$

A normalization of the radius coordinate to the planet's radius R in those functions, leads to the form

$$\begin{aligned}\psi = \frac{R}{\mu_0}\sum_{l=1}^{\infty}\sum_{m=0}^{\infty} P_l^m(\cos\vartheta)\Bigg\{ &\left[C_l^m\left(\frac{r}{R}\right)^l + \left(1-C_l^m\right)\left(\frac{R}{r}\right)^{l+1}\right] g_l^m\cos(m\varphi) \\ &+ \left[S_l^m\left(\frac{r}{R}\right)^l + \left(1-S_l^m\right)\left(\frac{R}{r}\right)^{l+1}\right] h_l^m\sin(m\varphi)\Bigg\}\end{aligned}$$

of equation (2.4). The sum over l starts with 1 as, due to the non-existence of magnetic monopoles ($\nabla\mathbf{B} = 0$), the $(l=0)$-term vanishes. The items g_l^m and h_l^m are the Schmidt coefficients, which are of the unit of the magnetic induction, i.e. commonly Tesla (T) or Gauss (G). The definition of those units reads as

$$\begin{aligned} 1\,\mathrm{T} &= 1\,\frac{\mathrm{V}\cdot\mathrm{s}}{\mathrm{m}^2} = 1\,\frac{\mathrm{kg}}{\mathrm{A}\cdot\mathrm{s}^2} \\ 1\,\mathrm{G} &= 10^{-4}\,\mathrm{T}, \end{aligned}$$

where the last equivalent of Tesla is in SI base units. The constants C_l^m and S_l^m, which are numbers between 0 and 1, quantify the fraction of the potential coming

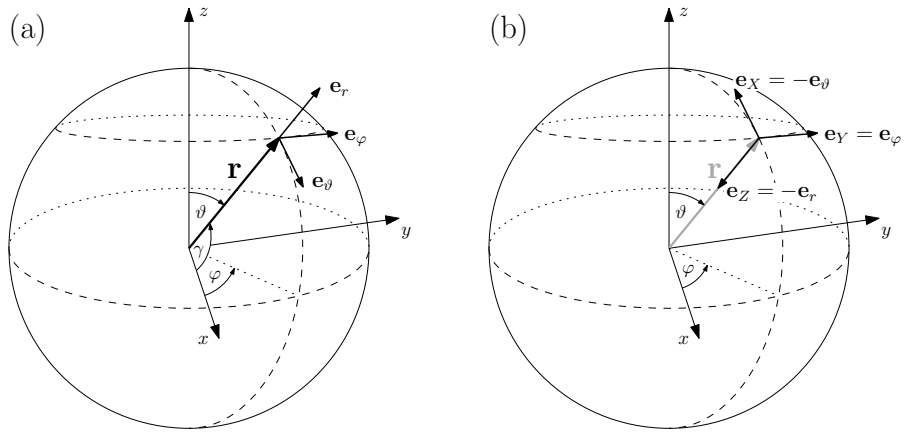

Figure 2.1: (a) definition of spherical coordinate system in use, the angle γ will be discussed in Section 2.2; (b) directions of X, Y and Z component of magnetic induction $\mathbf{B}$

from external sources $r > R$. Therefore $(1-C_l^m)$ and $(1-S_l^m)$ give the fraction from internal sources $r \leq R$. In case the external sources are negligible ($C_l^m, S_l^m \ll 1$), the expression for the potential may be simplified to

$$\psi(r,\vartheta,\varphi) = R\sum_{l=1}^{\infty}\sum_{m=0}^{\infty}\left(\frac{R}{r}\right)^{l+1} P_l^m(\cos\vartheta)\left[g_l^m\cos(m\varphi) + h_l^m\sin(m\varphi)\right]. \qquad (2.5)$$

This simplification is commonly used when describing planetary magnetic fields. However, it is not always justified. For example, in the case of Jupiter, the contributions from the current sheet are relevant for regions around Ganymede's orbit, and even at Europa it is not easy to justify neglecting them. Data supporting these statements is cited in Section 2.4. But without the simplifications in equation (2.5), the mathematical treatment is quite complex. A commonly used solution to this issue is to model the current sheet contribution and to subtract it from the measured magnetic field before starting the spherical harmonic analysis. This approach is closer described in Section 2.4.

One obtains the vector components of the magnetic induction $\mathbf{B}$ by applying the gradient to the potential ψ. It is common to give the vertical component Z of the planet's field and the north X and east Y directed parts of the horizontal component. The directions of those components are also depicted in Figure 2.1(b). They are calculated via the expressions

$$\begin{aligned}
\mathbf{B}_r &= -\frac{\partial\psi}{\partial r}\,\hat{\mathbf{e}}_r &&= -\,Z\,\hat{\mathbf{e}}_r \\
\mathbf{B}_\vartheta &= -\frac{1}{r}\frac{\partial\psi}{\partial\vartheta}\,\hat{\mathbf{e}}_\vartheta &&= -\,X\,\hat{\mathbf{e}}_\vartheta \\
\mathbf{B}_\varphi &= -\frac{1}{r\sin\vartheta}\frac{\partial\psi}{\partial\varphi}\,\hat{\mathbf{e}}_\varphi &&= +\,Y\,\hat{\mathbf{e}}_\varphi\,.
\end{aligned}$$

The item $\hat{\mathbf{e}}_j$, $j \in \{r,\vartheta,\varphi\}$, is the unit vector in r-, ϑ- and φ-direction, respectively.

2.2 Interpretation of the Schmidt Coefficients

The terms in equation (2.5) can be interpreted as the contributions to the potential from a dipole, quadrupole, etc. situated at the center of the planet. The first term of (2.5) is

$$g_1^0 \, P_1^0(\cos\vartheta)\frac{R^3}{r^2} = \left(\frac{g_1^0 \cdot 4\pi R^3}{\mu_0}\right)\frac{\mu_0}{4\pi}\frac{\cos\vartheta}{r^2}.$$

If one compares this to the potential of a magnetic dipole (e.g. Clauser 2014, p. 197)

$$\psi_{\text{dipole}} = \frac{\mu_0}{4\pi}\frac{\mathbf{M}\cdot\mathbf{r}}{r^3} = \frac{\mu_0}{4\pi}\frac{M\cos\vartheta}{r^2}$$

$$\mathbf{M} \text{ ... dipole moment, } M = |\mathbf{M}|,\ [M] = \mathrm{A\,m^2},$$

it is obvious that the g_1^0-term describes the potential of a planet-centered dipole along z with the magnetic moment $M = \left(\frac{g_1^0 \cdot 4\pi R^3}{\mu_0}\right)$. In case the magnetic moment is given in units of $\mathrm{T\,m^3}$ or $\mathrm{G\,m^3}$, μ_0 needs to be substituted by 4π in the equations above. A similar argument holds for the g_1^1-term

$$\left(\frac{g_1^1 \cdot 4\pi R^3}{\mu_0}\right)\frac{\mu_0}{4\pi}\frac{\cos\varphi\sin\vartheta}{r^2} = \left(\frac{g_1^1 \cdot 4\pi R^3}{\mu_0}\right)\frac{\mu_0}{4\pi}\frac{\cos\gamma}{r^2},$$

where γ is the angle between the radius vector and the x-axis, as can also be seen in Figure 2.1(a). The relation that $\cos\gamma = \cos\varphi\sin\vartheta$ can be easily derived from trigonometric considerations. That term, therefore, describes the potential of a dipole along x. The h_1^1-term finally describes a dipole along y. In total, the ($l = 1$)-terms can be interpreted as the potential of a centered, tilted dipole with the magnetic moment

$$M = \frac{4\pi R^3}{\mu_0}\sqrt{(g_1^0)^2 + (g_1^1)^2 + (h_1^1)^2}$$

Similar arguments show that the ($l = 2$)-terms describe a planet-centered quadrupole, ($l = 3$) an octupole, etc. Alternatively the ($l = 1$)- and ($l = 2$)-terms can be combined to describe the potential of an eccentric, tilted dipole. The magnetic moment and tilt of such a dipole are the same as in the planet-centered case, but its location is shifted to $\Delta x = \eta R,\ \Delta y = \zeta R,\ \Delta z = \xi R$, in a Cartesian, planet-centered coordinate system like the one depicted in Figure 2.1. The coefficients $\eta,\ \zeta$ and ξ can be obtained from the Schmidt coefficients via the relations

$$\begin{aligned}
\xi &= (L_0 - g_1^0 E)/(3B_0^2) & L_0 &= 2g_1^0 g_2^0 + \sqrt{3}\cdot(g_1^1 g_2^1 + h_1^1 h_2^1)\\
\eta &= (L_1 - g_1^1 E)/(3B_0^2) & L_1 &= -g_1^1 g_2^0 + \sqrt{3}\cdot(g_1^0 g_2^1 + g_1^1 g_2^2 + h_1^1 h_2^2)\\
\zeta &= (L_2 - h_1^1 E)/(3B_0^2) & L_2 &= -h_1^1 g_2^0 + \sqrt{3}\cdot(g_1^0 h_2^1 + h_1^1 g_2^2 + g_1^1 h_2^2)\\
& & E &= (L_0 g_1^0 + L_1 g_1^1 + L_2 h_1^1)/(4B_0^2)\\
& & B_0^2 &= (g_1^0)^2 + (g_1^1)^2 + (h_1^1)^2.
\end{aligned}$$

Those equations are taken from Fraser-Smith (1987), where the reader is referred to for a more detailed description.

2.3 Magnetic Field Lines

Magnetic fields are usually visualized by depicting magnetic field lines. The definition of a field line requires that on any point, the local vector field forms a tangent to the line. This requirement can be formulated as (see e.g. Blackwell et al. 2001 or Callen 2006)

$$\frac{\mathrm{d}\mathbf{x}(s)}{\mathrm{d}s} = \hat{\mathbf{B}}(\mathbf{x}(s)), \tag{2.6}$$

where $\mathbf{x}(s)$ is the trajectory of the field line, and $\hat{\mathbf{B}}(\mathbf{x}(s))$ is the direction of the magnetic induction at the position $\mathbf{x}(s)$. In the parametrization $\mathbf{x}(s)$ of the field line, the parameter s is usually taken to be the distance along the line. The vector $\hat{\mathbf{B}}$ is the unit vector defined as $\hat{\mathbf{B}} = \mathbf{B}/|\mathbf{B}|$. In many cases the differential equation (2.6) has to be solved numerically. This is especially true for a planetary magnetic field described by spherical harmonics, if one uses terms of higher order than a simple dipole. How this was done in the presented work specifically is detailed in Section 4.2.

2.4 Modeling of the Jovian Current Sheet

In Section 2.1 the necessity for the modeling of the Jovian current sheet was briefly mentioned. A commonly used model is that developed by Connerney et al. (1981). This model was also used for the definition of the VIP4 (Connerney et al. 1998) and VIPAL (Hess et al. 2011) models, which are used in the analysis in Chapter 4. More recent models of the current sheet, including a more detailed description, do exist – see e.g. Khurana (1997) and Khurana and Schwarzl (2005). However, those models do not improve the mapping of magnetic field lines from the orbits of Europa and Ganymede to Jupiter's polar regions. They mainly offer improvements for regions father out (beyond $\sim 30\ R_\mathrm{J}$). For this reason Hess et al. (2011) decided to use the Connerney et al. (1981) model, a decision taken for the following analysis in this work as well. Thus it shall be described in Section 2.4.2 in some detail. Unless noted otherwise, the description there follows Connerney et al. (1981). Before, Section 2.4.1 gives some physical evidence for the existence of a current sheet in the Jovian magnetosphere and for its shape.

2.4.1 Observational Evidence for the Current Sheet

Already measurements performed by the Pioneer 10 and 11 probes showed a strong deviation of the magnetic field from the dipolar configuration in the magnetic equatorial regions (e.g. Smith et al. 1974). The Voyager 1 and 2 spacecraft supplied additional measurements of the region. Connerney et al. (1981) show the most striking characteristics based on plots of the perturbation magnetic field. Those plots depict the difference between the observed magnetic field and the one predicted by a spherical harmonic model, in their case the GSFC O_4 model (Acuña and Ness 1976). Exemplary, in Figure 2.2 a graph by Connerney et al. (1981) is

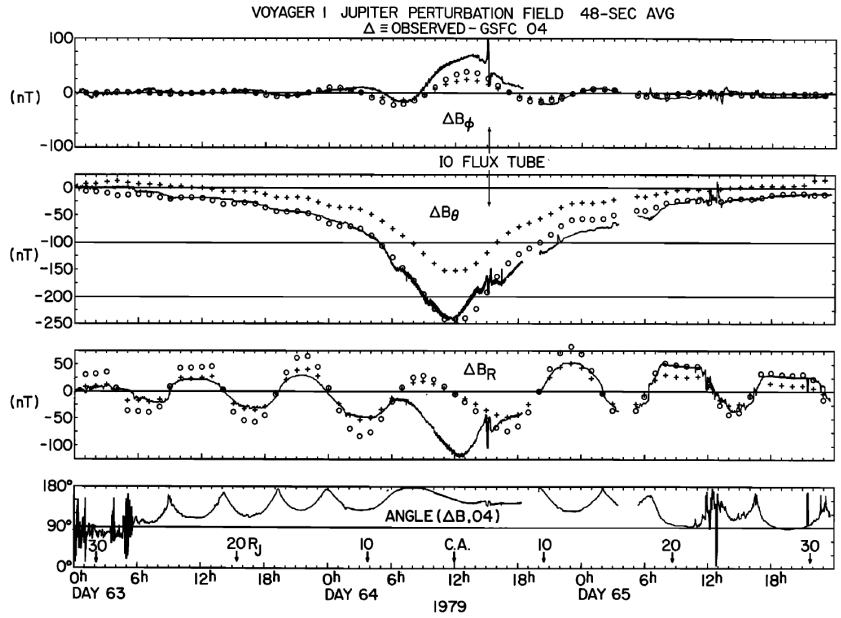

Figure 2.2: Comparison of the perturbation field measured by Voyager 1 with the one generated by an annular current sheet. The model parameters are given in the text; the crosses (+) were computed using a smaller current density and a smaller sheet outer radius than for the open circles (∘). In the text the slightly altered notation of ΔB_φ, ΔB_ϑ, ΔB_r, instead of ΔB_ϕ, ΔB_θ, ΔB_R is used. Source: Connerney et al. (1981)

reproduced, which shows the perturbation field from Voyager 1 measurements. The plots show the three components ΔB_φ, ΔB_ϑ, ΔB_r of the perturbation field in spherical coordinates (z-axis parallel to the magnetic dipole axis) and the angle between the perturbation field and the O_4 model. The notation has been adapted slightly with respect to Connerney et al. (1981), to match the rest of this work. The φ-component is small. The ϑ-component is slowly increasing with decreasing r, and it is anti-parallel to the internal dipole field. The radial component is also increasing when approaching Jupiter, and even slower than the ϑ-component. Additionally it displays an ∼10-hour periodicity, with the sign of ΔB_r changing twice every 10 hours. The angle of the perturbation field varies from about 90° to almost 180°. All of these phenomena can be reproduced by the model of a thin, annular current sheet with azimuthal currents, through which the spacecraft repeatedly passes. A comparison of the perturbation field with the spacecraft trajectory suggests that the plane of symmetry of the current sheet lies in or near the magnetic equatorial plane.

In Figure 2.2 a field modeled according to the description in the following section 2.4.2 is plotted on top of the measured perturbation field ΔB. The parameters used are: $R_0 = 5\ R_\mathrm{J}$, $D = 2.5\ R_\mathrm{J}$ and (i) $R_1 = 50\ R_\mathrm{J}$, $I_0 = 25.6 \cdot 10^6$ A/R_J = 0.34 A/m for the open circles, and (ii) $R_1 = 30\ R_\mathrm{J}$, $I_0 = 17.1 \cdot 10^6$ A/R_J = 0.24 A/m for the crosses.

The contribution of the current sheet to the magnetic field is clearly non-negligible in the region of Europa and Ganymede: at 15 R_J the magnitude of the current sheet field is comparable in magnitude to the internal field (Connerney et al. 1981). The field geometry is altered on a global scale by the current sheet – reaching up

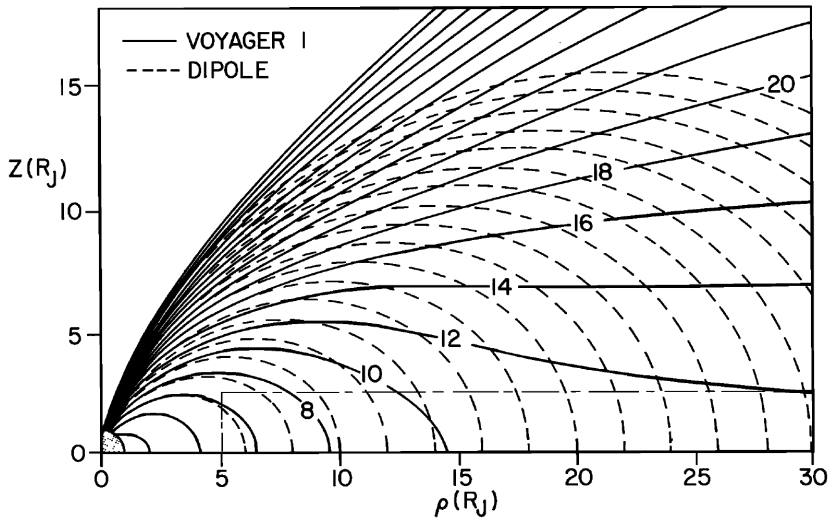

Figure 2.3: Comparison of magnetic field lines of a model including the contribution of a current sheet (continuous lines) to the ones produces by a dipolar internal field alone (dashed lines). The model parameters are given in the text and correspond to the ones depicted by open circles in Figure 2.2. The coordinate system is a cylindrical one, with the z-axis parallel to the magnetic dipole axis. Source: Connerney et al. (1981)

to high latitudes. This is best to be seen in Figure 2.3, which has been taken from Connerney et al. (1981) as well. The graph shows a comparison of the magnetic field lines of a model where the current sheet is taken into account with the ones generated by a dipole alone. The current sheet model used for Figure 2.3 is the one marked by open circles in Figure 2.2.

2.4.2 Mathematical Description of the Current Sheet

The modeled current sheet was derived by analyzing the difference between the magnetic field as predicted by the GSFC O_4 model (Acuña and Ness 1976) and that measured by the Voyager spacecraft. Based on those measurements the model describes a planar current sheet positioned in the magnetic equatorial plane. For the following derivations a cylindric coordinate system is used. The vertical component z is parallel to the O_4 model dipole axis. The radial component ρ and the angle φ are measured in the magnetic equatorial plane. The geometry of the problem is visualized in Figure 2.4. If the current is assumed to consist of an azimuthal component only, the magnetic vector potential $\mathbf{A}$ has only a φ-component as well

$$\mathbf{A} = A(\rho, z)\,\hat{\mathbf{e}}_\varphi\,.$$

The magnetic field is the curl of the vector potential, i.e. in cylindrical coordinates and using the properties of $\mathbf{A}$

$$\mathbf{B} = \nabla \times \mathbf{A} = -\frac{\partial A}{\partial z}\,\hat{\mathbf{e}}_\rho + \frac{1}{\rho}\frac{\partial}{\partial \rho}(\rho A)\,\hat{\mathbf{e}}_z\,.$$

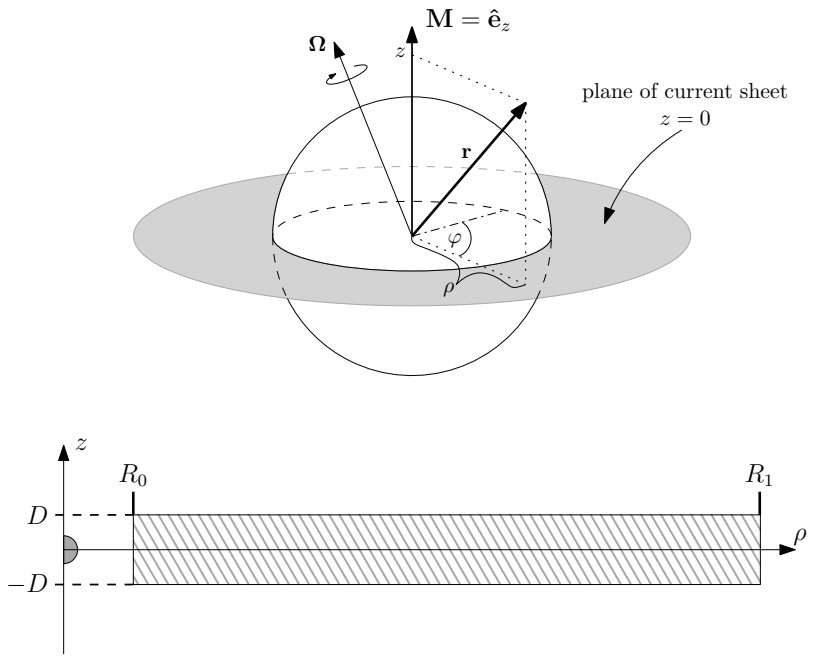

Figure 2.4: Geometry of the current sheet model. Top: Sketch of the planet Jupiter with its rotational axis $\mathbf{\Omega}$, the magnetic dipole axis $\mathbf{M}$, and the magnetic equatorial plane, depicted in gray. The components of a vector $\mathbf{r}$ in the used cylindrical coordinate system are given. Any angles in the sketch are for illustrative purposes only and are not to scale. Bottom: Cut through the current sheet in the ρz-plane. The dimensions correspond to those given in Table 2.1

If the region is current free, the curl of $\mathbf{B}$ vanishes, i.e. $\nabla \times \mathbf{B} = 0$, which implies for A

$$-\frac{\partial^2 A}{\partial z^2} + \frac{A}{\rho^2} - \frac{1}{\rho}\frac{\partial A}{\partial \rho} - \frac{\partial^2 A}{\partial \rho^2} = 0\,.$$

Separating the variables in the above equation, i.e. assuming $A(\rho, z) = \alpha(\rho) \cdot \beta(z)$, the physically acceptable solutions of the differential equation are of the form

$$A^{\pm} = J_1(\lambda\rho)\, e^{\mp\lambda z},$$

where the upper sign is for $z > 0$ and the lower one for $z < 0$. In Connerney et al. (1981), this is stated exactly the other way round. However, from physical considerations (otherwise A diverges for $|z| \to \infty$), and from the following derivations it is obvious that the definition Connerney et al. (1981) actually used, is the one given here. The factor $J_1(\lambda\rho)$ is Bessel's equation which remains finite at the origin. One obtains the general solution as

$$A^{\pm} = \int_0^{\infty} C(\lambda)\, J_1(\lambda\rho)\, e^{\mp\lambda z} \mathrm{d}\lambda\,. \tag{2.7}$$

The function $C(\lambda)$ has to be determined in a way that $A^{\pm}$ fulfills the boundary conditions. This condition is the reversal of B_ρ across the sheet. For a current sheet confined to the $(z{=}0)$-plane this is given as

$$\left.\frac{\partial A^+}{\partial z}\right|_{z=0} = \left.\frac{\partial A^-}{\partial z}\right|_{z=0} - \mu_0 I(\rho)\,, \tag{2.8}$$

with $I(\rho)$ being the surface current density in the plane. A sheet of finite thickness is obtained from the solution to this situation by superposition later on. A combination of equations (2.7) and (2.8), and the Fourier-Bessel equation

$$f(\beta) = \int_0^{\infty} f(\lambda) \int_0^{\infty} J_1(\lambda r)\, J_1(\beta r)\, \lambda r \,\mathrm{d}r \,\mathrm{d}\lambda$$

leads to the expression

$$C(\lambda) = \frac{\mu_0}{2} \int_0^{\infty} J_1(\lambda\rho)\, I(\rho) \rho \,\mathrm{d}\rho$$

for $C(\lambda)$. For some current densities this integral is solvable immediately. One possibility for $I(\rho)$ is

$$I(\rho) = \begin{cases} I_0/\rho & \text{for} \quad \rho > a \\ 0 & \text{for} \quad \rho < a \end{cases},$$

which describes a semi-infinite sheet, i.e. an annular sheet extending from an inner radius a outwards to infinity. In that case $C(\lambda) = \frac{\mu_0 I_0}{2}\frac{1}{\lambda} J_0(\lambda a)$ and the vector potential and magnetic field are given as

$$\begin{aligned} A^{\pm} &= \frac{\mu_0 I_0}{2} \int_0^{\infty} \frac{1}{\lambda} J_1(\lambda\rho)\, J_0(\lambda a)\, e^{\mp\lambda z}\,\mathrm{d}\lambda\,, \\ B_\rho &= \mathrm{sign}(z)\, \frac{\mu_0 I_0}{2} \int_0^{\infty} J_1(\lambda\rho)\, J_0(\lambda a)\, e^{-\lambda|z|}\,\mathrm{d}\lambda\,, \\ B_z &= \frac{\mu_0 I_0}{2} \int_0^{\infty} J_0(\lambda\rho)\, J_0(\lambda a)\, e^{-\lambda|z|}\,\mathrm{d}\lambda\,. \end{aligned}$$

For a finitely thick sheet, we take D to be the sheet's thickness and integrate over z to get

$$A^{\pm} = \mu_0 I_0 \int_0^\infty \frac{1}{\lambda^2} J_1(\lambda\rho)\, J_0(\lambda a)\, \sinh(\lambda D)\, e^{\mp\lambda z}\, \mathrm{d}\lambda\,, \tag{2.9}$$

$$B_\rho = \mathrm{sign}(z)\, \mu_0 I_0 \int_0^\infty \frac{1}{\lambda} J_1(\lambda\rho)\, J_0(\lambda a)\, \sinh(\lambda D)\, e^{-\lambda|z|}\, \mathrm{d}\lambda\,, \tag{2.10}$$

$$B_z = \mu_0 I_0 \int_0^\infty \frac{1}{\lambda} J_0(\lambda\rho)\, J_0(\lambda a)\, \sinh(\lambda D)\, e^{-\lambda|z|}\, \mathrm{d}\lambda\,, \tag{2.11}$$

which is valid outside of the sheet, i.e. for $|z| > D$. Inside, for $|z| < D$ the relations change to

$$A^{\mathrm{i}} = \mu_0 I_0 \int_0^\infty \frac{1}{\lambda^2} J_1(\lambda\rho)\, J_0(\lambda a)\, \left[1 - e^{-\lambda D}\cosh(\lambda z)\right]\, \mathrm{d}\lambda\,, \tag{2.12}$$

$$B_\rho^{\mathrm{i}} = \mu_0 I_0 \int_0^\infty \frac{1}{\lambda} J_1(\lambda\rho)\, J_0(\lambda a)\, \sinh(\lambda z)\, e^{-\lambda D}\, \mathrm{d}\lambda\,, \tag{2.13}$$

$$B_z^{\mathrm{i}} = \mu_0 I_0 \int_0^\infty \frac{1}{\lambda} J_0(\lambda\rho)\, J_0(\lambda a)\, \left[1 - e^{-\lambda D}\cosh(\lambda z)\right]\, \mathrm{d}\lambda\,. \tag{2.14}$$

For a finite annular current sheet

$$I(\rho) = \begin{cases} 0 & \text{for} \quad \rho < R_0 \\ I_0/\rho & \text{for} \quad R_0 < \rho < R_1 \\ 0 & \text{for} \quad \rho > R1 \end{cases},$$

the magnetic field and vector potential are obtained by superposition. A semi-infinite sheet of inner radius $a = R_1$ is subtracted from a semi-infinite sheet of $a = R_0$.

2.4.3 Analytical Approximation

For the original paper Connerney et al. (1981) evaluated equations (2.9) to (2.14) numerically. In this work, as in the VIPAL model, an analytical approximation which is given in the appendix to Connerney et al. (1981) is used. In parts the notation in this work is slightly different to the one used by Connerney et al. (1981). They do not distinguish between $F_{1,a}$, $F_{2,a}$ and $F_{1,\rho}$, $F_{2,\rho}$, but call the respective terms in all regions just F_1 and F_2. This distinction is introduced below, see equations (2.16) and (2.18), for clarity.

The integrals for B_ρ and B_z can be simplified and thus solved analytically if one of the arguments of the Bessel function is small. Therefore the ρz-space is separated into three different regions:

Region I	...	$\rho < a$
Region II	...	$\rho > a$ and $\lvert z\rvert > D$
Region III	...	$\rho > a$ and $\lvert z\rvert < D$

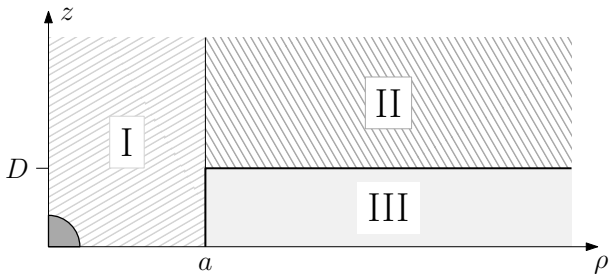

Figure 2.5: Visualization of the three regions used for the analytical approximation of the magnetic field of a semi-infinite current sheet. The dark gray quarter circle symbolizes Jupiter, the current sheet itself corresponds to Region III. As the situation is symmetrical for positive and negative z, only the positive half is depicted. For more detailed definitions of the variables used in the figure, the reader is referred to the text.

Those regions are depicted in Figure 2.5. In Region I, near the axis, where ρ is small, the approximations

$$\begin{aligned} J_1(\lambda\rho) &\simeq \frac{\lambda\rho}{2} && \text{in equation (2.10) and} \\ J_0(\lambda\rho) &\simeq 1 - \frac{\lambda^2\rho^2}{4} && \text{in equation (2.11)} \end{aligned}$$

can be used. The second approximation which is used for the z-component is to assume a thin sheet, so that the simplification

$$\int_0^\infty \frac{1}{\lambda} J_0(\lambda a)\, \sinh(\lambda D)\, e^{-\lambda z}\, \mathrm{d}\lambda \simeq 2D \int_0^\infty J_0(\lambda a)\, e^{-\lambda z}\, \mathrm{d}\lambda = \frac{2D}{(z^2+a^2)^{1/2}}$$

is valid. This results in the expressions

$$\begin{aligned} B_\rho^{\mathrm{I}} &= \left(\frac{\mu_0 I_0}{2}\right) \frac{\rho}{2} \left[\frac{1}{F_{1,a}} - \frac{1}{F_{2,a}}\right] \\ B_z^{\mathrm{I}} &= \left(\frac{\mu_0 I_0}{2}\right) \left[\frac{2D}{(z^2+a^2)^{1/2}} - \frac{\rho^2}{4}\left(\frac{z-D}{F_{1,a}^3} - \frac{z+D}{F_{2,a}^3}\right)\right] \end{aligned} \tag{2.15}$$

for the magnetic field in Region I. The terms $F_{1,a}$ and $F_{2,a}$ are defined as

$$\begin{aligned} F_{1,a} &= \left[(z-D)^2 + a^2\right]^{1/2} \\ F_{2,a} &= \left[(z+D)^2 + a^2\right]^{1/2} . \end{aligned} \tag{2.16}$$

Using a similar approach in Region II, here a is the small quantity, the magnetic field is given by

$$\begin{aligned} B_\rho^{\mathrm{II}} &= \left(\frac{\mu_0 I_0}{2}\right) \left[\frac{1}{\rho}(F_{1,\rho} - F_{2,\rho} + 2D) - \frac{a^2\rho}{4}\left(\frac{1}{F_{1,\rho}^3} - \frac{1}{F_{2,\rho}^3}\right)\right] \\ B_z^{\mathrm{II}} &= \left(\frac{\mu_0 I_0}{2}\right) \left[\frac{2D}{(z^2+\rho^2)^{1/2}} - \frac{a^2}{4}\left(\frac{z-D}{F_{1,\rho}^3} - \frac{z+D}{F_{2,\rho}^3}\right)\right] . \end{aligned} \tag{2.17}$$

Table 2.1: Properties of the current sheet in the used model, corresponding to the values stated in Connerney et al. (1981). Inner and outer edge refer to the inner and outer radius of the current sheet. The value and units of the surface current density are chosen for the resulting magnetic field to be expressed in nano-teslas.

Quantity	Symbol	Value
Inner edge	R_0	$5\ R_\mathrm{J}$
Outer edge	R_1	$50\ R_\mathrm{J}$
Half-thickness	D	$2.5\ R_\mathrm{J}$
Surface current density	I_0/ρ	$255\ \frac{\mathrm{nA}}{\mathrm{m}} \cdot \frac{2}{\mu_0}\frac{1}{\rho}$
		$= 0.41\ \frac{\mathrm{A}}{\mathrm{m}} \cdot \frac{1}{\rho}$

The terms $F_{1,\rho}$ and $F_{2,\rho}$ are defined similarly to the previous case, as

$$\begin{aligned} F_{1,\rho} &= \left[(z-D)^2+\rho^2\right]^{1/2} \\ F_{2,\rho} &= \left[(z+D)^2+\rho^2\right]^{1/2} . \end{aligned} \tag{2.18}$$

Finally inside the sheet, in Region III, we use again the approximation of small a to obtain

$$\begin{aligned} B_\rho^{\mathrm{III}} &= \left(\frac{\mu_0 I_0}{2}\right)\left[\frac{1}{\rho}(F_{1,\rho}-F_{2,\rho}+2z) - \frac{a^2\rho}{4}\left(\frac{1}{F_{1,\rho}^3}-\frac{1}{F_{2,\rho}^3}\right)\right] \\ B_z^{\mathrm{III}} &= B_z^{II} \end{aligned} \tag{2.19}$$

from equations (2.13) and (2.14), where we are using the same definitions of $F_{1,\rho}$ and $F_{2,\rho}$ as before. All the expressions above are valid for a semi-infinite sheet, The description of the finite sheet is derived by superposition as described above.

Connerney et al. (1981) suggest values for R_0, R_1, D and $\frac{\mu_0 I_0}{2}$. Those are also the values used in the calculations for Chapter 4, as given in Table 2.1.

Chapter 3

Interaction of Satellites and Magnetosphere

The first indications of the interaction of the Jovian magnetosphere with its moons was found in the radio domain, where Bigg (1964) described the high correlation between Io phase and Jovian decametric radio emission. The auroral footprints themselves were first detected in the infrared, where the interaction with Io caused excitation of H_3^+ in Jupiter's ionosphere (Connerney et al. 1993). Observations of footprints of the other satellites, Europa and Ganymede in IR continued to elude (Bonfond 2013) – a fact that has changed with the first observations of the Jovian Infrared Auroral Mapper (JIRAM) on board the Juno spacecraft (Mura et al. 2017). Io's footprint has even been imaged in the visible range (Vasavada et al. 1999, Gladstone et al. 2007). The spectral range where the wealth of data is largest, however, and where footprints of the three mentioned satellites are detected repeatedly, is the ultraviolet. This is also the spectral range which will be considered for the main analyses performed in this thesis. Figure 3.1 shows an example of an observation in the IR (Juno JIRAM), the visible (Galileo SSI) and the Far-UV (Hubble Space Telescope (HST) STIS). In the visible and UV image the footprints are marked by yellow arrows, in the IR image, the footprint contours, as modeled by the VIP4 model, are drawn with dashed lines outside of the instrument's field of view. The footprint positions as modeled by VIP4 at the time of image acquisition are marked by white dots and labeled with the moons' initials (Mura et al. 2017).

In the next sections, first, the general footprint morphology as seen in observations, mainly in the UV, will be described. Secondly, the theory for the footprints' formation, which has been derived from the observed morphologies will be reproduced. The characteristics are always best studied for the Io footprint. However, hints of those characteristics are also discernible for the other satellites, why they are assumed to stem from universal processes, common to all of the satellites (Bonfond et al. 2017a).

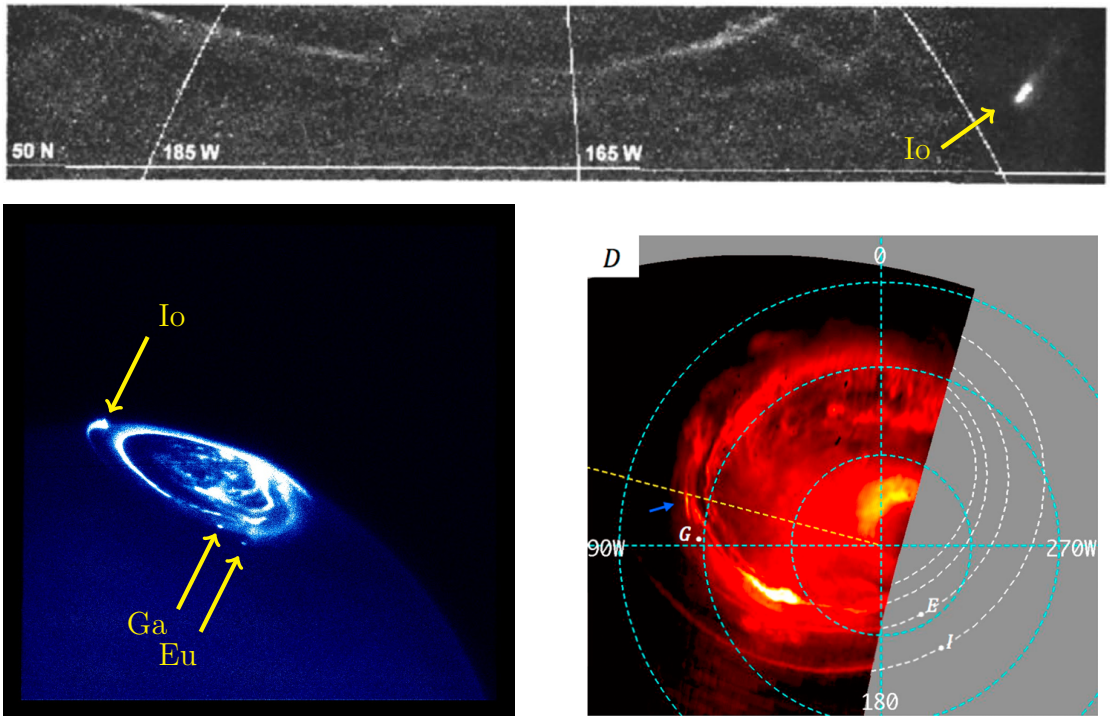

Figure 3.1: Satellite footprint aurorae in different spectral ranges.
Top: Io footprint in visible, observed by Galileo SSI on Jupiter's Northern hemisphere (Image source: Vasavada et al. 1999).
Bottom left: Io, Europa (Eu) and Ganymede (Ga) footprints in UV, observed by HST STIS on Jupiter's Northern hemisphere (image aquired via APIS database: Lamy et al. 2015).
Bottom right: infrared aurorae triggered by Europa (E – only tail visible, very close to main aurora), Io (I – only tail) and Ganymede (G – spots marked by blue arrow) observed by Juno JIRAM on Jupiter's Southern hemisphere (Image source: Mura et al. 2017, images with better visibility for Europa's tail can be found there)

3.1 Footprint Morphology

Auroral footprints are the auroral features found on a giant planet, here Jupiter, close to the magnetic field lines connected to one of their moons (in the case of Jupiter Io, Europa or Ganymede). A footprint remains fixed to its moon – as Jupiter rotates, the fooprints therefore move with respect to the planetary surface and the auroral main emission (Clarke et al. 2002, Bonfond et al. 2017b). Each moon's auroral footprint positions follow a closed contour in a Jovicentric coordinate system (Bonfond 2013). This shape is called the footprint path/footpath or footprint oval (despite potentially not being oval-shaped at all). A satellite's footprint path is acquired by mapping its orbit along magnetic field lines to the planet's surface. Therefore, the path of Io, being the innermost of the Galilean moons, can be found at the lowest latitudes, while Europa's and Ganymede's are situated at ever higher latitudes. Just as the satellites' orbits do not cross each other, neither do the footpaths. Due to the inhomogeneity of the magnetic field, they can, however, have a varying distance between one another depending on System III longitude.

Io's footprint has been discovered not to consist of a single, but of multiple distinct auroral emission spots (Connerney and Satoh 2000, Gérard et al. 2006, Bonfond et al. 2008). Also for Ganymede a secondary spot has been observed in UV imagery (Bonfond et al. 2013). The multiple spots move with respect to one another, i.e. their separation changes, as the moon triggering them moves up and down with respect to the centrifugal equator. The centrifugal equatorial plane is the surface consisting of the points on any given field line which are farthest away from the rotational axis (Hill et al. 1974, see also Section 4.4, and Figure 4.4 in there). Additionally to its multiplicity, the Io footprint also features a long (depending on instrument sensitivity dozens to hundreds of degrees SIII longitude) downstream tail (Clarke et al. 2002). Such a tail can also temporarily be observed for Europa and Ganymede in HST images (Grodent et al. 2006, Bonfond et al. 2017b). Recent Juno JIRAM data shows both the multiple Ganymede footprints and the Europa tail as well (Mura et al. 2017).

Different theories have been put forward in the past to interpret these features. In the following section, some of the currently used ones, which do well at explaining the mentioned behavior, will be described. There is of course the possibility that especially in light of new Juno discoveries, new/other models will gain higher approval in the future.

3.2 Formation Mechanism

The plasma in the inner and middle Jovian magnetosphere is coupled to the planet's rotation, i.e. it is corotating with the planet (although starting to "slip" in the middle magnetosphere region, Hill et al. 1983). Therefore, the azimuthal speed of the plasma is much higher than the orbital velocity of the moons – although their relative velocity u is still considerably slower than the local Alfvén velocity v_A (Kivelson et al. 2004). The moons constitute an obstacle for the plasma and it is diverted from its path. That diversion of the flow is carried by shear Alfvén waves. These waves continue to propagate along the magnetic field towards Jupiter's Northern and Southern hemisphere. Due to the waves' finite propagation speed, the local Alfvén velocity, the field aligned currents carried by them appear to be bent in the downstream direction by the angle

$$\theta_\mathrm{A} = \tan^{-1}\left(\frac{u}{v_\mathrm{A}}\right)$$

with respect to the background magnetic field in the satellite rest frame. These bent, disturbed regions are referred to as Alfvén wings (Goertz 1980, Neubauer 1980; description based on Kivelson et al. 2004). Figure 3.2 shows a sketch of the Alfvén wings close to the satellite including the angle θ_A.

Once the Alfvén waves reach high altitudes, below about 1 R_J above the Jovian surface, they accelerate electrons down- and upwards (Jones and Su 2008, Hess et al. 2010), i.e. towards both the closer and the opposite hemisphere – more on that in the next section. Some of these electrons precipitate into Jupiter's ionosphere, where they trigger the auroral emissions.

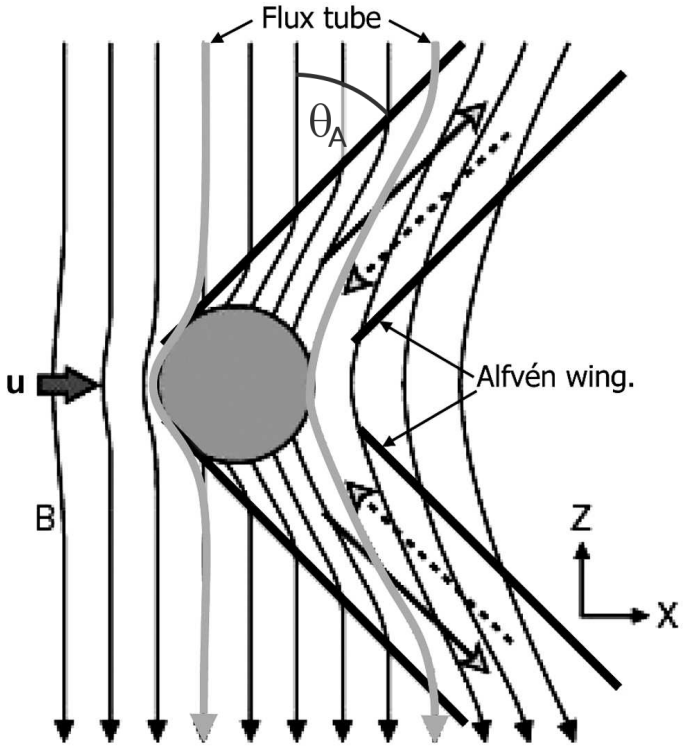

Figure 3.2: Sketch of the Alfvén wing interaction at a satellite. The viewing direction is from outside the moon's orbit towards Jupiter, in the rest frame of the moon. **B** denotes the Jovian magnetic field, pointing towards South, **u** is the relative velocity of plasma and moon. The bounds of the Alfvén wing are marked with heavy black lines. The open-headed arrows inside the Alfvén wing show the current paths; solid arrows are currents flowing on the "observer's side" of the wing (i.e. radially farther out), dashed arrows are on "Jupiter's side" (i.e. radially farther in). The interaction there does not affect the field strength, so when the distance between field lines appears to change, the lines are actually bent out of the image plane. The flux tube, marked in gray, are those field lines which pass through the moon (Image source: Kivelson et al. 2004, slightly modified).

3.2.1 Generation of Multiple Spots

Until now the description only explains the formation of one emission spot per satellite. In Section 3.1, however, the multiple footprints observed for Io and Ganymede were mentioned. The general theory is that they are formed by a combination of reflection of Alfvén waves and the electrons accelerated towards the opposite hemisphere, as mentioned before.

The interaction path followed in the previous section gives rise to the so called Main Alfvén Wing (MAW) spot. In the region of the plasma sheet (or the torus in the case of Io – but as the future analysis is concerned with Europa and Ganymede, solely the term "sheet" shall be used), the plasma density is relatively high, and it decreases sharply at the edge of the sheet. In the low density region outside, the Alfvén waves accelerate to a velocity close to the speed of light. At the boundary itself, a part of the wave is reflected (Neubauer 1980). Those reflected waves travel towards the opposite hemisphere again, and the part of them that manages to leave

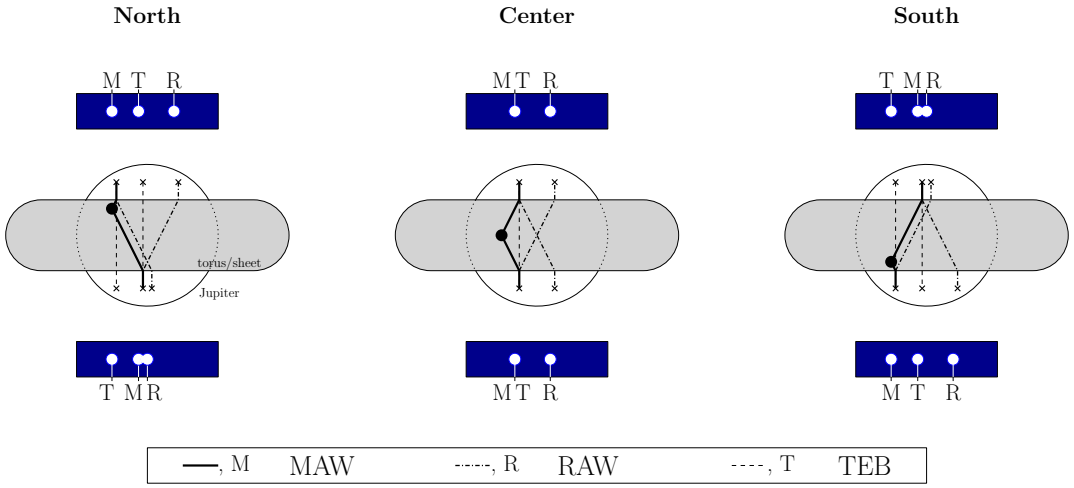

Figure 3.3: Sketch of the effect of satellite centrifugal latitude on the configuration of it auroral footprint spots. The left, middle, and right drawing show the situation when the moon (black dot) is at the Northern edge, in the center and at the Southern edge of the plasma torus/sheet (gray bar), respectively. Each situation shows the view from outside the moon's orbit looking inwards at Jupiter (white circle). The panels at the top and bottom symbolize the auroral pattern triggered in the Northern and Southern Jovian ionosphere, respectively. The solid lines stand for the main and the dash-dotted for the reflected Alfvén wing. The dashed line denotes the trans-hemispheric electron beam. In reality those lines are obviously not straight, but curved as the magnetic field lines. A more detailed description of the situations is given in the text. Figure based on the ones in Bonfond et al. (2008) and Bonfond et al. (2017a).

the sheet there, accelerate electrons to trigger aurorae as well. The auroral emission triggered by those waves is called the Reflected Alfvén Wing (RAW) spot. The third kind of spot is termed Trans-hemispheric Electron Beam (TEB) spot. It is formed by the electrons accelerated by the main Alfvén wing towards the opposite hemisphere (Bonfond et al. 2008). Those electrons have very high kinetic energies; therefore they are approximately following the magnetic field.

Thus, in total, there should be a minimum of three spots per satellite. Their position with respect to each other changes depending on their position with respect to the high-density region (Bonfond et al. 2008). The plasma sheet is centered around the centrifugal equator, i.e. tilted compared to the orbital plane of the satellites. Consequently, during the course of their orbits, they move up and down in the plasma sheet. This latitudinal position affects the distance the Alfvén waves of the MAW and RAW have to travel in a high-density environment, i.e. at low velocity. Figure 3.3 shows a sketch of the interaction geometry for different satellite positions. The panels at the top and bottom present qualitative sketches of the expected auroral features. In reality the spots exhibit different brightness – that is not accounted for in this sketch. When the moon is close to the Northern edge of the sheet (situation to the left), the MAW towards North is soon in the low-density environment, while the wing towards South has to travel at low speed for a long time. Also, as the boundary where reflection can occur is close, the southward RAW travels almost

along the same path as the southward MAW – their aurorae are very close, or even overlap. The Northern RAW has a very long way to travel – almost twice the width of the plasma sheet. It is therefore very far from the Northern MAW. While the TEB in the North is between the MAW and RAW, it is actually preceding the MAW in the South and forms a leading spot. In the situation where the moon is precisely at the center of the sheet, both main wing travel the same distance through the sheet, and the TEBs overlap with the MAWs. Also both reflected wings traverse the same distance within the sheet and therefore exhibit the same distance to the MAW in both hemispheres – the situation should be fully symmetric. The situation when the moon is close to the Southern edge, is equivalent to the first situation, only with the role of Northern and Southern hemisphere switched.

As an additional comment, it shall be mentioned that there exist other potential explanations for the satellite footprint multiplicity. Jacobsen et al. (2007) suggest that the multiple spots originate not in standard reflection (i.e. as an RAW), but are due to interference patterns of multiply reflected Alfvén waves. Future studies are to shed light onto this issue. As the previously mentioned theory of MAW/RAW/TEB is applied in the study of Bonfond et al. (2017b), the supplementary information of which forms the basis of the following analyses, it shall be the working theory here as well.

When one maps the size of the footprints back along the magnetic field lines to the equatorial plane, it can give some indication to the size of the interaction region. While a reliable estimation of size is difficult due to projection effects depending on viewing geometry, there exist estimates for the size of both the Europa, as well as the Ganymede footprint. For the size of the interaction region corresponding to the Europa spot Grodent et al. (2006) give an upper limit of $\sim$15 Europa diameters. Additionally there is the Europa tail which can be occasionally observed, for which they give an estimate of about 70 Europa diameters. This indicates that the interaction region may also include a plasma plume in the downstream wake, which was also suggested to exist by Kivelson et al. (1999). The diameter of the Ganymede interaction region has been analyzed by Grodent et al. (2009) to be in the range of about 8-20 Ganymede radii. They therefore argued for the interaction not to be governed by the satellite itself, but by the extent of its mini-magnetosphere (Kivelson et al. 1996). A more exhaustive summary of these and other satellite footprints' characteristics can, e.g. be found in Bonfond (2013).

Chapter 4

Comparison of Magnetic Field Models with Observations

In this chapter, two magnetic field models often used in the literature, VIP4 by Connerney et al. (1998) and VIPAL by Hess et al. (2011), are compared to one another by comparing their predictions to observational data. Auroral footprint positions of the satellites Europa and Ganymede, as detected by Bonfond et al. (2017b), are compared to the magnetic footprints of the satellites calculated using the magnetic field models. Such modeled footprints are obtained by tracing the position of a moon along magnetic field lines (which are determined by the magnetic field models) to the planetary surface. More information on the observational data used for the analysis is given in Section 4.1. The method to iteratively trace the magnetic field lines is described in Section 4.2, and the two magnetic field models are presented in Section 4.3. Eventually, in Section 4.4 the steps of the analysis are described in detail, and their results are shown. Those findings are discussed in view of existing literature. Also they are compared to a shortened version of the analysis performed on a new magnetic field model based on Juno measurements (JRM09 by Connerney et al. 2018) in Section 4.5.

4.1 Observational Data Used

The comparison undertaken in this chapter is based on Far-UV aurora observations of Jupiter obtained by the Hubble Space Telescope (HST). They were imaged using the Space Telescope Imaging Spectrograph (STIS) and the Advanced Camera for Surveys (ACS) in the years 1997 to 2014. An analysis of the imagery itself would have exceeded the scope of this work. For that reason the footprint positions published as supporting information to Bonfond et al. (2017b) form the basis of the presented study. That supporting information includes a description of the data analysis performed to determine the locations of the footprints' Main Alfvén Wing (MAW; see Chapter 3) spot in the images and the data lists themselves. The locations are listed for the satellites Io, Europa and Ganymede and both Jovian

hemispheres. Here only the data for Europa and Ganymede have been used. The footprint location lists are also included in this thesis in Table B.1 in Appendix B.

4.2 Tracing of Magnetic Field Lines

For the present thesis a numerical solution as mentioned in Section 2.3 has been implemented in a MATLAB script. The reader can find all used scripts in Appendix E. The line tracing is an iterative process. The set of points representing one field line is determined by propagating from one starting point, along the magnetic field direction, using an Euler integration method (see Section A.1 in Appendix A for details on this method). In the script developed here, the calculation is to start in the equatorial plane at the orbital positions of Europa or Ganymede. From there the field lines are traced to high latitudes, where they impinge on the planet. To get the line segment between a given position $\mathbf{x}_i$ and the next point $\mathbf{x}_{i+1}$, first the local magnetic field at $\mathbf{x}_i$ is determined. This field consists of (i) the component coming from internal sources, which is described by the gradient of the magnetic potential ψ, and (ii) the contribution of the current sheet $\mathbf{B}_{\mathrm{cs}}$ (see Section 2.4), i.e.

$$\mathbf{B}(\mathbf{x}_i) = \underbrace{-\nabla\psi(\mathbf{x}_i)}_{\text{(i)}} + \underbrace{\mathbf{B}_{\mathrm{cs}}(\mathbf{x}_i)}_{\text{(ii)}} .$$

Therefore, first the magnetic potential ψ, see equation (2.5), is calculated. For the numerical solution this is done on a "micro-grid" consisting of six points around $\mathbf{x}_i$. These points are spaced at a distance of $h/2$ behind and ahead of $\mathbf{x}_i$ along the x-, y- and z-axis. The geometry of the micro-grid is visualized in Figure 4.1. The quantity h specifies the distance between $\mathbf{x}_i$ and $\mathbf{x}_{i+1}$,

$$h = |\mathbf{x}_i - \mathbf{x}_{i+1}|.$$

This distance is a constant given in the beginning of the program, i.e. it is the same for all pairs $\{\mathbf{x}_i, \mathbf{x}_{i+1}\}$.

The reader may have noticed the discrepancy in coordinate systems in use; equation (2.5) specifies the potential in spherical coordinates, while the micro-grid is defined in Cartesian coordinates. The reason for this is that the mathematics of deriving the magnetic potential are easier in spherical coordinates, but subsequent calculations are more straightforward in Cartesian ones. Therefore the principle coordinate system in use is Cartesian. For determining the magnetic potential at each point of the micro-grid, its position is first transformed into the spherical coordinate system in which equation (2.5) is given.

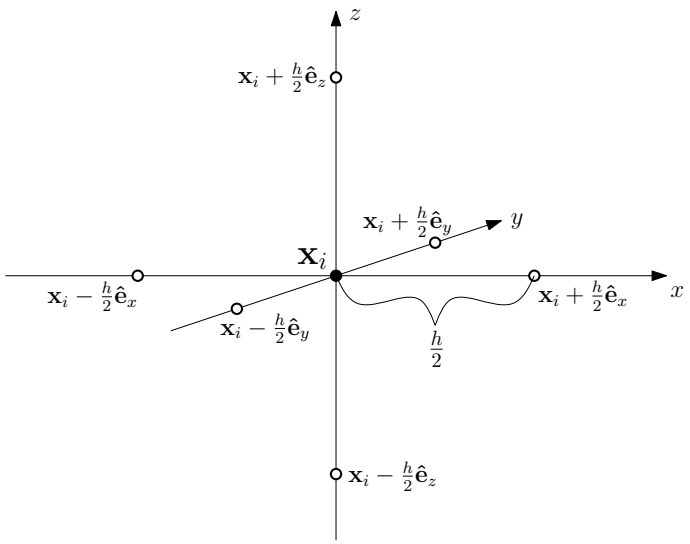

Figure 4.1: Visualization of the "micro-grid" used for the determination of the local magnetic field; the naming convention of variables corresponds to that used and explained in the text.

The internal magnetic field at the position $\mathbf{x}_i$ is obtained by numerically approximating the gradient in equation (2.3) by finite differences. This means, the internal magnetic field $\mathbf{B}^{\text{int}}(\mathbf{x}_i)$ is determined as

$$B_x^{\text{int}}(\mathbf{x}_i) = -\frac{\partial\psi}{\partial x}\bigg|_{\mathbf{x}_i} \approx -\frac{1}{h}\Big[\psi(\mathbf{x}_i + \tfrac{h}{2}\hat{\mathbf{e}}_x) - \psi(\mathbf{x}_i - \tfrac{h}{2}\hat{\mathbf{e}}_x)\Big],$$

$$B_y^{\text{int}}(\mathbf{x}_i) = -\frac{\partial\psi}{\partial y}\bigg|_{\mathbf{x}_i} \approx -\frac{1}{h}\Big[\psi(\mathbf{x}_i + \tfrac{h}{2}\hat{\mathbf{e}}_y) - \psi(\mathbf{x}_i - \tfrac{h}{2}\hat{\mathbf{e}}_y)\Big],$$

$$B_z^{\text{int}}(\mathbf{x}_i) = -\frac{\partial\psi}{\partial z}\bigg|_{\mathbf{x}_i} \approx -\frac{1}{h}\Big[\psi(\mathbf{x}_i + \tfrac{h}{2}\hat{\mathbf{e}}_z) - \psi(\mathbf{x}_i - \tfrac{h}{2}\hat{\mathbf{e}}_z)\Big],$$

where $\hat{\mathbf{e}}_x$, $\hat{\mathbf{e}}_y$, and $\hat{\mathbf{e}}_z$ specify the unit vectors in x, y, and z direction, respectively. To this the magnetic field generated by the current sheet $\mathbf{B}^{\text{sheet}}(\mathbf{x}_i)$, derived as described in Section 2.4, is added. In concrete terms, this means that depending on whether the point $\mathbf{x}_i$ is located in region I, II or III (see Figure 2.5), the current sheet field is calculated using the expressions 2.15, 2.17 or 2.19, respectively. As these equations yield the magnetic field components in cylindrical coordinates, they are converted to Cartesian ones before adding them to $\mathbf{B}^{\text{int}}(\mathbf{x}_i)$. Using the final magnetic field vector $\mathbf{B}(\mathbf{x}_i) = \mathbf{B}^{\text{int}}(\mathbf{x}_i) + \mathbf{B}^{\text{sheet}}(\mathbf{x}_i)$, the position of the point $\mathbf{x}_{i+1}$ is determined as

$$\mathbf{x}_{i+1} = \mathbf{x}_i + \sigma \cdot h\,\frac{\mathbf{B}(\mathbf{x}_i)}{|\mathbf{B}(\mathbf{x}_i)|} \quad \text{with} \quad \sigma = \pm 1.$$

In the equation above σ specifies the direction in which the magnetic field line should be traced. If $\sigma = +1$ the line is traced in the direction of the magnetic field vector,

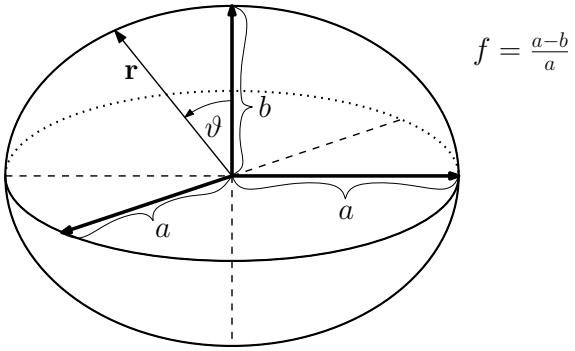

Figure 4.2: Definition of the semi-major axes a and b of an oblate spheroid – f is the flattening of the spheroid. This is the shape assumed for the planetary body in the field line tracing model. In the case of Jupiter $a = 1\ R_\mathrm{J} = 71492$ km and $f = 0.064935$. The angle ϑ marks the co-latitude, as used in equation 4.1.

i.e. towards the planetary magnetic South pole, if the current position is outside of the planet. If $\sigma = -1$ the field line is traced in the opposite direction, i.e. outside the planet towards magnetic North. Of course, in the case of Jupiter treated here, the magnetic North pole lies in the geographic Northern hemisphere and the magnetic South pole in the geographic Southern hemisphere. This equation corresponds to the Euler integration method mentioned above.

As long as $\mathbf{x}_{i+1}$ is situated outside of the planet, the calculation is repeated. The planet's shape is assumed to be an ellipsoid, or, to be precise, an oblate spheroid of flattening $f = (a - b)/a$, where a and b are the spheroid's semi-major axes, as given in Figure 4.2. In the case of Jupiter the semi-major axis a is one Jovian radius, i.e. $a = 1\ R_\mathrm{J} = 71492$ km and the flattening used is $f = 0.064935$. The dependence of the planetary radius R_P, to which the current position's radial component is compared, on the current co-latitude ϑ is given as

$$|\mathbf{x}_{i+1}| < R_\mathrm{P}(\vartheta_{i+1}) = a \cdot \left[1 + \frac{f\,(2-f)}{(1-f)^2}\,\cos^2\vartheta_{i+1}\right]^{-1/2}. \tag{4.1}$$

In case the above statement is true, the calculation is terminated. The line calculated that way is saved as an array of N points. As already stated above, the main purpose of the program is to trace a magnetic field line, starting at the position of Europa or Ganymede to a point where the line impinges on the planet. This point can either be in the Northern or Southern hemisphere. The final result shall be a comparison of aurora observations with magnetic footprints. One observation is only covering one hemisphere. Therefore for one starting position not the entire field line (from Northern to Southern hemisphere) is calculated, but only the part leading to the observed one.

Estimates of the achieved accuracies in the determination of the field lines have been obtained as follows. The setting is visualized in Figure 4.3. From starting positions spaced at 10° intervals around the orbit of Europa and Ganymede field lines were

calculated both towards the Northern (marked with "N←Sat" in Figure 4.3) and Southern (marked with "S←Sat" in Figure 4.3) hemisphere. Next from the Northern footprints obtained thus, field lines were traced to the South polar regions (marked with "N→S" in Figure 4.3). That way for each starting position along the orbit two footprint positions in the South polar region are obtained. Due to accumulated numerical uncertainties those two endpoints will not overlap exactly. Their distance δ_S on the planet's surface is given in kilometers in Table 4.1. The distance between the starting positions in the equatorial plane, and the points where the field lines which are being traced back from the North polar regions cross that plane, is determined as well. That point is calculated using the `intersectLinePlane` function of the geom3d MATLAB library by Legland (2017). In Table 4.1 the absolute distance $\delta_{eq,tot}$ between the point where the field line crosses the equator and the starting point is given, as well as the radial $\delta_{eq,r}$ and longitudinal $\delta_{eq,\varphi}$ offset. For these estimates the VIPAL magnetic field model (Hess et al. 2011) and a step size $h = 0.01\ R_J$ were used, so h is the same as used for the analysis described in Section 4.4.

From Table 4.1 it can be seen that the distance between the points in the equatorial plane, $\delta_{eq,tot}$ and $\delta_{eq,r}$, is in the order of tens of satellite radii. The distances are larger for Ganymede than for Europa, due to the greater orbital radius and thus longer field lines, which leads to greater accumulated numerical errors. The longitudinal offset $\delta_{eq,\varphi}$ is sometimes positive, sometimes negative, but always below 1°. This implies that the main deviation of the field lines in the equatorial plane is in the radial direction – which is to be expected from the numerical method used (see Appendix A.1). In the Southern hemisphere, the distance between the footprints is a few hundreds of kilometers – on average approx. 400 km (see last line of Table 4.1), which is about an order of magnitude smaller than the distances between modeled and observed footprints, as will be shown in Section 4.4. In Table 4.1, the minimum values of each column are underlined, and the maximum values are written in bold letters. While the minimum deviations all occur in the interval from 20° and 50° satellite central meridian longitude (CML), the maxima show a wider spread. Noteworthy is especially the separation of maxima in the equatorial and polar regions: while the polar deviation reaches is maximum for Europa and Ganymede at 70° and 100°, respectively, the equatorial maxima are between 270° and 330°. However, while not being at their maximum, the polar deviations in the range of the equatorial maxima (270° to 330°), are also among the highest.

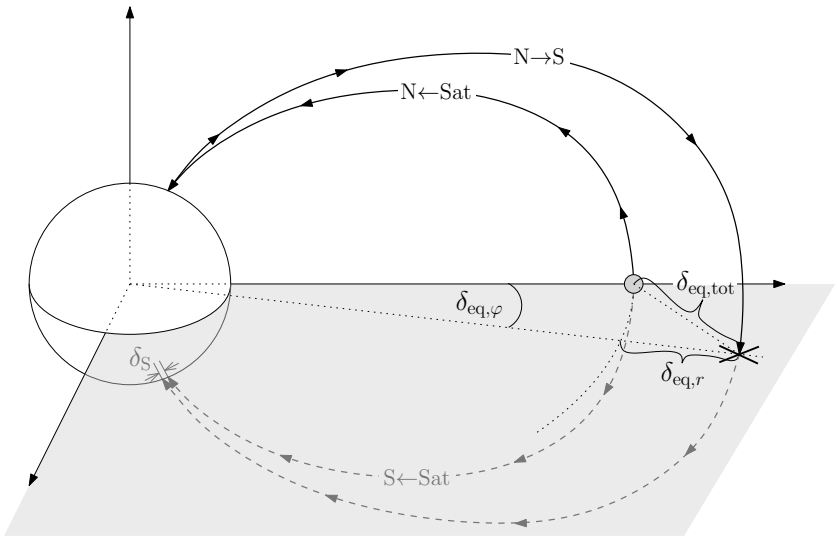

Figure 4.3: Sketch of the setting used to obtain an estimate of the line tracing accuracy – not to scale. The big white sphere symbolizes Jupiter, the small gray one stands for one of the satellites and marks the starting point for the field line calculation. The gray plane is the equatorial plane, field lines below that are drawn gray, above in black. From the satellite's orbit field lines are traced towards the Northern and Southern hemisphere, afterwards from the Northern footprint to the South ("N→S"). The point where the "N→S"-line crosses the equatorial plane is marked with a cross. The total, radial and longitudinal distance from that cross to the starting point are labeled with $\delta_{\mathrm{eq,tot}}$, $\delta_{\mathrm{eq},r}$ and $\delta_{\mathrm{eq},\varphi}$, respectively. The distance between the footprints in the Southern hemisphere is marked with δ_{S}.

Table 4.1: Accuracy estimates of field line calculations. In the table below, the first column states the System III Central Meridian Longitude (CML) φ_0 of the starting position. For an explanation of the quantities in the remaining columns, see text and Figure 4.3. Underlined entries mark the minimum, bold letters the maximum value of each column. The bottom row lists the average for each column.
For the calculations of the values below the following quantities have been used: orbital radius of Europa $a_{\mathrm{Eu}} = 670\,900$ km $= 9.38\ R_{\mathrm{J}}$, orbital radius of Ganymede $a_{\mathrm{Ga}} = 1\,070\,400$ km $= 14.97\ R_{\mathrm{J}}$, satellite radius of Europa $R_{\mathrm{Eu}} = 1\,560$ km, satellite radius of Ganymede $R_{\mathrm{Ga}} = 2\,634$ km

	Europa				Ganymede			
$\varphi_0/^\circ$	δ_{S}/km	$\delta_{\mathrm{eq,tot}}/R_{\mathrm{Eu}}$	$\delta_{\mathrm{eq},r}/R_{\mathrm{Eu}}$	$\delta_{\mathrm{eq},\varphi}/^\circ$	δ_{S}/km	$\delta_{\mathrm{eq,tot}}/R_{\mathrm{Ga}}$	$\delta_{\mathrm{eq},r}/R_{\mathrm{Ga}}$	$\delta_{\mathrm{eq},\varphi}/^\circ$
0	189.00	6.90	6.29	0.38	175.19	6.92	6.12	0.45
10	166.99	5.37	5.00	0.26	114.83	4.22	3.58	0.31
20	263.27	4.34	4.28	0.10	61.61	2.83	2.72	0.11
30	124.65	5.76	5.68	-0.13	126.42	3.77	3.69	-0.11
40	485.33	8.69	8.37	-0.31	145.57	8.56	8.29	-0.30
50	291.02	12.28	11.98	-0.35	237.74	13.94	13.66	-0.39
60	623.94	14.77	14.57	-0.32	284.01	18.93	18.74	-0.37
70	**745.98**	16.22	16.10	-0.26	518.90	22.53	22.41	-0.32
80	420.69	16.41	16.36	-0.18	292.14	24.76	24.69	-0.26
90	393.07	16.03	16.01	-0.12	428.61	25.37	25.33	-0.19
100	721.89	15.37	15.36	-0.08	**649.81**	25.21	25.19	-0.14
110	252.25	14.85	14.84	-0.06	393.35	24.47	24.46	-0.11
120	288.51	14.15	14.14	-0.05	247.95	23.55	23.54	-0.09
130	222.45	13.65	13.64	-0.06	378.28	22.47	22.46	-0.09
140	319.10	13.36	13.35	-0.07	204.11	21.61	21.60	-0.09
150	191.95	13.39	13.38	-0.08	196.76	21.42	21.41	-0.10
160	516.59	13.62	13.61	-0.09	106.83	21.20	21.18	-0.10
170	225.04	13.93	13.91	-0.09	365.02	20.94	20.93	-0.10
180	216.67	14.43	14.42	-0.09	386.23	21.51	21.49	-0.10
190	272.29	14.97	14.95	-0.09	381.56	21.82	21.81	-0.10
200	489.43	15.32	15.31	-0.08	240.32	22.68	22.68	-0.09
210	502.75	16.29	16.28	-0.07	450.47	24.33	24.32	-0.07
220	272.36	17.02	17.01	-0.06	259.06	25.35	25.34	-0.05
230	359.57	18.00	17.99	-0.04	225.89	27.91	27.91	-0.03
240	261.08	19.01	19.01	-0.01	436.46	30.14	30.14	0.00
250	491.43	20.20	20.20	0.03	400.04	33.39	33.39	0.05
260	375.15	21.28	21.27	0.09	298.73	35.42	35.41	0.12
270	653.59	21.80	**21.76**	0.17	380.30	37.78	37.75	0.20
280	449.79	**21.81**	21.72	0.26	484.34	**38.44**	**38.38**	0.29
290	398.20	20.79	20.62	0.35	544.20	36.63	36.52	0.37
300	348.68	19.26	18.98	0.43	424.96	33.74	33.57	0.46
310	380.56	17.18	16.77	0.49	237.00	28.86	28.61	0.51
320	347.88	14.96	14.42	0.52	298.19	23.58	23.23	0.55
330	365.48	12.88	12.20	**0.54**	256.18	18.75	18.28	**0.57**
340	336.42	10.66	9.92	0.51	229.41	14.16	13.60	0.55
350	236.41	8.71	7.95	0.47	219.58	10.32	9.65	0.51
Avg.	366.65	14.55	14.38	0.05	307.78	22.15	22.00	0.05

4.3 Magnetic Field Models

In the analysis described in Section 4.4, two magnetic field models are compared in their correspondence to observational data. Those two models are the VIP4 model by Connerney et al. (1998) and the VIPAL model by Hess et al. (2011). In the following, those models, their definition and basic assumptions shall be described. The spherical harmonic coefficients, or Schmidt coefficients, defining the two models are given in Table 4.2.

Table 4.2: Schmidt coefficients in units of Gauss (G) of the two magnetic field models VIP4 and VIPAL. Details on the definition, usage and interpretation of Schmidt coefficients can be found in Chapter 2.

		VIP4		VIPAL	
l	m	g_l^m	h_l^m	g_l^m	h_l^m
1	0	4.20543	0	4.200000	0
	1	-0.65920	0.24992	-0.697496	0.197345
2	0	-0.05118	0	0.644083	0
	1	-0.61904	-0.36052	-0.872434	-0.392307
	2	0.49690	0.05250	0.959767	0.602976
3	0	-0.01576	0	-0.105791	0
	1	-0.52036	-0.08804	-0.588712	-0.227086
	2	0.24386	0.40829	0.624723	0.519474
	3	-0.17597	-0.31586	0.462077	-0.104386
4	0	-0.16758	0	-0.746610	0
	1	0.22210	0.07557	0.339530	0.317345
	2	-0.06074	0.40411	-0.338022	-0.213050
	3	-0.20243	-0.16597	0.185097	0.055605
	4	0.06643	0.03866	-0.155423	0.034880
5	0	–	–	-0.065951	0
	1	–	–	0.062428	0.202157
	2	–	–	-0.156685	-0.128328
	3	–	–	-0.188082	0.023776
	4	–	–	-0.007754	0.002504
	5	–	–	-0.072790	-0.195294

4.3.1 VIP4

Developed by Connerney et al. (1998), the VIP4 model was the first to include not only magnetic field measurements by spacecraft, but also the constraint provided by the auroral emissions at the Io footprint. Its name ("VIP4") refers to the fact that it is a fourth degree/order model ("4"), using observations from Voyager ("V"), of the Io footprint ("I"), and from Pioneer ("P").

For modeling, infrared imagery of the Io footprint auroral emission was used. The data had been acquired at NASA's Infrared Telescope Facility (IRTF) on Mauna

Kea, Hawaii, and with the wide field and planetary camera (WFPC2) and faint object camera (FOC) on the Hubble Space Telescope. The data cover a wide range in system III longitude, however, the most northern longitudes between $\lambda_{III} = 0°$ and $\lambda_{III} = 150°$ were very sparsely sampled. The magnetometer data used for the development of VIP4 had been obtained by (i) the Pioneer 11 vector helium magnetometer, (ii) the Voyager 1 fluxgate magnetometer, and (iii) the Ulysses fluxgate magnetometer. Although the Ulysses data have not been used together with either Pioneer 11 or Voyager 1 observations, as the magnetosphere had been in an unusual state during that time. For more details on the assumed uncertainties and weighting factors for the modeling, please refer to Connerney et al. (1998).

In the VIP4 model the Io footprint was not used to constrain the magnetic field longitudinally in any way. The only requirement in the modeling process was that when tracing along the magnetic field from an observed footprint to the equatorial plane, the end point would have to lie on Io's orbit.

4.3.2 VIPAL

The VIPAL model, developed by Hess et al. (2011), intends to improve on the VIP4 model by also using the longitudinal position of the auroral footprint as a constraint. In this model the main input comes from Io's footprint, the magnetic field measurements from spacecraft are only used to normalize the result.

Hess et al. (2011) used far ultraviolet observations of the H_2 and H emissions from the Space Telescope Imaging Spectrograph (STIS) and the Advanced Camera for Surveys (ACS) instruments of the Hubble Space Telescope (HST). Those data have the advantage of a better spatial resolution compared to the infrared data used by Connerney et al. (1998) for VIP4. Another adjustment performed by Hess et al. (2011) with respect to VIP4, was to include magnetic anomaly proposed by Grodent et al. (2008) in their modeling efforts. When analyzing HST ACS images of Jupiter's northern aurora, Grodent et al. (2008) found that they could better reproduce the observed footprint contours of Io, Europa and Ganymede if they added a localized magnetic field anomaly to the VIP4 model. This improved the agreement between modeled and observed footprints in the "auroral kink sector", in the region between 80° and 150° System III longitude. That anomaly had not been included in a spherical decomposition of the Jovian magnetic field before.

As already stated, the VIPAL model also puts a longitudinal constraint on the footprint mapping, i.e. the field line traced from a footprint towards the equator must not only end up at Io's orbit, but also close to the satellite's longitudinal position. However, it shall not end up exactly at the moon, but downstream of it, as during the finite travel time of the perturbation towards the planet, the logitudinal position of the moon with respect to the planet changes. The basic assumption underlying the longitudinal constraint of the VIPAL model is that of the Alfvénic interaction between the satellite and Jupiter's magnetosphere. This interaction is explained in Chapter 3. Based on this Alfvèn wing theory, an expected lead angle between the actual satellite position and that location which maps to the auroral

emission is determined as a function of Io's position. That lead angle enters the longitudinal constraint. Therefore the resulting magnetic field model is dependent on the theory of satellite magnetosphere interaction.

The name of the model is an acronym, similar to VIP4. The first three letters are defined in the same way as for VIP4 (Voyager, Io footprint, Pioneer). The last two stand for the northern magnetic anomaly ("A") and the longitudinal constraint ("L").

4.4 Results of Model Comparison

The algorithm described in Section 4.2 leads from the position of a satellite, via one of the magnetic field models described in Section 4.3, to a magnetic footprint on the Jovian surface. Now one can compare the calculated position of a satellite's magnetic footprint at a certain time to the aurora triggered by the same satellite at the same time. Ideally those two would both lie on the same footprint path. The footprint path of a satellite is obtained by mapping the entire orbit of that satellite onto the planet. Most of the time, they should not totally coincide, due to the finite travel time of the Alfvén waves towards Jupiter – see Chapter 3. This lead angle has not been taken into account explicitly in this analysis. However it will be considered qualitatively. It must not be negative, as this would violate causality. Also the change of the lead angle with satellite longitude should show some specific characteristics. A change of the lead angle can be attributed to a change in the distance over which the Alfvén waves have to travel through an environment of higher density. This may be caused by the moon's change of position compared to that environment. For simplicity, one can assume for the environment to be more or less stable, and the highest density to be found in the plane of the centrifugal equator. The centrifugal equator plane is defined as the surface comprised of the points on any given field line which are farthest away from the rotational axis (see Figure 4.4, Hill et al. 1974). In that case, the lead angle as a function of longitude should follow a somewhat sinusoidal behavior. This would be due to the fact that the moons' orbits are confined to the rotational equatorial plane, which is tilted with respect to the centrifugal equator. That causes an up- and downward movement of the satellites compared to the centrifugal equator on their orbits. This behavior will be tested in the analysis.

This aforementioned study of the lead angle is only part of a broader analysis investigating the distances between calculated and observed satellite footprints, of Europa and Ganymede, on the surface of Jupiter. In the first step the absolute distance between the footprints is analyzed. The second step then no longer compares the calculated footprints to their observed counterparts, but analyzes their distance from the corresponding point[1] on a footprint path provided by Bonfond et al. (2017b) in the supplementary material. These paths are best fit contours of the observed footprint locations. The material gives the planeto-centric latitude

[1] What "corresponding point" means in this context will be explained in more detail in Section 4.4.3

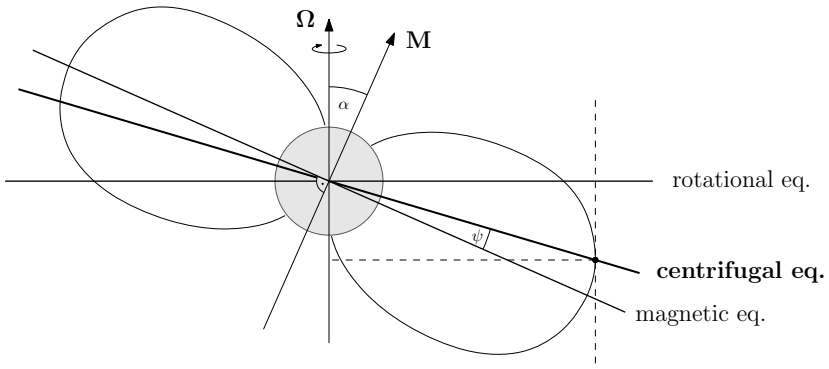

Figure 4.4: Definition of the centrifugal equator – the surface defined by the points on any given field line which are farthest away from the rotational axis; the sketch shows the meridian plane containing the rotational axis $\mathbf{\Omega}$ and the magnetic dipole moment $\mathbf{M}$. In this plane the angle ψ between the magnetic and the centrifugal equator is maximum. For a dipolar configuration and small tilt angles α between magnetic and rotational axis $\psi \simeq \alpha/3$ (Hill et al. 1974), e.g. for Jupiter $\alpha \simeq 9.6°$ and $\psi \simeq 3.2°$

and System III longitude of the footprint path as a function of satellite System III longitude. The distance to the point on the reference path is split into a part along, and one normal to the path. The result shall provide a metric to compare magnetic field models, here VIP4 and VIPAL, in their suitability of mapping the positions of Europa and Ganymede to the planet. This metric evaluates the models' performance in the different hemispheres, split into longitudinal regions, as a model may do better in one and worse in the other longitude range. This is of course especially true for the magnetic anomaly region in the Northern hemisphere. Although especially in that part the analysis is complicated as well, due to a lack in observational data there.

4.4.1 Observational Uncertainties and Their Role in the Analysis

The observational data provided by Bonfond et al. (2017b) includes error estimates of the listed auroral footprint positions. These are also given in Appendix B. These uncertainties mainly stem from the uncertainty in determining the planet's center with the limb fitting method used (Bonfond et al. 2009). The listed uncertainties are based on the assumption of a center location uncertainty of 3 pixels for ACS, and 8 pixels for STIS observations (Bonfond et al. 2017b, supporting information). In Figure 4.5 the error bars for all observations are displayed, as well as the footprints calculated using the two magnetic field models under consideration. From those plots the following observations can be made for Ganymede: for VIPAL the modeled footprints are almost always within the area covered by the error bars. Only in the region of the magnetic anomaly in the North (between approximately 270° and 140° (via 0°) System III longitude) and between 320° and 15° (via 0°) in the South the

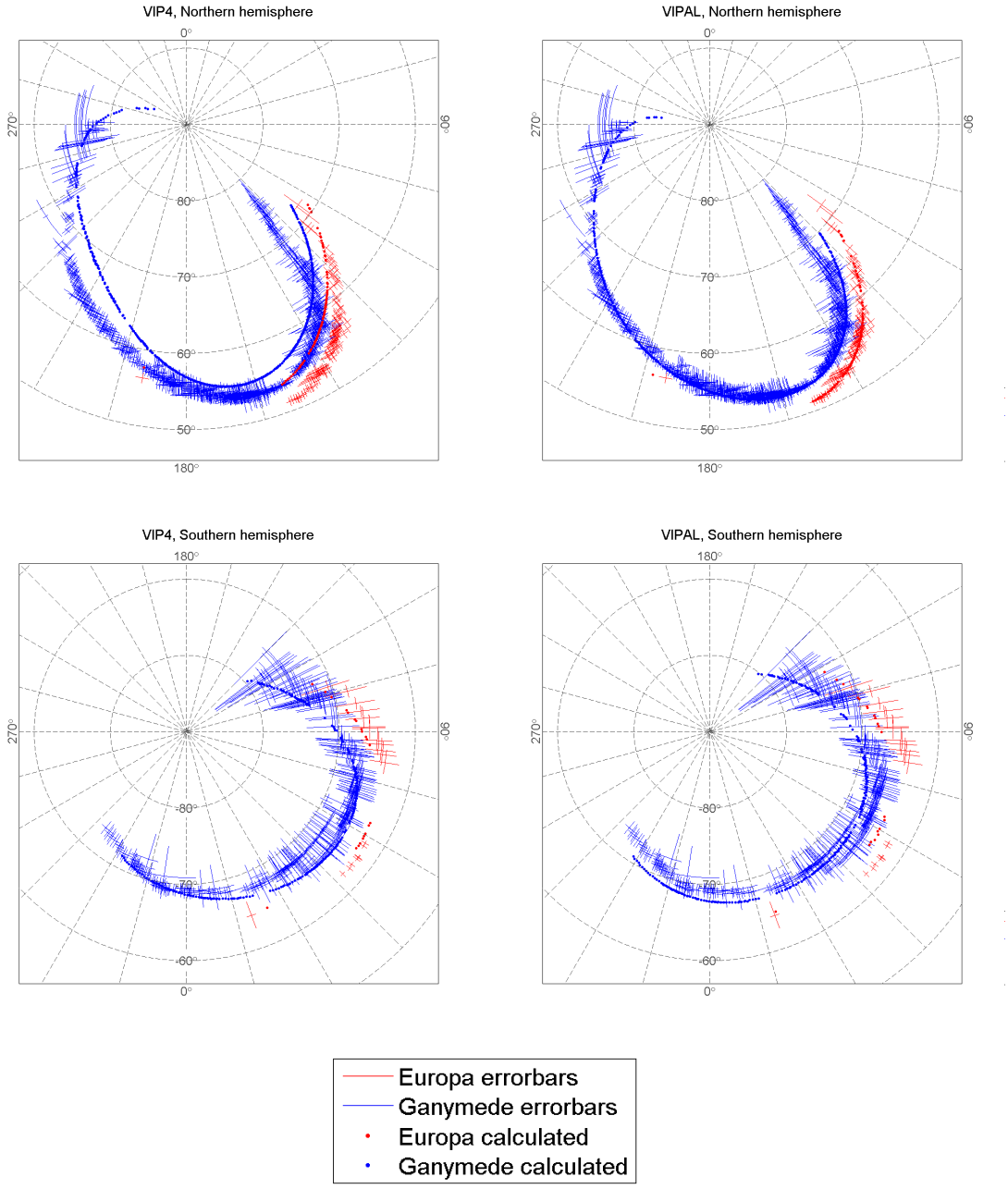

Figure 4.5: Observed and modeled satellite footprints. Observed footprints are marked with error bars indicating the observational uncertainties. Calculated footprints are depicted by filled circles. Data for Ganymede is shown in blue, for Europa in red. The top row shows the Northern, the bottom the Southern hemisphere of Jupiter, in the left column the modeled footprints were calculated using the VIP4 (Connerney et al. 1998), in the right column using the VIPAL (Hess et al. 2011) model.

deviations are beyond the error bars. For the VIP4 model the agreement in the South seems generally better. In the North however, strong deviations between the modeled footprint path and the observations become obvious – for wide longitude ranges they are clearly greater than the uncertainties. For Europa the analysis that can be made is very limited, due to the small number of available observations. However the agreement seems to be slightly worse than for Ganymede, for both models. In the North, the trends described for Ganymede seem to be valid for Europa as well.

The statements made above give only a qualitative impression. A more quantitative analysis follows in the next sections. Also those statements do not imply that the calculated footprint for one observation only, actually coincides with the area covered by the observation's error bars. It may only be within the region covered by the overlapping error bars of neighboring observations. In the following sections this factor will be taken into account as well.

In Figure 4.5 the error bars are rather dominant. They clutter the image too much for any additional information to be discernible. Therefore, in later figures displaying the entire polar region the error bars will no longer be included.

4.4.2 Absolute Distances to Observations

In this section the deviations between the observed footprints and their modeled counterparts shall be studied in more detail. For each of Europa's and Ganymede's observed auroral footprints listed in the supplementary data to Bonfond et al. (2017b), a modeled footprint had been calculated: The satellite location at the time the observation was performed, had been traced along magnetic field lines, given by a certain magnetic field model, to Jupiter's surface. Now, the distance between each observed footprint and the modeled one corresponding to the same point in time, i.e. the same satellite central meridian longitude (CML), is determined. That distance is measured on the planet's surface. Figure 4.6 shows the modeled footprints and the corresponding observations in a polar projection. The four panels show the two hemispheres, each modeled using the VIP4 and the VIPAL model. This picture gives already a qualitative impression of the model's strengths and weaknesses. In the Northern hemisphere, the deviations between observation and model are much smaller for the VIPAL than for the VIP4 model. The only region where the deviations are considerable for the VIPAL model as well, is the region of the magnetic anomaly, i.e. for longitudes between $\sim 135^\circ$ (the limit of available data) and $\sim 140^\circ$. In the Southern hemisphere the results obtained from the two models appear quite similar, neither of the two models seems to reproduce the observational data properly. These statements are based mainly on the analysis of the Ganymede footprints. While the data gathered for Europa show signs of a similar trend, the data are scarce, thus only tentative statements can be given.

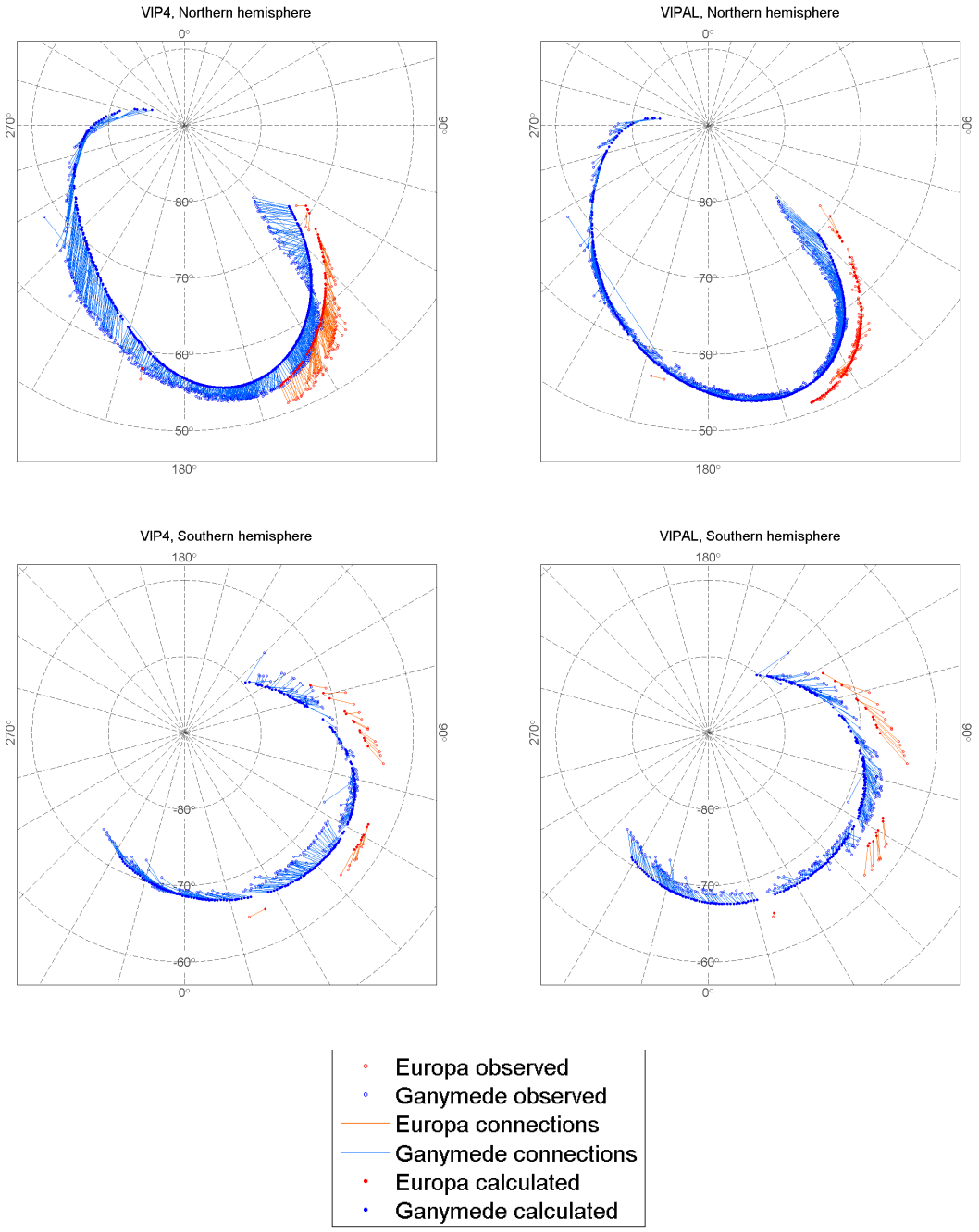

Figure 4.6: Observed and modeled satellite footprints. Calculated footprints are depicted by filled circles, observed footprints by open circles. Modeled and observed footprints corresponding to the same satellite CML are connected by a line. Data for Ganymede is shown in blue, for Europa in red; connectors for Ganymede are drawn in light-blue, for Europa in orange. The top row shows the Northern, the bottom the Southern hemisphere of Jupiter, in the left column the modeled footprints were calculated using the VIP4 (Connerney et al. 1998), in the right column using the VIPAL (Hess et al. 2011) model.

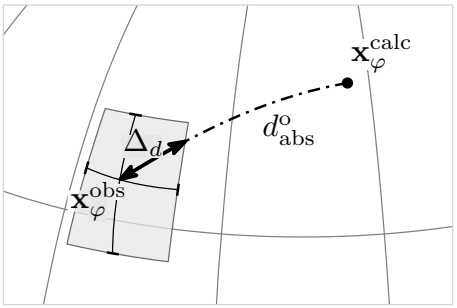

Figure 4.7: Definition of the uncertainty values plotted in Figure 4.8. The points $\mathbf{x}_\varphi^{\mathrm{obs}}$ and $\mathbf{x}_\varphi^{\mathrm{calc}}$ mark an observed and a calculated footprint on Jupiter's surface. The observed point includes error bars which span a quadrangle (gray shaded). The distance between the two footprints is $d^{\mathrm{o}}_{\mathrm{abs}}$, the uncertainty for Figure 4.8 is the part of $d^{\mathrm{o}}_{\mathrm{abs}}$ overlapping the quadrangle, labeled Δ_d.

When looking at Figure 4.6, especially at the upper right panel (VIPAL, Northern hemisphere), an outlier in the data is evident. For the observation

Obs. ID	o5hya4iaq	Calculated latitude	56.95°
Date	09/21/1999	Calculated longitude	188.26°
Time	21:05:30	Observed latitude	67.99°
Satellite	Ganymede	Observed longitude	236.91°
Satellite CML	212.89°	Distance	31594 km

the calculated and observed footprints lie in entirely different regions on the planet – the listed observed footprint appears to be erroneous. This outlier is excluded in further analyses.

To obtain a more quantitative view on the deviations between models and observations, in Figure 4.8, the distances between the calculated and observed footprints are plotted as a function of satellite longitude. In the plots, the observational error is included as well. Figure 4.7 helps to explain the custom definition of this error used henceforth. The figure shows one observed footprint $\mathbf{x}_\varphi^{\mathrm{obs}}$ and one calculated footprint $\mathbf{x}_\varphi^{\mathrm{calc}}$ on Jupiter's surface. Both points correspond to the same satellite longitude φ (and of course the same satellite). In the observations by Bonfond et al. (2017b), the uncertainties are specified in longitudinal and latitudinal direction. In both directions, an error in positive, as well as in negative direction is given, which are usually not of the same magnitude. Therefore the area of uncertainty around an observed point cannot be described by a simple ellipse. For simplicity, it was decided to use an upper limit to the error given: the area of uncertainty is considered to be a quadrangle, the East-West limits of which are given by the longitudinal error bars, and the North-South limits by the latitudinal error bars. This quadrangle is visualized by the light gray area around $\mathbf{x}_\varphi^{\mathrm{obs}}$ in Figure 4.7. The distance plotted as points (blue for Ganymede, red for Europa) in Figure 4.8 is represented by the line $d^{\mathrm{o}}_{\mathrm{abs}}$ in Figure 4.7, which connects $\mathbf{x}_\varphi^{\mathrm{obs}}$ to $\mathbf{x}_\varphi^{\mathrm{calc}}$. The part of this line which overlaps with the area of uncertainty is labeled Δ_d – this is the magnitude of the error plotted as a gray area in Figure 4.8.

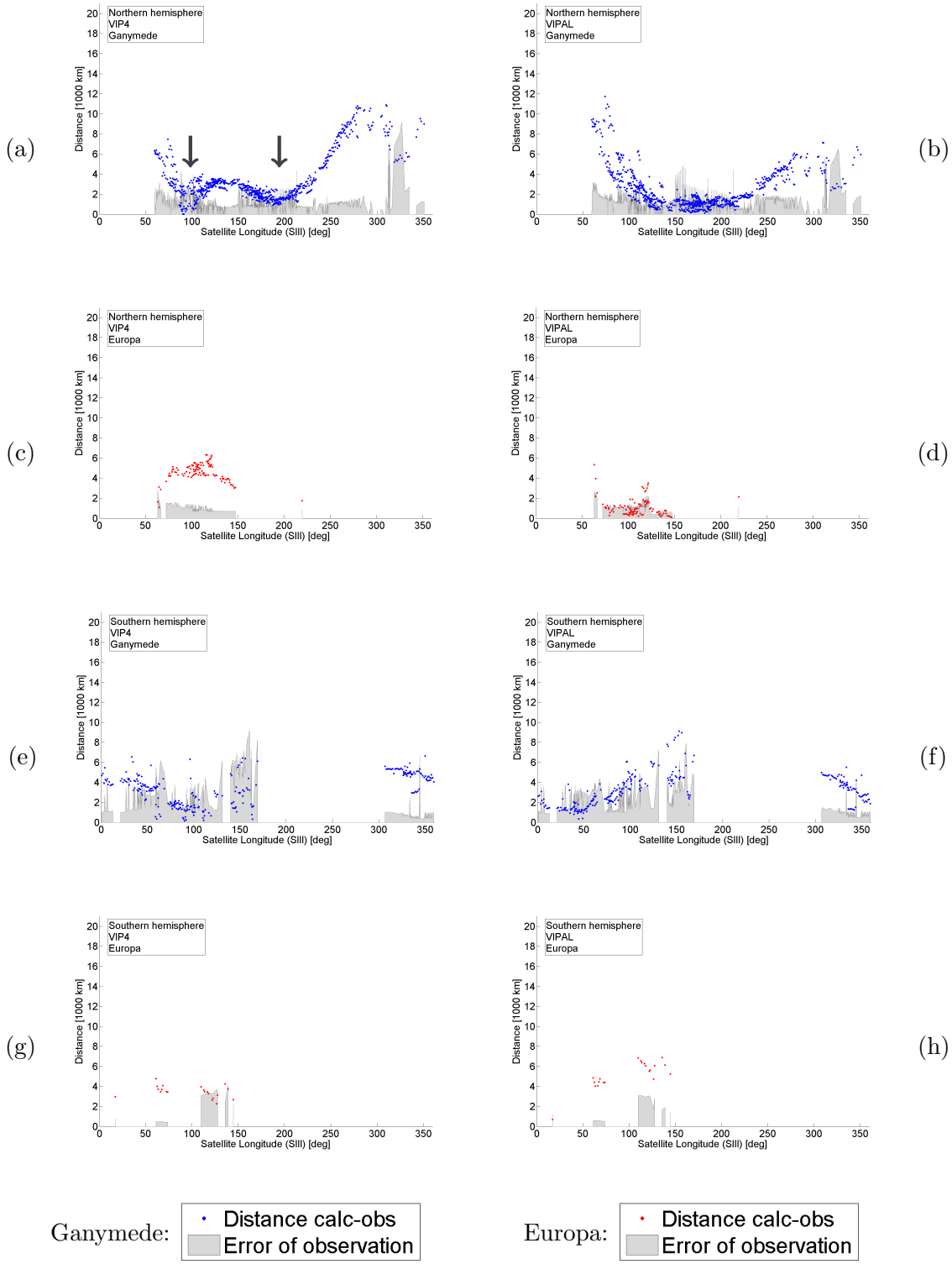

Figure 4.8: Absolute distances between observed and modeled satellite footprints as a function of satellite CML. The distances are depicted by dots, where data for Ganymede is shown in blue, for Europa in red. The observational error is shown as a gray-shaded area. In the left column the modeled footprints were calculated using the VIP4 (Connerney et al. 1998), in the right column using the VIPAL (Hess et al. 2011) model. Panels (a)-(d) show data from the Northern, panels (e)-(h) from the Southern hemisphere of Jupiter.

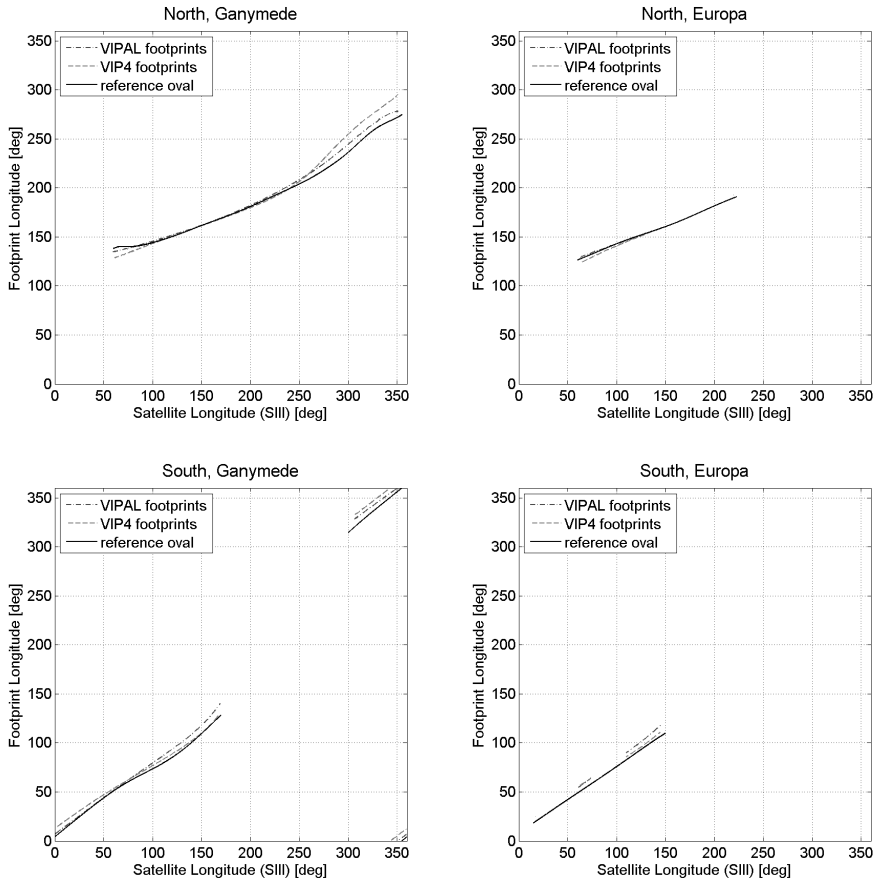

Figure 4.9: Relationship between satellite CML and longitude of the footprint on Jupiter's surface. The left column shows the data for Ganymede, the right column the data for Europa. The top row shows the Northern, the bottom the Southern hemisphere. Each panel contains the longitudinal behavior of the observational reference oval, and that of the VIPAL and VIP4 models.

The plots in Figure 4.8 show again in greater clarity and better quantifiable, what seemed to be inferable from the previous polar plots as well. To be able to better compare the plots in Figure 4.8, and similar following ones, the reader is referred to Figure 4.9. The plots there show the relationship between satellite CML and footprint longitude for Europa and Ganymede, in both Jovian hemispheres. Using the relationship there, the mentioned figures can be correlated. In general, from Figure 4.8, it becomes obvious that the numerical errors in footprint modeling play only a minor role (see Table 4.1); they are always well below 1000 km, and on average at approx. 400 km. The observational errors are mostly 1000 km and more, and the deviations between model and observation are frequently even beyond that. Panels (a) and (b) show the distances between observed and modeled footprints for Ganymede in the Northern hemisphere. For VIP4, (a), the deviations between observation and model are usually beyond the observational uncertainty. There are two points where the distances drop below the error: one at 100° and one at 200° satellite CML (marked by arrows). Figure 4.9 shows that on the planet, these regions correspond to approx. 150° and 180° longitude. A comparison to

the left upper panel of Figure 4.6, reveals that the minimum at 100° satellite CML results from a crossing of the calculated footprint oval and the observed ones. The maximum deviation is at approx. 300° satellite CML, and reaches around 8 000 to 10 000 km. For VIPAL the distances are slightly smaller, often within the error bars of the observations, but the maximum deviations still reach to 8 000 to 10 000 km. However, this happens in a different region than for VIP4, at 50-100°. For Europa's Northern footprints (Figure 4.8 (c) & (d)), at least where data is available, the improvement VIPAL offers is substantial. The deviations are reduced from approx. 5 000 km for VIP4, to mostly below 2 000 km for VIPAL, which is within the range covered by the error bars. In the Southern hemisphere (panels (e)-(h)), the amount of data, as well as their quality are lower. While the distances between model and observation in those panels differ between the models, they both exhibit a large scatter and generally overlap the error bars. No clear preference for either of the two models can be inferred from the plots in this region. The data for Europa in the South are extremely scare (Figure 4.8 (g) & (h)). The results for VIP4 even seem to be slightly better than for VIPAL, but the data points are too few to be certain.

This analysis treated the absolute distances between calculated and observed footprints. It did not take into account whether this distance was along the footprint oval, corresponding to a lead angle, or normal to it. As already mentioned in the beginning of this section, a certain lead angle is to be expected, and dictated by the processes of the interaction – see Chapter 3 for details. A distance normal to the oval, however, is undesirable and should be minimized. These considerations are the basis of the next analysis step.

4.4.3 Distances Relative to Footprint Oval

This section is no longer concerned with the auroral footprint observations themselves, but with the reference oval fitted to them by Bonfond et al. (2017b). The ovals are given, with reduced accuracy, in Appendix C. These ovals specify the latitude and longitude of a satellite's auroral footprint as a function of satellite CML. As the ovals were obtained by fitting a curve to the observational data, their reliability depends on the number of data points available. Figure 4.10 shows histograms which give the number of observations in 10° satellite CML bins. Ganymede's oval in the Northern hemisphere is based on a large number of observations, especially between ∼80° and ∼250° it is well founded. In the South, the number of data points is considerably smaller, and, as can be seen from Figure 4.5 or Figure 4.8, also the error bars are larger. Therefore the oval is less well constrained. For Europa in the North, the number of observations per bin is similar to Ganymede in the South. As the error bars are also smaller here, the mid-section of this oval is more reliable. Towards the ends, however, the number of data points decreases considerably. The end point at ∼220° is only constrained by one data point which is set apart from the others by a gap of approximately 50°. Thus, the oval can only be considered properly defined between ∼80° and 150°. The situation is worst, however, for the Southern Europan oval. It is only constrained by a small number of data points (no more than 5 per bin), which several tens-of-degrees wide gaps in between. As

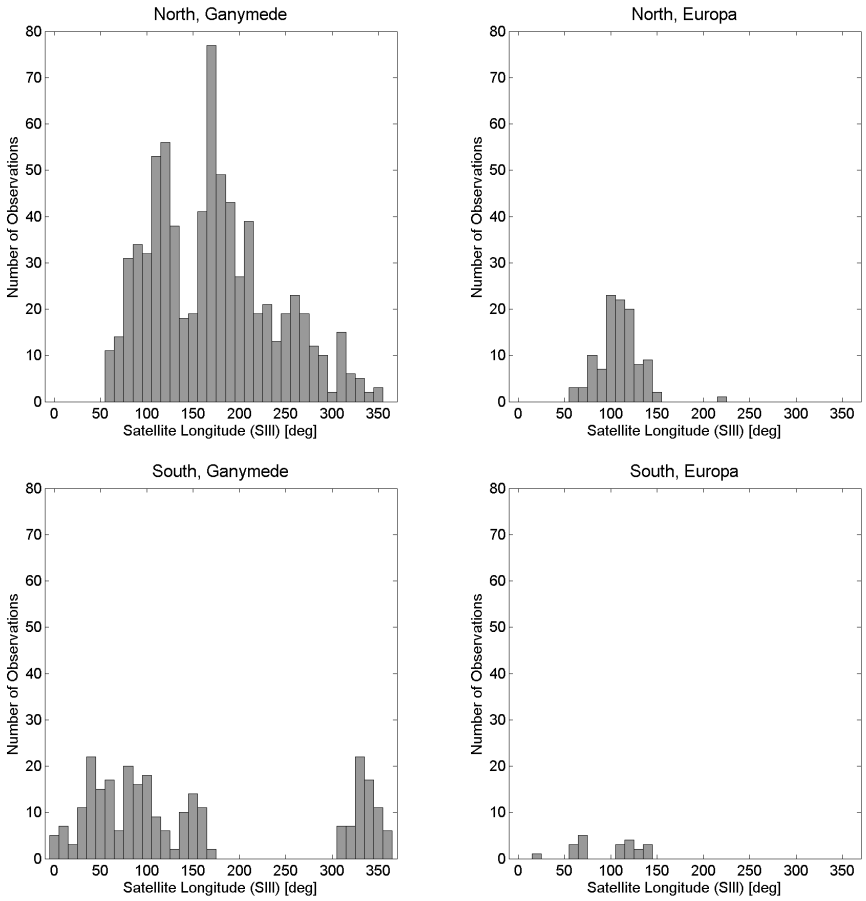

Figure 4.10: Histograms of the observational data available as a function of satellite CML. The left column shows the data for Ganymede, the right column the data for Europa. The top row shows the Northern, the bottom the Southern hemisphere.

already indicated previously, any statements about this data set have to be regarded with severe caution.

The reason, why the amount of data available is so heterogeneous, is mainly due to the observing geometry. From Earth, Jupiter's nightside hemisphere is not observable. Also, an auroral footprint in the regions above/below approx. ±75-80° latitude appears always in a quite unfavorable observing geometry, very close to the limb. This also increases the observational uncertainty in those regions (Grodent et al. 2008). Additionally, due to the hemispherical asymmetry of the Jovian magnetic field, the Northern aurorae (including footprints) reach closer to the equator than the Southern ones. This generally simplifies their observation (Grodent 2015), which explains the difference in the number and quality of observations between North and South. Furthermore, observers preferably chose the imaged longitudes in such a way that the magnetic pole of the respective hemisphere pointed towards the Earth (Bonfond et al. 2017b). Europa's footprint, specifically, is imaged so rarely because of its low brightness. Even in favorable viewing geometries it is not always observable (Grodent et al. 2008).

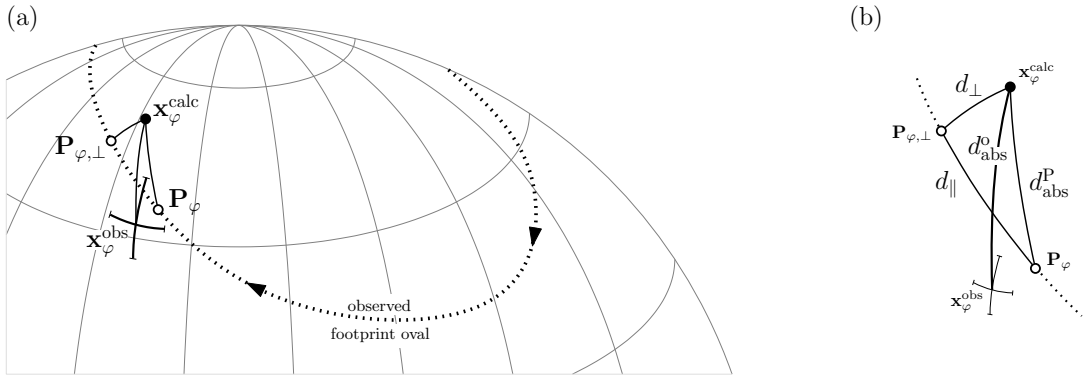

Figure 4.11: Footprint distances measured in the analysis. Panel (a) is a sketch of a calculated and an observed footprint and the point on the reference oval all corresponding to the same satellite CML. Panel (b) marks the distances between them (distances exaggerated and error bars shortened with respect to panel (a) for clarity). See text for detailed description.

As the footprints were only modeled for those satellite longitudes where actual observational data was available, the following study automatically avoids the regions where the ovals are least reliable, i.e. not constrained by any data points at all. In the next analysis steps, the distance between the footprint oval and the calculated footprint is measured in two directions. The reader is referred to Figure 4.11 as a guide for the following explanation. In the course of the entire analysis, for each satellite CML φ, four points are of relevance:

(i) the observed footprint $\mathbf{x}_\varphi^{\mathrm{obs}}$ – this was mainly considered in the previous section and is now of lesser importance

(ii) the calculated point $\mathbf{x}_\varphi^{\mathrm{calc}}$; there are of course separate calculated points for the different magnetic field models – this explanation is concerned with the analysis for one model alone

(iii) the point of the reference oval $\mathbf{P}_\varphi$ corresponding to the same satellite CML φ

(iv) the point of the reference oval $\mathbf{P}_{\varphi,\perp}$ which is closest to the calculated point $\mathbf{x}_\varphi^{\mathrm{calc}}$

These points are all sketched on the Jovian surface in Figure 4.11 (a). In Figure 4.11 (b), only those points, without the planet, are repeated, with the distances between them being exaggerated compared to part (a). In part (b) four distances are marked:

(i) $d_{\mathrm{abs}}^{\mathrm{o}}$ ... the absolute distance between calculated $\mathbf{x}_\varphi^{\mathrm{calc}}$ and observed footprint $\mathbf{x}_\varphi^{\mathrm{obs}}$, which has been analyzed in Section 4.4.2

(ii) $d_{\mathrm{abs}}^{\mathrm{P}}$ ... the absolute distance between calculated footprint $\mathbf{x}_\varphi^{\mathrm{calc}}$ and the point $\mathbf{P}_\varphi$. This distance is marked in Figure 4.13.

(iii) $d_\perp$ ... the absolute distance between calculated footprint $\mathbf{x}_\varphi^{\text{calc}}$ and the point $\mathbf{P}_{\varphi,\perp}$; this is the distance between the oval and $\mathbf{x}_\varphi^{\text{calc}}$, normal to the oval. This distance is marked in Figure 4.14

(iv) $d_\parallel$ ... the distance, projected onto the oval, i.e. between $\mathbf{P}_{\varphi,\perp}$ and $\mathbf{P}_\varphi$; this is the distance between $\mathbf{P}_\varphi$ and $\mathbf{x}_\varphi^{\text{calc}}$ along the oval

Items (iii) and (iv) will be used for the following analysis. The values of the distances listed as items (i) to (iii) are all non-negative. The distance along the oval $d_\parallel$, however, is defined in a way that it can be negative. Due to the rotation of Jupiter, the auroral footprints propagate along the oval towards higher System III longitudes. This propagation is marked in Figure 4.11 (a) by arrowheads on the oval. The calculated footprint is propagated along the magnetic field lines from the position of a satellite at the moment of observation; it represents an "instantaneous" transfer of information. In reality, the propagation of the disturbance caused by the satellite, takes a finite amount of time to reach the planetary surface. Therefore the observed footprint corresponds to an "earlier" position of the satellite. For the magnetic field model not violate causality, the calculated footprint has to be located at a position "ahead" of the observed one – this is the situation depicted in Figure 4.11. In such a configuration, $d_\parallel$ is defined to be positive. In the opposite scenario, where the calculated footprint lags "behind" the observed one, thus violating causality, $d_\parallel$ is defined to be negative.

In Figure 4.13, each calculated footprint is connected to its corresponding point $\mathbf{P}_\varphi$ on the oval, i.e. the distances $d_{\text{abs}}^{\text{P}}$ are marked. This image shall serve as an overview of the footprint paths and give a first glimpse into the longitudinal behavior, i.e. it already indicates regions where negative $d_\parallel$ can be expected. For example, for VIP4 in the region between $\sim$150° and $\sim$180°, Ganymede's calculated footprints seem to be lagging behind the observed ones. And for this model Europa's footprints appear to violate causality over the entire range.

Figure 4.12 shows a sketch of this situation to clarify the above statement. The same nomenclature is used here as in Figure 4.11, except for the fact that for simplicity in this explanation instead of the index φ, a running integer index $(1, 2, 3, ...)$ is used. For different positions of the satellite $(1, 2, ..., 5)$ different footprints are calculated using a specific magnetic field model $(\mathbf{x}_1^{\text{calc}}, ..., \mathbf{x}_5^{\text{calc}})$. To each of these five positions corresponds also a point on the reference oval $(\mathbf{P}_1, ..., \mathbf{P}_5)$. Figure 4.12 shall show these points and the oval in a polar projection, just like the ones in e.g. Figure 4.13. As Jupiter rotates, the footprint would propagate with time along the oval in the direction of the arrows. Each point $\mathbf{x}_i^{\text{calc}}$ is connected to the corresponding point $\mathbf{P}_i$. Also, to make it easier to see whether the modeled point is "ahead" of or "behind" the observed one, in each point $\mathbf{P}_i$, the local normal to the reference oval is marked. If the connecting line is tilted to the left with respect to the normal, the modeled footprint is "ahead", i.e. $d_\parallel$ would be positive. If it is tilted to the right, it is "behind", implying negative $d_\parallel$. In the left part of the image, for points 4 and 5, the modeled footprint is ahead of the observed one, as it should be for a causal model. For points 1 and 2, the calculated point is lagging behind: this is the non-causal case. The point 3 is the limiting case, the connection line is exactly

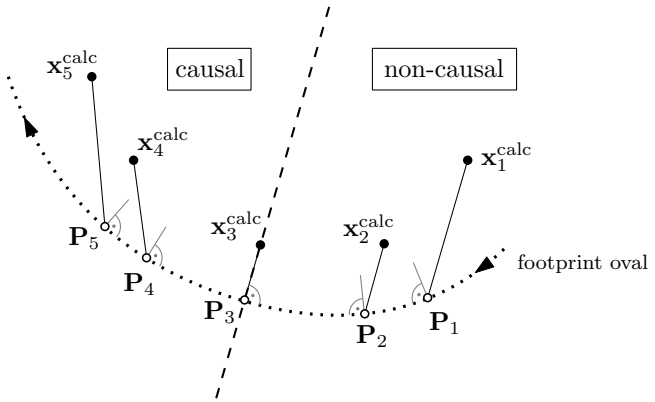

Figure 4.12: Sketch explaining the identification of areas of non-causality in polar plots like Figure 4.13. Nomenclature and symbology are similar to Figure 4.11; the dashed line through $\mathbf{P}_i$, normal to the footprint oval, separates areas where the model behaves causally/non-causally. For a detailed explanation see text.

perpendicular to the oval, $d_{\parallel}$ would be zero. This would be the case of instantaneous information transfer.

Figure 4.14 also shows the reference ovals and the calculated footprints, but there the normal distance $d_{\perp}$ is marked. There it is evident that towards the ends of the ovals, some calculated footprints are no longer connected to the path. This is the case if the calculated footprints reach higher longitudes than the ovals (e.g. in the North for Ganymede beyond $\sim$270°, or in the South beyond $\sim$120°); in that case no normal distance can be determined, and those points are excluded from further analysis.

Figure 4.15 shows the final results of the analysis. The left column contains the data for VIP4, the right for VIPAL. Overall, it is clearly evident that the footprints' longitudinal position was of no concern for the development of VIP4 (Connerney et al. 1998), but for VIPAL it was (Hess et al. 2011). VIPAL manages to improve on many of the non-causalities VIP4 suffers from. For Ganymede, in the Northern hemisphere (panel (a)), VIP4 exhibits a region of non-causality between $\sim$80°and $\sim$160°. The separation normal to the oval is rather large, often around 3 000 km. The maximum distance along the oval is 10 000 km at $\sim$280°. VIPAL (panel (b)) eliminates the non-causality entirely, and reduces the normal distance considerably to below 2 000 km. The maximum separation along the oval is approx. 8 000 km. But being located at $\sim$50°, it is in an entirely different area than for VIP4. For Europa (panels (c) and (d)), the situation is similar. The Europan footprint also features a strong non-causality around 100° with VIP4, which is even more pronounced than for Ganymede. This non-causality is strongly diminished with VIPAL, the remaining, slightly non-causal points are negligible given the observational errors. The normal separation is strongly reduced as well, to very close to zero, perfectly overlapping given the error bars.

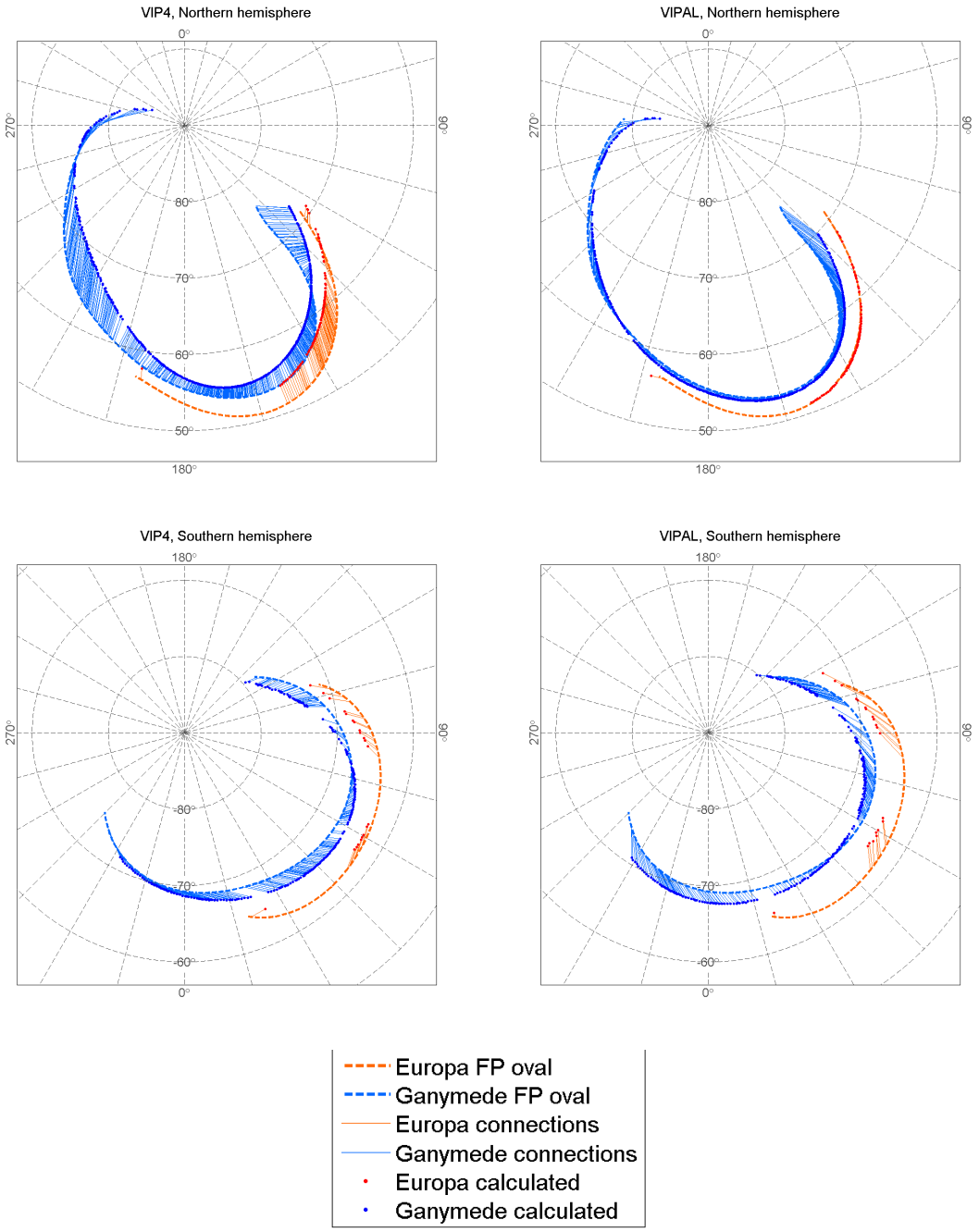

Figure 4.13: Reference oval of observations and modeled satellite footprints. Calculated footprints are depicted by filled circles, the reference oval by a dashed line. Modeled footprints and the point on the oval corresponding to the same satellite CML are connected by a line, i.e. $d^{\mathrm{P}}_{\mathrm{abs}}$ is marked. Modeled data for Ganymede is shown in blue, for Europa in red; oval and connectors for Ganymede are drawn in light-blue, for Europa in orange. The top row shows the Northern, the bottom the Southern hemisphere of Jupiter, in the left column the modeled footprints were calculated using the VIP4 (Connerney et al. 1998), in the right column using the VIPAL (Hess et al. 2011) model.

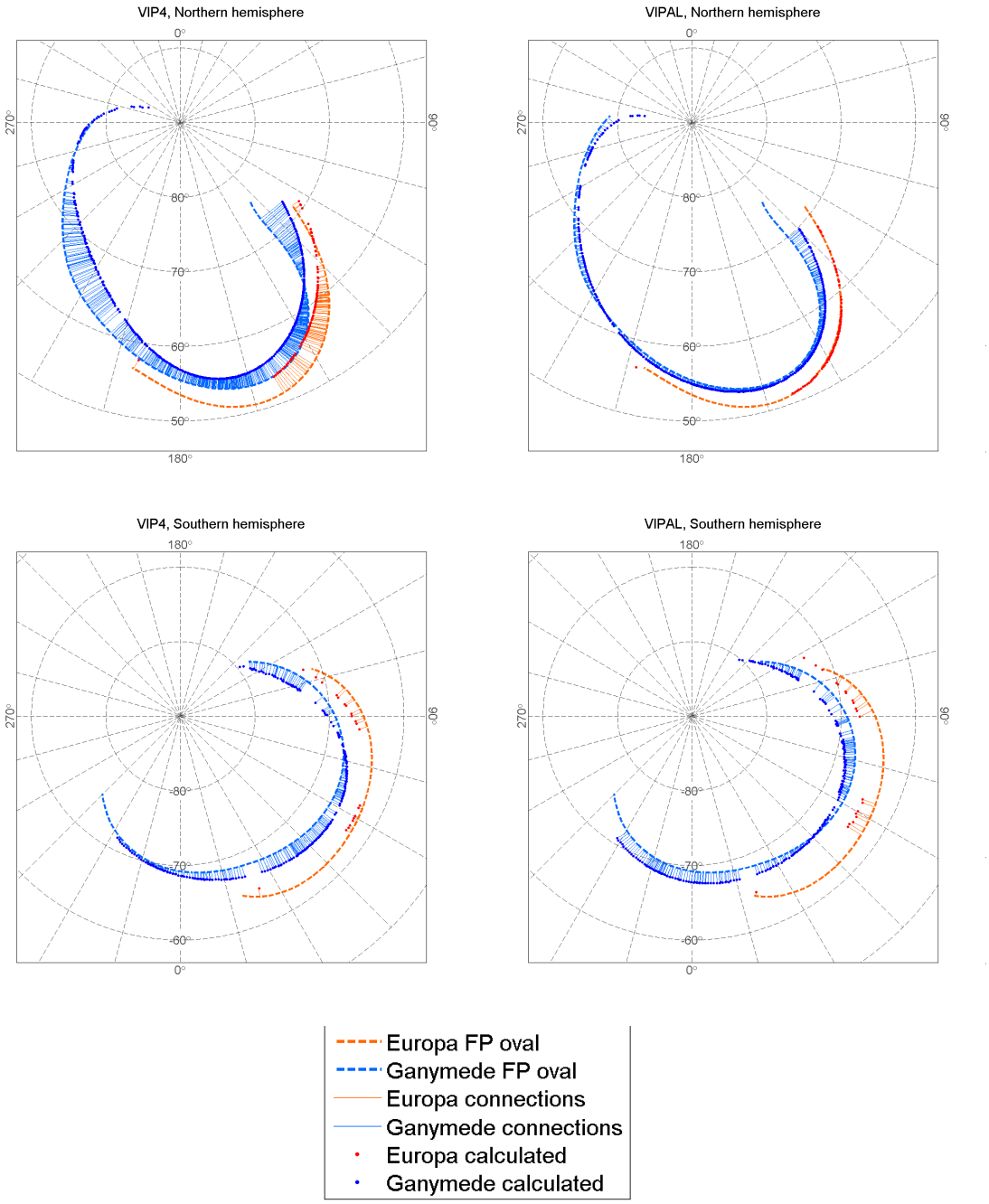

Figure 4.14: Reference oval of observations and modeled satellite footprints. Calculated footprints are depicted by filled circles, the reference oval by a dashed line. Each of the modeled footprints is connected to the point of the oval closest to it, i.e. $d_\perp$ is marked. Modeled data for Ganymede is shown in blue, for Europa in red; oval and connectors for Ganymede are drawn in light-blue, for Europa in orange. The top row shows the Northern, the bottom the Southern hemisphere of Jupiter, in the left column the modeled footprints were calculated using the VIP4 (Connerney et al. 1998), in the right column using the VIPAL (Hess et al. 2011) model.

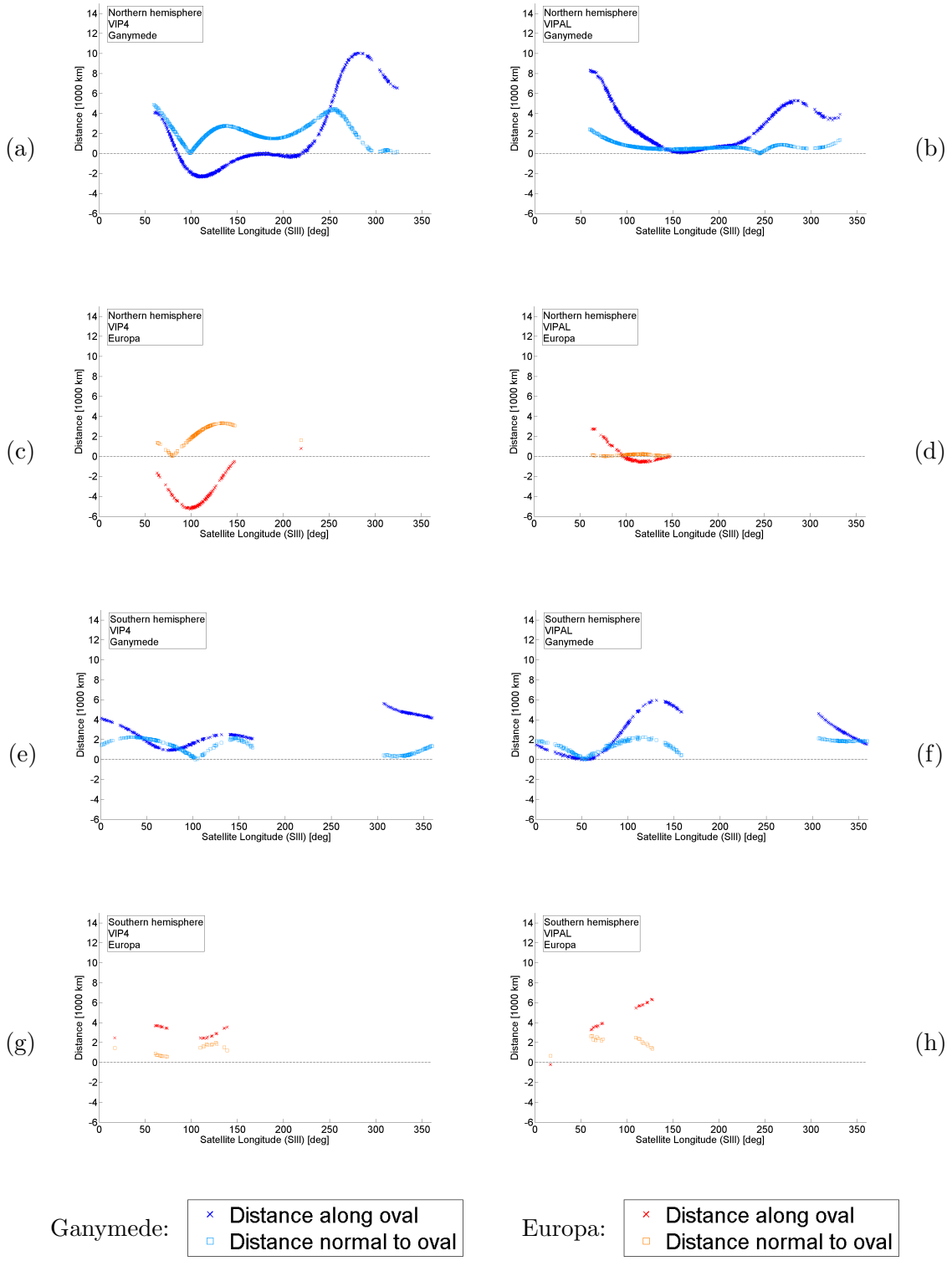

Figure 4.15: Distances between observed reference oval and modeled satellite footprints as a function of satellite CML. The distances are split into a part along (crosses; Ganymede blue, Europa red) and a part normal (open squares; Ganymede light-blue, Europa orange) to the oval. In the left column the modeled footprints were calculated using the VIP4 (Connerney et al. 1998), in the right column using the VIPAL (Hess et al. 2011) model. Panels (a)-(d) show data from the Northern, panels (e)-(h) from the Southern hemisphere of Jupiter.

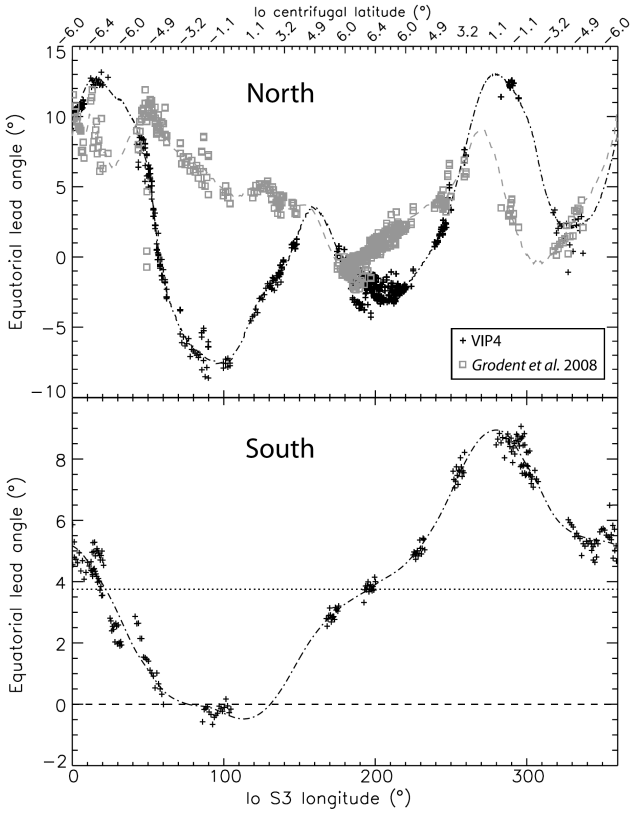

Figure 4.16: Io lead angles for Northern and Southern footprints as computed by Bonfond et al. (2009, for details on their derivation see there). The data set of interest here is for the VIP4 model (black crosses). The plot has been taken from Bonfond et al. (2009), and was slightly altered (the secondary x-axis showing the centrifugal latitude was taken from Figure 4 in the same publication and adapted).

In the Southern hemisphere (panels (e)-(f)), the contrast between VIP4 and VIPAL is much less distinct. Neither of the two models has issues with causality in the observed regions. The normal, as well as the longitudinal separations are of a comparable magnitude for both satellites. Although, it has to be stressed again that the data for Europa are very sparse. The maximum of the distance of Ganymedean footprints along the oval is larger for VIPAL (panel (f)) than for VIP4 (panel (e)), but without a further study including detailed wave propagation (see Chapter 3), there is no saying if this is justified or not.

The parallel deviation analyzed here, is closely related to the lead angle. That quantity measures the longitudinal angular separation between the calculated and observed footprint. Bonfond et al. (2009) studied the dependence of Io's lead angle as a function of Io's SIII longitude for the VIP4 model and compared the results to the Grodent et al. (2008) model. They showed the lead angle to be highly dependent on the magnetic field model in use. They also remarked on the negative lead angles, corresponding to a negative parallel distance here, present for VIP4, and took them to point to inaccuracies in the model, as no theory for footprint generation would predict their occurrence – the same interpretation as used here. Figure 4.16 shows a plot of the lead angle taken from Bonfond et al. (2009). Though it shows data for the

Io footprint, it shows some qualitative similarities to Ganymede's parallel deviations studied here (again, the lack of data for Europa prevents any real comparison there). The resemblance is most striking in the Northern hemisphere, i.e. between Figure 4.15 (a) and Figure 4.16 (top, black crosses). The negative lead angles for Io are at similar longitudes as for Ganymede (around 100°). The second minimum in the Io plot (at ∼200°), is not as pronounced in the Ganymede plot, where it only features as a plateau. Also the maximum at ∼280° is present in both. In the South (Figure 4.15 (e)), the similarities are not as strong – especially as for Ganymede the range between ∼270° and ∼300° is missing. Bonfond et al. (2009) also remark that neither the Northern nor the Southern dependence of the lead angle follows what is to be expected from an Alfvén wing model. To the plots in Figure 4.16 an axis showing the centrifugal latitude of Io has been added. As Ganymede orbits in approximately the same plane as Io (Jacobsen 2003), its centrifugal latitude should reach its extrema at similar longitudes, although their value will be different. For the North, the Alfvén wing model would predict a maximum lead angle for the southernmost satellite latitudes and a maximum for the northernmost ones (and vice versa for the South). The Io lead angle for the VIP4 model in the North, featuring too many extrema, therefore does not fit the expected trend at all. And also the South, despite being more regular, contradicts the model – the minimum and maximum lead angle are found at the same centrifugal latitudes. One comment shall be made regarding the behavior of the parallel distance for the VIPAL model (Figure 4.15 (b) and (f)): they appear to follow the trend predicted by the Alfvén wing model better. However, this is not surprising, as the theory of Alfvénic interaction is assumed as the basis of the azimuthal constraint in the definition of the model itself (Hess et al. 2011).

4.5 Short Analysis of the JRM09 Model's Performance

Recently, Connerney et al. (2018) published a new model based on Juno magnetic field measurements. This model, referred to as "JRM09" model (Juno Reference Model through Perijove 9), is a subset of Schmidt coefficients up to degree and order 10 from a degree and order 20 model. The reason for this is that the complexity of the Jovian magnetic field, as already observed in the first Juno perijove passes (Bolton et al. 2017, Connerney et al. 2017), warrants a degree and order 20 model. However, the eight perijove passes which supplied the data for the model (PJ1 and PJ3-PJ9; data from PJ2 was lost, due to the spacecraft entering a safe mode), are only sufficient to resolve the coefficients up to degree and order 10. The Schmidt coefficients of this model are reproduced in Appendix D.

Connerney et al. (2018) also provide satellite footprints calculated with JRM09 in the supplementary information to their paper. In this material they list the latitudinal and longitudinal position of the footprints as a function of satellite SIII longitude, in 5° longitude steps. These data have been processed here via the same pipeline as described in Section 4.4.3, with the aim of achieving a preliminary comparison with the results obtained for VIP4 and VIPAL. This is particularly interesting, as the JRM09 model was developed based solely on magnetic field measurements, while VIP4 and VIPAL are also constrained by the Io footprint. Comparing it to satellite footprint therefore offers a fully independent test.

Figure 4.17 shows polar projections of the data and comparing them to the observed oval. Due to the available dataset, the calculated points here cover the entire longitude range, and not only the observed points. In the North, the JRM09 model already appears to do much better than VIP4 and appears qualitatively similar to VIPAL. From the polar projection alone it is hard to make any statements about the South. In Figure 4.18 the distances of JRM09 footprints parallel and perpendicular to the observed oval are plotted. First the behavior for Ganymede shall be discussed. Panel (a) now quantitatively shows the improvement of JRM09 compared to VIP4 (Figure 4.15 (a)): the normal deviations are much smaller (below 2000 km), and the non-causalities are gone. Also the trend appears smoother. Interestingly, the plot for JRM09 looks quite similar to the one for VIPAL in Figure 4.15 (b), especially in the parallel distances: the extrema are at similar longitudes and of similar magnitude. This can be interpreted as evidence that the assumptions used for the development of VIPAL may not have been too far from reality. In the South (panel (d) in Figure 4.18 and panels (e)-(f) in Figure 4.15) statements are difficult. The normal deviations are slightly smaller than for the old models. The longitudinal trend is, to some degree, qualitatively similar for all three models. An analysis for Europa is, as always, hindered by the lack of observational data. In the North, in the small range where the observed oval is acceptably constrained (i.e. between $\sim$50° and 150°), the parallel deviation is comparable to VIPAL, although, intriguingly, the normal distances are indeed smaller for VIPAL. In the South, where data for Europa is even more sparse, any comparison to the older models would be hardly more than speculation.

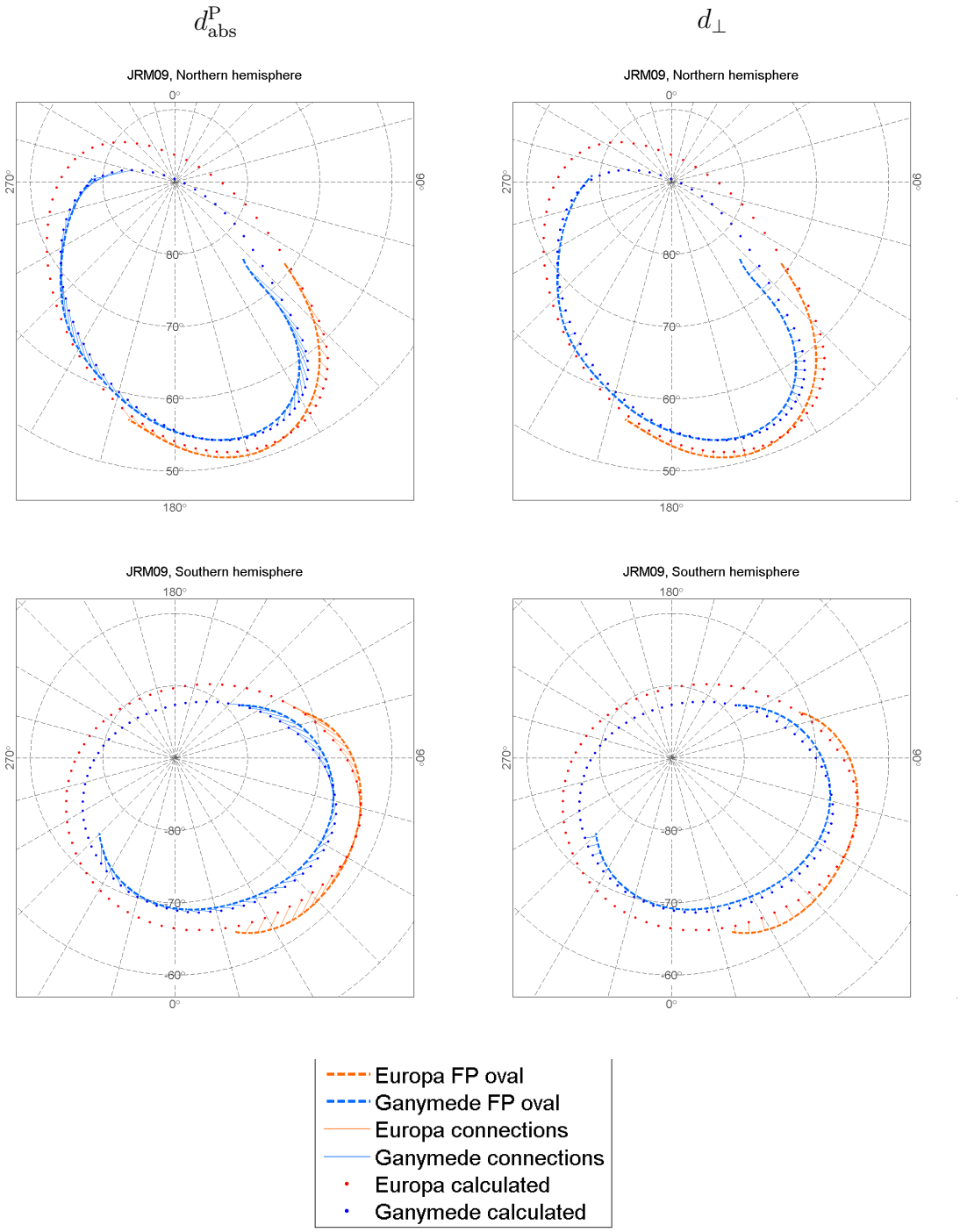

Figure 4.17: Reference oval of observations and modeled satellite footprints for the JRM09 model. Calculated footprints are depicted by filled circles, the reference oval by a dashed line. In the left column, modeled footprints and the point on the oval corresponding to the same satellite CML are connected by a line (i.e. $d^{\mathrm{P}}_{\mathrm{abs}}$ is marked). In the right column each of the modeled footprints is connected to the point of the oval closest to it (i.e. $d_{\perp}$ is marked). Modeled data for Ganymede is shown in blue, for Europa in red; oval and connectors for Ganymede are drawn in light-blue, for Europa in orange. The top row shows the Northern, the bottom the Southern hemisphere of Jupiter.

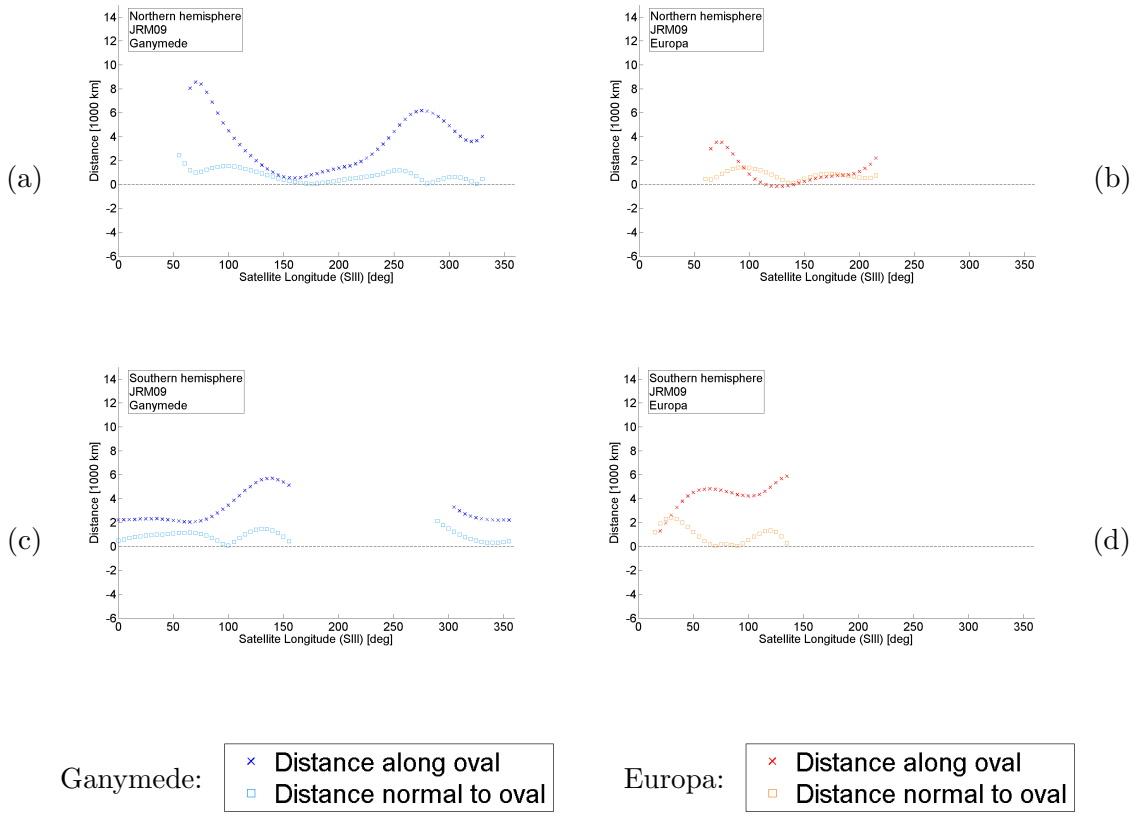

Figure 4.18: Distances between observed reference oval and modeled satellite footprints as a function of satellite CML for the JRM09 model. The distances are split into a part along (crosses; Ganymede blue, Europa red) and a part normal (open squares; Ganymede light-blue, Europa orange) to the oval. The left column shows the data for Ganymede, the right for Europa. The top row features data for the Northern, the bottom for the Southern hemisphere of Jupiter.

Chapter 5

Conclusion

This thesis results in the development of a metric for the comparison of Jovian magnetic field models. The metric quantifies the applicability of the models for the mapping of Europa's and Ganymede's footprints onto the planet. This is achieved comparing the modeled footprints to HST UV aurora observations by Bonfond et al. (2017b). The deviations between model and observation are measured in kilometers on the planets surface. A reference oval fitted to the observations by Bonfond et al. (2017b) is used to analyze the deviations split into a part parallel to the oval (i.e. roughly longitudinally), and one normal to it. This analysis is capable of clearly indicating regions where a model violates causality. The main limitation of the metric stems from the availability of observational data. Ganymede's footprint is well sampled in much of the Northern hemisphere, but the observations still do not cover the entire CML range. Longitudinal cover is worse in the Southern hemisphere, and even where observations exist, they are less numerous. Europa's footprint is sparsely sampled in the North (both with respect to longitudinal range, as well as point density), and the data points available for the South are hardly more than a handful. A higher number of observations would certainly be desirable to strengthen the base of the analysis.

The metric has been applied in its full version to the two magnetic field models VIP4 (Connerney et al. 1998) and VIPAL (Hess et al. 2011). Also a slightly modified, shortened analysis of the JRM09 model (Connerney et al. 2018) has been performed. The results of this analysis can be summarized as follows. Due to the missing longitudinal constraint in its definition, the VIP4 model shows significant non-causalities for some longitudes in Jupiter's Northern hemisphere. Also the general longitudinal trend is not compatible with any behavior predicted by an Alfvén wing model of footprint formation. Especially in the Northern hemisphere, the results for VIPAL and JRM09 are rather similar – a fact that appears to speak in favor of VIPAL, as JRM09 is only based on Juno magnetic field measurements, without any additional constraints via footprints or the like. Neither of them features (significant) non-causalities, they both show a similar longitudinal trend, which, qualitatively, fits an Alfvénic interaction model better. Also the normal deviations of both of these models is smaller than for VIP4. In the South all models are qualitatively similar. Their average normal deviations are alike, none of the models feature any

non-causalities – at least in the CML ranges covered by observations. Due to the limited availability of data, the general longitudinal trend is hard to evaluate. In particular it is not possible to determine whether it is fitting an Alfvén wing model or not.

Bibliography

Acuña, M. H. and N. F. Ness (1976). The main magnetic field of Jupiter. *J. Geophys. Res.* 81.16, pp. 2917–2922.

Bigg, E. K. (1964). Influence of the satellite Io on Jupiter's decametric emission. *Nature* 203.4949, p. 1008.

Blackwell, B. D., B. F. McMillan, A. C. Searle, and H. J. Gardner (2001). Algorithms for real time magnetic field tracing and optimization. *Comput. Phys. Commun.* 142.1-3, pp. 243–247.

Bolton, S. J., A. Adriani, V. Adumitroaie, M. Allison, J. Anderson, S. Atreya, J. Bloxham, S. Brown, J. E. P. Connerney, E. DeJong, et al. (2017). Jupiter's interior and deep atmosphere: The initial pole-to-pole passes with the Juno spacecraft. *Science* 356.6340, pp. 821–825.

Bonfond, B. (2013). When Moons Create Aurora: The Satellite Footprints on Giant Planets. In: *Auroral Phenomenology and Magnetospheric Processes: Earth And Other Planets*. Ed. by A. Keiling, E. Donovan, F. Bagenal, and T. Karlsson. American Geophysical Union, pp. 133–140.

Bonfond, B., D. Grodent, J.-C. Gérard, A. Radioti, J. Saur, and S. Jacobsen (2008). UV Io footprint leading spot: A key feature for understanding the UV Io footprint multiplicity? *Geophys. Res. Lett.* 35.5.

Bonfond, B., D. Grodent, J.-C. Gérard, A. Radioti, V. Dols, P. A. Delamere, and J. T. Clarke (2009). The Io UV footprint: Location, inter-spot distances and tail vertical extent. *J. Geophys. Res.: Space Physics* 114.A7.

Bonfond, B., S. Hess, F. Bagenal, J.-C. Gérard, D. Grodent, A. Radioti, J. Gustin, and J. T Clarke (2013). The multiple spots of the Ganymede auroral footprint. *Geophys. Res. Lett.* 40.19, pp. 4977–4981.

Bonfond, B., D. Grodent, S.V. Badman, J. Saur, J.-C. Gérard, and A. Radioti (2017a). Similarity of the Jovian satellite footprints: Spots multiplicity and dynamics. *Icarus* 292, pp. 208 –217.

Bonfond, B., J. Saur, D. Grodent, S. V. Badman, D. Bisikalo, V. Shematovich, J.-C. Gérard, and A. Radioti (2017b). The tails of the satellite auroral footprints at Jupiter. *J. Geophys. Res.: Space Physics* 122.8, pp. 7985–7996.

Burke, B. F. and K. L. Franklin (1955). Observations of a variable radio source associated with the planet Jupiter. *J. Geophys. Res.* 60.2, pp. 213–217.

Callen, J. D. (2006). *Fundamentals of Plasma Physics*. University of Wisconsin. Madison.

Clarke, J. T., J. Ajello, G. Ballester, L. Ben Jaffel, J. E. P. Connerney, J.-C. Gérard, G. R. Gladstone, D. Grodent, W. Pryor, J. Trauger, et al. (2002). Ultraviolet

emissions from the magnetic footprints of Io, Ganymede and Europa on Jupiter. *Nature* 415.6875, p. 997.

Clauser, C. (2014). Magnetfeld und Magnetosphäre der Erde. In: *Einführung in die Geophysik – Globale physikalische Felder und Prozesse in der Erde*. Berlin Heidelberg: Springer Spektrum. Chap. 5, pp. 189–245.

Connerney, J. E. P. and T. Satoh (2000). The H_3^+ ion: A remote diagnostic of the Jovian magnetosphere. *Philos. Trans. Royal Soc. A* 358.1774, pp. 2471–2483.

Connerney, J. E. P., M. H. Acuña, and N. F. Ness (1981). Modeling the Jovian current sheet and inner magnetosphere. *J. Geophys. Res.: Space Physics* 86.A10, pp. 8370–8384.

Connerney, J. E. P., R. Baron, T. Satoh, and T. Owen (1993). Images of Excited H_3^+ at the Foot of the lo Flux Tube in Jupiter's Atmosphere. *Science* 262.5136, pp. 1035–1038.

Connerney, J. E. P., M. H. Acuna, N. F. Ness, and T. Satoh (1998). New models of Jupiter's magnetic field constrained by the Io flux tube footprint. *J. Geophys. Res.: Space Physics* 103.A6, pp. 11929–11939.

Connerney, J. E. P., A. Adriani, F. Allegrini, F. Bagenal, S. J. Bolton, B. Bonfond, S. W. H. Cowley, J.-C. Gerard, G. R. Gladstone, D. Grodent, et al. (2017). Jupiter's magnetosphere and aurorae observed by the Juno spacecraft during its first polar orbits. *Science* 356.6340, pp. 826–832.

Connerney, J. E. P., S. Kotsiaros, R. J. Oliversen, J. R. Espley, J. L. Joergensen, P. S. Joergensen, J. M. G. Merayo, M. Herceg, J. Bloxham, K. M. Moore, et al. (2018). A New Model of Jupiter's Magnetic Field From Juno's First Nine Orbits. *Geophys. Res. Lett.* 45.6, pp. 2590–2596.

Fraser-Smith, A. C. (1987). Centered and eccentric geomagnetic dipoles and their poles, 1600-1985. *Rev. Geophys.* 25.1, pp. 1–16.

Gérard, J.-C., A. Saglam, D. Grodent, and J. T. Clarke (2006). Morphology of the ultraviolet Io footprint emission and its control by Io's location. *J. Geophys. Res.: Space Physics* 111.A4.

Gershenfeld, N. A. (1999). The nature of mathematical modeling. In: 4th ed. reprint 2002. Cambridge: Cambridge University Press. Chap. 6, pp. 67–70.

Gladstone, G. R., S. A. Stern, D. C. Slater, M. Versteeg, M. W. Davis, K. D. Retherford, L. A. Young, A. J. Steffl, H. Throop, J. Wm. Parker, et al. (2007). Jupiter's Nightside Airglow and Aurora. *Science* 318.5848, pp. 229–231.

Goertz, C.K. (1980). Io's interaction with the plasma torus. *J. Geophys. Res.: Space Physics* 85.A6, pp. 2949–2956.

Grodent, D. (2015). A brief review of ultraviolet auroral emissions on giant planets. *Space Sci. Rev.* 187.1-4, pp. 23–50.

Grodent, D., J.-C. Gérard, J. Gustin, B. H. Mauk, J. E. P. Connerney, and J. T. Clarke (2006). Europa's FUV auroral tail on Jupiter. *Geophys. Res. Lett.* 33.6.

Grodent, D., B. Bonfond, J.-C. Gérard, A. Radioti, J. Gustin, J. T. Clarke, J. Nichols, and J. E. P. Connerney (2008). Auroral evidence of a localized magnetic anomaly in Jupiter's northern hemisphere. *J. Geophys. Res.: Space Physics* 113.A9.

Grodent, D., B. Bonfond, A. Radioti, J.-C. Gérard, X. Jia, J. D. Nichols, and J. T. Clarke (2009). Auroral footprint of Ganymede. *J. Geophys. Res.: Space Physics* 114.A7212.

Hess, S. L. G., P. Delamere, V. Dols, B. Bonfond, and D. Swift (2010). Power transmission and particle acceleration along the Io flux tube. *J. Geophys. Res.: Space Physics* 115.A6.

Hess, S. L. G., B. Bonfond, P. Zarka, and D. Grodent (2011). Model of the Jovian magnetic field topology constrained by the Io auroral emissions. *J. Geophys. Res.: Space Physics* 116.A05217.

Hill, T. W., A. J. Dessler, and F. C. Michel (1974). Configuration of the Jovian magnetosphere. *Geophys. Res. Lett.* 1.1, pp. 3–6.

Hill, T. W., A. J. Dessler, and C. K. Goertz (1983). Magnetospheric models. In: *Physics of the Jovian Magnetosphere*. Ed. by A. J. Dessler, pp. 353–394.

Jacobsen, R. A. (2003). *JUP230 – JPL satellite ephemeris*. Jet Propulsion Laboratory, Pasadena, CA.

Jacobsen, S., F. M. Neubauer, J. Saur, and N. Schilling (2007). Io's nonlinear MHD-wave field in the heterogeneous Jovian magnetosphere. *Geophys. Res. Lett.* 34.10.

Jones, S. T. and Y.-J. Su (2008). Role of dispersive Alfvén waves in generating parallel electric fields along the Io-Jupiter fluxtube. *Journal of Geophysical Research: Space Physics* 113.A12.

Khurana, K. K. (1997). Euler potential models of Jupiter's magnetospheric field. *J. Geophys. Res.: Space Physics* 102.A6, pp. 11295–11306.

Khurana, K. K. and H. K. Schwarzl (2005). Global structure of Jupiter's magnetospheric current sheet. *J. Geophys. Res.: Space Physics* 110.A7.

Kivelson, M. G., K. K. Khurana, C. T. Russell, R. J. Walker, J. Warnecke, F. V. Coroniti, C. Polanskey, D. J. Southwood, and G. Schubert (1996). Discovery of Ganymede's magnetic field by the Galileo spacecraft. *Nature* 384.6609, p. 537.

Kivelson, M. G., K. K. Khurana, D. J. Stevenson, L. Bennett, S. Joy, C. T. Russell, R. J. Walker, C. Zimmer, and C. Polanskey (1999). Europa and Callisto: Induced or intrinsic fields in a periodically varying plasma environment. *J. Geophys. Res.: Space Physics* 104.A3, pp. 4609–4625.

Kivelson, M. G., F. Bagenal, W. S. Kurth, F. M. Neubauer, C. Paranicas, and J. Saur (2004). Magnetospheric Interactions with Satellites. In: *Jupiter: The planet, satellites and magnetosphere*. Ed. by F. Bagenal, T. E. Dowling, and W. B. McKinnon. Cambridge University Press. Chap. 21, pp. 513–536.

Lamy, L., R. Prangé, F. Henry, and P. Le Sidaner (2015). The Auroral Planetary Imaging and Spectroscopy (APIS) service. *Astronomy and Computing* 11, Part B. The Virtual Observatory: {II}, pp. 138–145.

Legland, D. (2017). *geom3d MATLAB library*. Version 1.20, 05-May-2017. URL: `http://de.mathworks.com/matlabcentral/fileexchange/24484-geom3d`.

Merrill, R. T., M. W. McElhinny, and P. L. McFadden (1998). The Present Geomagnetic Field: Analysis and Description from Historical Observations. In: *The magnetic field of the earth: paleomagnetism, the core, and the deep mantle*. Vol. 63. International Geophysics Series. Academic Press. Chap. 2.

Mura, A., A. Adriani, F. Altieri, J. E. P. Connerney, S. J. Bolton, M. L. Moriconi, J.-C. Gérard, W. S. Kurth, B. M. Dinelli, F. Fabiano, et al. (2017). Infrared

observations of Jovian aurora from Juno's first orbits: main oval and satellite footprints. *Geophys. Res. Lett.* 44.11, pp. 5308–5316.

Neubauer, F. M. (1980). Nonlinear standing Alfvén wave current system at Io: Theory. *J. Geophys. Res.: Space Physics* 85.A3, pp. 1171–1178.

Smith, E. J., L. Davis, D. E. Jones, P. J. Coleman, D. S. Colburn, P. Dyal, C. P. Sonett, and A. M. A. Frandsen (1974). The planetary magnetic field and magnetosphere of Jupiter: Pioneer 10. *J. Geophys. Res.* 79.25, pp. 3501–3513.

Vasavada, A. R., A. H. Bouchez, A. P. Ingersoll, B. Little, and C. D. Anger (1999). Jupiter's visible aurora and Io footprint. *J. Geophys. Res.* 104.E11, pp. 27133–27142.

von Laven, K. (2015). *Spherical To Azimuthal Equidistant MATLAB library*. Version 1.6, 13-Mar-2015. URL: `https://de.mathworks.com/matlabcentral/fileexchange/28848-spherical-to-azimuthal-equidistant`.

Appendix A

Mathematical Concepts

A.1 Euler Integration Method

The Euler method is a very simple technique of numerically solving ordinary differential equations (ODEs). The descriptions in this section mainly follow the ones in (Gershenfeld 1999). An ordinary differential equation of first order is an equation of the form

$$\frac{\mathrm{d}y}{\mathrm{d}x} = f(x, y). \tag{A.1}$$

Due to the dependence of the left-hand side on y, such an equation cannot be solved by plain integration – often iterative, numerical solutions are required. In case the ODE is of first order, and the value $y(x')$ is known, for a small quantity h, the value of $y(x' + h)$ can be approximated by the Taylor series

$$y(x' + h) = y(x') + h \left.\frac{\mathrm{d}y}{\mathrm{d}x}\right|_{x'} + \frac{h^2}{2} \left.\frac{\mathrm{d}^2y}{\mathrm{d}x^2}\right|_{x'} + \mathcal{O}(h^3).$$

For the Euler method, only the first two terms are used, i.e.

$$y(x' + h) = y(x') + h \left.\frac{\mathrm{d}y}{\mathrm{d}x}\right|_{x'} + \mathcal{O}(h^2).$$

Using the original definition of the ODE in equation (A.1), one obtains the expression

$$y(x' + h) \approx y(x') + hf(x', y(x')),$$

which is defining the Euler method. Figure A.1 shows a sketch visualizing this procedure. Due to the large error, of the order $\mathcal{O}(h^2)$, acquired at each step, the Euler method needs a very small step size h to converge satisfactorily. If the step size is too large, the solution may begin to oscillate and can even diverge, which Gershenfeld (1999) demonstrates using the following example: the differential equation

$$\frac{\mathrm{d}y}{\mathrm{d}x} = Ay,$$

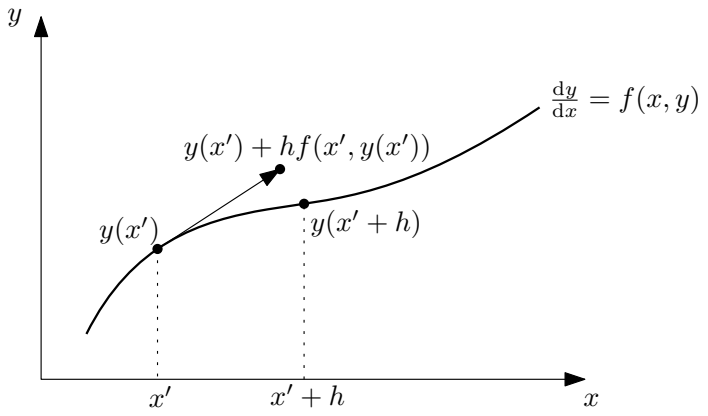

Figure A.1: Sketch of the principle of the Euler method. The value of $y(x' + h)$ is approximated by $y(x') + hf(x', y(x'))$, i.e. by adding the step width h, multiplied with the local slope, to $y(x')$. Figure based on Gershenfeld (1999).

can be solved exactly by the expression

$$y(x) = y(0)e^{Ax}.$$

The Euler approximation yields

$$y(x + h) = y(x) + hAy(x) = (1 + hA)y(x),$$

which is equivalent to the expression

$$y(x) = (1 + hA)^{x/h}y(0)$$

for $y(x)$. This equation shows the following behavior for different ranges of hA:

$0 < hA$	...	diverges (similar to exact solution)
$-1 < hA < 0$	...	decays to 0 (similar to exact solution)
$-2 < hA < -1$	...	magnitude of solution decays, but is oscillating
$hA < -2$	...	magnitude of solution diverges

This can also be seen in Figure A.2. By taking more terms of the Taylor series into account one can improve on the convergence. This leads to Runge-Kutta methods of different order (for details see e.g. Gershenfeld 1999). However, those methods come at the cost of greater complexity, and thus also increasing computational time.

One comment regarding the applicability of Euler, and similar, methods to ODEs of higher order: The above derivations have been performed for a differential equation of first order. They can, however, be easily modified to be usable for higher order equations. The procedure relies on the fact that the methods are immediately

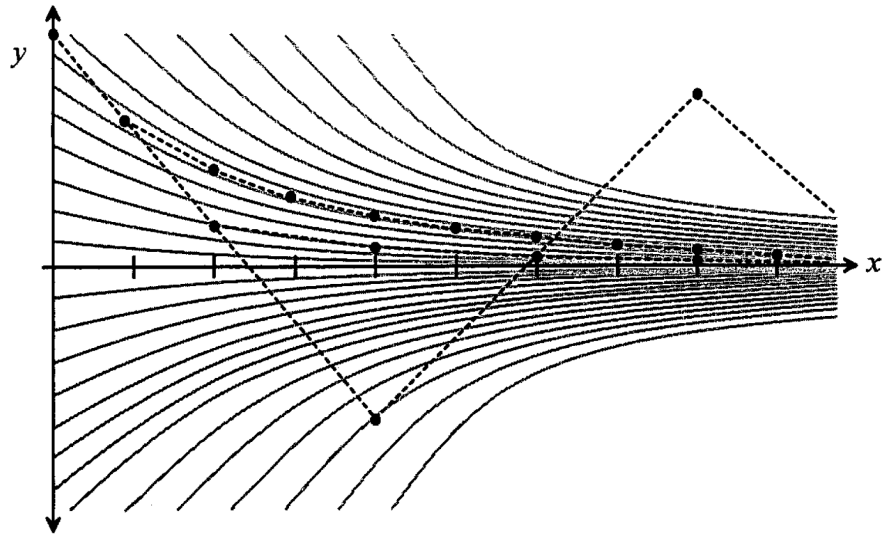

Figure A.2: Behavior of the Euler method for different step sizes. The solid curves show a family of functions $y(0)e^{Ax}$ for different $y(0)$. The dashed curves show the Euler approximation for different step sizes (Source: Gershenfeld 1999).

applicable to a system of differential equations

$$\begin{aligned}
\frac{\mathrm{d}y_1}{\mathrm{d}x} &= f_1(x, y_1, y_2, ..., y_N) \\
\frac{\mathrm{d}y_2}{\mathrm{d}x} &= f_2(x, y_1, y_2, ..., y_N) \\
&\vdots \\
\frac{\mathrm{d}y_N}{\mathrm{d}x} &= f_N(x, y_1, y_2, ..., y_N),
\end{aligned}$$

by applying them to each equation separately. This helps in solving a differential equation of higher order

$$\frac{\mathrm{d}^N y}{\mathrm{d}x^N} = f\left(x, y, \frac{\mathrm{d}y}{\mathrm{d}x}, ..., \frac{\mathrm{d}^{N-1} y}{\mathrm{d}x^{N-1}}\right),$$

by using the fact that such an equation can be written as a system of ODEs of first order, via the definition

$$y^{(1)} \equiv \frac{\mathrm{d}y}{\mathrm{d}x}, \quad ..., \quad y^{(N)} \equiv \frac{\mathrm{d}^N y}{\mathrm{d}x^N},$$

as

$$\begin{aligned}
\frac{\mathrm{d}y}{\mathrm{d}x} &= y^{(1)} \\
\frac{\mathrm{d}y^{(1)}}{\mathrm{d}x} &= y^{(2)} \\
&\vdots \\
\frac{\mathrm{d}y^{(N-1)}}{\mathrm{d}x} &= y^{(N)} \\
\frac{\mathrm{d}y^{(N)}}{\mathrm{d}x} &= f_N(x, y, y^{(1)}, y^{(2)}, ..., y^{(N-1)}).
\end{aligned}$$

This system can be solved again by the approximations discussed before.

Appendix B

List of Observed Footprint Positions

Table B.1: Auroral footprints' main Alfvén wing (MAW) spot locations for Europa and Ganymede observed on the Northern and Southern Jovian hemispheres as published as supporting information to Bonfond et al. (2017b).

The columns contain the following data:
1. "Sat." ... satellite triggering the auroral footprint, Eu = Europa, Ga = Ganymede
2. "Hem." ... observed hemisphere, N = North, S = South
3. "Obs ID" ... ID of the HST observation
4. "Date" ... date at the center of the (sub-)exposure, format "YYYY/MM/DD"
5. "Time" ... time at the center of the (sub-)exposure, format "hh:mm:ss"
6. "φ_{Sat}" ... System III longitude of the satellite
7. "φ_{fp}" ... System III longitude of the spot in degrees
8. "λ_{fp}" ... planeto-centric latitude of the spot in degrees
9. "$\Delta^{+}(\varphi_{\mathrm{fp}})$" & 10. "$\Delta^{-}(\varphi_{\mathrm{fp}})$" ... uncertainty range on the spot longitudes in degrees
11. "$\Delta^{+}(\lambda_{\mathrm{fp}})$" & 12. "$\Delta^{-}(\lambda_{\mathrm{fp}})$" ... uncertainty range on the spot latitudes in degrees

Sat.	Hem.	Obs ID	Date	Time	φ_{Sat}	φ_{fp}	λ_{fp}	$\Delta^{+}(\varphi_{\mathrm{fp}})$	$\Delta^{-}(\varphi_{\mathrm{fp}})$	$\Delta^{+}(\lambda_{\mathrm{fp}})$	$\Delta^{-}(\lambda_{\mathrm{fp}})$
Eu	N	j93e03bvq	2005/04/18	11:13:55	64.582	129.952	69.218	132.240	128.042	70.928	67.662
Eu	N	j93e03bwq	2005/04/18	11:17:05	66.277	130.184	68.725	132.243	128.437	70.383	67.208
Eu	N	j93e03c1q	2005/04/18	11:28:30	72.391	131.435	65.545	132.778	130.226	66.937	64.240
Eu	N	j93e03c4q	2005/04/18	11:33:10	74.889	132.672	64.433	133.866	131.583	65.752	63.189
Eu	N	j93e03c5q	2005/04/18	11:35:30	76.139	133.081	64.040	134.208	132.046	65.336	62.816
Eu	N	j93e03c6q	2005/04/18	11:37:50	77.388	133.702	63.639	134.775	132.711	64.911	62.434
Eu	N	j93e03c7q	2005/04/18	11:40:10	78.638	134.150	63.034	135.159	133.214	64.273	61.858
Eu	N	j93e03caq	2005/04/18	11:46:05	81.806	135.568	62.119	136.464	134.640	63.312	60.983
Eu	N	j93e03cbq	2005/04/18	11:49:15	83.501	135.935	61.617	136.829	134.962	62.786	60.501
Eu	N	j93e03ccq	2005/04/18	11:52:25	85.197	136.499	61.320	137.431	135.482	62.476	60.216
Eu	N	j93e04e7q	2005/04/25	11:41:30	63.217	125.709	71.957	129.200	122.981	74.214	70.006
Eu	N	j93e04e8q	2005/04/25	11:44:40	64.913	126.625	70.099	129.427	124.308	72.062	68.345
Eu	N	j93ea4eaq	2005/04/25	12:39:52	94.470	139.794	58.644	140.607	138.952	59.766	57.565
Eu	N	j93ea4ebq	2005/04/25	12:43:02	96.165	140.108	58.572	140.938	139.210	59.692	57.495
Eu	N	j93ea4edq	2005/04/25	12:46:12	97.861	140.958	57.853	141.799	140.050	58.945	56.801
Eu	N	j93ea4eeq	2005/04/25	12:49:22	99.557	141.604	57.911	142.487	140.649	59.007	56.855
Eu	N	j93ea4efq	2005/04/25	12:52:07	101.029	142.690	57.482	143.576	141.732	58.562	56.441
Eu	N	j93ea4egq	2005/04/25	12:54:27	102.278	142.764	57.029	143.676	141.779	58.094	56.003
Eu	N	j93ea4ehq	2005/04/25	12:56:47	103.528	143.595	56.792	144.517	142.601	57.848	55.772
Eu	N	j93ea4eiq	2005/04/25	12:59:07	104.777	144.147	56.439	145.082	143.140	57.483	55.431
Eu	N	j93ea4ekq	2005/04/25	13:03:47	107.276	144.766	56.008	145.751	143.704	57.040	55.011
Eu	N	j93ea4elq	2005/04/25	13:06:07	108.525	145.669	55.609	146.654	144.609	56.628	54.624
Eu	N	j93ea4emq	2005/04/25	13:08:27	109.775	145.893	55.501	146.909	144.798	56.517	54.518
Eu	N	j93ea4enq	2005/04/25	13:11:12	111.247	146.528	54.888	147.550	145.429	55.886	53.922
Eu	N	j93ea4eoq	2005/04/25	13:14:22	112.943	146.945	54.843	148.010	145.798	55.841	53.877
Eu	N	j93ea4epq	2005/04/25	13:17:32	114.638	147.743	54.576	148.830	146.571	55.567	53.616
Eu	N	j93ea4eqq	2005/04/25	13:20:22	116.155	148.344	54.312	149.454	147.148	55.296	53.359
Eu	N	j9du01cuq	2006/02/07	10:19:43	133.198	154.592	51.802	155.335	153.821	52.370	51.244
Eu	N	j9du01cvq	2006/02/07	10:22:08	134.488	155.072	51.791	155.831	154.282	52.357	51.233

Table B.1: Auroral footprints' main Alfvén wing (MAW) spot locations for Europa and Ganymede observed on the Northern and Southern Jovian hemispheres as published as supporting information to Bonfond et al. (2017b). (*continued*)

Sat.	Hem.	Obs ID	Date	Time	φ_{Sat}	φ_{fp}	λ_{fp}	$\Delta^{+}(\varphi_{\mathrm{fp}})$	$\Delta^{-}(\varphi_{\mathrm{fp}})$	$\Delta^{+}(\lambda_{\mathrm{fp}})$	$\Delta^{-}(\lambda_{\mathrm{fp}})$
Eu	N	j9du01cwq	2006/02/07	10:24:33	135.778	155.445	51.966	156.229	154.629	52.536	51.406
Eu	N	j9du01cxq	2006/02/07	10:26:58	137.068	156.114	51.586	156.902	155.295	52.148	51.032
Eu	N	j9du01cyq	2006/02/07	10:29:23	138.358	156.685	51.393	157.483	155.854	51.953	50.843
Eu	N	j9du01czq	2006/02/07	10:31:48	139.648	157.422	51.204	158.229	156.584	51.760	50.656
Eu	N	j9du01d0q	2006/02/07	10:34:13	140.938	157.883	51.198	158.708	157.024	51.754	50.651
Eu	N	j9rlb1idq	2007/02/21	15:43:30	219.511	189.876	56.283	191.445	188.421	56.970	55.614
Eu	N	j9rlb2mdq	2007/02/22	10:33:00	102.004	140.835	56.634	141.989	139.749	57.332	55.954
Eu	N	j9rlb2mfq	2007/02/22	10:37:40	104.491	141.766	55.919	142.827	140.765	56.597	55.256
Eu	N	j9rlb2miq	2007/02/22	10:42:20	106.978	143.066	55.646	144.072	142.113	56.317	54.991
Eu	N	j9rlb2mmq	2007/02/22	10:51:58	112.111	145.115	54.880	145.995	144.276	55.529	54.244
Eu	N	j9rlb2mnq	2007/02/22	10:54:18	113.355	145.506	54.639	146.354	144.697	55.282	54.008
Eu	N	j9rlb2moq	2007/02/22	10:56:38	114.598	146.186	54.612	147.017	145.392	55.254	53.982
Eu	N	j9rlb2mrq	2007/02/22	11:03:38	118.329	147.675	53.914	148.428	146.954	54.540	53.300
Eu	N	j9rlb2mvq	2007/02/22	11:13:16	123.463	149.653	53.006	150.310	149.019	53.612	52.411
Eu	N	j9rlb2mwq	2007/02/22	11:15:36	124.706	150.053	52.976	150.693	149.436	53.581	52.382
Eu	N	j9rlb6a1q	2007/02/26	15:17:37	89.934	138.991	60.083	140.414	137.440	60.877	59.315
Eu	N	j9rlb6a2q	2007/02/26	15:19:57	91.179	139.202	59.911	140.659	137.614	60.702	59.145
Eu	N	j9rlb6a3q	2007/02/26	15:22:17	92.424	139.919	59.485	141.370	138.339	60.264	58.730
Eu	N	j9rlb6a6q	2007/02/26	15:26:57	94.914	141.379	58.432	142.804	139.833	59.184	57.703
Eu	N	j9rlb6a7q	2007/02/26	15:29:35	96.319	141.806	58.056	143.249	140.242	58.800	57.335
Eu	N	j9rlb6a8q	2007/02/26	15:31:55	97.564	142.534	57.661	143.974	140.974	58.395	56.948
Eu	N	j9rlb6a9q	2007/02/26	15:34:15	98.809	142.514	57.524	144.000	140.901	58.259	56.812
Eu	N	j9rlb6aaq	2007/02/26	15:36:35	100.054	143.269	56.928	144.738	141.678	57.648	56.229
Eu	N	j9rlb6abq	2007/02/26	15:38:55	101.299	143.975	56.758	145.459	142.366	57.475	56.062
Eu	N	j9rlb6acq	2007/02/26	15:41:15	102.544	143.900	56.840	145.452	142.212	57.563	56.139
Eu	N	j9rlb6adq	2007/02/26	15:43:35	103.789	144.377	56.480	145.942	142.677	57.196	55.785
Eu	N	j9rlb6aeq	2007/02/26	15:45:55	105.034	144.851	56.125	146.428	143.135	56.835	55.436
Eu	N	j9rlb6afq	2007/02/26	15:48:15	106.279	145.830	55.747	147.397	144.127	56.449	55.066
Eu	N	j9rlb6agq	2007/02/26	15:50:53	107.685	146.696	55.589	148.283	144.971	56.288	54.910
Eu	N	j9rlb6ahq	2007/02/26	15:53:13	108.930	146.639	55.277	148.269	144.864	55.973	54.601
Eu	N	j9rlb6aiq	2007/02/26	15:55:33	110.175	147.614	54.912	149.235	145.850	55.600	54.243
Eu	N	j9rlb6ajq	2007/02/26	15:57:53	111.420	148.585	54.551	150.199	146.831	55.232	53.888
Eu	N	j9rlb6akq	2007/02/26	16:00:13	112.665	148.722	54.432	150.387	146.907	55.115	53.769
Eu	N	j9rli5nyq	2007/03/02	08:48:44	79.016	136.072	63.100	138.285	133.541	64.025	62.220
Eu	N	j9rli5o8q	2007/03/02	09:00:24	85.246	138.757	61.379	141.021	136.173	62.252	60.545
Eu	N	j9rlc3afq	2007/03/05	05:38:33	125.860	150.871	52.711	151.355	150.374	53.289	52.142
Eu	N	j9rlc3agq	2007/03/05	05:40:53	127.103	151.021	52.557	151.520	150.507	53.133	51.990
Eu	N	j9rlc3akq	2007/03/05	05:48:11	130.994	152.776	52.260	153.308	152.228	52.833	51.697
Eu	N	j9rlc3alq	2007/03/05	05:50:31	132.237	153.237	52.288	153.782	152.674	52.862	51.724
Eu	N	j9rlc3amq	2007/03/05	05:52:51	133.481	153.595	51.953	154.150	153.022	52.522	51.394
Eu	N	j9rlc3anq	2007/03/05	05:55:11	134.725	154.406	51.790	154.967	153.827	52.357	51.233
Eu	N	j9rlc3asq	2007/03/05	06:06:51	140.943	156.673	51.411	157.298	156.028	51.974	50.856
Eu	N	j9rlc3atq	2007/03/05	06:09:29	142.346	157.466	51.439	158.103	156.807	52.004	50.884
Eu	N	j9rlc3auq	2007/03/05	06:11:49	143.590	157.972	51.294	158.619	157.301	51.857	50.740
Eu	N	j9rlc3avq	2007/03/05	06:14:09	144.833	158.416	51.330	159.079	157.728	51.895	50.775
Eu	N	j9rlc3awq	2007/03/05	06:16:29	146.077	159.016	51.361	159.693	158.313	51.927	50.805
Eu	N	j9rlc3axq	2007/03/05	06:18:49	147.321	159.519	51.219	160.208	158.804	51.783	50.665
Eu	N	j9rlj6t5q	2007/03/09	09:11:34	75.851	134.220	64.181	135.930	132.304	65.097	63.306
Eu	N	j9rlj6tbq	2007/03/09	09:18:34	79.588	135.719	62.514	137.388	133.868	63.369	61.694
Eu	N	j9rlj6tcq	2007/03/09	09:19:44	80.211	136.163	62.528	137.846	134.295	63.384	61.706
Eu	N	j9rlj6tiq	2007/03/09	09:26:44	83.949	137.585	61.459	139.294	135.692	62.283	60.666
Eu	N	j9rli7toq	2007/03/09	10:25:38	115.404	152.022	53.682	154.171	149.596	54.365	53.024
Eu	N	j9rli7tqq	2007/03/09	10:27:58	116.650	152.296	53.393	154.503	149.792	54.075	52.737
Eu	N	j9rli7tsq	2007/03/09	10:30:18	117.896	152.317	53.475	154.648	149.642	54.168	52.811
Eu	N	j9rli7tuq	2007/03/09	10:32:38	119.142	152.877	53.172	155.250	150.143	53.864	52.511
Eu	N	j9rli7twq	2007/03/09	10:34:58	120.388	153.670	53.034	156.083	150.876	53.726	52.372
Eu	N	j9rli7txq	2007/03/09	10:36:08	121.012	154.120	52.875	156.540	151.318	53.565	52.215
Eu	N	j9rli7tyq	2007/03/09	10:37:18	121.635	154.568	52.717	156.993	151.756	53.405	52.059
Eu	N	j9rle1cgq	2007/05/22	19:54:06	101.157	143.605	56.708	144.693	142.454	57.246	56.182
Eu	N	j9rle1chq	2007/05/22	19:55:16	101.781	143.985	56.534	145.073	142.835	57.068	56.010
Eu	N	j9rle1ciq	2007/05/22	19:56:26	102.405	144.714	56.359	145.792	143.574	56.890	55.838
Eu	N	j9rle1cjq	2007/05/22	19:57:36	103.029	144.921	56.187	146.004	143.776	56.716	55.669
Eu	N	j9rle1ckq	2007/05/22	19:58:46	103.653	144.953	56.018	146.047	143.797	56.545	55.502
Eu	N	j9rle1clq	2007/05/22	19:59:56	104.277	144.358	56.371	145.509	143.137	56.907	55.847
Eu	N	j9rle1cmq	2007/05/22	20:01:06	104.901	145.160	55.853	146.280	143.975	56.379	55.338
Eu	N	j9rle1cnq	2007/05/22	20:02:16	105.525	145.332	55.857	146.468	144.129	56.384	55.341
Eu	N	j9rle1coq	2007/05/22	20:03:26	106.149	145.534	55.690	146.676	144.324	56.215	55.176
Eu	N	j9rle1cpq	2007/05/22	20:04:36	106.773	146.272	55.520	147.404	145.073	56.042	55.009
Eu	N	j9rle1cqq	2007/05/22	20:05:46	107.397	146.474	55.355	147.613	145.268	55.875	54.846
Eu	N	j9rle1ctq	2007/05/22	20:09:16	109.269	147.254	54.867	148.408	146.033	55.381	54.363
Eu	N	j9rle1d0q	2007/05/22	20:22:18	116.240	150.501	53.469	151.730	149.197	53.969	52.980
Eu	N	j9rle1d2q	2007/05/22	20:24:38	117.488	150.811	53.329	152.070	149.471	53.829	52.840
Eu	N	j9rle1d3q	2007/05/22	20:25:48	118.112	151.129	53.336	152.403	149.772	53.837	52.846
Eu	N	j9rle1d4q	2007/05/22	20:26:58	118.736	150.851	53.354	152.163	149.451	53.857	52.861
Eu	N	j9rle1d5q	2007/05/22	20:28:08	119.360	151.609	53.195	152.910	150.223	53.696	52.705
Eu	N	j9rle1d6q	2007/05/22	20:29:18	119.985	151.517	53.211	152.849	150.094	53.713	52.719
Eu	N	j9rle1d7q	2007/05/22	20:30:28	120.609	151.875	53.061	153.212	150.447	53.562	52.571
Eu	N	j9rle1d8q	2007/05/22	20:31:38	121.233	152.232	52.912	153.574	150.798	53.412	52.423
Eu	N	j9rle1daq	2007/05/22	20:33:58	122.481	152.469	52.782	153.851	150.988	53.282	52.292
Eu	S	o5hye3zpq	1999/08/08	13:40:18	126.717	96.729	-66.969	98.626	94.802	-64.501	-69.806
Eu	S	o5g2a3caq	1999/08/15	14:26:02	135.708	99.583	-67.481	101.666	97.534	-64.991	-70.362
Eu	S	o5g2a3cbq	1999/08/15	14:31:54	138.849	104.151	-68.260	106.330	102.012	-65.666	-71.304
Eu	S	o5g2a3cfq	1999/08/15	14:42:46	144.667	107.630	-70.567	110.018	105.287	-67.659	-74.164
Eu	S	o6ba04bqq	2000/12/18	10:05:04	17.096	19.446	-64.444	20.788	18.006	-62.705	-66.335
Eu	S	o6ba01odq	2000/12/28	08:53:50	109.907	81.132	-63.649	84.752	77.982	-61.814	-65.667

Table B.1: Auroral footprints' main Alfvén wing (MAW) spot locations for Europa and Ganymede observed on the Northern and Southern Jovian hemispheres as published as supporting information to Bonfond et al. (2017b). (*continued*)

Sat.	Hem.	Obs ID	Date	Time	φ_{Sat}	φ_{fp}	λ_{fp}	$\Delta^{+}(\varphi_{\mathrm{fp}})$	$\Delta^{-}(\varphi_{\mathrm{fp}})$	$\Delta^{+}(\lambda_{\mathrm{fp}})$	$\Delta^{-}(\lambda_{\mathrm{fp}})$
Eu	S	o6ba01ofq	2000/12/28	08:59:02	112.690	83.381	-64.148	87.028	80.215	-62.276	-66.214
Eu	S	o6ba01ogq	2000/12/28	09:01:04	113.778	84.455	-64.354	88.136	81.264	-62.466	-66.442
Eu	S	o6ba01oiq	2000/12/28	09:06:16	116.561	86.284	-64.761	89.928	83.121	-62.842	-66.887
Eu	S	o6ba01ojq	2000/12/28	09:08:18	117.649	87.357	-64.973	91.039	84.169	-63.037	-67.123
Eu	S	o6ba01olq	2000/12/28	09:15:58	121.752	91.118	-65.950	94.981	87.806	-63.925	-68.226
Eu	S	o6ba01olq	2000/12/28	09:17:28	122.554	91.484	-65.983	95.296	88.208	-63.956	-68.259
Eu	S	o6ba01onq	2000/12/28	09:27:02	127.674	94.402	-66.737	98.112	91.209	-64.652	-69.093
Eu	S	j9rle4baq	2007/05/21	20:10:20	61.133	47.720	-62.317	48.455	47.013	-61.776	-62.867
Eu	S	j9rle4bbq	2007/05/21	20:12:40	62.377	50.065	-62.076	50.810	49.349	-61.539	-62.622
Eu	S	j9rle4bcq	2007/05/21	20:15:00	63.620	51.216	-62.269	51.962	50.499	-61.729	-62.818
Eu	S	j9rle4beq	2007/05/21	20:19:40	66.107	53.293	-62.147	54.021	52.592	-61.609	-62.694
Eu	S	j9rle4bfq	2007/05/21	20:22:00	67.351	53.800	-62.036	54.508	53.118	-61.500	-62.581
Eu	S	j9rle4bgq	2007/05/21	20:24:20	68.595	53.873	-62.128	54.559	53.212	-61.591	-62.674
Eu	S	j9rle4bjq	2007/05/21	20:31:38	72.485	57.164	-62.377	57.837	56.515	-61.836	-62.927
Eu	S	j9rle4bkq	2007/05/21	20:33:58	73.729	58.068	-62.411	58.732	57.427	-61.870	-62.962
Ga	N	j93e03bvq	2005/04/18	11:13:55	158.601	163.376	53.683	167.295	160.061	55.097	52.329
Ga	N	j93e03bwq	2005/04/18	11:17:05	160.404	164.161	53.705	167.946	160.940	55.120	52.351
Ga	N	j93e03bxq	2005/04/18	11:20:15	162.208	164.969	53.729	168.630	161.837	55.144	52.375
Ga	N	j93e03byq	2005/04/18	11:23:25	164.011	165.618	53.760	169.147	162.582	55.175	52.405
Ga	N	j93e03c0q	2005/04/18	11:26:10	165.577	166.615	53.952	170.109	163.607	55.376	52.589
Ga	N	j93e03c1q	2005/04/18	11:28:30	166.906	167.101	53.802	170.475	164.180	55.219	52.446
Ga	N	j93e03c2q	2005/04/18	11:30:50	168.235	167.473	53.832	170.752	164.623	55.250	52.475
Ga	N	j93e03c4q	2005/04/18	11:33:10	169.564	168.233	54.027	171.484	165.407	55.453	52.662
Ga	N	j93e03c5q	2005/04/18	11:35:30	170.893	168.794	54.054	171.972	166.023	55.481	52.689
Ga	N	j93e03c6q	2005/04/18	11:37:50	172.221	169.030	54.094	172.112	166.333	55.522	52.727
Ga	N	j93e03c7q	2005/04/18	11:40:10	173.550	169.613	54.123	172.630	166.966	55.553	52.755
Ga	N	j93e03c8q	2005/04/18	11:42:55	175.116	170.113	53.992	173.018	167.553	55.415	52.629
Ga	N	j93e03caq	2005/04/18	11:46:05	176.920	171.074	54.204	173.935	168.549	55.637	52.833
Ga	N	j93e03cbq	2005/04/18	11:49:15	178.723	171.869	54.250	174.653	169.406	55.685	52.877
Ga	N	j93e03ccq	2005/04/18	11:52:25	180.527	172.523	54.480	175.246	170.109	55.926	53.098
Ga	N	j93ea3cdq	2005/04/18	12:44:26	210.150	185.447	56.840	186.133	184.786	57.419	56.271
Ga	N	j93ea3ceq	2005/04/18	12:47:36	211.953	186.169	56.927	186.836	185.525	57.508	56.356
Ga	N	j93ea3cgq	2005/04/18	12:50:46	213.757	186.890	57.016	187.539	186.263	57.599	56.443
Ga	N	j93ea3chq	2005/04/18	12:53:56	215.560	187.727	57.473	188.369	187.107	58.066	56.891
Ga	N	j93ea3ciq	2005/04/18	12:56:41	217.126	188.539	57.728	189.173	187.927	58.327	57.141
Ga	N	j93ea3cjq	2005/04/18	12:59:01	218.455	188.885	57.811	189.503	188.289	58.412	57.223
Ga	N	j93ea3ckq	2005/04/18	13:01:21	219.784	189.489	57.686	190.090	188.908	58.285	57.100
Ga	N	j93ea3clq	2005/04/18	13:03:41	221.113	190.030	57.946	190.622	189.457	58.550	57.354
Ga	N	j93ea3cmq	2005/04/18	13:06:01	222.442	190.523	58.020	191.101	189.963	58.627	57.426
Ga	N	j93ea3cnq	2005/04/18	13:08:21	223.770	191.199	58.272	191.770	190.646	58.884	57.673
Ga	N	j93ea3coq	2005/04/18	13:10:41	225.099	191.836	58.336	192.396	191.295	58.950	57.735
Ga	N	j93ea3cpq	2005/04/18	13:13:01	226.428	192.678	58.770	193.237	192.138	59.394	58.160
Ga	N	j93ea3cqq	2005/04/18	13:15:46	227.994	193.533	58.644	194.076	193.008	59.266	58.037
Ga	N	j93ea3crq	2005/04/18	13:18:56	229.798	194.220	59.139	194.751	193.707	59.772	58.520
Ga	N	j93ea3csq	2005/04/18	13:22:06	231.601	195.016	59.236	195.529	194.519	59.872	58.614
Ga	N	j93ea3ctq	2005/04/18	13:24:56	233.215	195.763	59.125	196.258	195.279	59.759	58.505
Ga	N	j93ea4eaq	2005/04/25	12:39:52	188.939	176.845	55.083	179.728	174.283	56.683	53.561
Ga	N	j93ea4ebq	2005/04/25	12:43:02	190.742	177.728	55.236	180.558	175.210	56.844	53.708
Ga	N	j93ea4edq	2005/04/25	12:46:12	192.546	178.470	55.414	181.240	175.999	57.031	53.878
Ga	N	j93ea4eeq	2005/04/25	12:49:22	194.349	179.071	55.618	181.779	176.652	57.245	54.072
Ga	N	j93ea4efq	2005/04/25	12:52:07	195.915	179.694	55.580	182.329	177.334	57.205	54.036
Ga	N	j93ea4egq	2005/04/25	12:54:27	197.244	180.383	55.695	182.986	178.049	57.327	54.146
Ga	N	j93ea4ehq	2005/04/25	12:56:47	198.573	180.785	55.858	183.344	178.487	57.498	54.301
Ga	N	j93ea4eiq	2005/04/25	12:59:07	199.901	181.632	56.153	184.191	179.336	57.810	54.581
Ga	N	j93ea4ejq	2005/04/25	13:01:27	201.230	181.880	56.142	184.367	179.643	57.799	54.571
Ga	N	j93ea4ekq	2005/04/25	13:03:47	202.559	182.716	56.238	185.180	180.499	57.900	54.663
Ga	N	j93ea4elq	2005/04/25	13:06:07	203.888	183.120	56.408	185.545	180.937	58.080	54.824
Ga	N	j93ea4emq	2005/04/25	13:08:27	205.216	183.668	56.555	186.059	181.514	58.236	54.964
Ga	N	j93ea4enq	2005/04/25	13:11:12	206.782	184.047	56.574	186.368	181.950	58.255	54.981
Ga	N	j93ea4eoq	2005/04/25	13:14:22	208.586	184.957	56.749	187.241	182.892	58.441	55.147
Ga	N	j93ea4epq	2005/04/25	13:17:32	210.389	185.865	56.926	188.113	183.831	58.630	55.315
Ga	N	j93ea4eqq	2005/04/25	13:20:22	212.003	186.542	57.315	188.774	184.525	59.042	55.683
Ga	N	j9du01cjq	2006/02/07	09:55:33	154.321	163.199	53.496	163.751	162.666	54.109	52.895
Ga	N	j9du01ckq	2006/02/07	09:57:58	155.698	163.503	53.255	164.032	162.990	53.862	52.658
Ga	N	j9du01clq	2006/02/07	10:00:23	157.075	163.994	53.410	164.510	163.494	54.020	52.812
Ga	N	j9du01cmq	2006/02/07	10:02:48	158.452	164.641	53.379	165.143	164.152	53.987	52.781
Ga	N	j9du01coq	2006/02/07	10:05:13	159.829	165.451	53.354	165.943	164.954	53.962	52.757
Ga	N	j9du01cpq	2006/02/07	10:07:38	161.205	166.100	53.324	166.594	165.592	53.930	52.728
Ga	N	j9du01cqq	2006/02/07	10:10:03	162.582	166.579	53.483	167.088	166.054	54.093	52.886
Ga	N	j9du01crq	2006/02/07	10:12:28	163.959	167.064	53.449	167.586	166.525	54.057	52.853
Ga	N	j9du01csq	2006/02/07	10:14:53	165.336	167.712	53.422	168.246	167.162	54.029	52.826
Ga	N	j9du01ctq	2006/02/07	10:17:18	166.713	168.198	53.390	168.745	167.634	53.996	52.795
Ga	N	j9du01cuq	2006/02/07	10:19:43	168.090	168.821	53.559	169.383	168.241	54.168	52.962
Ga	N	j9du01cvq	2006/02/07	10:22:08	169.467	169.303	53.529	169.878	168.708	54.137	52.933
Ga	N	j9du01cwq	2006/02/07	10:24:33	170.843	169.948	53.505	170.535	169.340	54.112	52.910
Ga	N	j9du01cxq	2006/02/07	10:26:58	172.220	170.716	53.683	171.317	170.094	54.292	53.084
Ga	N	j9du01cyq	2006/02/07	10:29:23	173.597	171.356	53.660	171.970	170.722	54.269	53.062
Ga	N	j9du01czq	2006/02/07	10:31:48	174.974	171.782	53.831	172.415	171.126	54.443	53.231
Ga	N	j9du01d0q	2006/02/07	10:34:13	176.351	172.416	53.810	173.061	171.746	54.421	53.210
Ga	N	j9du02f3q	2006/02/28	22:21:08	165.191	167.595	53.399	168.123	167.075	54.081	52.732
Ga	N	j9du02f4q	2006/02/28	22:23:33	166.568	168.252	53.287	168.772	167.741	53.967	52.622
Ga	N	j9du02f5q	2006/02/28	22:25:58	167.945	168.775	53.401	169.288	168.270	54.084	52.733
Ga	N	j9du02f6q	2006/02/28	22:28:23	169.322	169.290	53.517	169.796	168.792	54.202	52.845
Ga	N	j9du02f8q	2006/02/28	22:30:48	170.699	169.956	53.584	170.456	169.464	54.271	52.911
Ga	N	j9du02f9q	2006/02/28	22:33:13	172.076	170.296	53.574	170.786	169.813	54.261	52.901

Table B.1: Auroral footprints' main Alfvén wing (MAW) spot locations for Europa and Ganymede observed on the Northern and Southern Jovian hemispheres as published as supporting information to Bonfond et al. (2017b). (*continued*)

Sat.	Hem.	Obs ID	Date	Time	φ_{Sat}	φ_{fp}	λ_{fp}	$\Delta^{+}(\varphi_{\mathrm{fp}})$	$\Delta^{-}(\varphi_{\mathrm{fp}})$	$\Delta^{+}(\lambda_{\mathrm{fp}})$	$\Delta^{-}(\lambda_{\mathrm{fp}})$
Ga	N	j9du02faq	2006/02/28	22:35:38	173.452	171.115	53.594	171.600	170.620	54.282	52.920
Ga	N	j9du02fbq	2006/02/28	22:38:03	174.829	171.606	53.714	172.099	171.090	54.406	53.037
Ga	N	j9du02fcq	2006/02/28	22:40:28	176.206	172.426	53.557	172.928	171.901	54.246	52.883
Ga	N	j9du02fdq	2006/02/28	22:42:53	177.583	173.074	53.629	173.592	172.531	54.320	52.953
Ga	N	j9du02feq	2006/02/28	22:45:18	178.960	173.532	53.931	174.075	172.962	54.630	53.248
Ga	N	j9du02ffq	2006/02/28	22:47:43	180.337	174.012	53.878	174.572	173.423	54.575	53.195
Ga	N	j9du02fgq	2006/02/28	22:50:08	181.713	174.317	53.876	174.900	173.704	54.575	53.193
Ga	N	j9du02fhq	2006/02/28	22:52:33	183.090	175.111	53.901	175.708	174.483	54.601	53.217
Ga	N	j9du02fiq	2006/02/28	22:54:58	184.467	175.691	54.159	176.312	175.036	54.865	53.469
Ga	N	j9du02fjq	2006/02/28	22:57:23	185.844	176.652	54.134	177.283	175.988	54.840	53.443
Ga	N	j9du02fkq	2006/02/28	22:59:48	187.221	177.069	54.266	177.725	176.377	54.976	53.572
Ga	N	j9du02flq	2006/02/28	23:02:13	188.598	177.610	54.529	178.293	176.887	55.246	53.829
Ga	N	j9du03b3q	2006/03/27	09:02:45	258.040	207.026	62.581	210.282	204.290	63.464	61.754
Ga	N	j9du03b4q	2006/03/27	09:05:10	259.416	210.112	63.574	213.918	207.017	64.521	62.698
Ga	N	j9du03b5q	2006/03/27	09:07:35	260.793	209.687	63.444	213.149	206.814	64.365	62.585
Ga	N	j9du03b6q	2006/03/27	09:10:00	262.169	208.764	63.058	211.805	206.180	63.941	62.227
Ga	N	j9du03b8q	2006/03/27	09:12:25	263.545	211.059	63.790	214.403	208.268	64.714	62.926
Ga	N	j9du03b9q	2006/03/27	09:14:50	264.922	211.761	63.967	215.052	209.005	64.894	63.100
Ga	N	j9du03baq	2006/03/27	09:17:15	266.298	212.470	64.147	215.715	209.748	65.077	63.277
Ga	N	j9du03bbq	2006/03/27	09:19:40	267.675	213.188	64.330	216.390	210.497	65.263	63.456
Ga	N	j9du03bcq	2006/03/27	09:22:05	269.051	213.913	64.516	217.075	211.251	65.453	63.638
Ga	N	j9du03bdq	2006/03/27	09:24:30	270.428	215.276	64.987	218.561	212.532	65.949	64.090
Ga	N	j9du03beq	2006/03/27	09:26:55	271.804	216.351	65.204	219.650	213.598	66.174	64.299
Ga	N	j9du03bfq	2006/03/27	09:29:20	273.181	216.407	65.355	219.577	213.746	66.323	64.451
Ga	N	j9du03bgq	2006/03/27	09:31:45	274.557	217.152	65.555	220.294	214.512	66.529	64.645
Ga	N	j9du03bhq	2006/03/27	09:34:10	275.933	218.876	66.077	222.206	216.109	67.083	65.142
Ga	N	j9du03biq	2006/03/27	09:36:35	277.310	218.059	65.672	221.009	215.560	66.639	64.766
Ga	N	j9du03bjq	2006/03/27	09:39:00	278.686	218.820	65.879	221.750	216.337	66.853	64.967
Ga	N	j9du03bkq	2006/03/27	09:41:25	280.063	219.848	66.367	222.864	217.307	67.366	65.434
Ga	N	j9du03blq	2006/03/27	09:43:50	281.439	220.934	66.604	223.977	218.378	67.615	65.662
Ga	N	j9du04ewq	2006/04/14	03:55:46	87.956	141.551	63.934	144.460	137.955	66.083	61.979
Ga	N	j9du04exq	2006/04/14	03:58:10	89.323	142.078	63.383	144.977	138.520	65.474	61.472
Ga	N	j9du04eyq	2006/04/14	04:00:36	90.710	142.432	63.082	145.373	138.826	65.143	61.195
Ga	N	j9du04ezq	2006/04/14	04:03:00	92.077	142.774	62.787	145.758	139.120	64.819	60.922
Ga	N	j9du04f1q	2006/04/14	04:05:26	93.463	142.765	62.482	145.820	139.023	64.485	60.640
Ga	N	j9du04f2q	2006/04/14	04:07:50	94.830	143.579	61.744	146.570	139.951	63.681	59.955
Ga	N	j9du04f3q	2006/04/14	04:10:16	96.217	144.196	61.249	147.179	140.596	63.143	59.494
Ga	N	j9du04f4q	2006/04/14	04:12:40	97.584	144.619	60.759	147.607	141.024	62.612	59.035
Ga	N	j9du04f5q	2006/04/14	04:15:06	98.970	145.255	60.285	148.237	141.680	62.102	58.592
Ga	N	j9du04f6q	2006/04/14	04:17:30	100.337	145.468	60.026	148.507	141.822	61.823	58.348
Ga	N	j9du04f7q	2006/04/14	04:19:56	101.724	146.117	59.568	149.152	142.488	61.332	57.919
Ga	N	j9du04f8q	2006/04/14	04:22:20	103.091	146.751	59.120	149.783	143.135	60.852	57.496
Ga	N	j9du04f9q	2006/04/14	04:24:46	104.477	146.940	59.086	150.067	143.192	60.816	57.464
Ga	N	j9du04faq	2006/04/14	04:27:10	105.844	147.765	58.652	150.876	144.048	60.353	57.055
Ga	N	j9du04fbq	2006/04/14	04:29:36	107.231	148.002	58.418	151.177	144.201	60.103	56.833
Ga	N	j9du04fcq	2006/04/14	04:32:00	108.598	148.647	57.993	151.823	144.852	59.652	56.431
Ga	N	j9du04fdq	2006/04/14	04:34:26	109.984	149.251	57.775	152.465	145.406	59.420	56.224
Ga	N	j9du04feq	2006/04/14	04:36:50	111.351	149.897	57.362	153.115	146.053	58.982	55.833
Ga	N	j9rlb1i3q	2007/02/21	15:22:12	162.177	165.263	53.564	166.282	164.294	54.178	52.962
Ga	N	j9rlb1i4q	2007/02/21	15:24:32	163.506	165.738	53.561	166.733	164.790	54.174	52.960
Ga	N	j9rlb1i5q	2007/02/21	15:26:52	164.836	166.591	53.559	167.572	165.656	54.172	52.959
Ga	N	j9rlb1i8q	2007/02/21	15:31:32	167.494	167.755	53.558	168.697	166.856	54.169	52.958
Ga	N	j9rlb1i9q	2007/02/21	15:34:10	168.995	167.827	53.762	168.742	166.953	54.377	53.158
Ga	N	j9rlb1iaq	2007/02/21	15:36:30	170.324	168.402	53.562	169.290	167.552	54.173	52.961
Ga	N	j9rlb1ibq	2007/02/21	15:38:50	171.653	168.843	53.767	169.718	168.006	54.383	53.163
Ga	N	j9rlb1icq	2007/02/21	15:41:10	172.983	169.716	53.769	170.580	168.890	54.385	53.165
Ga	N	j9rlb1idq	2007/02/21	15:43:30	174.312	170.058	53.775	170.899	169.252	54.391	53.170
Ga	N	j9rlb1ieq	2007/02/21	15:45:50	175.641	170.675	53.983	171.507	169.879	54.604	53.374
Ga	N	j9rlb1ifq	2007/02/21	15:48:10	176.971	171.376	53.988	172.193	170.593	54.609	53.379
Ga	N	j9rlb1igq	2007/02/21	15:50:30	178.300	171.812	54.201	172.616	171.041	54.826	53.588
Ga	N	j9rlb1ihq	2007/02/21	15:52:50	179.630	172.435	54.003	173.217	171.684	54.625	53.393
Ga	N	j9rlb1iiq	2007/02/21	15:55:28	181.130	173.754	54.210	174.537	173.003	54.836	53.596
Ga	N	j9rlb1ijq	2007/02/21	15:57:48	182.459	174.285	54.219	175.051	173.550	54.845	53.605
Ga	N	j9rlb1ikq	2007/02/21	16:00:08	183.789	174.819	54.229	175.569	174.100	54.856	53.614
Ga	N	j9rlb1ilq	2007/02/21	16:02:28	185.118	175.247	54.447	175.983	174.539	55.079	53.828
Ga	N	j9rlb1imq	2007/02/21	16:04:48	186.447	175.782	54.459	176.502	175.089	55.091	53.840
Ga	N	j9rlb2mdq	2007/02/22	10:33:00	97.873	142.819	60.767	144.362	141.405	61.592	59.970
Ga	N	j9rlb2meq	2007/02/22	10:35:20	99.203	143.259	60.722	144.755	141.886	61.544	59.928
Ga	N	j9rlb2mfq	2007/02/22	10:37:40	100.533	143.725	60.432	145.156	142.408	61.243	59.649
Ga	N	j9rlb2mgq	2007/02/22	10:40:00	101.862	144.245	59.906	145.599	142.994	60.699	59.139
Ga	N	j9rlb2miq	2007/02/22	10:42:20	103.192	144.550	59.618	145.840	143.353	60.400	58.861
Ga	N	j9rlb2mlq	2007/02/22	10:49:38	107.351	146.104	58.559	147.229	145.051	59.306	57.833
Ga	N	j9rlb2mmq	2007/02/22	10:51:58	108.681	146.460	58.516	147.550	145.438	59.260	57.792
Ga	N	j9rlb2mnq	2007/02/22	10:54:18	110.010	146.827	58.475	147.883	145.835	59.216	57.753
Ga	N	j9rlb2moq	2007/02/22	10:56:38	111.340	147.080	58.200	148.088	146.131	58.933	57.487
Ga	N	j9rlb2mpq	2007/02/22	10:58:58	112.669	147.271	58.155	148.242	146.355	58.885	57.444
Ga	N	j9rlb2mqq	2007/02/22	11:01:18	113.999	147.970	57.901	148.911	147.081	58.623	57.197
Ga	N	j9rlb2mrq	2007/02/22	11:03:38	115.329	148.486	57.642	149.392	147.629	58.358	56.945
Ga	N	j9rlb2msq	2007/02/22	11:06:16	116.829	149.028	56.938	149.881	148.219	57.635	56.258
Ga	N	j9rlb2mtq	2007/02/22	11:08:36	118.159	149.594	56.690	150.417	148.811	57.380	56.016
Ga	N	j9rlb2muq	2007/02/22	11:10:56	119.488	149.988	56.439	150.779	149.233	57.122	55.772
Ga	N	j9rlb2mvq	2007/02/22	11:13:16	120.818	150.400	56.191	151.162	149.673	56.868	55.530
Ga	N	j9rlb2mwq	2007/02/22	11:15:36	122.147	151.014	55.951	151.751	150.309	56.622	55.296
Ga	N	j9rlb3pyq	2007/02/23	08:56:43	143.541	160.464	53.598	162.129	158.645	54.302	52.913
Ga	N	j9rlb3pzq	2007/02/23	08:59:03	144.871	161.321	53.467	163.003	159.481	54.170	52.784
Ga	N	j9rlb3q0q	2007/02/23	09:01:23	146.200	161.883	53.362	163.600	160.002	54.066	52.679
Ga	N	j9rlb3q1q	2007/02/23	09:03:43	147.530	162.114	53.465	163.902	160.145	54.175	52.777

Table B.1: Auroral footprints' main Alfvén wing (MAW) spot locations for Europa and Ganymede observed on the Northern and Southern Jovian hemispheres as published as supporting information to Bonfond et al. (2017b). (*continued*)

Sat.	Hem.	Obs ID	Date	Time	φ_{Sat}	φ_{fp}	λ_{fp}	$\Delta^{+}(\varphi_{\mathrm{fp}})$	$\Delta^{-}(\varphi_{\mathrm{fp}})$	$\Delta^{+}(\lambda_{\mathrm{fp}})$	$\Delta^{-}(\lambda_{\mathrm{fp}})$
Ga	N	j9rlb3q3q	2007/02/23	09:06:03	148.860	163.249	53.311	165.039	161.277	54.018	52.625
Ga	N	j9rlb3q4q	2007/02/23	09:08:41	150.360	163.585	53.597	168.266	157.391	55.577	51.785
Ga	N	j9rlb3q5q	2007/02/23	09:11:01	151.690	164.081	53.498	168.869	157.686	55.484	51.684
Ga	N	j9rlb3q6q	2007/02/23	09:13:21	153.019	164.846	53.553	169.739	158.247	55.552	51.732
Ga	N	j9rlb3q7q	2007/02/23	09:15:41	154.349	165.308	53.456	170.322	158.469	55.464	51.633
Ga	N	j9rlb3q8q	2007/02/23	09:18:01	155.678	166.043	53.513	171.174	158.961	55.537	51.681
Ga	N	j9rlb3q9q	2007/02/23	09:20:21	157.008	166.054	53.630	171.441	158.413	55.691	51.780
Ga	N	j9rlb3qaq	2007/02/23	09:22:41	158.337	166.369	53.721	171.969	158.226	55.814	51.856
Ga	N	j9rlb3qbq	2007/02/23	09:25:01	159.667	167.168	53.419	172.804	158.925	55.502	51.565
Ga	N	j9rlb3qcq	2007/02/23	09:27:21	160.996	168.270	53.269	173.925	159.971	55.348	51.421
Ga	N	j9rlg7cpq	2007/02/27	10:29:40	237.324	195.955	59.811	198.790	193.482	60.620	59.029
Ga	N	j9rlg7crq	2007/02/27	10:32:00	238.653	197.061	60.088	199.916	194.572	60.906	59.298
Ga	N	j9rlg7csq	2007/02/27	10:34:20	239.982	197.875	60.375	200.723	195.393	61.202	59.577
Ga	N	j9rlg7ctq	2007/02/27	10:36:40	241.311	198.991	60.659	201.863	196.490	61.496	59.852
Ga	N	j9rlg7cvq	2007/02/27	10:39:00	242.640	199.234	60.686	201.993	196.819	61.522	59.880
Ga	N	j9rlg7cwq	2007/02/27	10:41:38	244.140	199.394	61.006	202.076	197.038	61.851	60.191
Ga	N	j9rlg7cxq	2007/02/27	10:43:58	245.469	200.233	61.308	202.917	197.875	62.163	60.484
Ga	N	j9rlg7cyq	2007/02/27	10:46:18	246.798	200.806	61.333	203.420	198.503	62.187	60.509
Ga	N	j9rlg7czq	2007/02/27	10:48:38	248.127	201.927	61.631	204.569	199.603	62.497	60.797
Ga	N	j9rlg7d0q	2007/02/27	10:50:58	249.456	202.499	61.952	205.125	200.188	62.829	61.108
Ga	N	j9rlg7d1q	2007/02/27	10:53:18	250.785	203.626	62.259	206.285	201.292	63.147	61.404
Ga	N	j9rlg7d2q	2007/02/27	10:55:38	252.114	204.212	62.288	206.804	201.929	63.177	61.433
Ga	N	j9rlg7d3q	2007/02/27	10:57:58	253.443	205.067	62.610	207.671	202.776	63.511	61.745
Ga	N	j9rlg7d4q	2007/02/27	11:00:18	254.772	205.663	62.642	208.205	203.421	63.543	61.776
Ga	N	j9rlg7d5q	2007/02/27	11:02:56	256.272	206.717	62.663	209.219	204.506	63.564	61.797
Ga	N	j9rlg7d6q	2007/02/27	11:05:16	257.601	207.574	62.992	210.091	205.353	63.907	62.114
Ga	N	j9rlg7d7q	2007/02/27	11:07:36	258.930	207.432	62.754	209.789	205.337	63.656	61.886
Ga	N	j9rlg7d8q	2007/02/27	11:09:56	260.259	208.545	63.074	210.934	206.427	63.989	62.195
Ga	N	j9rlg7d9q	2007/02/27	11:12:16	261.588	209.400	63.411	211.805	207.271	64.341	62.520
Ga	N	j9rlb8geq	2007/02/28	05:39:03	172.025	168.837	53.904	170.740	167.096	54.559	53.267
Ga	N	j9rlb8gfq	2007/02/28	05:40:13	172.690	169.018	53.889	170.886	167.305	54.542	53.254
Ga	N	j9rlb8ggq	2007/02/28	05:41:23	173.354	169.204	53.874	171.040	167.518	54.526	53.241
Ga	N	j9rlb8ghq	2007/02/28	05:42:33	174.019	169.652	53.867	171.472	167.980	54.517	53.235
Ga	N	j9rlb8giq	2007/02/28	05:43:43	174.683	169.848	53.853	171.637	168.201	54.502	53.222
Ga	N	j9rlb8gjq	2007/02/28	05:44:53	175.348	169.800	53.833	171.545	168.189	54.479	53.204
Ga	N	j9rlb8gkq	2007/02/28	05:46:03	176.013	170.316	54.026	172.069	168.700	54.676	53.394
Ga	N	j9rlb8glq	2007/02/28	05:47:13	176.677	170.772	54.020	172.511	169.169	54.668	53.388
Ga	N	j9rlb8gmq	2007/02/28	05:48:23	177.342	170.739	54.001	172.437	169.170	54.647	53.372
Ga	N	j9rlb8gnq	2007/02/28	05:49:33	178.006	171.256	54.196	172.960	169.681	54.845	53.563
Ga	N	j9rlb8goq	2007/02/28	05:50:43	178.671	171.422	53.983	173.081	169.886	54.626	53.356
Ga	N	j9rlb8gpq	2007/02/28	05:51:53	179.336	172.179	54.183	173.857	170.626	54.831	53.552
Ga	N	j9rlb8gqq	2007/02/28	05:53:03	180.000	172.163	54.166	173.804	170.642	54.812	53.537
Ga	N	j9rlb8grq	2007/02/28	05:54:13	180.665	172.157	54.149	173.762	170.667	54.793	53.522
Ga	N	j9rlb8gsq	2007/02/28	05:55:23	181.329	172.394	54.139	173.976	170.923	54.781	53.512
Ga	N	j9rlb8gtq	2007/02/28	05:56:33	181.994	173.141	54.340	174.742	171.656	54.987	53.710
Ga	N	j9rlb8gvq	2007/02/28	06:03:45	186.096	174.551	54.480	176.032	173.169	55.123	53.853
Ga	N	j9rlb8gwq	2007/02/28	06:04:55	186.760	175.061	54.679	176.549	173.674	55.326	54.049
Ga	N	j9rlb8gxq	2007/02/28	06:06:05	187.425	175.604	55.086	177.115	174.197	55.742	54.448
Ga	N	j9rlb8gyq	2007/02/28	06:07:15	188.090	175.859	55.078	177.350	174.469	55.732	54.440
Ga	N	j9rlb8gzq	2007/02/28	06:08:25	188.754	176.340	55.074	177.821	174.958	55.727	54.436
Ga	N	j9rlb8h0q	2007/02/28	06:09:35	189.419	176.157	55.058	177.601	174.808	55.709	54.423
Ga	N	j9rlb8h1q	2007/02/28	06:10:45	190.083	176.204	55.047	177.621	174.879	55.696	54.413
Ga	N	j9rlb8h2q	2007/02/28	06:11:55	190.748	176.909	55.046	178.326	175.584	55.696	54.413
Ga	N	j9rlb8h3q	2007/02/28	06:13:05	191.413	177.416	55.250	178.840	176.085	55.904	54.612
Ga	N	j9rlb8h4q	2007/02/28	06:14:15	192.077	177.252	55.236	178.641	175.951	55.888	54.600
Ga	N	j9rlb8h5q	2007/02/28	06:15:25	192.742	177.312	55.227	178.677	176.034	55.877	54.592
Ga	N	j9rlb8h6q	2007/02/28	06:16:35	193.406	177.816	55.432	179.187	176.532	56.086	54.794
Ga	N	j9rlb8h7q	2007/02/28	06:17:45	194.071	178.768	55.856	180.178	177.451	56.521	55.209
Ga	N	j9rlb8h8q	2007/02/28	06:18:55	194.736	178.373	55.420	179.712	177.118	56.072	54.783
Ga	N	j9rlb8h9q	2007/02/28	06:20:05	195.400	178.445	55.411	179.761	177.210	56.063	54.776
Ga	N	j9rlb8haq	2007/02/28	06:21:15	196.065	179.360	55.414	180.684	178.119	56.065	54.778
Ga	N	j9rlc0neq	2007/03/02	07:15:39	68.005	138.915	71.508	141.540	136.763	72.929	70.211
Ga	N	j9rlc0nfq	2007/03/02	07:17:59	69.334	139.702	71.544	142.278	137.590	72.969	70.245
Ga	N	j9rlc0ngq	2007/03/02	07:20:19	70.664	139.960	70.720	142.227	138.056	72.062	69.484
Ga	N	j9rlc0niq	2007/03/02	07:22:39	71.993	140.068	69.956	142.079	138.347	71.230	68.774
Ga	N	j9rlc0njq	2007/03/02	07:25:17	73.494	140.215	69.642	142.069	138.613	70.890	68.480
Ga	N	j9rlc0nkq	2007/03/02	07:27:37	74.823	140.023	68.584	141.625	138.611	69.753	67.487
Ga	N	j9rlc0nlq	2007/03/02	07:29:57	76.153	139.954	67.948	141.400	138.665	69.075	66.886
Ga	N	j9rlc0nmq	2007/03/02	07:32:17	77.483	140.237	67.319	141.564	139.042	68.406	66.290
Ga	N	j9rlc0nnq	2007/03/02	07:34:37	78.812	140.345	66.728	141.561	139.241	67.781	65.727
Ga	N	j9rlc0noq	2007/03/02	07:36:57	80.142	140.401	66.491	141.539	139.361	67.532	65.501
Ga	N	j9rlc0npq	2007/03/02	07:39:17	81.471	140.392	65.944	141.436	139.431	66.957	64.979
Ga	N	j9rlc0nqq	2007/03/02	07:41:37	82.801	140.526	65.721	141.507	139.619	66.723	64.765
Ga	N	j9rlc0nrq	2007/03/02	07:43:57	84.130	140.570	64.899	141.461	139.739	65.862	63.978
Ga	N	j9rlc0nsq	2007/03/02	07:46:35	85.631	141.149	64.381	141.985	140.367	65.321	63.479
Ga	N	j9rlc0ntq	2007/03/02	07:48:55	86.960	141.557	63.594	142.333	140.825	64.501	62.721
Ga	N	j9rlc0nuq	2007/03/02	07:51:15	88.290	141.843	63.398	142.579	141.147	64.298	62.533
Ga	N	j9rlc0nvq	2007/03/02	07:53:35	89.619	142.137	62.933	142.829	141.480	63.815	62.083
Ga	N	j9rlc0nwq	2007/03/02	07:55:55	90.949	142.466	62.477	143.117	141.796	63.343	61.642
Ga	N	j9rli5nyq	2007/03/02	08:48:44	121.043	151.420	55.875	152.422	150.359	56.545	55.220
Ga	N	j9rli5nzq	2007/03/02	08:49:54	121.708	151.927	55.884	152.934	150.860	56.555	55.229
Ga	N	j9rli5o0q	2007/03/02	08:51:04	122.373	152.381	55.691	153.387	151.317	56.358	55.040
Ga	N	j9rli5o1q	2007/03/02	08:52:14	123.038	152.290	55.729	153.318	151.201	56.397	55.076
Ga	N	j9rli5o2q	2007/03/02	08:53:24	123.702	152.748	55.537	153.773	151.662	56.202	54.888
Ga	N	j9rli5o3q	2007/03/02	08:54:34	124.367	152.852	55.566	153.895	151.747	56.232	54.915
Ga	N	j9rli5o4q	2007/03/02	08:55:44	125.032	153.112	55.385	154.158	152.003	56.048	54.738
Ga	N	j9rli5o5q	2007/03/02	08:56:54	125.697	153.212	55.414	154.276	152.084	56.079	54.766

Table B.1: Auroral footprints' main Alfvén wing (MAW) spot locations for Europa and Ganymede observed on the Northern and Southern Jovian hemispheres as published as supporting information to Bonfond et al. (2017b). (*continued*)

Sat.	Hem.	Obs ID	Date	Time	φ_{Sat}	φ_{fp}	λ_{fp}	$\Delta^{+}(\varphi_{\mathrm{fp}})$	$\Delta^{-}(\varphi_{\mathrm{fp}})$	$\Delta^{+}(\lambda_{\mathrm{fp}})$	$\Delta^{-}(\lambda_{\mathrm{fp}})$
Ga	N	j9rli5o6q	2007/03/02	08:58:04	126.361	153.472	55.235	154.540	152.341	55.896	54.590
Ga	N	j9rli5o7q	2007/03/02	08:59:14	127.026	153.568	55.265	154.653	152.416	55.928	54.618
Ga	N	j9rli5o8q	2007/03/02	09:00:24	127.691	153.658	55.295	154.762	152.485	55.959	54.647
Ga	N	j9rli5o9q	2007/03/02	09:01:34	128.356	154.091	54.911	155.184	152.932	55.567	54.270
Ga	N	j9rli5oaq	2007/03/02	09:02:44	129.020	154.592	54.921	155.691	153.426	55.578	54.280
Ga	N	j9rli5obq	2007/03/02	09:03:54	129.685	154.855	54.746	155.958	153.685	55.400	54.108
Ga	N	j9rli5ocq	2007/03/02	09:05:04	130.350	154.943	54.777	156.065	153.751	55.432	54.137
Ga	N	j9rli5odq	2007/03/02	09:06:14	131.015	155.619	54.582	156.732	154.438	55.234	53.946
Ga	N	j9rli5ofq	2007/03/02	09:13:26	135.117	156.160	54.778	157.399	154.839	55.439	54.132
Ga	N	j9rlc1qmq	2007/03/03	04:05:51	60.320	138.229	76.153	141.350	133.271	78.388	74.340
Ga	N	j9rlc1qnq	2007/03/03	04:08:11	61.649	138.516	75.684	141.625	133.738	77.805	73.935
Ga	N	j9rlc1qoq	2007/03/03	04:10:31	62.978	139.295	75.202	142.327	134.788	77.215	73.515
Ga	N	j9rlc1qpq	2007/03/03	04:12:51	64.308	139.900	74.266	142.746	135.896	76.098	72.690
Ga	N	j9rlc1qrq	2007/03/03	04:15:11	65.637	139.848	73.902	142.749	135.816	75.680	72.362
Ga	N	j9rlc1qsq	2007/03/03	04:17:49	67.137	138.363	74.133	141.675	133.613	75.975	72.556
Ga	N	j9rlc1qtq	2007/03/03	04:20:09	68.467	139.158	73.278	142.269	134.884	74.981	71.790
Ga	N	j9rlc1qvq	2007/03/03	04:22:29	69.796	139.924	72.476	142.872	136.003	74.069	71.064
Ga	N	j9rlc1qwq	2007/03/03	04:24:49	71.125	140.671	71.719	143.484	137.023	73.222	70.371
Ga	N	j9rlc1r1q	2007/03/03	04:34:09	76.443	140.603	68.269	143.135	137.543	69.480	67.146
Ga	N	j9rlc1r3q	2007/03/03	04:36:29	77.772	140.196	68.405	142.899	136.894	69.636	67.267
Ga	N	j9rlc1r4q	2007/03/03	04:39:07	79.272	142.284	67.128	144.702	139.411	68.266	66.065
Ga	N	j9rlc1r5q	2007/03/03	04:41:27	80.601	142.021	66.081	144.378	139.252	67.161	65.066
Ga	N	j9rlc1r7q	2007/03/03	04:43:47	81.931	142.429	65.591	144.775	139.684	66.648	64.596
Ga	N	j9rlc1r8q	2007/03/03	04:46:07	83.260	142.671	64.857	144.980	139.987	65.879	63.891
Ga	N	j9rlc1r9q	2007/03/03	04:48:27	84.589	142.576	64.701	144.965	139.791	65.721	63.737
Ga	N	j9rlc5klq	2007/03/07	06:04:00	168.304	166.602	53.786	169.197	164.323	54.466	53.134
Ga	N	j9rlc5kmq	2007/03/07	06:05:10	168.969	166.652	53.762	169.171	164.428	54.437	53.113
Ga	N	j9rlc5knq	2007/03/07	06:06:20	169.634	167.034	53.749	169.518	164.837	54.423	53.102
Ga	N	j9rlc5koq	2007/03/07	06:07:30	170.298	167.104	53.726	169.520	164.957	54.395	53.082
Ga	N	j9rlc5kpq	2007/03/07	06:08:40	170.963	167.496	53.715	169.880	165.373	54.382	53.072
Ga	N	j9rlc5kqq	2007/03/07	06:09:50	171.627	167.706	53.889	170.067	165.602	54.557	53.244
Ga	N	j9rlc5krq	2007/03/07	06:11:00	172.292	168.104	53.877	170.435	166.023	54.544	53.234
Ga	N	j9rlc5ksq	2007/03/07	06:12:10	172.957	167.907	53.846	170.153	165.890	54.508	53.206
Ga	N	j9rlc5ktq	2007/03/07	06:13:20	173.621	168.727	54.042	171.008	166.684	54.709	53.399
Ga	N	j9rlc5kuq	2007/03/07	06:14:30	174.286	168.838	54.022	171.066	166.837	54.685	53.381
Ga	N	j9rlc5kvq	2007/03/07	06:15:40	174.950	169.250	54.012	171.452	167.268	54.674	53.372
Ga	N	j9rlc5kwq	2007/03/07	06:16:50	175.615	169.664	54.002	171.841	167.702	54.662	53.363
Ga	N	j9rlj6t4q	2007/03/09	09:10:24	115.422	149.278	57.087	150.049	148.467	57.757	56.431
Ga	N	j9rlj6t5q	2007/03/09	09:11:34	116.087	149.696	56.886	150.467	148.885	57.553	56.235
Ga	N	j9rlj6t6q	2007/03/09	09:12:44	116.751	150.034	56.900	150.813	149.214	57.567	56.248
Ga	N	j9rlj6t7q	2007/03/09	09:13:54	117.416	150.186	56.920	150.978	149.353	57.588	56.268
Ga	N	j9rlj6t8q	2007/03/09	09:15:04	118.081	150.425	56.729	151.221	149.589	57.393	56.080
Ga	N	j9rlj6t9q	2007/03/09	09:16:14	118.746	150.851	56.531	151.647	150.015	57.191	55.886
Ga	N	j9rlj6taq	2007/03/09	09:17:24	119.410	150.821	56.560	151.633	149.966	57.221	55.913
Ga	N	j9rlj6tbq	2007/03/09	09:18:34	120.075	150.786	56.588	151.615	149.913	57.251	55.941
Ga	N	j9rlj6tcq	2007/03/09	09:19:44	120.740	151.034	56.400	151.867	150.157	57.059	55.756
Ga	N	j9rlj6tdq	2007/03/09	09:20:54	121.405	151.183	56.422	152.029	150.292	57.082	55.777
Ga	N	j9rlj6teq	2007/03/09	09:22:04	122.069	151.538	56.027	152.378	150.654	56.679	55.390
Ga	N	j9rlj6tfq	2007/03/09	09:23:14	122.734	151.874	56.042	152.723	150.981	56.694	55.405
Ga	N	j9rlj6tgq	2007/03/09	09:24:24	123.399	152.315	55.850	153.163	151.423	56.499	55.216
Ga	N	j9rlj6thq	2007/03/09	09:25:34	124.064	152.466	55.873	153.327	151.560	56.522	55.238
Ga	N	j9rlj6tiq	2007/03/09	09:26:44	124.728	152.986	55.881	153.851	152.075	56.530	55.245
Ga	N	j9rli7tkq	2007/03/09	10:20:58	155.630	164.888	53.250	166.207	163.479	53.876	52.638
Ga	N	j9rli7tlq	2007/03/09	10:22:08	156.295	165.369	53.262	166.696	163.949	53.889	52.649
Ga	N	j9rli7tmq	2007/03/09	10:23:18	156.960	165.621	53.286	166.966	164.181	53.915	52.673
Ga	N	j9rli7tnq	2007/03/09	10:24:28	157.624	165.868	53.311	167.232	164.407	53.941	52.696
Ga	N	j9rli7toq	2007/03/09	10:25:38	158.289	166.344	53.324	167.717	164.872	53.954	52.708
Ga	N	j9rli7tpq	2007/03/09	10:26:48	158.954	166.351	53.362	167.753	164.846	53.995	52.744
Ga	N	j9rli7tqq	2007/03/09	10:27:58	159.619	166.602	53.205	168.012	165.088	53.836	52.589
Ga	N	j9rli7trq	2007/03/09	10:29:08	160.283	166.816	53.414	168.258	165.263	54.050	52.793
Ga	N	j9rli7tsq	2007/03/09	10:30:18	160.948	167.302	53.244	168.742	165.752	53.878	52.626
Ga	N	j9rli7ttq	2007/03/09	10:31:28	161.613	167.527	53.271	168.989	165.953	53.906	52.651
Ga	N	j9rli7tuq	2007/03/09	10:32:38	162.278	167.747	53.297	169.231	166.147	53.934	52.676
Ga	N	j9rli7tvq	2007/03/09	10:33:48	162.942	167.962	53.325	169.468	166.335	53.964	52.702
Ga	N	j9rli7twq	2007/03/09	10:34:58	163.607	168.171	53.352	169.701	166.517	53.993	52.728
Ga	N	j9rli7txq	2007/03/09	10:36:08	164.272	168.626	53.366	170.168	166.958	54.008	52.741
Ga	N	j9rli7tyq	2007/03/09	10:37:18	164.937	168.827	53.395	170.394	167.129	54.038	52.768
Ga	N	j9rli7tzq	2007/03/09	10:38:28	165.601	169.021	53.423	170.614	167.293	54.069	52.795
Ga	N	j9rli7u1q	2007/03/09	10:45:40	169.704	171.043	53.374	172.747	169.182	54.026	52.741
Ga	N	j9rli9ltq	2007/03/17	05:30:05	72.382	140.797	72.558	142.598	138.561	73.984	71.269
Ga	N	j9rli9lvq	2007/03/17	05:31:45	73.331	141.150	72.148	142.940	138.951	73.531	70.892
Ga	N	j9rlk9mcq	2007/03/17	05:55:09	86.663	141.818	64.629	143.452	139.991	65.535	63.764
Ga	N	j9rlk9mdq	2007/03/17	05:56:49	87.613	141.522	64.679	143.224	139.613	65.590	63.809
Ga	N	j9rlk9meq	2007/03/17	05:58:29	88.562	142.148	64.153	143.813	140.289	65.042	63.302
Ga	N	j9rlk9mfq	2007/03/17	06:00:09	89.512	142.188	63.925	143.875	140.305	64.807	63.081
Ga	N	j9rlk9mgq	2007/03/17	06:01:49	90.461	142.491	63.690	144.187	140.598	64.564	62.853
Ga	N	j9rlk9mhq	2007/03/17	06:03:29	91.411	142.535	63.469	144.255	140.617	64.337	62.638
Ga	N	j9rlk9miq	2007/03/17	06:05:09	92.360	142.924	62.983	144.623	141.035	63.833	62.167
Ga	N	j9rlk9mjq	2007/03/17	06:06:49	93.310	142.530	63.295	144.331	140.515	64.161	62.465
Ga	N	j9rli8gsq	2007/03/22	22:50:44	86.394	138.665	66.042	141.825	135.977	67.050	65.088
Ga	N	j9rli8gtq	2007/03/22	22:52:24	87.343	138.730	65.749	141.714	136.169	66.739	64.810
Ga	N	j9rli8gvq	2007/03/22	22:54:04	88.293	139.736	65.749	142.720	137.175	66.738	64.809
Ga	N	j9rli8gxq	2007/03/22	22:55:44	89.242	138.687	64.871	141.283	136.413	65.812	63.973
Ga	N	j9rli8gzq	2007/03/22	22:57:24	90.192	139.693	64.871	142.289	137.419	65.812	63.972
Ga	N	j9rli8h1q	2007/03/22	22:59:04	91.142	140.194	64.902	142.754	137.949	65.844	64.003
Ga	N	j9rli8h3q	2007/03/22	23:00:44	92.091	139.432	64.378	141.758	137.367	65.293	63.502
Ga	N	j9rli8h5q	2007/03/22	23:02:24	93.041	140.200	64.082	142.459	138.187	64.983	63.217

Table B.1: Auroral footprints' main Alfvén wing (MAW) spot locations for Europa and Ganymede observed on the Northern and Southern Jovian hemispheres as published as supporting information to Bonfond et al. (2017b). (*continued*)

Sat.	Hem.	Obs ID	Date	Time	φ_{Sat}	φ_{fp}	λ_{fp}	$\Delta^{+}(\varphi_{\mathrm{fp}})$	$\Delta^{-}(\varphi_{\mathrm{fp}})$	$\Delta^{+}(\lambda_{\mathrm{fp}})$	$\Delta^{-}(\lambda_{\mathrm{fp}})$
Ga	N	j9rli8h7q	2007/03/22	23:04:04	93.991	140.493	64.130	142.711	138.514	65.033	63.264
Ga	N	j9rlk8hiq	2007/03/22	23:22:26	104.456	144.360	59.961	145.743	143.070	60.710	59.234
Ga	N	j9rlk8hjq	2007/03/22	23:24:06	105.405	144.398	60.040	145.751	143.134	60.791	59.311
Ga	N	j9rlk8hoq	2007/03/22	23:32:26	110.153	146.411	58.366	147.556	145.330	59.070	57.680
Ga	N	j9rlk8hpq	2007/03/22	23:34:06	111.103	146.697	58.429	147.824	145.631	59.135	57.741
Ga	N	j9rld0htq	2007/05/11	15:23:05	165.284	166.330	53.232	166.878	165.795	53.746	52.727
Ga	N	j9rld0huq	2007/05/11	15:25:25	166.613	166.811	53.311	167.349	166.286	53.826	52.804
Ga	N	j9rld0hvq	2007/05/11	15:27:45	167.943	167.383	53.221	167.909	166.870	53.735	52.716
Ga	N	j9rld0hwq	2007/05/11	15:30:05	169.272	167.998	53.291	168.516	167.493	53.806	52.784
Ga	N	j9rld0hyq	2007/05/11	15:32:25	170.601	168.612	53.361	169.121	168.116	53.877	52.852
Ga	N	j9rld0i0q	2007/05/11	15:37:23	173.431	169.401	53.885	169.891	168.923	54.411	53.368
Ga	N	j9rld0i1q	2007/05/11	15:39:43	174.760	170.113	53.785	170.594	169.645	54.309	53.270
Ga	N	j9rld0i2q	2007/05/11	15:42:03	176.090	170.581	53.872	171.051	170.121	54.398	53.355
Ga	N	j9rld0i3q	2007/05/11	15:44:23	177.419	171.044	53.960	171.505	170.595	54.488	53.441
Ga	N	j9rld0i5q	2007/05/11	15:49:03	180.078	172.224	53.952	172.665	171.792	54.480	53.432
Ga	N	j9rld0i6q	2007/05/11	15:51:23	181.407	172.691	54.368	173.126	172.266	54.904	53.842
Ga	N	j9rld0i9q	2007/05/11	15:58:41	185.566	174.897	54.091	175.315	174.467	54.623	53.568
Ga	N	j9rld0iaq	2007/05/11	16:01:01	186.896	175.472	54.335	175.904	175.027	54.872	53.808
Ga	N	j9rld0ibq	2007/05/11	16:03:21	188.225	175.906	54.431	176.353	175.445	54.970	53.902
Ga	N	j9rld1nfq	2007/05/12	21:45:06	123.345	151.171	55.852	152.049	150.246	56.425	55.290
Ga	N	j9rld1ngq	2007/05/12	21:47:26	124.675	151.623	55.619	152.514	150.685	56.189	55.060
Ga	N	j9rld1nhq	2007/05/12	21:49:46	126.004	152.117	55.544	153.026	151.158	56.114	54.985
Ga	N	j9rld1niq	2007/05/12	21:52:06	127.333	152.567	55.315	153.490	151.594	55.882	54.760
Ga	N	j9rld1nkq	2007/05/12	21:54:26	128.663	153.194	55.073	154.126	152.212	55.637	54.521
Ga	N	j9rld1nlq	2007/05/12	21:57:04	130.163	153.317	55.053	154.285	152.296	55.617	54.499
Ga	N	j9rld1nmq	2007/05/12	21:59:24	131.492	153.940	54.815	154.918	152.909	55.376	54.265
Ga	N	j9rld1nnq	2007/05/12	22:01:44	132.822	154.563	54.580	155.550	153.521	55.138	54.032
Ga	N	j9rld1noq	2007/05/12	22:04:04	134.151	154.840	54.531	155.855	153.767	55.090	53.983
Ga	N	j9rld1npq	2007/05/12	22:06:24	135.480	155.269	54.317	156.301	154.178	54.873	53.771
Ga	N	j9rld1nqq	2007/05/12	22:08:44	136.810	155.903	54.237	156.953	154.793	54.793	53.692
Ga	N	j9rld1nrq	2007/05/12	22:11:04	138.139	156.339	54.175	157.414	155.201	54.732	53.630
Ga	N	j9rld1nsq	2007/05/12	22:13:24	139.468	156.763	54.115	157.864	155.596	54.672	53.569
Ga	N	j9rld1ntq	2007/05/12	22:16:02	140.969	157.739	53.873	158.846	156.566	54.427	53.330
Ga	N	j9rld1nuq	2007/05/12	22:18:22	142.298	158.335	53.652	159.455	157.147	54.203	53.111
Ga	N	j9rld1nvq	2007/05/12	22:20:42	143.627	159.137	53.559	160.271	157.933	54.110	53.020
Ga	N	j9rld1nwq	2007/05/12	22:23:02	144.957	159.529	53.505	160.693	158.292	54.057	52.964
Ga	N	j9rld1nxq	2007/05/12	22:25:22	146.286	160.113	53.433	161.301	158.850	53.985	52.893
Ga	N	j9rld2oeq	2007/05/13	17:29:06	77.865	141.454	70.493	144.031	138.320	71.584	69.485
Ga	N	j9rld2ofq	2007/05/13	17:31:26	79.194	141.069	70.217	143.727	137.832	71.296	69.219
Ga	N	j9rld6bpq	2007/05/17	20:01:34	205.324	182.703	55.639	183.773	181.686	56.172	55.115
Ga	N	j9rld6bqq	2007/05/17	20:03:54	206.653	183.488	56.008	184.559	182.470	56.548	55.478
Ga	N	j9rld6brq	2007/05/17	20:06:14	207.982	184.254	56.203	185.318	183.244	56.746	55.669
Ga	N	j9rld6bsq	2007/05/17	20:08:34	209.311	184.680	56.227	185.718	183.693	56.771	55.693
Ga	N	j9rld6buq	2007/05/17	20:10:54	210.641	185.116	56.253	186.129	184.152	56.797	55.718
Ga	N	j9rld6bvq	2007/05/17	20:13:32	212.141	185.587	56.646	186.590	184.632	57.198	56.104
Ga	N	j9rld6bwq	2007/05/17	20:15:52	213.470	186.354	56.848	187.351	185.406	57.403	56.302
Ga	N	j9rld6bxq	2007/05/17	20:18:12	214.799	186.961	56.872	187.938	186.031	57.428	56.326
Ga	N	j9rld6byq	2007/05/17	20:20:32	216.128	187.568	57.081	188.534	186.647	57.641	56.532
Ga	N	j9rld6bzq	2007/05/17	20:22:52	217.457	188.181	57.107	189.130	187.277	57.668	56.557
Ga	N	j9rld6c1q	2007/05/17	20:27:32	220.115	189.232	57.541	190.157	188.350	58.110	56.983
Ga	N	j9rld6c2q	2007/05/17	20:29:52	221.445	189.991	57.753	190.910	189.115	58.327	57.191
Ga	N	j9rld6c3q	2007/05/17	20:32:30	222.945	190.950	57.777	191.855	190.087	58.351	57.214
Ga	N	j9rld6c4q	2007/05/17	20:34:50	224.274	191.547	57.997	192.443	190.693	58.576	57.430
Ga	N	j9rld6c5q	2007/05/17	20:37:10	225.603	192.169	58.029	193.048	191.331	58.608	57.461
Ga	N	j9rld6c6q	2007/05/17	20:39:30	226.932	192.794	58.061	193.657	191.971	58.641	57.492
Ga	N	j9rld6c7q	2007/05/17	20:41:50	228.261	193.508	58.473	194.372	192.684	59.062	57.896
Ga	N	j9rld7cgq	2007/05/18	17:02:39	203.730	182.223	55.788	183.616	180.689	57.267	54.378
Ga	N	j9rld7chq	2007/05/18	17:04:59	205.059	182.903	55.840	184.327	181.330	57.324	54.428
Ga	N	j9rld7ciq	2007/05/18	17:07:19	206.388	183.682	56.054	185.143	182.065	57.549	54.631
Ga	N	j9rld7cjq	2007/05/18	17:09:39	207.718	184.499	56.097	185.987	182.850	57.596	54.671
Ga	N	j9rld7ckq	2007/05/18	17:11:59	209.047	185.264	56.313	186.791	183.565	57.824	54.876
Ga	N	j9rld7clq	2007/05/18	17:14:19	210.376	185.866	56.542	187.442	184.108	58.067	55.094
Ga	N	j9rld7cmq	2007/05/18	17:16:39	211.706	186.514	56.599	188.127	184.711	58.129	55.147
Ga	N	j9rld7cnq	2007/05/18	17:19:17	213.206	187.492	56.645	188.129	186.828	57.210	56.090
Ga	N	j9rld7coq	2007/05/18	17:21:37	214.535	188.063	56.879	188.722	187.375	57.449	56.319
Ga	N	j9rld7cpq	2007/05/18	17:23:57	215.864	188.776	57.103	189.454	188.067	57.679	56.539
Ga	N	j9rld7cqq	2007/05/18	17:26:17	217.194	189.395	57.163	190.090	188.668	57.741	56.598
Ga	N	j9rld7crq	2007/05/18	17:28:37	218.523	190.086	57.391	190.802	189.335	57.974	56.821
Ga	N	j9rle6elq	2007/05/27	18:26:18	73.844	138.893	74.087	140.733	136.641	75.941	72.482
Ga	N	j9rle6emq	2007/05/27	18:28:38	75.174	140.076	72.774	141.740	138.275	74.422	71.307
Ga	N	j9rle6enq	2007/05/27	18:30:58	76.503	140.249	72.734	141.955	138.328	74.381	71.270
Ga	N	j9rle6eoq	2007/05/27	18:33:18	77.832	140.923	72.022	142.566	139.143	73.578	70.623
Ga	N	j9rle6epq	2007/05/27	18:35:38	79.161	141.529	71.026	143.086	139.864	72.470	69.708
Ga	N	j9rle6eqq	2007/05/27	18:37:58	80.491	142.087	69.943	143.559	140.522	71.284	68.705
Ga	N	j9rle6erq	2007/05/27	18:40:18	81.820	142.318	69.623	143.797	140.747	70.939	68.406
Ga	N	j9rle6esq	2007/05/27	18:42:56	83.320	142.063	68.743	143.516	140.523	69.990	67.580
Ga	N	j9rlf0k9q	2007/05/31	11:42:32	244.395	200.900	60.689	202.863	199.133	61.411	59.993
Ga	N	j9rlf0kaq	2007/05/31	11:44:52	245.724	201.634	60.961	203.589	199.874	61.689	60.259
Ga	N	j9rlf0kbq	2007/05/31	11:47:12	247.053	202.301	61.055	204.221	200.570	61.784	60.352
Ga	N	j9rlf0kcq	2007/05/31	11:49:32	248.382	202.710	61.122	204.576	201.023	61.849	60.420
Ga	N	j9rlf0keq	2007/05/31	11:51:52	249.711	203.717	61.429	205.598	202.019	62.165	60.720
Ga	N	j9rlf0kfq	2007/05/31	11:54:30	251.211	204.116	61.655	205.955	202.454	62.395	60.942
Ga	N	j9rlf0kgq	2007/05/31	11:56:50	252.539	205.123	61.971	206.980	203.449	62.720	61.250
Ga	N	j9rlf0khq	2007/05/31	11:59:10	253.868	205.551	62.045	207.359	203.917	62.794	61.323
Ga	N	j9rlf0kiq	2007/05/31	12:01:30	255.197	206.245	62.148	208.025	204.634	62.899	61.426
Ga	N	j9rlf0kjq	2007/05/31	12:03:50	256.526	206.942	62.253	208.695	205.355	63.005	61.529
Ga	N	j9rlf0kkq	2007/05/31	12:06:10	257.855	207.689	62.551	209.443	206.103	63.311	61.819

Table B.1: Auroral footprints' main Alfvén wing (MAW) spot locations for Europa and Ganymede observed on the Northern and Southern Jovian hemispheres as published as supporting information to Bonfond et al. (2017b). (*continued*)

Sat.	Hem.	Obs ID	Date	Time	φ_{Sat}	φ_{fp}	λ_{fp}	$\Delta^{+}(\varphi_{\mathrm{fp}})$	$\Delta^{-}(\varphi_{\mathrm{fp}})$	$\Delta^{+}(\lambda_{\mathrm{fp}})$	$\Delta^{-}(\lambda_{\mathrm{fp}})$
Ga	N	j9rlf0klq	2007/05/31	12:08:30	259.184	208.690	62.881	210.463	207.090	63.651	62.140
Ga	N	j9rlf0kmq	2007/05/31	12:10:50	260.513	209.135	62.963	210.865	207.572	63.733	62.221
Ga	N	j9rlf0knq	2007/05/31	12:13:28	262.013	210.269	63.102	211.991	208.712	63.877	62.357
Ga	N	j9rlf0koq	2007/05/31	12:15:48	263.342	211.012	63.413	212.737	209.455	64.197	62.659
Ga	N	j9rlf0kpq	2007/05/31	12:18:08	264.671	211.712	63.528	213.413	210.177	64.314	62.772
Ga	N	j9rlf0kqq	2007/05/31	12:20:28	266.000	212.702	63.875	214.424	211.151	64.673	63.108
Ga	N	j9rlf0krq	2007/05/31	12:22:48	267.329	213.400	63.993	215.099	211.870	64.794	63.224
Ga	N	j9rlf3qsq	2007/06/03	10:01:55	128.079	153.851	55.044	154.827	152.836	55.648	54.451
Ga	N	j9rlf3qtq	2007/06/03	10:04:15	129.408	154.397	54.791	155.382	153.373	55.390	54.202
Ga	N	j9rlf3quq	2007/06/03	10:06:35	130.737	154.850	54.737	155.855	153.804	55.336	54.150
Ga	N	j9rlf3qvq	2007/06/03	10:08:55	132.067	155.167	54.650	156.194	154.097	55.248	54.064
Ga	N	j9rlf3qxq	2007/06/03	10:11:15	133.396	155.826	54.439	156.862	154.745	55.032	53.856
Ga	N	j9rlf3qyq	2007/06/03	10:13:53	134.896	155.941	54.481	157.016	154.817	55.077	53.897
Ga	N	j9rlf3qzq	2007/06/03	10:16:13	136.225	155.452	54.889	156.598	154.249	55.494	54.296
Ga	N	j9rlf3r4q	2007/06/03	10:27:53	142.872	159.346	53.840	160.536	158.095	54.426	53.265
Ga	N	j9rlf3r5q	2007/06/03	10:30:13	144.201	160.087	53.675	161.290	158.821	54.258	53.102
Ga	N	j9rlf3r6q	2007/06/03	10:32:51	145.702	161.139	53.543	162.353	159.861	54.125	52.973
Ga	N	j9rlf3r9q	2007/06/03	10:39:51	149.690	162.879	53.187	164.160	161.526	53.763	52.621
Ga	N	j9rlf3raq	2007/06/03	10:42:11	151.019	163.868	53.092	165.159	162.503	53.667	52.527
Ga	N	j9rlf1qtq	2007/06/10	09:50:18	102.990	143.799	61.067	144.428	143.175	61.926	60.236
Ga	N	j9rlf1quq	2007/06/10	09:52:38	104.319	144.541	60.569	145.160	143.927	61.412	59.754
Ga	N	j9rlf1qvq	2007/06/10	09:54:58	105.648	144.913	60.138	145.522	144.307	60.967	59.335
Ga	N	j9rlf1qwq	2007/06/10	09:57:18	106.977	145.502	59.767	146.104	144.904	60.584	58.974
Ga	N	j9rlf1qyq	2007/06/10	09:59:38	108.307	146.104	59.401	146.699	145.513	60.208	58.619
Ga	N	j9rlf1qzq	2007/06/10	10:02:16	109.807	146.880	58.732	147.463	146.299	59.518	57.967
Ga	N	j9rlf1r0q	2007/06/10	10:04:36	111.136	147.317	58.332	147.894	146.742	59.108	57.577
Ga	N	j9rlf1r2q	2007/06/10	10:06:56	112.466	147.957	57.987	148.529	147.388	58.754	57.241
Ga	N	j9rlf1r3q	2007/06/10	10:09:16	113.795	148.418	57.600	148.984	147.846	58.357	56.863
Ga	N	j9rlf1r4q	2007/06/10	10:11:36	115.124	148.890	57.365	149.453	148.302	58.116	56.634
Ga	N	j9rlf1r6q	2007/06/10	10:13:56	116.453	149.370	56.988	149.930	148.772	57.730	56.265
Ga	N	j9rlf1r7q	2007/06/10	10:16:16	117.783	149.854	56.760	150.426	149.241	57.497	56.042
Ga	N	j9rlf1r8q	2007/06/10	10:18:36	119.112	150.147	56.633	150.742	149.510	57.367	55.917
Ga	N	j9rlf1raq	2007/06/10	10:21:14	120.612	150.619	56.508	151.236	149.957	57.240	55.794
Ga	N	j9rlf1rbq	2007/06/10	10:23:34	121.942	150.906	56.385	151.546	150.220	57.115	55.673
Ga	N	j9rlf1req	2007/06/10	10:28:14	124.600	152.090	55.853	152.750	151.383	56.571	55.152
Ga	N	j9rlf1rfq	2007/06/10	10:30:34	125.929	152.164	55.833	152.856	151.421	56.552	55.132
Ga	N	j9rlf1rgq	2007/06/10	11:26:05	157.557	165.161	53.267	166.364	163.850	53.957	52.595
Ga	N	j9rlf1riq	2007/06/10	11:28:25	158.886	165.249	53.361	166.516	163.864	54.056	52.684
Ga	N	j9rlf1rjq	2007/06/10	11:30:45	160.216	166.205	53.294	167.488	164.802	53.989	52.618
Ga	N	j9rlf1rkq	2007/06/10	11:33:05	161.545	166.927	53.195	168.234	165.495	53.890	52.519
Ga	N	j9rlf1rmq	2007/06/10	11:35:25	162.874	167.168	53.327	168.541	165.657	54.027	52.645
Ga	N	j9rlf1rnq	2007/06/10	11:38:03	164.374	167.917	53.362	169.335	166.350	54.065	52.677
Ga	N	j9rlf1roq	2007/06/10	11:40:23	165.704	168.840	53.298	170.279	167.249	54.001	52.614
Ga	N	j9rlf1rpq	2007/06/10	11:42:43	167.033	168.986	53.435	170.506	167.295	54.146	52.745
Ga	N	j9rlf1rqq	2007/06/10	11:45:03	168.362	169.887	53.373	171.431	168.167	54.084	52.682
Ga	N	j9rlf1rrq	2007/06/10	11:47:23	169.692	170.220	53.546	171.845	168.398	54.266	52.849
Ga	N	j9rlf1rsq	2007/06/10	11:49:43	171.021	170.939	53.618	172.616	169.051	54.343	52.917
Ga	N	j9rlf1rtq	2007/06/10	11:52:03	172.350	171.363	53.662	173.111	169.383	54.392	52.957
Ga	N	j9rlf1ruq	2007/06/10	11:54:23	173.679	172.212	53.603	173.994	170.188	54.334	52.897
Ga	N	j9rlfcbqq	2007/06/11	06:39:16	94.481	141.418	63.186	143.802	138.547	64.218	62.214
Ga	N	j9rlfcbrq	2007/06/11	06:41:36	95.810	142.046	62.602	144.393	139.236	63.609	61.651
Ga	N	j9rlfcbsq	2007/06/11	06:43:56	97.140	142.364	62.214	144.736	139.520	63.209	61.274
Ga	N	j9rlfcbuq	2007/06/11	06:46:16	98.469	142.360	62.015	144.823	139.389	63.009	61.077
Ga	N	j9rlfcbxq	2007/06/11	06:53:34	102.627	144.767	60.894	147.215	141.820	61.850	59.990
Ga	N	j9rlfcbyq	2007/06/11	06:55:54	103.956	144.358	60.680	146.946	141.205	61.641	59.776
Ga	N	j9rlfcbzq	2007/06/11	06:58:14	105.285	145.460	60.236	147.998	142.380	61.179	59.346
Ga	N	j9rlfcc0q	2007/06/11	07:00:34	106.614	145.600	59.901	148.209	142.412	60.841	59.016
Ga	N	j9rlfcc1q	2007/06/11	07:02:54	107.943	146.943	59.113	149.421	143.952	60.020	58.255
Ga	N	j9rlfcc2q	2007/06/11	07:05:14	109.272	147.358	58.828	149.890	144.284	59.732	57.974
Ga	N	j9rlfcc3q	2007/06/11	07:07:52	110.772	146.943	58.842	149.703	143.508	59.765	57.976
Ga	N	o43b05c1q	1997/09/20	15:36:06	204.479	182.973	56.093	183.776	182.188	56.601	55.592
Ga	N	o43b05c3q	1997/09/20	15:42:46	208.277	184.553	56.475	185.331	183.790	56.990	55.967
Ga	N	o43b09b3q	1997/12/01	04:06:46	182.710	172.205	53.922	175.139	172.413	54.543	53.310
Ga	N	o43b09b3q	1997/12/01	04:08:16	183.564	172.415	53.833	174.397	171.754	54.453	53.223
Ga	N	o43b09b3q	1997/12/01	04:09:46	184.419	173.450	54.047	174.551	171.862	54.671	53.434
Ga	N	o43b12xaq	1998/07/26	13:50:36	151.884	159.653	54.044	160.518	158.806	54.496	53.596
Ga	N	o43b2rxeq	1998/07/26	14:27:40	173.000	168.533	53.929	171.864	168.294	55.162	52.732
Ga	N	o43b2rxeq	1998/07/26	14:29:10	173.855	168.882	53.968	171.291	167.748	55.203	52.770
Ga	N	o43b2rxeq	1998/07/26	14:30:40	174.709	169.290	53.950	170.777	167.264	55.184	52.752
Ga	N	o43b2sxgq	1998/07/26	15:24:26	205.339	182.660	56.229	183.207	182.119	56.717	55.747
Ga	N	o43b2sxiq	1998/07/26	15:30:54	209.023	183.454	56.667	184.598	183.524	57.162	56.177
Ga	N	o43b13s8q	1998/11/26	00:53:16	154.754	163.302	53.970	164.512	162.123	55.248	52.732
Ga	N	o43b13saq	1998/11/26	00:59:48	158.476	164.769	53.958	165.208	164.334	54.433	53.488
Ga	N	o43b4askq	1998/11/26	02:38:40	214.791	189.394	57.562	190.297	188.442	58.072	57.058
Ga	N	o43b21caq	1999/06/28	17:06:52	192.973	177.632	55.310	178.226	177.039	55.899	54.729
Ga	N	o43b21cbq	1999/06/28	17:12:14	196.030	178.911	55.658	179.506	178.316	56.253	55.072
Ga	N	o43b21cdq	1999/06/28	17:18:02	199.334	181.161	55.789	181.757	180.567	56.386	55.201
Ga	N	o43b21cfq	1999/06/28	17:27:54	204.954	183.718	56.826	184.327	183.109	57.443	56.220
Ga	N	o43b21chq	1999/06/28	17:35:04	209.036	185.486	57.290	186.101	184.871	57.915	56.676
Ga	N	o43b21cjq	1999/06/28	17:42:14	213.118	187.382	57.542	188.000	186.764	58.170	56.923
Ga	N	o5g2d1c3q	1999/08/16	11:48:06	245.462	202.574	61.629	206.782	198.836	63.062	60.232
Ga	N	o5hya4i4q	1999/09/21	20:28:10	191.625	177.397	55.237	179.531	177.576	55.659	54.818
Ga	N	o5hya4i4q	1999/09/21	20:29:40	192.479	177.593	55.218	178.795	176.887	55.641	54.798
Ga	N	o5hya4i6q	1999/09/21	20:38:28	197.492	179.932	55.336	180.812	179.097	55.765	54.911
Ga	N	o5hya4iaq	1999/09/21	21:05:30	212.892	236.905	67.986	243.296	228.168	68.282	67.601
Ga	N	o6ba03ukq	2000/12/16	11:01:28	167.569	166.035	53.678	168.332	164.034	54.797	52.578
Ga	N	o6ba03ulq	2000/12/16	11:03:40	168.822	166.908	53.761	169.180	164.928	54.885	52.659

Table B.1: Auroral footprints' main Alfvén wing (MAW) spot locations for Europa and Ganymede observed on the Northern and Southern Jovian hemispheres as published as supporting information to Bonfond et al. (2017b). (*continued*)

Sat.	Hem.	Obs ID	Date	Time	φ_{Sat}	φ_{fp}	λ_{fp}	$\Delta^{+}(\varphi_{\mathrm{fp}})$	$\Delta^{-}(\varphi_{\mathrm{fp}})$	$\Delta^{+}(\lambda_{\mathrm{fp}})$	$\Delta^{-}(\lambda_{\mathrm{fp}})$
Ga	N	o6ba03unq	2000/12/16	11:09:00	171.859	168.059	53.808	170.177	166.204	54.941	52.699
Ga	N	o6ba03uoq	2000/12/16	11:11:12	173.112	168.725	53.895	170.806	166.901	55.032	52.782
Ga	N	o6ba03uqq	2000/12/16	11:16:36	176.188	170.013	53.935	171.960	168.296	55.078	52.816
Ga	N	o6ba03urq	2000/12/16	11:18:48	177.441	170.704	54.019	172.619	169.008	55.167	52.897
Ga	N	o6ba03utq	2000/12/16	11:26:32	181.846	172.979	54.502	176.238	172.729	55.672	53.359
Ga	N	o6ba03utq	2000/12/16	11:28:02	182.700	173.466	54.508	175.793	172.320	55.679	53.365
Ga	N	o6ba03utq	2000/12/16	11:29:32	183.554	173.751	54.592	175.141	171.709	55.767	53.445
Ga	N	o6ba03uvq	2000/12/16	12:20:08	212.374	186.495	56.877	187.029	185.963	57.350	56.409
Ga	N	o6ba03uwq	2000/12/16	12:22:20	213.627	187.265	56.952	187.798	186.734	57.427	56.484
Ga	N	o6ba03uyq	2000/12/16	12:27:42	216.684	188.479	57.174	189.007	187.953	57.652	56.702
Ga	N	o6ba03v4q	2000/12/16	13:57:14	267.678	213.588	64.438	214.189	212.989	65.040	63.848
Ga	N	o6ba03v6q	2000/12/16	14:01:20	270.013	214.846	64.897	215.457	214.236	65.509	64.298
Ga	N	o6ba03v7q	2000/12/16	14:03:12	271.076	215.440	64.979	216.052	214.828	65.592	64.378
Ga	N	o6ba03v9q	2000/12/16	14:08:16	273.962	216.805	65.428	217.428	216.182	66.051	64.818
Ga	N	o6ba03vaq	2000/12/16	14:10:08	275.025	217.377	65.510	218.003	216.752	66.134	64.898
Ga	N	o6ba03vcq	2000/12/16	14:15:08	277.873	219.100	66.091	219.740	218.460	66.728	65.467
Ga	N	o6ba03vdq	2000/12/16	14:17:00	278.936	219.588	66.064	220.228	218.948	66.701	65.441
Ga	N	o6ba03vfq	2000/12/16	14:22:04	281.822	221.096	66.757	221.755	220.436	67.410	66.119
Ga	N	o6ba03vhq	2000/12/16	14:28:24	285.429	224.492	67.563	226.782	223.130	69.406	65.841
Ga	N	o6ba03vhq	2000/12/16	14:29:54	286.283	224.988	67.659	226.380	222.711	69.508	65.931
Ga	N	o6ba03vjq	2000/12/16	14:39:28	291.732	227.931	69.138	228.665	227.196	69.854	68.441
Ga	N	o6ba03vkq	2000/12/16	14:41:20	292.795	228.785	69.003	229.515	228.054	69.716	68.311
Ga	N	o6baa4chq	2000/12/18	14:10:50	115.581	148.984	58.126	149.497	148.469	58.621	57.638
Ga	N	o6baa4cnq	2000/12/18	14:49:50	137.791	156.707	54.763	157.234	156.178	55.209	54.321
Ga	N	o6baa4crq	2000/12/18	15:44:08	168.715	169.679	53.502	170.466	168.850	53.920	53.088
Ga	N	o6baa4csq	2000/12/18	15:46:00	169.778	170.118	53.474	170.922	169.271	53.890	53.061
Ga	N	o6baa4cuq	2000/12/18	15:51:00	172.625	171.442	53.553	172.298	170.539	53.968	53.141
Ga	N	o6baa4cvq	2000/12/18	15:52:52	173.688	172.060	53.607	172.933	171.137	54.021	53.195
Ga	N	o6baa4cxq	2000/12/18	15:57:56	176.574	172.999	53.817	173.950	171.992	54.229	53.406
Ga	N	o6baa4cyq	2000/12/18	15:59:48	177.637	173.575	53.868	174.546	172.544	54.280	53.458
Ga	N	o6baa4d0q	2000/12/18	16:04:48	180.484	175.233	53.883	176.254	174.148	54.293	53.476
Ga	N	o6baa4d2q	2000/12/18	16:11:08	184.091	174.284	54.383	178.874	171.951	55.459	53.306
Ga	N	o6baa4d2q	2000/12/18	16:12:38	184.945	174.881	54.368	178.597	171.591	55.441	53.293
Ga	N	o6baa4d2q	2000/12/18	16:14:08	185.800	175.032	54.487	177.951	170.670	55.555	53.414
Ga	N	o6baa4d4q	2000/12/18	16:22:12	190.394	179.071	54.961	180.464	177.557	55.362	54.559
Ga	N	o6baa4d5q	2000/12/18	16:24:04	191.457	179.365	55.078	180.815	177.783	55.477	54.678
Ga	N	o6ba06s4q	2001/01/13	17:30:28	313.884	244.869	73.158	245.834	243.905	74.092	72.266
Ga	N	o6ba06s6q	2001/01/13	18:20:28	342.362	266.723	78.367	268.112	265.334	79.647	77.187
Ga	N	o6ba06s7q	2001/01/13	18:22:30	343.520	267.715	77.960	269.058	266.372	79.203	76.809
Ga	N	o6ba06s9q	2001/01/13	18:27:42	346.482	269.421	77.749	270.743	268.099	78.973	76.613
Ga	N	o6ba06saq	2001/01/13	18:29:44	347.640	271.293	78.157	272.659	269.927	79.417	76.992
Ga	N	o6ba06scq	2001/01/13	18:34:56	350.602	271.480	79.176	272.977	269.982	80.532	77.937
Ga	N	o6baa7xiq	2001/01/20	15:51:01	238.315	198.011	60.012	199.109	196.978	60.529	59.500
Ga	N	o6baa7y1q	2001/01/20	17:46:25	304.045	237.263	71.562	238.100	236.516	72.393	70.760
Ga	N	o6baa7y2q	2001/01/20	17:48:27	305.204	237.775	71.660	238.584	237.050	72.496	70.854
Ga	N	o6baa7y4q	2001/01/20	17:56:07	309.570	237.898	71.997	241.179	237.002	74.361	69.867
Ga	N	o6baa7y4q	2001/01/20	17:57:37	310.425	239.035	72.090	241.409	237.231	74.465	69.951
Ga	N	o6baa7y6q	2001/01/20	18:07:11	315.874	246.283	73.913	247.114	245.433	74.852	73.017
Ga	N	o6baa5bmq	2001/01/21	22:22:11	201.264	183.190	56.103	183.695	182.685	56.618	55.595
Ga	N	o8k801pvq	2003/02/26	00:22:19	257.326	210.295	63.041	214.596	209.448	63.722	62.375
Ga	N	o8k801pvq	2003/02/26	00:23:49	258.180	211.632	62.970	215.068	209.849	63.649	62.306
Ga	N	o8k801pvq	2003/02/26	00:25:19	259.035	213.873	63.123	216.641	211.018	63.806	62.456
Ga	N	o8k801pxq	2003/02/26	00:33:51	263.895	211.156	63.799	213.383	209.216	64.500	63.115
Ga	N	o8k801pyq	2003/02/26	00:36:37	265.471	212.912	64.281	215.245	210.891	64.995	63.585
Ga	N	o8k801q0q	2003/02/26	00:39:23	267.047	214.706	64.771	217.159	212.595	65.500	64.063
Ga	N	o8k801q2q	2003/02/26	00:42:09	268.622	216.405	65.165	218.953	214.224	65.905	64.445
Ga	N	o8k801q4q	2003/02/26	00:44:55	270.198	216.972	65.396	219.460	214.837	66.143	64.670
Ga	N	o8k801q6q	2003/02/26	00:47:41	271.774	217.430	65.520	219.827	215.366	66.272	64.791
Ga	N	o8k801q8q	2003/02/26	00:50:27	273.350	219.138	65.926	221.633	217.000	66.691	65.184
Ga	N	o8k801qbq	2003/02/26	00:57:14	277.213	221.278	66.359	225.243	220.686	67.140	65.601
Ga	N	o8k801qbq	2003/02/26	00:58:44	278.068	224.836	66.942	228.334	223.011	67.743	66.167
Ga	N	o8k801qbq	2003/02/26	01:00:14	278.922	226.841	67.007	229.587	223.996	67.810	66.230
Ga	N	o8k801qgq	2003/02/26	01:58:22	312.032	246.629	73.534	261.473	241.724	76.787	70.815
Ga	N	o8k801qgq	2003/02/26	01:59:52	312.887	249.892	74.000	266.974	243.246	77.366	71.215
Ga	N	o8k801qgq	2003/02/26	02:01:22	313.741	252.086	74.095	269.790	244.160	77.482	71.296
Ga	N	o8k801qiq	2003/02/26	02:09:54	318.601	258.906	75.296	286.323	249.988	79.013	72.316
Ga	N	o8k801qjq	2003/02/26	02:12:41	320.186	259.225	75.503	285.847	250.495	79.295	72.488
Ga	N	o8k801qlq	2003/02/26	02:15:26	321.753	259.950	75.898	288.787	251.118	79.833	72.814
Ga	N	o8k801qnq	2003/02/26	02:18:13	323.338	260.269	76.114	288.606	251.615	80.137	72.990
Ga	N	o8k801qpq	2003/02/26	02:20:58	324.904	259.845	76.278	285.984	251.609	80.375	73.123
Ga	N	o8k801qrq	2003/02/26	02:23:45	326.490	261.301	76.752	292.707	252.698	81.053	73.507
Ga	N	o8k801qtq	2003/02/26	02:29:41	329.869	266.516	77.119	273.405	262.020	78.607	75.782
Ga	N	o8k801qvq	2003/02/26	02:32:27	331.445	264.799	77.032	270.716	260.839	78.510	75.702
Ga	N	o8k801qxq	2003/02/26	02:35:13	333.020	265.953	77.688	272.588	261.700	79.255	76.295
Ga	N	o8k801qzq	2003/02/26	02:37:59	334.596	265.884	78.092	272.641	261.649	79.720	76.657
Ga	N	oc0va1r4q	2012/11/14	17:12:40	109.202	143.399	61.143	147.473	143.590	62.574	59.765
Ga	N	oc0va1r4q	2012/11/14	17:14:10	110.056	143.866	60.980	146.976	143.195	62.406	59.609
Ga	N	oc0va1r4q	2012/11/14	17:15:40	110.911	144.089	60.460	146.170	142.606	61.865	59.107
Ga	N	oc0va1r4q	2012/11/14	17:17:10	111.765	144.553	60.026	145.639	142.231	61.413	58.688
Ga	N	oc0va4e0q	2013/01/25	05:58:32	99.147	143.758	61.039	147.280	145.588	61.616	60.471
Ga	N	oc0va4e0q	2013/01/25	06:00:02	100.002	144.137	60.828	146.738	145.073	61.402	60.263
Ga	N	oc0va4e0q	2013/01/25	06:01:32	100.856	144.509	60.701	146.194	144.550	61.273	60.138
Ga	N	oc0va4e0q	2013/01/25	06:03:02	101.710	144.642	60.470	145.404	143.791	61.039	59.910
Ga	N	oc0va4e0q	2013/01/25	06:04:32	102.564	144.820	60.157	144.657	143.079	60.721	59.601
Ga	N	oc0va2wrq	2013/02/14	22:06:12	133.210	152.288	55.008	155.996	153.946	55.516	54.505
Ga	N	oc0va2wrq	2013/02/14	22:07:42	134.065	152.884	54.912	155.674	153.645	55.419	54.410
Ga	N	oc0va2wrq	2013/02/14	22:09:12	134.919	153.424	54.960	155.301	153.285	55.468	54.457

Table B.1: Auroral footprints' main Alfvén wing (MAW) spot locations for Europa and Ganymede observed on the Northern and Southern Jovian hemispheres as published as supporting information to Bonfond et al. (2017b). (*continued*)

Sat.	Hem.	Obs ID	Date	Time	φ_{Sat}	φ_{fp}	λ_{fp}	$\Delta^{+}(\varphi_{\mathrm{fp}})$	$\Delta^{-}(\varphi_{\mathrm{fp}})$	$\Delta^{+}(\lambda_{\mathrm{fp}})$	$\Delta^{-}(\lambda_{\mathrm{fp}})$
Ga	N	oc0va2wrq	2013/02/14	22:10:42	135.774	153.399	54.743	154.340	152.380	55.250	54.241
Ga	N	oc0va2wrq	2013/02/14	22:12:12	136.628	153.948	54.790	153.976	152.028	55.298	54.288
Ga	N	oc0va3jiq	2013/02/21	23:11:02	151.126	160.477	53.634	164.046	162.299	54.147	53.126
Ga	N	oc0va3jiq	2013/02/21	23:12:32	151.981	160.860	53.563	163.502	161.793	54.076	53.056
Ga	N	oc0va3jiq	2013/02/21	23:14:02	152.835	161.265	53.582	162.986	161.304	54.096	53.074
Ga	N	oc0va3jiq	2013/02/21	23:15:32	153.689	161.660	53.511	162.457	160.809	54.024	53.003
Ga	N	oc0va3jiq	2013/02/21	23:17:02	154.544	161.829	53.539	161.699	160.089	54.053	53.030
Ga	N	oc0va5rmq	2013/03/09	06:02:39	87.742	139.155	65.708	147.156	137.934	67.812	63.725
Ga	N	oc0va5rmq	2013/03/09	06:04:09	88.596	139.336	65.198	146.055	137.430	67.269	63.245
Ga	N	oc0va5rmq	2013/03/09	06:05:39	89.450	139.648	64.822	145.195	136.998	66.869	62.890
Ga	N	oc0va5rmq	2013/03/09	06:07:09	90.305	139.654	64.453	144.001	136.282	66.478	62.540
Ga	N	oc0va5rmq	2013/03/09	06:08:39	91.159	139.824	64.334	143.107	135.651	66.354	62.426
Ga	N	oc0va7obq	2013/12/21	07:31:58	105.507	144.981	59.428	154.015	150.849	60.893	58.024
Ga	N	oc0va7obq	2013/12/21	07:33:28	106.361	145.213	59.360	153.291	150.215	60.822	57.958
Ga	N	oc0va7obq	2013/12/21	07:34:58	107.215	145.427	59.076	152.526	149.579	60.527	57.685
Ga	N	oc0va7obq	2013/12/21	07:36:28	108.069	145.836	58.972	151.988	149.113	60.418	57.584
Ga	N	oc0va7obq	2013/12/21	07:37:58	108.923	146.084	58.797	151.274	148.499	60.236	57.416
Ga	N	oc0va7obq	2013/12/21	07:39:28	109.778	146.181	58.554	150.397	147.724	59.983	57.182
Ga	N	oc0va7obq	2013/12/21	07:40:58	110.632	146.456	58.486	149.723	147.094	59.912	57.116
Ga	N	oc0va7obq	2013/12/21	07:42:28	111.486	146.736	58.418	149.056	146.469	59.842	57.050
Ga	N	oc0va7obq	2013/12/21	07:43:58	112.340	146.868	58.280	148.229	145.698	59.699	56.918
Ga	N	oc0va7obq	2013/12/21	07:45:28	113.194	147.165	58.108	147.576	145.093	59.520	56.752
Ga	N	oc0va7obq	2013/12/21	07:46:58	114.049	147.472	57.937	146.971	144.498	59.341	56.586
Ga	N	oc0va7obq	2013/12/21	07:48:28	114.903	147.787	57.766	146.374	143.911	59.164	56.421
Ga	N	oc0va7obq	2013/12/21	07:49:58	115.757	148.123	57.493	145.795	143.347	58.880	56.159
Ga	N	oc0va7obq	2013/12/21	07:51:28	116.611	148.609	57.290	145.369	142.932	58.669	55.963
Ga	N	oc0va7obq	2013/12/21	07:52:58	117.466	148.950	57.122	144.799	142.371	58.494	55.800
Ga	N	oc0va7obq	2013/12/21	07:54:28	118.320	149.165	56.887	144.101	141.684	58.251	55.574
Ga	N	oc1z02twq	2014/01/02	09:20:33	290.350	228.935	69.655	234.173	230.864	70.337	68.993
Ga	N	oc1z02twq	2014/01/02	09:22:03	291.205	229.884	69.972	234.258	230.868	70.663	69.300
Ga	N	oc1z02twq	2014/01/02	09:23:33	292.059	230.974	70.246	234.487	231.012	70.947	69.567
Ga	N	oc1z02twq	2014/01/02	09:25:03	292.914	231.492	70.386	234.101	230.622	71.091	69.702
Ga	N	oc1z02twq	2014/01/02	09:26:33	293.768	231.436	70.387	233.096	229.695	71.093	69.702
Ga	N	oc1z02twq	2014/01/02	09:28:03	294.623	232.081	70.480	232.837	229.433	71.189	69.793
Ga	N	oc1z02twq	2014/01/02	09:29:33	295.477	232.297	70.388	232.104	228.778	71.094	69.703
Ga	N	oc1z02u2q	2014/01/02	09:50:25	307.364	240.939	72.894	246.576	242.877	73.698	72.121
Ga	N	oc1z02u2q	2014/01/02	09:51:55	308.218	242.045	73.211	246.841	243.021	74.029	72.426
Ga	N	oc1z02u2q	2014/01/02	09:53:25	309.073	243.171	73.534	247.133	243.180	74.366	72.736
Ga	N	oc1z02u2q	2014/01/02	09:54:55	309.927	242.192	73.048	245.066	241.448	73.860	72.269
Ga	N	oc1z02u2q	2014/01/02	09:56:25	310.782	243.616	73.639	245.715	241.855	74.478	72.837
Ga	N	oc1z02u2q	2014/01/02	09:57:55	311.636	244.885	73.915	246.149	242.157	74.766	73.100
Ga	N	oc1z02u2q	2014/01/02	09:59:25	312.491	244.698	73.912	244.998	241.113	74.764	73.097
Ga	N	oc1z02u2q	2014/01/02	10:00:55	313.345	244.821	73.799	244.153	240.381	74.647	72.989
Ga	N	oc1z03y3q	2014/01/03	04:28:06	223.992	191.404	58.913	195.655	194.226	59.375	58.457
Ga	N	oc1z03y3q	2014/01/03	04:29:36	224.847	191.886	59.033	195.227	193.803	59.497	58.576
Ga	N	oc1z03y3q	2014/01/03	04:31:06	225.701	192.259	59.184	194.691	193.272	59.650	58.725
Ga	N	oc1z03y3q	2014/01/03	04:32:36	226.555	192.737	59.305	194.260	192.845	59.773	58.845
Ga	N	oc1z03y3q	2014/01/03	04:34:06	227.410	193.214	59.427	193.828	192.418	59.896	58.964
Ga	N	oc1z03y3q	2014/01/03	04:35:36	228.264	193.690	59.549	193.394	191.989	60.020	59.085
Ga	N	oc1z03y3q	2014/01/03	04:37:06	229.118	194.164	59.671	192.959	191.558	60.144	59.205
Ga	N	oc1z03ybq	2014/01/03	04:57:58	241.003	199.365	60.625	203.712	202.451	61.112	60.145
Ga	N	oc1z03ybq	2014/01/03	04:59:28	241.857	199.817	60.750	203.255	201.999	61.239	60.268
Ga	N	oc1z03ybq	2014/01/03	05:00:58	242.711	200.152	60.906	202.680	201.430	61.397	60.422
Ga	N	oc1z03ybq	2014/01/03	05:02:28	243.566	200.599	61.031	202.217	200.972	61.525	60.545
Ga	N	oc1z03ybq	2014/01/03	05:03:58	244.420	201.043	61.157	201.751	200.512	61.652	60.669
Ga	N	oc1z03ybq	2014/01/03	05:05:28	245.274	201.485	61.283	201.283	200.049	61.780	60.793
Ga	N	oc1z03ybq	2014/01/03	05:06:58	246.129	201.836	61.276	200.721	199.500	61.774	60.786
Ga	N	oc1z03ybq	2014/01/03	05:08:28	246.983	202.359	61.536	200.339	199.114	62.038	61.043
Ga	N	oc1z04b4q	2014/01/04	01:11:20	212.014	186.805	57.952	188.710	186.304	59.138	56.804
Ga	N	oc1z04b4q	2014/01/04	01:12:50	212.869	186.938	58.102	187.972	185.490	59.293	56.950
Ga	N	oc1z04b4q	2014/01/04	01:14:20	213.723	187.324	58.202	187.476	184.941	59.396	57.047
Ga	N	oc1z04b4q	2014/01/04	01:15:50	214.577	187.706	58.302	186.975	184.387	59.499	57.144
Ga	N	oc1z04bbq	2014/01/04	01:41:02	228.928	193.563	59.162	198.597	195.307	60.385	57.980
Ga	N	oc1z04bbq	2014/01/04	01:42:32	229.782	194.031	59.237	198.183	194.838	60.463	58.053
Ga	N	oc1z04bbq	2014/01/04	01:44:02	230.636	194.790	59.263	198.044	194.681	60.490	58.078
Ga	N	oc1z04bbq	2014/01/04	01:45:32	231.490	195.104	59.363	197.485	194.047	60.594	58.176
Ga	N	oc1z04bbq	2014/01/04	01:47:02	232.344	195.494	59.565	197.007	193.483	60.803	58.371
Ga	N	oc1z04bbq	2014/01/04	01:48:32	233.198	195.875	59.769	196.522	192.906	61.013	58.568
Ga	N	oc1z04bbq	2014/01/04	01:50:02	234.053	196.320	59.845	196.088	192.411	61.092	58.642
Ga	N	oc1z05haq	2014/01/05	05:52:40	112.239	147.359	58.777	151.314	150.444	59.223	58.336
Ga	N	oc1z05haq	2014/01/05	05:54:10	113.093	147.550	58.547	150.604	149.722	58.990	58.109
Ga	N	oc1z05haq	2014/01/05	05:55:40	113.948	148.131	58.248	150.277	149.397	58.688	57.814
Ga	N	oc1z05haq	2014/01/05	05:57:10	114.802	148.336	58.021	149.581	148.689	58.458	57.590
Ga	N	oc1z05haq	2014/01/05	05:58:40	115.656	148.801	57.750	149.140	148.247	58.183	57.322
Ga	N	oc1z05haq	2014/01/05	06:00:10	116.510	149.019	57.526	148.457	147.552	57.956	57.101
Ga	N	oc1z05haq	2014/01/05	06:01:40	117.364	149.344	57.400	147.880	146.963	57.828	56.977
Ga	N	oc1z05hgq	2014/01/05	06:22:32	129.248	153.775	55.384	158.005	156.945	55.786	54.985
Ga	N	oc1z05hgq	2014/01/05	06:24:02	130.102	153.950	55.395	157.284	156.202	55.798	54.997
Ga	N	oc1z05hgq	2014/01/05	06:25:32	130.956	154.355	55.161	156.784	155.699	55.561	54.766
Ga	N	oc1z05hgq	2014/01/05	06:27:02	131.810	154.791	55.132	156.319	155.221	55.531	54.736
Ga	N	oc1z05hgq	2014/01/05	06:28:32	132.664	155.016	55.031	155.644	154.532	55.429	54.637
Ga	N	oc1z05hgq	2014/01/05	06:30:02	133.519	155.318	55.021	155.047	153.917	55.418	54.627
Ga	N	oc1z05hgq	2014/01/05	06:31:32	134.373	155.674	54.899	154.501	153.362	55.296	54.507
Ga	N	oc1z05hgq	2014/01/05	06:33:02	135.227	156.031	54.778	153.957	152.806	55.173	54.387
Ga	N	oc1z06ayq	2014/01/06	02:35:58	100.326	142.503	62.521	149.659	141.580	63.911	61.181
Ga	N	oc1z06ayq	2014/01/06	02:37:28	101.180	144.188	61.800	150.218	142.678	63.160	60.488
Ga	N	oc1z06ayq	2014/01/06	02:38:58	102.034	144.169	61.625	149.346	141.682	62.973	60.321

Table B.1: Auroral footprints' main Alfvén wing (MAW) spot locations for Europa and Ganymede observed on the Northern and Southern Jovian hemispheres as published as supporting information to Bonfond et al. (2017b). (*continued*)

Sat.	Hem.	Obs ID	Date	Time	φ_{Sat}	φ_{fp}	λ_{fp}	$\Delta^{+}(\varphi_{\mathrm{fp}})$	$\Delta^{-}(\varphi_{\mathrm{fp}})$	$\Delta^{+}(\lambda_{\mathrm{fp}})$	$\Delta^{-}(\lambda_{\mathrm{fp}})$
Ga	N	oc1z06ayq	2014/01/06	02:40:28	102.889	144.828	61.157	149.032	141.532	62.484	59.873
Ga	N	oc1z06ayq	2014/01/06	02:41:58	103.743	144.906	61.170	148.285	140.591	62.494	59.887
Ga	N	oc1z06ayq	2014/01/06	02:43:28	104.597	145.254	60.651	147.681	140.101	61.952	59.389
Ga	N	oc1z06ayq	2014/01/06	02:44:58	105.452	145.488	60.446	147.034	139.395	61.736	59.194
Ga	N	oc1z06b4q	2014/01/06	03:05:50	117.337	149.858	57.397	157.325	148.972	58.544	56.269
Ga	N	oc1z06b4q	2014/01/06	03:07:20	118.191	150.536	57.064	157.061	148.794	58.199	55.946
Ga	N	oc1z06b4q	2014/01/06	03:08:50	119.046	150.228	57.096	155.995	147.351	58.226	55.982
Ga	N	oc1z06b4q	2014/01/06	03:10:20	119.900	151.195	56.737	155.981	147.523	57.856	55.633
Ga	N	oc1z06b4q	2014/01/06	03:11:50	120.754	151.338	56.547	155.274	146.668	57.657	55.451
Ga	N	oc1z06b4q	2014/01/06	03:13:20	121.609	151.530	56.439	154.628	145.844	57.542	55.348
Ga	N	oc1z06b4q	2014/01/06	03:14:50	122.463	151.953	56.222	154.165	145.324	57.316	55.139
Ga	N	oc1z06b4q	2014/01/06	03:16:20	123.317	152.433	56.088	153.767	144.847	57.175	55.010
Ga	N	oc1z09faq	2014/01/10	04:19:20	200.507	180.577	55.669	186.786	181.960	56.874	54.500
Ga	N	oc1z09faq	2014/01/10	04:20:50	201.362	180.939	55.734	186.216	181.437	56.942	54.563
Ga	N	oc1z09faq	2014/01/10	04:22:20	202.216	181.092	55.693	185.416	180.722	56.900	54.523
Ga	N	oc1z09faq	2014/01/10	04:23:50	203.070	181.592	55.908	185.007	180.316	57.122	54.730
Ga	N	oc1z09faq	2014/01/10	04:25:20	203.925	182.255	56.036	184.762	180.072	57.255	54.855
Ga	N	oc1z09faq	2014/01/10	04:26:50	204.779	182.500	55.952	184.057	179.448	57.168	54.773
Ga	N	oc1z09faq	2014/01/10	04:28:20	205.633	183.000	56.167	183.649	179.043	57.391	54.981
Ga	N	oc1z09faq	2014/01/10	04:29:50	206.488	183.377	56.232	183.098	178.531	57.459	55.044
Ga	N	oc1z10hrq	2014/01/11	00:32:38	171.483	168.886	53.666	172.936	170.134	54.779	52.583
Ga	N	oc1z10hrq	2014/01/11	00:34:08	172.337	169.429	53.794	172.569	169.772	54.911	52.708
Ga	N	oc1z10hrq	2014/01/11	00:35:38	173.191	169.705	53.882	171.928	169.151	55.002	52.794
Ga	N	oc1z10hrq	2014/01/11	00:37:08	174.046	169.992	53.832	171.291	168.547	54.950	52.745
Ga	N	oc1z10hrq	2014/01/11	00:38:38	174.900	170.361	53.888	170.744	168.018	55.007	52.799
Ga	N	oc1z10hrq	2014/01/11	00:40:08	175.754	170.822	53.911	170.289	167.581	55.031	52.821
Ga	N	oc1z11lfq	2014/01/11	19:40:09	104.940	144.343	58.770	149.648	146.178	60.114	57.478
Ga	N	oc1z11lfq	2014/01/11	19:41:39	105.794	144.819	58.632	149.195	145.767	59.970	57.345
Ga	N	oc1z11lfq	2014/01/11	19:43:09	106.648	145.001	58.472	148.438	145.069	59.803	57.191
Ga	N	oc1z11lfq	2014/01/11	19:44:39	107.502	145.193	58.313	147.693	144.382	59.638	57.037
Ga	N	oc1z11lfq	2014/01/11	19:46:09	108.357	145.485	58.107	147.048	143.794	59.424	56.839
Ga	N	oc1z11lfq	2014/01/11	19:47:39	109.211	145.697	57.949	146.325	143.124	59.260	56.686
Ga	N	oc1z11lfq	2014/01/11	19:49:09	110.065	146.116	57.859	145.820	142.653	59.167	56.599
Ga	N	oc1z11llq	2014/01/11	20:10:01	121.947	148.461	57.081	153.521	150.864	58.358	55.848
Ga	N	oc1z11llq	2014/01/11	20:11:31	122.802	149.941	56.394	154.075	151.454	57.646	55.183
Ga	N	oc1z11llq	2014/01/11	20:13:01	123.656	150.515	55.848	153.714	151.147	57.081	54.655
Ga	N	oc1z11llq	2014/01/11	20:14:31	124.510	150.817	55.847	153.098	150.552	57.080	54.654
Ga	N	oc1z11llq	2014/01/11	20:16:01	125.364	151.153	55.695	152.512	149.996	56.922	54.507
Ga	N	oc1z11llq	2014/01/11	20:17:31	126.218	151.592	55.500	152.028	149.541	56.721	54.318
Ga	N	oc1z11llq	2014/01/11	20:19:01	127.072	151.843	55.392	151.358	148.900	56.608	54.213
Ga	N	oc1z11llq	2014/01/11	20:20:31	127.927	152.196	55.241	150.789	148.359	56.452	54.067
Ga	N	oc1z13b4q	2014/01/13	01:56:55	59.570	136.435	76.940	142.501	136.548	80.013	74.396
Ga	N	oc1z13b4q	2014/01/13	01:58:25	60.424	137.082	76.481	142.120	136.448	79.440	74.003
Ga	N	oc1z13b4q	2014/01/13	01:59:55	61.279	137.144	76.436	141.159	135.387	79.382	73.965
Ga	N	oc1z13b4q	2014/01/13	02:01:25	62.133	137.582	75.809	140.541	135.104	78.614	73.422
Ga	N	oc1z13b4q	2014/01/13	02:02:55	62.987	138.283	75.381	140.279	135.037	78.099	73.049
Ga	N	oc1z13b4q	2014/01/13	02:04:25	63.842	138.455	75.096	139.564	134.254	77.758	72.799
Ga	N	oc1z13b4q	2014/01/13	02:05:55	64.696	138.869	74.988	139.120	133.698	77.629	72.704
Ga	N	oc1z13baq	2014/01/13	02:26:47	76.581	141.518	68.228	147.380	142.558	70.026	66.555
Ga	N	oc1z13baq	2014/01/13	02:28:17	77.435	141.328	67.870	146.319	141.428	69.637	66.220
Ga	N	oc1z13baq	2014/01/13	02:29:47	78.289	141.351	67.187	145.410	140.604	68.900	65.581
Ga	N	oc1z13baq	2014/01/13	02:31:17	79.144	141.212	66.842	144.395	139.531	68.529	65.258
Ga	N	oc1z13baq	2014/01/13	02:32:47	79.998	141.289	66.186	143.538	138.758	67.825	64.640
Ga	N	oc1z13baq	2014/01/13	02:34:17	80.852	141.092	66.008	142.489	137.590	67.634	64.474
Ga	N	oc1z13baq	2014/01/13	02:35:47	81.707	141.200	65.904	141.731	136.739	67.522	64.376
Ga	N	oc1z13baq	2014/01/13	02:37:17	82.561	141.431	65.381	141.033	136.109	66.964	63.882
Ga	N	oc0va6xjq	2014/01/24	15:31:00	185.817	174.037	54.443	183.447	179.393	55.702	53.221
Ga	N	oc0va6xjq	2014/01/24	15:32:30	186.671	174.607	54.533	183.102	179.063	55.796	53.309
Ga	N	oc0va6xjq	2014/01/24	15:34:00	187.526	174.969	54.530	182.535	178.538	55.793	53.305
Ga	N	oc0va6xjq	2014/01/24	15:35:30	188.380	175.293	54.588	181.933	177.972	55.854	53.360
Ga	N	oc0va6xjq	2014/01/24	15:37:00	189.234	175.577	54.707	181.294	177.363	55.978	53.476
Ga	N	oc0va6xjq	2014/01/24	15:38:30	190.089	175.907	54.765	180.700	176.802	56.038	53.531
Ga	N	oc0va6xjq	2014/01/24	15:40:00	190.943	176.286	54.761	180.151	176.291	56.034	53.527
Ga	N	oc0va6xjq	2014/01/24	15:41:30	191.797	176.578	54.880	179.522	175.689	56.158	53.642
Ga	N	oc0va6xjq	2014/01/24	15:43:00	192.651	176.917	54.937	178.939	175.136	56.218	53.697
Ga	N	oc0va6xjq	2014/01/24	15:44:30	193.506	177.025	54.961	178.113	174.359	56.243	53.719
Ga	N	oc0va6xjq	2014/01/24	15:46:00	194.360	177.605	55.051	177.781	174.037	56.337	53.807
Ga	N	oc0va6xjq	2014/01/24	15:47:30	195.214	177.768	55.012	177.011	173.318	56.297	53.768
Ga	N	oc0va6xjq	2014/01/24	15:49:00	196.068	178.303	55.165	176.636	172.948	56.455	53.916
Ga	N	oc0va6xjq	2014/01/24	15:50:30	196.923	178.427	55.187	175.830	172.186	56.479	53.937
Ga	N	oc0va6xjq	2014/01/24	15:52:00	197.777	179.010	55.278	175.502	171.866	56.573	54.025
Ga	N	oc0va6xjq	2014/01/24	15:53:30	198.631	179.318	55.397	174.892	171.277	56.697	54.140
Ga	S	o43b06btq	1997/09/20	13:59:18	149.335	106.183	-73.468	112.203	102.620	-70.900	-76.521
Ga	S	o43b06bvq	1997/09/20	14:05:58	153.133	110.249	-74.362	117.286	106.373	-71.660	-77.647
Ga	S	o43b15xeq	1998/11/05	04:27:20	333.472	-16.757	-72.578	-12.373	-24.046	-69.835	-75.991
Ga	S	o5hy04hsq	1999/09/21	18:57:34	140.012	95.320	-70.515	101.650	91.853	-67.786	-73.915
Ga	S	o5hy04hsq	1999/09/21	18:59:04	140.867	96.088	-70.823	102.740	92.536	-68.047	-74.317
Ga	S	o5hy04huq	1999/09/21	19:10:34	147.418	100.051	-71.567	106.578	96.718	-68.691	-75.255
Ga	S	o5hy04hvq	1999/09/21	19:12:46	148.671	100.770	-71.678	107.226	97.497	-68.787	-75.398
Ga	S	o5hy04hxq	1999/09/21	19:17:58	151.633	102.773	-72.092	109.376	99.543	-69.134	-75.955
Ga	S	o5hy04hyq	1999/09/21	19:20:00	152.792	103.298	-72.022	109.541	100.205	-69.078	-75.845
Ga	S	o5hy04i0q	1999/09/21	19:25:12	155.754	105.709	-72.680	112.641	102.520	-69.620	-76.775
Ga	S	o5hy04i2q	1999/09/21	19:31:36	159.400	112.014	-74.679	127.770	107.531	-71.176	-80.339
Ga	S	o5hy04i2q	1999/09/21	19:33:06	160.255	114.310	-75.704	135.941	108.943	-71.932	-81.682
Ga	S	o5hya1qgq	1999/10/21	01:46:14	39.755	33.276	-67.018	36.807	30.852	-64.840	-69.504

Table B.1: Auroral footprints' main Alfvén wing (MAW) spot locations for Europa and Ganymede observed on the Northern and Southern Jovian hemispheres as published as supporting information to Bonfond et al. (2017b). (*continued*)

Sat.	Hem.	Obs ID	Date	Time	φ_{Sat}	φ_{fp}	λ_{fp}	$\Delta^{+}(\varphi_{\mathrm{fp}})$	$\Delta^{-}(\varphi_{\mathrm{fp}})$	$\Delta^{+}(\lambda_{\mathrm{fp}})$	$\Delta^{-}(\lambda_{\mathrm{fp}})$
Ga	S	o5hya1qoq	1999/10/21	03:04:06	84.108	65.235	-67.450	67.285	63.271	-65.254	-69.946
Ga	S	o5hya1qwq	1999/10/21	03:42:00	105.696	76.659	-66.801	78.403	74.962	-64.685	-69.181
Ga	S	o6baa3w3q	2000/12/16	17:30:52	29.352	386.054	-67.438	392.753	381.886	-65.088	-70.207
Ga	S	o6baa3w3q	2000/12/16	17:32:22	30.206	388.738	-67.928	396.554	384.111	-65.509	-70.827
Ga	S	o6ba04btq	2000/12/18	10:55:00	4.056	5.521	-69.116	10.776	-1.836	-66.861	-71.812
Ga	S	o6ba04bzq	2000/12/18	11:35:18	27.006	23.582	-68.270	29.519	14.667	-66.073	-70.923
Ga	S	o6ba04c1q	2000/12/18	12:31:18	58.898	51.955	-65.646	57.865	42.984	-63.681	-67.952
Ga	S	o6ba04c2q	2000/12/18	12:33:22	60.075	53.108	-65.598	59.019	44.130	-63.637	-67.900
Ga	S	o6ba04c4q	2000/12/18	12:38:34	63.036	54.227	-65.843	60.653	43.553	-63.840	-68.258
Ga	S	o6ba04c5q	2000/12/18	12:40:34	64.175	55.241	-65.748	61.670	44.532	-63.752	-68.153
Ga	S	o6ba04c7q	2000/12/18	12:45:46	67.136	49.615	-66.227	58.817	39.520	-64.062	-67.646
Ga	S	o6ba04c8q	2000/12/18	12:47:50	68.313	52.141	-65.928	60.718	40.196	-63.818	-67.647
Ga	S	o6baa6suq	2001/01/13	20:39:30	61.550	409.767	-65.306	420.594	403.920	-62.972	-68.147
Ga	S	o6baa6swq	2001/01/13	21:33:16	92.173	69.511	-66.045	75.658	65.545	-63.724	-68.732
Ga	S	o6baa6sxq	2001/01/13	21:35:18	93.331	70.702	-66.333	77.070	66.648	-63.982	-69.069
Ga	S	o6baa6szq	2001/01/13	21:40:30	96.293	72.255	-66.278	78.144	68.442	-63.940	-68.984
Ga	S	o6baa6t0q	2001/01/13	21:42:32	97.451	72.861	-66.257	78.575	69.139	-63.924	-68.952
Ga	S	o6baa6t2q	2001/01/13	21:47:44	100.412	75.018	-66.517	80.672	71.349	-64.162	-69.246
Ga	S	o6baa6t3q	2001/01/13	21:49:46	101.570	75.753	-66.650	81.380	72.111	-64.282	-69.395
Ga	S	o6baa6t5q	2001/01/13	21:54:58	104.532	77.605	-66.908	83.100	74.057	-64.518	-69.686
Ga	S	o6baa6t6q	2001/01/13	21:57:00	105.690	78.037	-67.035	83.430	74.557	-64.634	-69.827
Ga	S	o6baa6t8q	2001/01/13	22:04:40	110.057	81.880	-68.349	88.143	78.093	-65.787	-71.401
Ga	S	o6baa6t8q	2001/01/13	22:06:10	110.911	82.738	-68.677	89.299	78.848	-66.073	-71.803
Ga	S	o6baa6taq	2001/01/13	22:15:44	116.360	84.299	-69.320	90.210	80.820	-66.657	-72.536
Ga	S	o6baa6tcq	2001/01/13	22:19:46	118.657	86.341	-69.660	92.461	82.812	-66.952	-72.958
Ga	S	o6baa6tiq	2001/01/13	23:45:34	167.524	120.872	-76.832	133.849	117.537	-72.705	-83.727
Ga	S	o6ba07wuq	2001/01/20	12:42:18	130.825	91.935	-70.179	112.117	85.156	-67.371	-74.209
Ga	S	o6ba07x0q	2001/01/20	13:21:54	153.380	111.732	-74.935	134.317	102.161	-71.232	-78.225
Ga	S	o6ba05aaq	2001/01/21	16:00:48	344.056	350.990	-70.838	363.624	345.330	-67.847	-74.794
Ga	S	o6ba05agq	2001/01/21	16:40:24	6.610	370.089	-69.001	377.079	366.090	-66.314	-72.263
Ga	S	o6ba05aiq	2001/01/21	17:30:22	35.067	33.510	-67.730	37.716	30.807	-65.230	-70.646
Ga	S	o6ba05ajq	2001/01/21	17:32:24	36.225	34.845	-68.044	39.259	32.053	-65.506	-71.023
Ga	S	o6ba05alq	2001/01/21	17:37:36	39.187	36.358	-67.618	40.199	33.860	-65.136	-70.504
Ga	S	o6ba05amq	2001/01/21	17:39:38	40.345	37.931	-67.797	41.935	35.354	-65.293	-70.719
Ga	S	o6ba05aoq	2001/01/21	17:44:50	43.306	40.133	-67.577	43.840	37.712	-65.101	-70.451
Ga	S	o6ba05apq	2001/01/21	17:46:52	44.464	40.425	-67.207	43.790	38.133	-64.776	-70.009
Ga	S	o6ba05arq	2001/01/21	17:52:04	47.426	41.544	-66.039	44.161	39.423	-63.739	-68.645
Ga	S	o6ba05asq	2001/01/21	17:54:06	48.584	43.058	-66.638	45.914	40.874	-64.274	-69.337
Ga	S	o6ba05auq	2001/01/21	18:01:46	52.950	47.210	-67.869	50.479	44.906	-65.360	-70.790
Ga	S	o6ba05auq	2001/01/21	18:03:16	53.805	41.490	-68.351	43.772	39.275	-65.796	-71.338
Ga	S	o6ba05awq	2001/01/21	18:12:50	59.253	49.894	-65.889	51.971	47.868	-63.611	-68.459
Ga	S	o6ba05ayq	2001/01/21	18:16:52	61.550	51.794	-65.996	53.870	49.769	-63.708	-68.580
Ga	S	o6ba05b4q	2001/01/21	19:42:39	110.406	80.636	-68.556	82.703	78.580	-65.991	-71.556
Ga	S	o6ba05b6q	2001/01/21	20:43:08	144.853	108.300	-72.312	110.803	103.575	-69.167	-76.419
Ga	S	o6ba05b7q	2001/01/21	20:45:10	146.011	109.841	-72.327	112.344	105.210	-69.179	-76.437
Ga	S	o6ba05b9q	2001/01/21	20:50:22	148.972	112.162	-73.235	114.872	106.129	-69.912	-77.779
Ga	S	o6ba05baq	2001/01/21	20:52:24	150.130	113.328	-73.479	116.101	106.881	-70.107	-78.159
Ga	S	o6ba05bcq	2001/01/21	20:57:36	153.092	116.324	-73.984	119.236	108.830	-70.504	-78.981
Ga	S	o6ba05bdq	2001/01/21	20:59:38	154.250	117.119	-74.229	120.162	108.774	-70.693	-79.411
Ga	S	o6ba05bfq	2001/01/21	21:04:50	157.211	120.413	-74.781	123.605	110.385	-71.119	-80.434
Ga	S	o6ba05bgq	2001/01/21	21:06:52	158.369	121.528	-75.058	124.838	110.152	-71.329	-81.012
Ga	S	o6ba05biq	2001/01/21	21:14:32	162.736	123.654	-77.745	128.820	108.087	-73.217	-83.042
Ga	S	o6ba05biq	2001/01/21	21:16:02	163.590	124.244	-78.536	129.996	107.265	-73.724	-83.198
Ga	S	o6ba05bkq	2001/01/21	21:25:36	169.038	135.044	-75.170	138.054	125.071	-71.420	-81.180
Ga	S	j9rlb0g7q	2007/02/20	15:45:00	74.859	58.875	-66.312	62.781	55.502	-65.598	-67.041
Ga	S	j9rlb0g8q	2007/02/20	15:47:20	76.188	60.236	-66.564	64.206	56.815	-65.844	-67.299
Ga	S	j9rlb0g9q	2007/02/20	15:49:40	77.517	61.224	-66.574	65.146	57.839	-65.853	-67.310
Ga	S	j9rlb0gaq	2007/02/20	15:52:00	78.846	61.048	-66.360	64.730	57.844	-65.643	-67.094
Ga	S	j9rlb0gbq	2007/02/20	15:54:20	80.175	61.656	-66.378	65.257	58.515	-65.659	-67.114
Ga	S	j9rlb0gcq	2007/02/20	15:56:58	81.675	64.389	-66.602	68.172	61.108	-65.879	-67.342
Ga	S	j9rlb0gdq	2007/02/20	15:59:18	83.004	64.984	-66.621	68.682	61.769	-65.896	-67.362
Ga	S	j9rlb0geq	2007/02/20	16:01:38	84.333	65.592	-66.638	69.209	62.439	-65.912	-67.381
Ga	S	j9rlb0gfq	2007/02/20	16:03:58	85.662	66.210	-66.655	69.749	63.118	-65.928	-67.399
Ga	S	j9rlb0ggq	2007/02/20	16:06:18	86.991	67.544	-66.909	71.139	64.408	-66.176	-67.660
Ga	S	j9rlc6p1q	2007/03/08	07:10:30	306.590	319.856	-73.546	322.321	317.727	-72.551	-74.592
Ga	S	j9rlc6p2q	2007/03/08	07:12:50	307.920	321.956	-73.511	324.464	319.790	-72.518	-74.555
Ga	S	j9rlc6p3q	2007/03/08	07:15:10	309.249	322.610	-73.207	324.993	320.540	-72.228	-74.235
Ga	S	j9rlc6p4q	2007/03/08	07:17:30	310.579	324.019	-73.206	326.402	321.949	-72.228	-74.234
Ga	S	j9rlc6p6q	2007/03/08	07:19:50	311.908	324.707	-72.907	326.976	322.726	-71.941	-73.919
Ga	S	j9rlc6p7q	2007/03/08	07:22:28	313.409	326.298	-72.906	328.566	324.317	-71.941	-73.918
Ga	S	j9rlc6p8q	2007/03/08	07:24:48	314.738	327.375	-72.921	329.624	325.410	-71.955	-73.934
Ga	S	j9rlc6p9q	2007/03/08	07:27:08	316.068	329.409	-72.561	331.627	327.462	-71.611	-73.556
Ga	S	j9rlc6paq	2007/03/08	07:29:28	317.397	329.510	-72.624	331.656	327.627	-71.671	-73.622
Ga	S	j9rlc6pbq	2007/03/08	07:31:48	318.727	330.266	-72.332	332.317	328.457	-71.392	-73.316
Ga	S	j9rlc6pcq	2007/03/08	07:34:08	320.056	331.048	-72.043	333.012	329.309	-71.115	-73.013
Ga	S	j9rlc6pdq	2007/03/08	07:36:28	321.386	332.458	-72.042	334.421	330.719	-71.114	-73.012
Ga	S	j9rlc6peq	2007/03/08	07:38:48	322.715	333.265	-71.757	335.148	331.591	-70.841	-72.714
Ga	S	j9rlc6pfq	2007/03/08	07:41:08	324.045	334.645	-72.071	336.574	332.935	-71.141	-73.042
Ga	S	j9rlc6pgq	2007/03/08	07:43:46	325.545	336.852	-72.358	338.867	335.074	-71.417	-73.343
Ga	S	j9rlc6phq	2007/03/08	07:46:06	326.875	337.987	-71.740	339.884	336.299	-70.824	-72.696
Ga	S	j9rlc6piq	2007/03/08	07:48:26	328.204	337.528	-71.826	339.332	335.923	-70.907	-72.785
Ga	S	j9rlc6pjq	2007/03/08	07:50:46	329.534	339.057	-71.208	340.780	337.511	-70.314	-72.140
Ga	S	j9rlc6pkq	2007/03/08	07:53:06	330.863	339.793	-71.542	341.525	338.244	-70.634	-72.488
Ga	S	j9rlj8h9q	2007/03/22	23:07:25	95.899	63.773	-69.573	66.374	60.864	-68.742	-70.430
Ga	S	j9rlj8hbq	2007/03/22	23:09:05	96.849	66.473	-66.741	68.558	64.197	-65.991	-67.511
Ga	S	j9rlj8hcq	2007/03/22	23:10:45	97.799	69.883	-66.766	71.860	67.732	-66.014	-67.539
Ga	S	j9rlj8hdq	2007/03/22	23:12:25	98.748	70.439	-66.990	72.463	68.231	-66.232	-67.768

Table B.1: Auroral footprints' main Alfvén wing (MAW) spot locations for Europa and Ganymede observed on the Northern and Southern Jovian hemispheres as published as supporting information to Bonfond et al. (2017b). (*continued*)

Sat.	Hem.	Obs ID	Date	Time	φ_{Sat}	φ_{fp}	λ_{fp}	$\Delta^{+}(\varphi_{\mathrm{fp}})$	$\Delta^{-}(\varphi_{\mathrm{fp}})$	$\Delta^{+}(\lambda_{\mathrm{fp}})$	$\Delta^{-}(\lambda_{\mathrm{fp}})$
Ga	S	j9rlj8heq	2007/03/22	23:14:05	99.698	71.469	-67.278	73.528	69.220	-66.512	-68.065
Ga	S	j9rlj8hfq	2007/03/22	23:15:45	100.647	73.911	-67.174	75.891	71.753	-66.411	-67.960
Ga	S	j9rlj8hgq	2007/03/22	23:17:25	101.597	72.996	-67.214	75.070	70.730	-66.450	-67.999
Ga	S	j9rlj8hhq	2007/03/22	23:19:05	102.547	73.024	-67.377	75.167	70.677	-66.610	-68.166
Ga	S	j9rlj0wsq	2007/04/13	17:58:27	326.329	337.365	-71.137	338.749	335.836	-70.355	-71.947
Ga	S	j9rlj0wtq	2007/04/13	17:59:37	326.994	337.301	-71.383	338.742	335.705	-70.592	-72.203
Ga	S	j9rlj0wuq	2007/04/13	18:00:47	327.658	338.229	-71.123	339.635	336.676	-70.341	-71.933
Ga	S	j9rlj0wvq	2007/04/13	18:01:57	328.323	338.713	-71.382	340.153	337.116	-70.591	-72.202
Ga	S	j9rlj0wwq	2007/04/13	18:03:07	328.988	339.418	-71.382	340.859	337.822	-70.591	-72.202
Ga	S	j9rlj0wxq	2007/04/13	18:04:17	329.653	340.073	-71.115	341.489	338.507	-70.333	-71.924
Ga	S	j9rlj0wyq	2007/04/13	18:05:27	330.317	340.725	-70.851	342.119	339.188	-70.078	-71.651
Ga	S	j9rlj0wzq	2007/04/13	18:06:37	330.982	340.936	-71.100	342.374	339.345	-70.319	-71.909
Ga	S	j9rlj0x0q	2007/04/13	18:07:47	331.647	341.367	-71.093	342.817	339.764	-70.312	-71.902
Ga	S	j9rlj0x1q	2007/04/13	18:08:57	332.312	341.760	-70.822	343.196	340.175	-70.050	-71.621
Ga	S	j9rlj0x2q	2007/04/13	18:10:07	332.977	342.195	-70.815	343.641	340.598	-70.043	-71.613
Ga	S	j9rlj0x3q	2007/04/13	18:11:17	333.641	-17.371	-70.807	-15.913	-18.979	-70.035	-71.606
Ga	S	j9rlj0x4q	2007/04/13	18:12:27	334.306	-16.665	-70.807	-15.208	-18.274	-70.035	-71.605
Ga	S	j9rlj0x5q	2007/04/13	18:13:37	334.971	-15.993	-70.546	-14.560	-17.572	-69.783	-71.336
Ga	S	j9rlj0x6q	2007/04/13	18:14:47	335.636	-15.287	-70.546	-13.854	-16.866	-69.783	-71.335
Ga	S	j9rld8daq	2007/05/19	18:22:52	349.835	-8.162	-69.973	-5.950	-10.617	-69.283	-70.682
Ga	S	j9rld8dbq	2007/05/19	18:25:12	351.164	-2.222	-69.473	-0.307	-4.326	-68.794	-70.171
Ga	S	j9rld8dcq	2007/05/19	18:27:32	352.494	-1.579	-69.436	0.367	-3.718	-68.759	-70.132
Ga	S	j9rld8ddq	2007/05/19	18:29:52	353.823	-0.682	-69.411	1.285	-2.845	-68.734	-70.106
Ga	S	j9rld8dfq	2007/05/19	18:32:12	355.152	0.730	-69.411	2.696	-1.433	-68.734	-70.106
Ga	S	j9rld8dgq	2007/05/19	18:34:50	356.653	1.289	-69.360	3.298	-0.922	-68.685	-70.053
Ga	S	j9rld8dhq	2007/05/19	18:37:10	357.982	2.541	-68.883	4.493	0.401	-68.220	-69.562
Ga	S	j9rld8diq	2007/05/19	18:39:30	359.312	4.372	-68.672	6.276	2.287	-68.015	-69.346
Ga	S	j9rld8djq	2007/05/19	18:41:50	0.641	4.415	-69.068	6.437	2.192	-68.402	-69.752
Ga	S	j9rld8dkq	2007/05/19	18:44:10	1.970	5.049	-69.029	7.103	2.788	-68.364	-69.711
Ga	S	j9rld8dlq	2007/05/19	18:46:30	3.300	7.851	-68.634	9.785	5.732	-67.978	-69.307
Ga	S	j9rld8dmq	2007/05/19	18:48:50	4.629	8.321	-68.818	10.324	6.122	-68.158	-69.495
Ga	S	j9rld8dnq	2007/05/19	18:51:10	5.958	9.405	-68.570	11.390	7.228	-67.916	-69.240
Ga	S	j9rld8doq	2007/05/19	18:53:48	7.459	11.176	-68.350	13.124	9.044	-67.702	-69.015
Ga	S	j9rld8dpq	2007/05/19	18:56:08	8.788	11.899	-68.544	13.905	9.698	-67.891	-69.213
Ga	S	j9rld8dqq	2007/05/19	18:58:28	10.117	13.494	-68.324	15.462	11.339	-67.677	-68.988
Ga	S	j9rld8drq	2007/05/19	19:00:48	11.447	14.398	-68.298	16.387	12.219	-67.652	-68.961
Ga	S	j9rld8dsq	2007/05/19	19:03:08	12.776	15.300	-68.272	17.310	13.098	-67.626	-68.933
Ga	S	j9rle3eyq	2007/05/24	16:40:10	72.290	57.377	-66.028	60.150	54.875	-65.436	-66.631
Ga	S	j9rle3ezq	2007/05/24	16:42:30	73.619	58.241	-66.069	60.977	55.768	-65.476	-66.674
Ga	S	j9rle3f0q	2007/05/24	16:44:50	74.948	58.840	-66.131	61.524	56.410	-65.535	-66.737
Ga	S	j9rle3f1q	2007/05/24	16:47:10	76.277	60.250	-66.130	62.935	57.820	-65.535	-66.737
Ga	S	j9rle3f3q	2007/05/24	16:49:30	77.606	60.859	-66.191	63.493	58.470	-65.593	-66.800
Ga	S	j9rle3f4q	2007/05/24	16:52:08	79.106	61.368	-66.049	63.901	59.064	-65.453	-66.657
Ga	S	j9rle3f5q	2007/05/24	16:54:28	80.435	62.260	-66.088	64.763	59.980	-65.491	-66.697
Ga	S	j9rle3f6q	2007/05/24	16:56:48	81.764	62.898	-66.146	65.358	60.655	-65.547	-66.757
Ga	S	j9rle3f7q	2007/05/24	16:59:08	83.094	63.287	-66.002	65.657	61.119	-65.404	-66.611
Ga	S	j9rle3f8q	2007/05/24	17:01:28	84.423	64.448	-66.241	66.841	62.262	-65.638	-66.856
Ga	S	j9rle3f9q	2007/05/24	17:03:48	85.752	65.105	-66.297	67.459	62.952	-65.693	-66.914
Ga	S	j9rle3faq	2007/05/24	17:06:08	87.081	65.777	-66.131	68.060	63.684	-65.529	-66.745
Ga	S	j9rle3fbq	2007/05/24	17:08:28	88.410	66.931	-66.371	69.235	64.820	-65.764	-66.990
Ga	S	j9rle3fcq	2007/05/24	17:11:06	89.910	68.766	-66.576	71.117	66.616	-65.965	-67.199
Ga	S	j9rle3fdq	2007/05/24	17:13:26	91.239	69.926	-66.820	72.301	67.757	-66.203	-67.449
Ga	S	j9rle3feq	2007/05/24	17:15:46	92.568	70.099	-66.686	72.377	68.011	-66.072	-67.313
Ga	S	j9rle3ffq	2007/05/24	17:18:06	93.897	70.068	-66.569	72.246	68.066	-65.956	-67.195
Ga	S	j9rle3fgq	2007/05/24	17:20:26	95.226	71.696	-66.776	73.917	69.657	-66.159	-67.407
Ga	S	j9rleaceq	2007/05/26	18:27:32	334.156	-14.662	-71.471	-13.041	-16.425	-70.652	-72.322
Ga	S	j9rleacfq	2007/05/26	18:29:52	335.485	-12.023	-69.425	-10.649	-13.494	-68.672	-70.202
Ga	S	j9rleachq	2007/05/26	18:32:12	336.815	-11.009	-69.347	-9.629	-12.487	-68.596	-70.121
Ga	S	j9rleaciq	2007/05/26	18:34:32	338.144	-9.993	-69.268	-8.608	-11.477	-68.520	-70.040
Ga	S	j9rleacjq	2007/05/26	18:36:52	339.474	-9.173	-69.151	-7.778	-10.665	-68.407	-69.919
Ga	S	j9rleaclq	2007/05/26	18:39:12	340.803	-7.958	-69.112	-6.560	-9.453	-68.369	-69.879
Ga	S	j9rleacmq	2007/05/26	18:41:32	342.132	-7.327	-68.957	-5.918	-8.834	-68.218	-69.718
Ga	S	j9rleacnq	2007/05/26	18:43:52	343.462	-6.602	-69.090	-5.159	-8.148	-68.348	-69.856
Ga	S	j9rleacvq	2007/05/26	19:49:47	21.017	20.424	-67.826	22.198	18.517	-67.124	-68.546
Ga	S	j9rleacxq	2007/05/26	19:52:07	22.346	21.215	-67.984	23.032	19.259	-67.278	-68.708
Ga	S	j9rleacyq	2007/05/26	19:54:27	23.676	22.686	-67.707	24.469	20.769	-67.009	-68.423
Ga	S	j9rleaczq	2007/05/26	19:56:47	25.005	23.286	-67.824	25.115	21.317	-67.123	-68.543
Ga	S	j9rlead1q	2007/05/26	19:59:07	26.334	24.510	-67.784	26.342	22.537	-67.084	-68.502
Ga	S	j9rlead2q	2007/05/26	20:01:45	27.835	25.727	-67.704	27.565	23.748	-67.007	-68.419
Ga	S	j9rlead3q	2007/05/26	20:04:05	29.164	26.118	-67.779	28.008	24.080	-67.081	-68.496
Ga	S	j9rlead4q	2007/05/26	20:06:25	30.493	27.153	-67.699	29.049	25.108	-67.003	-68.413
Ga	S	j9rlead5q	2007/05/26	20:08:45	31.823	28.564	-67.699	30.460	26.519	-67.003	-68.413
Ga	S	j9rlead6q	2007/05/26	20:11:05	33.152	25.918	-69.005	28.179	23.445	-68.279	-69.750
Ga	S	j9rlead7q	2007/05/26	20:13:25	34.482	27.713	-68.761	29.918	25.306	-68.041	-69.499
Ga	S	j9rlead8q	2007/05/26	20:15:45	35.811	31.376	-67.692	33.333	29.262	-66.997	-68.404
Ga	S	j9rlead9q	2007/05/26	20:18:05	37.140	32.409	-67.611	34.373	30.287	-66.919	-68.320
Ga	S	j9rleadaq	2007/05/26	20:20:43	38.641	33.313	-67.764	35.327	31.133	-67.068	-68.476
Ga	S	j9rleadbq	2007/05/26	20:23:03	39.970	34.655	-67.449	36.634	32.518	-66.762	-68.153
Ga	S	j9rleadcq	2007/05/26	20:25:23	41.299	34.509	-68.029	36.635	32.199	-67.329	-68.746
Ga	S	j9rleaddq	2007/05/26	20:27:43	42.629	36.594	-67.560	38.626	34.394	-66.871	-68.266
Ga	S	j9rleadeq	2007/05/26	20:30:03	43.958	36.559	-67.863	38.700	34.231	-67.168	-68.575
Ga	S	j9rlf2p7q	2007/06/02	08:27:38	333.959	342.661	-70.778	343.588	341.789	-69.981	-71.603
Ga	S	j9rlf2p8q	2007/06/02	08:29:58	335.288	343.884	-70.096	344.771	343.046	-69.322	-70.897
Ga	S	j9rlf2p9q	2007/06/02	08:32:18	336.618	345.068	-70.135	345.950	344.234	-69.359	-70.936
Ga	S	j9rlf2paq	2007/06/02	08:34:38	337.947	345.792	-70.250	346.660	344.972	-69.471	-71.055
Ga	S	j9rlf2pcq	2007/06/02	08:36:58	339.276	347.153	-70.025	348.009	346.343	-69.254	-70.823
Ga	S	j9rlf2pdq	2007/06/02	08:39:36	340.777	347.788	-69.954	348.614	347.006	-69.186	-70.749

Table B.1: Auroral footprints' main Alfvén wing (MAW) spot locations for Europa and Ganymede observed on the Northern and Southern Jovian hemispheres as published as supporting information to Bonfond et al. (2017b). (*continued*)

Sat.	Hem.	Obs ID	Date	Time	φ_{Sat}	φ_{fp}	λ_{fp}	$\Delta^{+}(\varphi_{\mathrm{fp}})$	$\Delta^{-}(\varphi_{\mathrm{fp}})$	$\Delta^{+}(\lambda_{\mathrm{fp}})$	$\Delta^{-}(\lambda_{\mathrm{fp}})$
Ga	S	j9rlf2peq	2007/06/02	08:41:56	342.106	348.706	-69.807	349.512	347.942	-69.044	-70.596
Ga	S	j9rlf2pfq	2007/06/02	08:44:16	343.435	349.889	-69.845	350.690	349.129	-69.080	-70.635
Ga	S	j9rlf2pgq	2007/06/02	08:46:36	344.765	351.269	-69.624	352.061	350.518	-68.866	-70.407
Ga	S	j9rlf2phq	2007/06/02	08:48:56	346.094	352.426	-69.442	353.203	351.686	-68.690	-70.219
Ga	S	j9rlf2piq	2007/06/02	08:51:16	347.423	353.809	-69.225	354.578	353.077	-68.480	-69.995
Ga	S	j9rlf2pjq	2007/06/02	08:53:36	348.753	355.220	-69.225	355.989	354.488	-68.480	-69.994
Ga	S	j9rlf2pkq	2007/06/02	08:55:56	350.082	355.939	-69.119	356.687	355.227	-68.376	-69.884
Ga	S	j9rlf2plq	2007/06/02	08:58:34	351.582	357.976	-69.046	358.732	357.256	-68.306	-69.810
Ga	S	j9rlf2pmq	2007/06/02	09:00:54	352.912	-0.857	-68.869	-0.113	-1.566	-68.134	-69.626
Ga	S	j9rlf2pnq	2007/06/02	09:03:14	354.241	0.113	-68.940	0.848	-0.588	-68.203	-69.700
Ga	S	j9rlf2poq	2007/06/02	09:05:34	355.570	1.066	-68.799	1.785	0.379	-68.066	-69.553
Ga	S	j9rlf2ppq	2007/06/02	09:07:54	356.900	1.812	-68.905	2.517	1.137	-68.170	-69.663
Ga	S	ob3001xqq	2009/09/11	03:50:40	38.998	32.864	-68.084	36.927	26.802	-66.041	-70.351
Ga	S	ob3001xqq	2009/09/11	03:52:10	39.853	33.771	-68.084	37.833	27.708	-66.041	-70.351
Ga	S	ob3001xqq	2009/09/11	03:53:40	40.707	38.088	-67.977	41.661	32.881	-65.945	-70.227
Ga	S	ob3001xqq	2009/09/11	03:55:10	41.562	38.995	-67.977	42.568	33.788	-65.945	-70.227
Ga	S	ob3001xqq	2009/09/11	03:56:40	42.416	39.280	-67.823	42.885	34.038	-65.804	-70.056
Ga	S	ob3001xqq	2009/09/11	03:58:10	43.271	39.016	-67.935	42.808	33.445	-65.905	-70.181
Ga	S	ob3001xqq	2009/09/11	03:59:40	44.125	39.609	-67.858	43.418	34.019	-65.835	-70.096
Ga	S	ob3001xqq	2009/09/11	04:01:10	44.980	40.029	-68.009	43.954	34.220	-65.973	-70.266
Ga	S	ob3001xqq	2009/09/11	04:02:40	45.834	39.990	-67.779	43.966	34.119	-65.762	-70.010
Ga	S	ob3001xqq	2009/09/11	04:04:10	46.689	40.581	-67.703	44.575	34.688	-65.692	-69.925
Ga	S	ob3001xqq	2009/09/11	04:05:40	47.543	41.077	-67.740	45.140	35.058	-65.726	-69.967
Ga	S	ob3001xqq	2009/09/11	04:07:10	48.398	43.342	-67.932	47.283	37.513	-65.903	-70.180
Ga	S	ob3001xqq	2009/09/11	04:08:40	49.253	44.423	-67.705	48.266	38.794	-65.695	-69.926
Ga	S	ob3001xqq	2009/09/11	04:10:10	50.107	44.748	-67.970	48.758	38.794	-65.936	-70.222
Ga	S	ob3001xqq	2009/09/11	04:11:40	50.962	45.655	-67.970	49.665	39.701	-65.936	-70.222
Ga	S	ob3001xqq	2009/09/11	04:13:10	51.816	47.058	-67.818	50.949	41.330	-65.798	-70.053
Ga	S	ob3001xqq	2009/09/11	04:14:40	52.671	47.965	-67.818	51.856	42.237	-65.798	-70.053
Ga	S	ob3001xqq	2009/09/11	04:16:10	53.525	48.783	-67.932	52.724	42.954	-65.903	-70.180
Ga	S	ob3001xqq	2009/09/11	04:17:40	54.380	49.778	-67.818	53.670	44.051	-65.798	-70.053
Ga	S	ob3001xqq	2009/09/11	04:19:10	55.234	50.189	-67.970	54.199	44.235	-65.936	-70.222
Ga	S	ob3001xqq	2009/09/11	04:20:40	56.089	51.592	-67.818	55.484	45.865	-65.798	-70.053
Ga	S	ob3001xqq	2009/09/11	04:22:10	56.943	51.908	-68.084	55.971	45.846	-66.041	-70.351
Ga	S	ob3001xqq	2009/09/11	04:23:40	57.798	53.317	-67.932	57.259	47.488	-65.903	-70.180
Ga	S	ob3001xqq	2009/09/11	04:25:10	58.652	54.313	-67.818	58.204	48.585	-65.798	-70.053
Ga	S	ob3001xqq	2009/09/11	04:26:40	59.507	54.724	-67.970	58.733	48.770	-65.936	-70.222
Ga	S	ob3001xqq	2009/09/11	04:28:10	60.361	55.630	-67.970	59.640	49.676	-65.936	-70.222
Ga	S	ob3001xqq	2009/09/11	04:29:40	61.216	57.033	-67.818	60.925	51.306	-65.798	-70.053
Ga	S	ob3001xqq	2009/09/11	04:31:10	62.070	57.350	-68.084	61.412	51.287	-66.041	-70.351
Ga	S	ob3001xqq	2009/09/11	04:32:40	62.925	58.351	-67.970	62.361	52.397	-65.936	-70.222
Ga	S	oc0v04dyq	2013/01/25	05:39:36	88.365	69.231	-66.409	71.667	66.438	-64.098	-69.034
Ga	S	oc0v04dyq	2013/01/25	05:41:06	89.219	70.105	-66.158	72.513	67.394	-63.872	-68.746
Ga	S	oc0v04dyq	2013/01/25	05:42:36	90.073	70.729	-66.462	73.184	67.869	-64.145	-69.097
Ga	S	oc0v04dyq	2013/01/25	05:44:06	90.928	71.591	-66.086	74.003	68.856	-63.807	-68.664
Ga	S	oc0v04dyq	2013/01/25	05:45:36	91.782	72.213	-66.390	74.671	69.328	-64.079	-69.015
Ga	S	oc0vb4e2q	2013/01/25	06:17:28	109.930	82.268	-67.633	85.598	76.921	-65.157	-70.531
Ga	S	oc0vb4e2q	2013/01/25	06:18:58	110.784	82.362	-67.757	85.840	76.708	-65.263	-70.688
Ga	S	oc0vb4e2q	2013/01/25	06:20:28	111.638	83.846	-68.181	87.379	77.991	-65.638	-71.191
Ga	S	oc0vb4e2q	2013/01/25	06:21:58	112.493	83.342	-67.883	86.977	77.354	-65.371	-70.848
Ga	S	oc0v02wpq	2013/02/14	21:47:16	122.426	84.417	-69.076	86.669	82.022	-66.350	-72.309
Ga	S	oc0v02wpq	2013/02/14	21:48:46	123.281	85.182	-69.300	87.461	82.754	-66.543	-72.584
Ga	S	oc0v02wpq	2013/02/14	21:50:16	124.135	86.394	-69.595	88.696	83.938	-66.798	-72.949
Ga	S	oc0v02wpq	2013/02/14	21:51:46	124.989	86.851	-69.527	89.159	84.388	-66.739	-72.865
Ga	S	oc0v02wpq	2013/02/14	21:53:16	125.844	87.158	-69.689	89.501	84.650	-66.878	-73.065
Ga	S	oc0vb2wtq	2013/02/14	22:25:08	143.995	103.300	-73.435	106.305	99.926	-69.982	-78.182
Ga	S	oc0vb2wtq	2013/02/14	22:26:38	144.849	104.742	-73.521	107.734	101.381	-70.051	-78.315
Ga	S	oc0vb2wtq	2013/02/14	22:28:08	145.703	105.251	-73.627	108.284	101.835	-70.134	-78.484
Ga	S	oc0vb2wtq	2013/02/14	22:29:38	146.558	105.606	-74.244	108.789	101.975	-70.616	-79.503
Ga	S	oc0v03jgq	2013/02/21	22:52:36	140.627	102.532	-72.193	105.281	99.795	-68.851	-76.575
Ga	S	oc0v03jgq	2013/02/21	22:54:06	141.481	103.653	-72.428	106.439	100.879	-69.042	-76.915
Ga	S	oc0v03jgq	2013/02/21	22:55:36	142.335	104.293	-72.908	107.155	101.444	-69.428	-77.625
Ga	S	oc0v03jgq	2013/02/21	22:57:06	143.190	104.631	-72.664	107.450	101.822	-69.232	-77.259
Ga	S	oc0v03jgq	2013/02/21	22:58:36	144.044	106.196	-73.407	109.143	103.262	-69.824	-78.399
Ga	S	oc0vb3jkq	2013/02/21	23:29:58	161.910	124.588	-76.938	128.986	120.876	-72.445	-85.232
Ga	S	oc0vb3jkq	2013/02/21	23:31:28	162.765	125.803	-77.290	129.642	121.988	-72.685	-83.783
Ga	S	oc0vb3jkq	2013/02/21	23:32:58	163.619	127.039	-77.655	132.123	123.112	-72.928	-85.259
Ga	S	oc0vb3jkq	2013/02/21	23:34:28	164.474	127.945	-77.655	133.029	124.019	-72.928	-85.259
Ga	S	oc0v05r9q	2013/03/09	05:43:43	76.959	61.419	-66.265	63.857	58.212	-63.639	-69.296
Ga	S	oc0v05r9q	2013/03/09	05:45:13	77.813	61.380	-66.487	63.864	57.913	-63.833	-69.561
Ga	S	oc0v05r9q	2013/03/09	05:46:43	78.668	61.971	-66.505	64.465	58.437	-63.848	-69.585
Ga	S	oc0v05r9q	2013/03/09	05:48:13	79.522	62.560	-66.524	65.064	58.958	-63.864	-69.608
Ga	S	oc0v05r9q	2013/03/09	05:49:43	80.376	62.451	-66.921	65.049	58.461	-64.211	-70.086
Ga	S	oc0vb5ruq	2013/03/09	06:21:35	98.525	73.756	-67.251	77.423	67.663	-64.475	-70.545
Ga	S	oc0vb5ruq	2013/03/09	06:23:05	99.379	74.663	-67.251	78.330	68.569	-64.475	-70.545
Ga	S	oc0vb5ruq	2013/03/09	06:24:35	100.233	75.570	-67.251	79.237	69.476	-64.475	-70.545
Ga	S	oc0vb5ruq	2013/03/09	06:26:05	101.087	75.458	-67.146	79.239	69.165	-64.379	-70.429

Appendix C

Observed Footprint Reference Ovals

Table C.1: Reduced accuracy representation of the reference ovals fitted to auroral footprints by Bonfond et al. (2017b).

The columns contain the following data:
1. "φ_{Sat}" ... System III CML of the satellite
2, 4, 6, 8. "$\varphi_{\mathrm{fp,xx}}$" ... System III CML of the spot in degrees
3, 5, 7, 9. "$\lambda_{\mathrm{fp,xx}}$" ... planeto-centric latitude of the spot in degrees

G ... Ganymede, N ... Northern hemisphere, E ... Europa, S ... Southern hemisphere

φ_{Sat}	$\varphi_{\mathrm{fp,GN}}$	$\lambda_{\mathrm{fp,GN}}$	$\varphi_{\mathrm{fp,GS}}$	$\lambda_{\mathrm{fp,GS}}$	$\varphi_{\mathrm{fp,EN}}$	$\lambda_{\mathrm{fp,EN}}$	$\varphi_{\mathrm{fp,ES}}$	$\lambda_{\mathrm{fp,ES}}$
0	-	-	4.29	-69.00	-	-	-	-
1	-	-	5.10	-68.96	-	-	-	-
2	-	-	5.91	-68.93	-	-	-	-
3	-	-	6.72	-68.89	-	-	-	-
4	-	-	7.54	-68.86	-	-	-	-
5	-	-	8.35	-68.83	-	-	-	-
6	-	-	9.16	-68.79	-	-	-	-
7	-	-	9.97	-68.76	-	-	-	-
8	-	-	10.78	-68.73	-	-	-	-
9	-	-	11.59	-68.70	-	-	-	-
10	-	-	12.41	-68.67	-	-	-	-
11	-	-	13.22	-68.64	-	-	-	-
12	-	-	14.03	-68.61	-	-	-	-
13	-	-	14.84	-68.58	-	-	-	-
14	-	-	15.65	-68.55	-	-	-	-
15	-	-	16.46	-68.52	-	-	-	-
16	-	-	17.27	-68.49	-	-	19.12	-64.54
17	-	-	18.08	-68.46	-	-	19.79	-64.38
18	-	-	18.88	-68.43	-	-	20.46	-64.22
19	-	-	19.69	-68.40	-	-	21.14	-64.08
20	-	-	20.50	-68.36	-	-	21.81	-63.93
21	-	-	21.30	-68.33	-	-	22.49	-63.80
22	-	-	22.10	-68.30	-	-	23.17	-63.67
23	-	-	22.91	-68.26	-	-	23.86	-63.55
24	-	-	23.71	-68.23	-	-	24.54	-63.43
25	-	-	24.51	-68.19	-	-	25.22	-63.32
26	-	-	25.31	-68.16	-	-	25.90	-63.22
27	-	-	26.11	-68.12	-	-	26.59	-63.12
28	-	-	26.91	-68.08	-	-	27.27	-63.03
29	-	-	27.70	-68.04	-	-	27.96	-62.95
30	-	-	28.50	-68.00	-	-	28.64	-62.87

Table C.1: Reference ovals fitted to auroral footprints by Bonfond et al. (2017b). (*cont.*)

φ_{Sat}	$\varphi_{\mathrm{fp,GN}}$	$\lambda_{\mathrm{fp,GN}}$	$\varphi_{\mathrm{fp,GS}}$	$\lambda_{\mathrm{fp,GS}}$	$\varphi_{\mathrm{fp,EN}}$	$\lambda_{\mathrm{fp,EN}}$	$\varphi_{\mathrm{fp,ES}}$	$\lambda_{\mathrm{fp,ES}}$
31	-	-	29.29	-67.96	-	-	29.32	-62.79
32	-	-	30.08	-67.92	-	-	30.01	-62.72
33	-	-	30.87	-67.88	-	-	30.69	-62.66
34	-	-	31.66	-67.84	-	-	31.37	-62.60
35	-	-	32.45	-67.80	-	-	32.06	-62.54
36	-	-	33.23	-67.75	-	-	32.74	-62.49
37	-	-	34.01	-67.71	-	-	33.42	-62.44
38	-	-	34.79	-67.67	-	-	34.10	-62.40
39	-	-	35.57	-67.62	-	-	34.78	-62.36
40	-	-	36.35	-67.58	-	-	35.46	-62.32
41	-	-	37.12	-67.54	-	-	36.14	-62.29
42	-	-	37.89	-67.50	-	-	36.81	-62.26
43	-	-	38.66	-67.45	-	-	37.49	-62.23
44	-	-	39.42	-67.41	-	-	38.17	-62.21
45	-	-	40.18	-67.37	-	-	38.84	-62.19
46	-	-	40.94	-67.33	-	-	39.52	-62.17
47	-	-	41.69	-67.29	-	-	40.19	-62.16
48	-	-	42.44	-67.25	-	-	40.86	-62.15
49	-	-	43.18	-67.21	-	-	41.53	-62.14
50	-	-	43.92	-67.18	-	-	42.21	-62.13
51	-	-	44.65	-67.14	-	-	42.88	-62.12
52	-	-	45.38	-67.10	-	-	43.55	-62.12
53	-	-	46.11	-67.07	-	-	44.22	-62.12
54	-	-	46.82	-67.04	-	-	44.89	-62.12
55	-	-	47.54	-67.01	-	-	45.55	-62.12
56	-	-	48.24	-66.98	-	-	46.22	-62.13
57	-	-	48.94	-66.95	-	-	46.89	-62.13
58	-	-	49.64	-66.93	-	-	47.56	-62.14
59	-	-	50.32	-66.90	-	-	48.22	-62.15
60	-	-	51.00	-66.88	-	-	48.89	-62.16
61	138.71	75.67	51.68	-66.86	126.85	71.02	49.56	-62.17
62	139.15	75.31	52.35	-66.84	127.29	70.60	50.22	-62.18
63	139.49	74.96	53.01	-66.82	127.72	70.18	50.89	-62.19
64	139.76	74.60	53.66	-66.80	128.14	69.76	51.56	-62.21
65	139.95	74.24	54.31	-66.79	128.56	69.34	52.22	-62.22
66	140.08	73.87	54.94	-66.78	128.97	68.91	52.89	-62.24
67	140.16	73.50	55.58	-66.77	129.38	68.49	53.56	-62.26
68	140.20	73.12	56.20	-66.76	129.78	68.06	54.22	-62.28
69	140.21	72.73	56.82	-66.75	130.19	67.64	54.89	-62.30
70	140.20	72.33	57.43	-66.74	130.59	67.22	55.55	-62.32
71	140.18	71.93	58.03	-66.74	131.00	66.80	56.22	-62.34
72	140.15	71.52	58.63	-66.73	131.41	66.38	56.89	-62.37
73	140.11	71.10	59.22	-66.73	131.82	65.96	57.56	-62.39
74	140.09	70.68	59.80	-66.73	132.23	65.55	58.22	-62.41
75	140.07	70.26	60.38	-66.73	132.64	65.14	58.89	-62.44
76	140.06	69.83	60.95	-66.74	133.06	64.74	59.56	-62.47
77	140.07	69.40	61.51	-66.74	133.47	64.34	60.23	-62.50
78	140.09	68.97	62.07	-66.75	133.89	63.95	60.90	-62.53
79	140.13	68.54	62.63	-66.76	134.32	63.56	61.57	-62.56
80	140.19	68.12	63.17	-66.76	134.74	63.17	62.25	-62.59
81	140.27	67.69	63.72	-66.77	135.16	62.80	62.92	-62.62
82	140.37	67.27	64.25	-66.79	135.59	62.42	63.59	-62.65
83	140.48	66.85	64.79	-66.80	136.02	62.06	64.26	-62.69
84	140.61	66.44	65.32	-66.81	136.44	61.70	64.94	-62.72
85	140.75	66.04	65.84	-66.83	136.87	61.35	65.61	-62.76
86	140.91	65.64	66.37	-66.85	137.30	61.01	66.29	-62.80
87	141.09	65.25	66.89	-66.86	137.72	60.67	66.97	-62.84
88	141.28	64.87	67.40	-66.88	138.15	60.34	67.65	-62.88
89	141.47	64.49	67.92	-66.90	138.57	60.02	68.33	-62.92
90	141.68	64.13	68.43	-66.93	138.99	59.70	69.01	-62.97
91	141.90	63.77	68.94	-66.95	139.42	59.40	69.69	-63.01
92	142.13	63.42	69.46	-66.98	139.83	59.10	70.37	-63.06
93	142.37	63.08	69.97	-67.00	140.25	58.81	71.05	-63.11
94	142.61	62.75	70.48	-67.03	140.67	58.52	71.73	-63.16
95	142.86	62.43	70.99	-67.06	141.08	58.25	72.42	-63.21
96	143.11	62.11	71.50	-67.09	141.49	57.98	73.10	-63.27

Table C.1: Reference ovals fitted to auroral footprints by Bonfond et al. (2017b). (*cont.*)

φ_{Sat}	$\varphi_{\mathrm{fp,GN}}$	$\lambda_{\mathrm{fp,GN}}$	$\varphi_{\mathrm{fp,GS}}$	$\lambda_{\mathrm{fp,GS}}$	$\varphi_{\mathrm{fp,EN}}$	$\lambda_{\mathrm{fp,EN}}$	$\varphi_{\mathrm{fp,ES}}$	$\lambda_{\mathrm{fp,ES}}$
97	143.38	61.80	72.02	-67.12	141.89	57.71	73.79	-63.32
98	143.64	61.50	72.53	-67.16	142.30	57.46	74.48	-63.38
99	143.91	61.21	73.05	-67.19	142.70	57.21	75.17	-63.44
100	144.19	60.93	73.57	-67.23	143.10	56.97	75.86	-63.51
101	144.47	60.65	74.10	-67.27	143.49	56.74	76.55	-63.57
102	144.75	60.38	74.63	-67.31	143.88	56.51	77.24	-63.64
103	145.03	60.12	75.16	-67.35	144.27	56.29	77.93	-63.71
104	145.32	59.87	75.70	-67.40	144.65	56.08	78.62	-63.78
105	145.62	59.62	76.24	-67.44	145.04	55.87	79.32	-63.86
106	145.91	59.37	76.79	-67.49	145.41	55.67	80.01	-63.94
107	146.21	59.14	77.34	-67.55	145.79	55.48	80.70	-64.02
108	146.51	58.91	77.90	-67.60	146.16	55.29	81.40	-64.10
109	146.82	58.68	78.47	-67.66	146.53	55.10	82.10	-64.19
110	147.12	58.46	79.04	-67.71	146.89	54.93	82.79	-64.28
111	147.44	58.25	79.62	-67.78	147.26	54.75	83.49	-64.37
112	147.75	58.04	80.21	-67.84	147.61	54.59	84.19	-64.47
113	148.07	57.83	80.81	-67.91	147.97	54.43	84.89	-64.57
114	148.39	57.63	81.41	-67.98	148.32	54.27	85.59	-64.67
115	148.71	57.43	82.03	-68.05	148.68	54.12	86.28	-64.78
116	149.04	57.24	82.65	-68.13	149.03	53.97	86.98	-64.89
117	149.37	57.06	83.28	-68.21	149.37	53.83	87.68	-65.00
118	149.71	56.88	83.93	-68.29	149.72	53.69	88.38	-65.12
119	150.05	56.70	84.58	-68.38	150.06	53.56	89.08	-65.24
120	150.39	56.53	85.24	-68.47	150.40	53.43	89.78	-65.36
121	150.73	56.36	85.91	-68.57	150.74	53.30	90.48	-65.49
122	151.08	56.20	86.59	-68.67	151.08	53.18	91.18	-65.63
123	151.43	56.04	87.28	-68.77	151.41	53.06	91.88	-65.76
124	151.79	55.88	87.98	-68.88	151.75	52.95	92.58	-65.90
125	152.15	55.74	88.69	-68.99	152.08	52.84	93.27	-66.05
126	152.51	55.59	89.41	-69.11	152.41	52.73	93.97	-66.20
127	152.87	55.45	90.14	-69.23	152.75	52.62	94.67	-66.36
128	153.24	55.32	90.89	-69.35	153.08	52.52	95.36	-66.51
129	153.61	55.19	91.64	-69.48	153.41	52.43	96.06	-66.68
130	153.98	55.06	92.40	-69.62	153.74	52.33	96.75	-66.85
131	154.36	54.94	93.17	-69.76	154.07	52.24	97.44	-67.02
132	154.74	54.83	93.96	-69.90	154.40	52.15	98.13	-67.20
133	155.12	54.72	94.75	-70.05	154.74	52.07	98.81	-67.38
134	155.50	54.61	95.55	-70.21	155.07	51.99	99.50	-67.57
135	155.88	54.51	96.36	-70.37	155.40	51.91	100.18	-67.76
136	156.26	54.42	97.18	-70.53	155.74	51.83	100.86	-67.96
137	156.65	54.33	98.01	-70.70	156.07	51.76	101.54	-68.16
138	157.03	54.24	98.85	-70.88	156.41	51.69	102.21	-68.37
139	157.42	54.16	99.70	-71.06	156.75	51.62	102.89	-68.59
140	157.81	54.09	100.55	-71.24	157.09	51.56	103.55	-68.81
141	158.20	54.02	101.42	-71.43	157.43	51.49	104.22	-69.03
142	158.58	53.95	102.29	-71.63	157.77	51.43	104.87	-69.26
143	158.97	53.89	103.17	-71.82	158.12	51.38	105.53	-69.50
144	159.36	53.84	104.05	-72.03	158.46	51.33	106.18	-69.74
145	159.75	53.78	104.94	-72.24	158.81	51.28	106.82	-69.98
146	160.13	53.74	105.84	-72.45	159.17	51.23	107.46	-70.23
147	160.52	53.70	106.75	-72.67	159.52	51.19	108.09	-70.49
148	160.90	53.66	107.66	-72.89	159.88	51.14	108.71	-70.76
149	161.29	53.62	108.57	-73.11	160.24	51.11	109.32	-71.02
150	161.67	53.59	109.49	-73.34	160.60	51.07	-	-
151	162.05	53.57	110.42	-73.57	160.97	51.04	-	-
152	162.43	53.54	111.35	-73.80	161.33	51.01	-	-
153	162.81	53.53	112.28	-74.04	161.71	50.99	-	-
154	163.19	53.51	113.22	-74.28	162.08	50.97	-	-
155	163.57	53.50	114.16	-74.52	162.46	50.95	-	-
156	163.94	53.49	115.11	-74.77	162.84	50.94	-	-
157	164.32	53.49	116.06	-75.01	163.22	50.92	-	-
158	164.69	53.49	117.01	-75.26	163.61	50.92	-	-
159	165.06	53.49	117.96	-75.51	164.00	50.91	-	-
160	165.43	53.49	118.92	-75.76	164.39	50.91	-	-
161	165.80	53.50	119.88	-76.01	164.79	50.92	-	-
162	166.17	53.51	120.84	-76.27	165.19	50.93	-	-

Table C.1: Reference ovals fitted to auroral footprints by Bonfond et al. (2017b). (*cont.*)

φ_{Sat}	$\varphi_{\mathrm{fp,GN}}$	$\lambda_{\mathrm{fp,GN}}$	$\varphi_{\mathrm{fp,GS}}$	$\lambda_{\mathrm{fp,GS}}$	$\varphi_{\mathrm{fp,EN}}$	$\lambda_{\mathrm{fp,EN}}$	$\varphi_{\mathrm{fp,ES}}$	$\lambda_{\mathrm{fp,ES}}$
163	166.54	53.52	121.80	-76.52	165.59	50.94	-	-
164	166.91	53.54	122.77	-76.77	165.99	50.96	-	-
165	167.27	53.56	123.74	-77.02	166.40	50.98	-	-
166	167.64	53.58	124.71	-77.27	166.81	51.00	-	-
167	168.01	53.60	125.68	-77.52	167.23	51.03	-	-
168	168.37	53.63	126.66	-77.77	167.65	51.06	-	-
169	168.74	53.66	127.64	-78.01	168.07	51.10	-	-
170	169.11	53.69	-	-	168.49	51.14	-	-
171	169.47	53.72	-	-	168.91	51.18	-	-
172	169.84	53.76	-	-	169.34	51.23	-	-
173	170.21	53.79	-	-	169.77	51.29	-	-
174	170.58	53.83	-	-	170.20	51.34	-	-
175	170.95	53.88	-	-	170.64	51.41	-	-
176	171.32	53.92	-	-	171.08	51.47	-	-
177	171.70	53.97	-	-	171.51	51.54	-	-
178	172.07	54.02	-	-	171.95	51.62	-	-
179	172.45	54.07	-	-	172.40	51.69	-	-
180	172.83	54.12	-	-	172.84	51.78	-	-
181	173.22	54.18	-	-	173.28	51.86	-	-
182	173.60	54.24	-	-	173.73	51.95	-	-
183	173.99	54.30	-	-	174.18	52.04	-	-
184	174.38	54.36	-	-	174.62	52.14	-	-
185	174.77	54.43	-	-	175.07	52.24	-	-
186	175.17	54.50	-	-	175.52	52.34	-	-
187	175.57	54.57	-	-	175.97	52.45	-	-
188	175.97	54.64	-	-	176.42	52.55	-	-
189	176.38	54.71	-	-	176.86	52.66	-	-
190	176.79	54.79	-	-	177.31	52.78	-	-
191	177.20	54.87	-	-	177.76	52.89	-	-
192	177.62	54.95	-	-	178.21	53.01	-	-
193	178.04	55.03	-	-	178.65	53.13	-	-
194	178.46	55.12	-	-	179.10	53.25	-	-
195	178.88	55.21	-	-	179.54	53.38	-	-
196	179.31	55.30	-	-	179.98	53.50	-	-
197	179.74	55.39	-	-	180.42	53.62	-	-
198	180.18	55.49	-	-	180.86	53.75	-	-
199	180.61	55.59	-	-	181.30	53.88	-	-
200	181.05	55.69	-	-	181.74	54.00	-	-
201	181.49	55.79	-	-	182.17	54.13	-	-
202	181.94	55.89	-	-	182.60	54.26	-	-
203	182.39	56.00	-	-	183.03	54.39	-	-
204	182.83	56.11	-	-	183.46	54.51	-	-
205	183.29	56.21	-	-	183.89	54.64	-	-
206	183.74	56.33	-	-	184.31	54.76	-	-
207	184.19	56.44	-	-	184.73	54.89	-	-
208	184.65	56.55	-	-	185.15	55.01	-	-
209	185.10	56.67	-	-	185.56	55.13	-	-
210	185.56	56.79	-	-	185.98	55.25	-	-
211	186.02	56.91	-	-	186.39	55.36	-	-
212	186.48	57.03	-	-	186.80	55.48	-	-
213	186.94	57.15	-	-	187.20	55.59	-	-
214	187.40	57.27	-	-	187.60	55.70	-	-
215	187.86	57.39	-	-	188.01	55.81	-	-
216	188.33	57.52	-	-	188.40	55.91	-	-
217	188.79	57.64	-	-	188.80	56.01	-	-
218	189.25	57.77	-	-	189.20	56.11	-	-
219	189.71	57.90	-	-	189.59	56.20	-	-
220	190.17	58.03	-	-	189.98	56.29	-	-
221	190.63	58.15	-	-	190.37	56.38	-	-
222	191.09	58.28	-	-	190.75	56.47	-	-
223	191.55	58.41	-	-	-	-	-	-
224	192.01	58.54	-	-	-	-	-	-
225	192.47	58.67	-	-	-	-	-	-
226	192.93	58.80	-	-	-	-	-	-
227	193.39	58.93	-	-	-	-	-	-
228	193.84	59.06	-	-	-	-	-	-

Table C.1: Reference ovals fitted to auroral footprints by Bonfond et al. (2017b). (*cont.*)

φ_{Sat}	$\varphi_{\mathrm{fp,GN}}$	$\lambda_{\mathrm{fp,GN}}$	$\varphi_{\mathrm{fp,GS}}$	$\lambda_{\mathrm{fp,GS}}$	$\varphi_{\mathrm{fp,EN}}$	$\lambda_{\mathrm{fp,EN}}$	$\varphi_{\mathrm{fp,ES}}$	$\lambda_{\mathrm{fp,ES}}$
229	194.30	59.19	-	-	-	-	-	-
230	194.76	59.32	-	-	-	-	-	-
231	195.21	59.45	-	-	-	-	-	-
232	195.67	59.57	-	-	-	-	-	-
233	196.12	59.70	-	-	-	-	-	-
234	196.58	59.83	-	-	-	-	-	-
235	197.04	59.96	-	-	-	-	-	-
236	197.49	60.08	-	-	-	-	-	-
237	197.95	60.21	-	-	-	-	-	-
238	198.41	60.34	-	-	-	-	-	-
239	198.87	60.46	-	-	-	-	-	-
240	199.32	60.59	-	-	-	-	-	-
241	199.79	60.71	-	-	-	-	-	-
242	200.25	60.83	-	-	-	-	-	-
243	200.71	60.96	-	-	-	-	-	-
244	201.18	61.08	-	-	-	-	-	-
245	201.65	61.21	-	-	-	-	-	-
246	202.12	61.33	-	-	-	-	-	-
247	202.59	61.45	-	-	-	-	-	-
248	203.07	61.58	-	-	-	-	-	-
249	203.55	61.70	-	-	-	-	-	-
250	204.04	61.83	-	-	-	-	-	-
251	204.53	61.95	-	-	-	-	-	-
252	205.02	62.08	-	-	-	-	-	-
253	205.52	62.20	-	-	-	-	-	-
254	206.02	62.33	-	-	-	-	-	-
255	206.53	62.46	-	-	-	-	-	-
256	207.05	62.59	-	-	-	-	-	-
257	207.57	62.72	-	-	-	-	-	-
258	208.09	62.85	-	-	-	-	-	-
259	208.62	62.99	-	-	-	-	-	-
260	209.16	63.13	-	-	-	-	-	-
261	209.71	63.26	-	-	-	-	-	-
262	210.26	63.41	-	-	-	-	-	-
263	210.81	63.55	-	-	-	-	-	-
264	211.38	63.70	-	-	-	-	-	-
265	211.95	63.85	-	-	-	-	-	-
266	212.52	64.01	-	-	-	-	-	-
267	213.11	64.16	-	-	-	-	-	-
268	213.70	64.33	-	-	-	-	-	-
269	214.29	64.49	-	-	-	-	-	-
270	214.89	64.66	-	-	-	-	-	-
271	215.50	64.83	-	-	-	-	-	-
272	216.12	65.01	-	-	-	-	-	-
273	216.74	65.19	-	-	-	-	-	-
274	217.37	65.38	-	-	-	-	-	-
275	218.01	65.57	-	-	-	-	-	-
276	218.65	65.77	-	-	-	-	-	-
277	219.29	65.97	-	-	-	-	-	-
278	219.95	66.17	-	-	-	-	-	-
279	220.61	66.38	-	-	-	-	-	-
280	221.27	66.59	-	-	-	-	-	-
281	221.95	66.80	-	-	-	-	-	-
282	222.62	67.02	-	-	-	-	-	-
283	223.31	67.24	-	-	-	-	-	-
284	224.00	67.47	-	-	-	-	-	-
285	224.70	67.70	-	-	-	-	-	-
286	225.41	67.93	-	-	-	-	-	-
287	226.13	68.16	-	-	-	-	-	-
288	226.85	68.39	-	-	-	-	-	-
289	227.59	68.63	-	-	-	-	-	-
290	228.33	68.86	-	-	-	-	-	-
291	229.09	69.10	-	-	-	-	-	-
292	229.85	69.34	-	-	-	-	-	-
293	230.63	69.58	-	-	-	-	-	-
294	231.42	69.81	-	-	-	-	-	-

Table C.1: Reference ovals fitted to auroral footprints by Bonfond et al. (2017b). (*cont.*)

φ_{Sat}	$\varphi_{\mathrm{fp,GN}}$	$\lambda_{\mathrm{fp,GN}}$	$\varphi_{\mathrm{fp,GS}}$	$\lambda_{\mathrm{fp,GS}}$	$\varphi_{\mathrm{fp,EN}}$	$\lambda_{\mathrm{fp,EN}}$	$\varphi_{\mathrm{fp,ES}}$	$\lambda_{\mathrm{fp,ES}}$
295	232.22	70.05	-	-	-	-	-	-
296	233.03	70.29	-	-	-	-	-	-
297	233.85	70.52	-	-	-	-	-	-
298	234.68	70.76	-	-	-	-	-	-
299	235.53	70.99	-	-	-	-	-	-
300	236.39	71.23	-	-	-	-	-	-
301	237.26	71.46	315.47	-75.09	-	-	-	-
302	238.14	71.69	316.37	-74.91	-	-	-	-
303	239.02	71.92	317.28	-74.72	-	-	-	-
304	239.92	72.14	318.17	-74.54	-	-	-	-
305	240.82	72.36	319.07	-74.36	-	-	-	-
306	241.74	72.58	319.95	-74.19	-	-	-	-
307	242.65	72.80	320.84	-74.02	-	-	-	-
308	243.57	73.02	321.72	-73.85	-	-	-	-
309	244.49	73.23	322.59	-73.68	-	-	-	-
310	245.41	73.44	323.47	-73.52	-	-	-	-
311	246.34	73.64	324.33	-73.36	-	-	-	-
312	247.25	73.84	325.20	-73.20	-	-	-	-
313	248.17	74.04	326.06	-73.05	-	-	-	-
314	249.08	74.24	326.91	-72.90	-	-	-	-
315	249.98	74.43	327.76	-72.75	-	-	-	-
316	250.87	74.61	328.61	-72.61	-	-	-	-
317	251.75	74.79	329.46	-72.47	-	-	-	-
318	252.61	74.97	330.30	-72.33	-	-	-	-
319	253.47	75.14	331.14	-72.19	-	-	-	-
320	254.31	75.31	331.97	-72.06	-	-	-	-
321	255.13	75.47	332.80	-71.94	-	-	-	-
322	255.93	75.63	333.63	-71.81	-	-	-	-
323	256.72	75.78	334.46	-71.69	-	-	-	-
324	257.48	75.93	335.28	-71.57	-	-	-	-
325	258.23	76.07	336.10	-71.46	-	-	-	-
326	258.96	76.21	336.92	-71.34	-	-	-	-
327	259.66	76.34	337.73	-71.23	-	-	-	-
328	260.35	76.47	338.55	-71.13	-	-	-	-
329	261.01	76.59	339.36	-71.02	-	-	-	-
330	261.65	76.71	340.17	-70.92	-	-	-	-
331	262.28	76.83	340.97	-70.82	-	-	-	-
332	262.88	76.94	341.78	-70.73	-	-	-	-
333	263.46	77.04	342.59	-70.64	-	-	-	-
334	264.03	77.15	343.39	-70.55	-	-	-	-
335	264.58	77.24	344.19	-70.46	-	-	-	-
336	265.11	77.34	345.00	-70.37	-	-	-	-
337	265.63	77.43	345.80	-70.29	-	-	-	-
338	266.13	77.52	346.60	-70.21	-	-	-	-
339	266.62	77.61	347.40	-70.14	-	-	-	-
340	267.11	77.69	348.20	-70.06	-	-	-	-
341	267.58	77.78	349.00	-69.99	-	-	-	-
342	268.05	77.86	349.80	-69.92	-	-	-	-
343	268.52	77.94	350.60	-69.85	-	-	-	-
344	268.98	78.02	351.40	-69.79	-	-	-	-
345	269.45	78.10	352.20	-69.72	-	-	-	-
346	269.92	78.18	353.00	-69.66	-	-	-	-
347	-89.61	78.26	353.81	-69.60	-	-	-	-
348	-89.13	78.34	354.61	-69.54	-	-	-	-
349	-88.63	78.43	355.41	-69.49	-	-	-	-
350	-88.12	78.51	356.22	-69.44	-	-	-	-
351	-87.59	78.60	357.02	-69.39	-	-	-	-
352	-87.05	78.69	357.83	-69.34	-	-	-	-
353	-86.47	78.79	358.63	-69.29	-	-	-	-
354	-85.88	78.89	359.44	-69.24	-	-	-	-
355	-	-	0.24	-69.20	-	-	-	-
356	-	-	1.05	-69.16	-	-	-	-
357	-	-	1.86	-69.11	-	-	-	-
358	-	-	2.67	-69.07	-	-	-	-
359	-	-	3.48	-69.04	-	-	-	-

Appendix D

JRM09 Model Schmidt Coefficients

Table D.1: Schmidt coefficients in units of Gauss (G) of the JRM09 model by Connerney et al. (2018). Details on the definition, usage and interpretation of Schmidt coefficients can be found in Chapter 2.

$l = 1$ to $l = 7$				$l = 8$ to $l = 10$			
l	m	g_l^m	h_l^m	l	m	g_l^m	h_l^m
1	0	4.102447	0	8	0	0.100592	0
1	1	-0.714983	0.213305	8	1	0.019344	-0.024097
2	0	0.116704	0	8	2	-0.067029	-0.116146
2	1	-0.568358	-0.420273	8	3	0.001537	0.092870
2	2	0.486895	0.193532	8	4	-0.041242	-0.009119
3	0	0.040186	0	8	5	-0.008672	0.027545
3	1	-0.377911	-0.329573	8	6	-0.037406	-0.024461
3	2	0.159263	0.420845	8	7	-0.007324	0.012073
3	3	-0.027105	-0.275442	8	8	-0.024332	-0.028873
4	0	-0.346454	0	9	0	0.096718	0
4	1	-0.082476	0.319945	9	1	-0.030462	-0.084674
4	2	-0.024061	0.278112	9	2	0.002609	-0.013838
4	3	-0.110838	-0.009261	9	3	0.020713	0.056977
4	4	-0.178372	0.003671	9	4	0.033296	-0.020563
5	0	-0.180236	0	9	5	-0.025231	0.030815
5	1	0.046839	0.453479	9	6	0.017871	-0.007212
5	2	0.161600	-0.007490	9	7	-0.011482	0.013525
5	3	-0.164020	0.062685	9	8	0.012765	-0.002101
5	4	-0.026007	0.108596	9	9	-0.019768	0.015676
5	5	-0.036607	0.096084	10	0	-0.022995	0
6	0	-0.208196	0	10	1	0.020097	-0.046926
6	1	0.099929	0.145331	10	2	0.021278	0.044458
6	2	0.117918	-0.105929	10	3	0.034983	-0.023786
6	3	-0.125747	0.005686	10	4	0.029676	-0.022043
6	4	0.026697	0.128717	10	5	0.000163	0.001641
6	5	0.011132	-0.041478	10	6	0.018065	-0.013616
6	6	0.075849	0.036044	10	7	-0.000465	-0.020315
7	0	0.005984	0	10	8	0.028978	0.014118
7	1	0.046659	-0.076263	10	9	0.005745	-0.007143
7	2	-0.064957	-0.109484	10	10	0.012989	0.016765
7	3	-0.025165	0.026333				
7	4	-0.064485	0.053942				
7	5	0.018553	-0.060508				
7	6	-0.028929	-0.015260				
7	7	0.029680	-0.056842				

Appendix E

MATLAB Scripts

E.1 General Overview

The following sections include the MATLAB code of the three most important programs and their subroutines developed for the analysis. Some of the functions are used multiple times – their code is only included once. However, for clarity, the list below shall give an overview of all the used functions. A higher list level is to be understood as, "subroutine of ...".

ModelComparisonMetric:

- ReadFPdata
- ReadJRM09data
- ReadFPpath
- distanceabsolute
  - skipgap
  - ptsintrack
- plotabsdistance
- disttopath
- plotdisttopath

FootprintComparison_PolarPlots:

- ReadFPdata
- PolarPlotSetup
- ProjectionParameters
- PlotFPpath
  - ReadFPpath

    - PolarProjection (using the `Spherical2AzimuthalEquidistant` function by von Laven 2015)

- ReadFPpath
- disttopath
- PlotFootprintConnections
    - PolarProjection
- PolarPlotFootprints
    - PolarProjection
    - LatLonErrorbars

FootprintComparison_v2:

- TraceFieldLines_fct_v3
    - CalcFieldLines_ell
        * srfdist_ell
        * MagneticField
            · MagneticPotential
            · currentsheet

E.2 ModelComparisonMetric

```
%% ModelComparisonMetric
%
% PURPOSE:
%   (1) Determine the distances between modeled and observed footprints
%       on the planetary surface for different magnetic field models (VIP4,
%       VIPAL). Plot the distances as a function of satellite SIII
%       longitude incl. a comparison to the observational error.
%   (2) Determine the distances between modeled footprints and the
%       corresponding point on the observed reference oval parallel and
%       normal to the oval for different magnetic field models (VIP4,
%       VIPAL, JRM09). Plot the distances as functions of satellite SIII
%       longitude.
%
% AUTHOR: Nina Sejkora
%
% DATE OF LAST REVISION: 26-Apr-2018
%
% INPUT ARGUMENTS:
%     * model ... magnetic field model for which to do the analysis.
%           Possible options: 'VIP4','VIPAL','JRM09'
%     * hemisphere ... hemisphere of Jupiter for which to do the analysis.
%           Possible options: 'North', 'South'
%     * configstructfile ... .mat-file containing the config information
```

```
%           where to find files, plot setup etc.
%     * imgprefix ... prefix of file name with which to save the image
%
% OUTPUT ARGUMENTS: -

function [  ] = ...
    ( model,hemisphere,configstructfile,imgprefix )

global JupiterRadius ;
JupiterRadius=71492000; %Jupiter equatorial radius in m
JupiterFlattening = 0.064935;

%ellipsoid describing Jupiter's shape
JupiterSpheroid = oblateSpheroid;
JupiterSpheroid.SemimajorAxis=JupiterRadius;
JupiterSpheroid.InverseFlattening=1/JupiterFlattening;


%% Test of input arguments

%check if correct number of input arguments are specified
minargs = 4;
maxargs = 4;
narginchk(minargs,maxargs)
%check if input arguments are of the correct data type (and size)
validateattributes(imgprefix,{'char'},{})
validateattributes(configstructfile,{'char'},{})
validateattributes(hemisphere,{'char'},{})
validateattributes(model,{'char'},{})

%check if the string specified for 'hemisphere' is valid
hemisphere = validatestring(hemisphere,{'North','South'});

%abbreviation for hemisphere (used in file names)
if strcmp(hemisphere,'North')
    hemshort='n';
else
    hemshort='s';
end

%check if the string specified for 'model' is valid
model = validatestring(model,{'VIP4','VIPAL','JRM09'});

%% load config file

configdata = load(configstructfile);
fn = fieldnames(configdata);
configdata=configdata.(fn{1});

%% in- & output file name

%current directory = where the program is located
programfolder = pwd;

%input: get absolute path of input folder (not all MATLAB functions take
%relative paths)
```

```
cd(configdata.FPDataFolder)
FPdatafolder = pwd;
cd(programfolder)

%input: get absolute path of input folder (not all MATLAB functions take
%relative paths)
cd(configdata.JRM09datafolder)
JRM09datafolder = pwd;
cd(programfolder)

%input: get absolute path of input folder (not all MATLAB functions take
%relative paths)
cd(configdata.FPpathFolder)
FPpathfolder = pwd;
cd(programfolder)

%output: get absolute path of output folder (not all MATLAB functions take
%relative paths)
cd(configdata.ImageFolder)
imgfolder = pwd;
cd(programfolder)

%image names
imgname_absGa = ...
    [imgfolder,'\',imgprefix,'_',hemshort,'_',model,'_absGa.png'];
imgname_pathGa = ...
    [imgfolder,'\',imgprefix,'_',hemshort,'_',model,'_pathGa.png'];
imgname_absEu = ...
    [imgfolder,'\',imgprefix,'_',hemshort,'_',model,'_absEu.png'];
imgname_pathEu = ...
    [imgfolder,'\',imgprefix,'_',hemshort,'_',model,'_pathEu.png'];


%% read calculated and observed footprint positions

if ~strcmp(model,'JRM09')
    [ ~,~,~,...
        startpos,startpos(:,2),startpos(:,3),...
        FPcalc,FPcalc(:,2),FPcalc(:,3),...
        FPobs,FPobsErr,FPobsErr(:,2),...
        FPobs(:,2),FPobsErr(:,3),FPobsErr(:,4),...
        ~ ] = ReadFPdata( FPdatafolder,hemshort,model,0 );
else
    [ startpos,startpos(:,2),FPcalc,FPcalc(:,2) ] = ...
        ReadJRM09data( JRM09datafolder,configdata.JRM09names,hemisphere );
    startpos = [startpos(:,1),zeros(size(startpos,1),1),startpos(:,2)];
    FPcalc = [zeros(size(FPcalc,1),1),FPcalc(:,1),FPcalc(:,2)];
end

%% read observed footprint path

[Eupath,Gapath] = ...
    ReadFPpath(FPpathfolder,configdata.FPpathFilenames,hemisphere);

%% determine absolute distance between observed and calculated FPs
```

```
136 if ~strcmp(model,'JRM09')
        [ absdistance,ErrtoCalc,ErroppCalc ] = ...
            distanceabsolute( FPcalc,FPobs,FPobsErr,...
            JupiterSpheroid,configdata.trackstepsize );
    end
141
    %% plot absolute distances

    xiscalc = configdata.xaxis_calclongitude;

146 if ~strcmp(model,'JRM09')
        fig_absdistGa = ...
            plotabsdistance( startpos(:,1),startpos(:,3),FPcalc(:,3),...
            absdistance,ErrtoCalc,...
            'Ganymede',model,hemisphere,configdata.PlotFontSize,xiscalc );
151     fig_absdistEu = ...
            plotabsdistance( startpos(:,1),startpos(:,3),FPcalc(:,3),...
            absdistance,ErrtoCalc,...
            'Europa',model,hemisphere,configdata.PlotFontSize,xiscalc );
    end
156
    %% determine distance along and normal to path

    [ ~,distalongGa,distnormalGa,~,~ ] = ...
        disttopath( FPcalc,startpos(:,1),startpos(:,3),...
161     Gapath,JupiterSpheroid,'Ganymede' );
    [ ~,distalongEu,distnormalEu,~,~ ] = ...
        disttopath( FPcalc,startpos(:,1),startpos(:,3),...
        Eupath,JupiterSpheroid,'Europa' );


166
    %% plot distances along and normal to path

    fig_disttopathGa = ...
        plotdisttopath( startpos(:,1),startpos(:,3),FPcalc(:,3),...
171     distalongGa,distnormalGa,'Ganymede',hemisphere,model,...
        configdata.PlotFontSize,xiscalc );
    fig_disttopathEu = ...
        plotdisttopath( startpos(:,1),startpos(:,3),FPcalc(:,3),...
        distalongEu,distnormalEu,'Europa',hemisphere,model,...
176     configdata.PlotFontSize,xiscalc );


    %% save images
    if ~strcmp(model,'JRM09')
181     handles_list = [fig_absdistGa,fig_absdistEu,...
            fig_disttopathGa,fig_disttopathEu];
    else
        handles_list = [fig_disttopathGa,fig_disttopathEu];
    end
186 %set paper size & position
    set(handles_list,'PaperUnits','centimeters');
    set(handles_list,'Units','centimeters');
    set(handles_list,'PaperPositionMode','manual');
    set(handles_list,'PaperPosition',[0,0,30,18]);
191 %print image to png-file
```

```
if ~strcmp(model,'JRM09')
    print(fig_absdistGa,imgname_absGa,'-dpng');
    print(fig_absdistEu,imgname_absEu,'-dpng');
end
print(fig_disttopathGa,imgname_pathGa,'-dpng');
print(fig_disttopathEu,imgname_pathEu,'-dpng');

%reset paper size and position to default values
set(handles_list,'PaperUnits','default');
set(handles_list,'Units','default');
set(handles_list,'PaperPositionMode','default');
set(handles_list,'PaperPosition','default');

end
```

E.2.1 ReadFPdata

```
%% ReadFPdata
%
% PURPOSE: Read in calculated and observed footprint data
%
% INPUT ARGUMENTS:
%     * datafolder ... directory where data files are located
%     * hemshort ... short label of the hemisphere of Jupiter for which to
%           read the data ('n' or 's')
%     * model ... magnetic field model ('VIP4' or 'VIPAL')
%     * headerout ... =1 if header of read file should be in the output
%
% OUTPUT ARGUMENTS:
%     * ObsID ... unique ID of the observation
%     * ObsDate ... date of the observation
%     * ObsTime ... time of the observation
%     * StartR ... radial distance at which the calculation started =
%           orbital distance of moon in RJ
%     * StartLat ... latitude at which calculation started (deg)
%     * StartLon ... longitude at which calculation started (deg, SIII)
%     * FPcalcR ... radial coordinate of calculated footprint
%     * FPcalcLat ... latitudinal position of calculated footprint (deg)
%     * FPcalcLon ... longitudinal position of calculated footprint (deg,
%           SIII)
%     * FPobsLat ... latitudinal position of observed footprint (deg)
%     * FPobsLatErr_plus ... latitudinal uncertainty of observation in
%           positive direction
%     * FPobsLatErr_minus ... latitudinal uncertainty of observation in
%               negative direction
%     *  FPobsLon ... longitudinal position of observed footprint (deg, SIII)
%     * FPobsLonErr_plus ... longitudinal uncertainty of observation in
%               positive direction
%     * FPobsLonErr_minus ... longitudinal uncertainty of observation in
%               positive direction
%     * Distance_km ... absolute distance between observed and calculated
%               footprint on planetary surface in km
%     * varargout ... contains file header if headerout = 1
```

```
function [ ObsID,ObsDate,ObsTime,...
    StartR,StartLat,StartLon,...
    FPcalcR,FPcalcLat,FPcalcLon,...
    FPobsLat,FPobsLatErr_plus,FPobsLatErr_minus,...
    FPobsLon,FPobsLonErr_plus,FPobsLonErr_minus,...
    Distance_km,varargout ] = ...
    ReadFPdata( datafolder,hemshort,model,headerout )

if isempty(model)
    fpfile = fopen([datafolder,'\fpcomp_',hemshort,'_VIPAL_v2.txt']);
else
    fpfile = fopen([datafolder,'\fpcomp_',hemshort,'_',model,'_v2.txt']);
end

if nargout==17 && headerout==1
    varargout = textscan(fpfile,'%s',7,'delimiter',char(10));
    fpdata = textscan(fpfile,...
        '%s␣%s␣%s␣%f␣%f␣%f␣%f␣%f␣%f␣%f␣%f␣%f␣%f␣%f␣%f␣%f',...
        'delimiter',',','whitespace','\r');
else
    fpdata = textscan(fpfile,...
        '%s␣%s␣%s␣%f␣%f␣%f␣%f␣%f␣%f␣%f␣%f␣%f␣%f␣%f␣%f␣%f',...
        'delimiter',',','whitespace','\r','HeaderLines',7);
end


ObsID = fpdata{1,1};
ObsDate = fpdata{1,2};
ObsTime = fpdata{1,3};
StartR = fpdata{1,4};
StartLat = fpdata{1,5};
StartLon = fpdata{1,6};
FPcalcR = fpdata{1,7};
FPcalcLat = fpdata{1,8};
FPcalcLon = fpdata{1,9};
FPobsLat = fpdata{1,10};
FPobsLatErr_plus = fpdata{1,11};
FPobsLatErr_minus = fpdata{1,12};
FPobsLon = fpdata{1,13};
FPobsLonErr_plus = fpdata{1,14};
FPobsLonErr_minus = fpdata{1,15};
Distance_km = fpdata{1,16};


end
```

E.2.2 ReadJRM09data

```
%% ReadJRM09data
%
% PURPOSE: read in calculated footprint data from JRM09 model
%
% INPUT ARGUMENTS:
%     * datafolder ... directory where data files are located
%     * filenames ... filenames of data files
```

```
%     * hemisphere ... hemisphere for which to read in data ('North', 'South')
%
% OUTPUT ARGUMENTS:
%     * StartR ...  radial distance at which the calculation started
%                 = orbital distance of moon in RJ
%     * StartLon ... longitude at which calculation started (deg, SIII)
%     * FPcalcLat ... latitudinal position of calculated footprint (deg)
%     * FPcalcLon ... longitudinal position of calculated footprint (deg, SIII)

function [ StartR,StartLon,FPcalcLat,FPcalcLon ] = ...
    ReadJRM09data( datafolder,filenames,hemisphere )

if strcmp(hemisphere,'North')
    datafile = [datafolder,'\',filenames{1}];
else
    datafile = [datafolder,'\',filenames{2}];
end

filehandle = fopen(datafile);

fpdata = textscan(filehandle,'%f␣%f␣%f␣%f␣%f␣%f␣%f␣%f␣%f',...
    'headerlines',3,'endofline','\n');
fpdata = cell2mat(fpdata);

fclose(filehandle);

StartR = ones(size(fpdata,1),1);
StartR = [9.4*StartR;15*StartR];
StartLon = [fpdata(:,1);fpdata(:,1)];
FPcalcLat = [fpdata(:,6);fpdata(:,8)];
FPcalcLon = [fpdata(:,7);fpdata(:,9)];


end
```

E.2.3 ReadFPpath

```
%% ReadFPpath
%
% PURPOSE: read in observed footprint oval data
%
% INPUT ARGUMENTS:
%     * datafolder ... directory where data files are located
%     * filenames ... filenames of data files
%     * hemisphere ... hemisphere for which to read in data ('North', 'South')
%
% OUTPUT ARGUMENTS:
%     * pathEu ...  footprint oval for Europa
%     * pathGa ... footprint oval for Ganymede


function [ pathEu,pathGa ] = ReadFPpath( datafolder,filenames,hemisphere )

if strcmp(hemisphere,'North')
```

```
    Eufile = [datafolder,'\',filenames{1}];
    Gafile = [datafolder,'\',filenames{3}];
else
    Eufile = [datafolder,'\',filenames{2}];
    Gafile = [datafolder,'\',filenames{4}];
end

fileEu = fopen(Eufile);
fileGa = fopen(Gafile);

pathEu = textscan(fileEu,'%f␣%f␣%f','headerlines',1,'endofline','\n');
pathEu = cell2mat(pathEu);

pathGa = textscan(fileGa,'%f␣%f␣%f','headerlines',1,'endofline','\n');
pathGa = cell2mat(pathGa);

fclose(fileEu);
fclose(fileGa);
end
```

E.2.4 distanceabsolute

```
%% distanceabsolute
%
% PURPOSE: determine absolute distance between calculated and
% observed footprints
%
% INPUT ARGUMENTS:
%     * calcpts ... calculated footprints
%     * obspts ... observed footprints
%     * obserr ... uncertainty of observed footprints
%     * JupiterSpheroid ... ellipsoid describing Jupiter's shape
%     * deltatrack ... stepsize
%
% OUTPUT ARGUMENTS:
%     * absdistance ...  absolute distance between footprints
%     * ErrtoCalc ... uncertainty in direction observed
%           -> calculated footprint
%     * ErroppCalc ... uncertainty in opposite direction


function [ absdistance,ErrtoCalc,ErroppCalc ] = ...
    distanceabsolute( calcpts,obspts,obserr,JupiterSpheroid,deltatrack )

%change left-handed SIII longitude to right-handed
calcpts(:,3)=360-calcpts(:,3);
obspts(:,2)=360-obspts(:,2);
obserr(:,3:4)=360-obserr(:,3:4);

%% absolute distance
% absolute distance between calculated and observed footprint in meters

absdistance = distance(calcpts(:,2:3),obspts,JupiterSpheroid);

%% comparison to observation errors
```

```
ErrtoCalc = zeros(length(calcpts(:,1)),1);
ErroppCalc = zeros(length(calcpts(:,1)),1);

for ind=1:length(calcpts(:,1))
    [antiobs,antiobs(2)]=antipode(obspts(ind,1),obspts(ind,2));
    [anticalc,anticalc(2)]=antipode(calcpts(ind,2),calcpts(ind,3));

    % error in direction of obs -> calc

    %if calculated FP is in the area covered by the observation error
    if  ingeoquad(calcpts(ind,2),calcpts(ind,3),...
            [obserr(ind,2),obserr(ind,1)],[obserr(ind,3),obserr(ind,4)])
        [trackErrtoCalc,trackErrtoCalc(:,2)] = ...
            track2(calcpts(ind,2),calcpts(ind,3),...
            antiobs(1),antiobs(2),...
            JupiterSpheroid,'degrees',...
            ptsintrack(distance(calcpts(ind,2:3),...
            antiobs,JupiterSpheroid),deltatrack));
    else
        [trackErrtoCalc,trackErrtoCalc(:,2)] = ...
            track2(obspts(ind,1),obspts(ind,2),...
            calcpts(ind,2),calcpts(ind,3),...
            JupiterSpheroid,'degrees',...
            ptsintrack(distance(calcpts(ind,2:3),...
            antiobs,JupiterSpheroid),deltatrack));
    end

    % error in opposite direction to obs -> calc
    [trackErroppCalc,trackErroppCalc(:,2)] = ...
        track2(obspts(ind,1),obspts(ind,2),...
        anticalc(1),anticalc(2),...
        JupiterSpheroid,'degrees',...
        ptsintrack(distance(calcpts(ind,2:3),...
        antiobs,JupiterSpheroid),deltatrack));

    trackinsideErrtoCalc = ...
        ingeoquad(trackErrtoCalc(:,1),trackErrtoCalc(:,2),...
        [obserr(ind,2),obserr(ind,1)],[obserr(ind,3),obserr(ind,4)]);
    firstoutsideErrtoCalc = find(trackinsideErrtoCalc==0,1,'first');
    ErrtoCalc(ind) = distance(trackErrtoCalc(firstoutsideErrtoCalc,:),...
        obspts(ind,:),JupiterSpheroid);

    trackinsideErroppCalc = ...
        ingeoquad(trackErroppCalc(:,1),trackErroppCalc(:,2),...
        [obserr(ind,2),obserr(ind,1)],[obserr(ind,3),obserr(ind,4)]);
    firstoutsideErroppCalc = find(trackinsideErroppCalc==0,1,'first');
    ErroppCalc(ind) = distance(trackErroppCalc(firstoutsideErroppCalc,:),...
        obspts(ind,:),JupiterSpheroid);
end



end
```

skipgap

```
%% skipgap
%
% PURPOSE: fill data gaps with zero or NaN
%
% INPUT ARGUMENTS:
%     * oldarray ... original data set
%     * fillvalue ... which value to use as fillvalue (string: 'zero','NaN')
%     * gapsize ... minimum size of gaps to skip
%
% OUTPUT ARGUMENTS:
%     * newarray ... array with fillvalues


function [ newarray ] = skipgap( oldarray,fillvalue,gapsize )

validateattributes(fillvalue,{'char'},{})
fillvalue = validatestring(fillvalue,{'zero','NaN'});

sortedarr=sortrows(oldarray,1);
diffarray = abs(diff(sortedarr(:,1)));
indgap = find(diffarray>gapsize);

if strcmp(fillvalue,'NaN')
    for i=1:length(indgap)
        sortedarr = [sortedarr(1:indgap(i),:);NaN([1,size(sortedarr,2)]);...
            sortedarr((indgap(i)+1):end,:)];
        indgap = indgap+1;
    end
else
    for i=1:length(indgap)
        sortedarr = [sortedarr(1:indgap(i),:);...
            [sortedarr(indgap(i),1)+eps(sortedarr(indgap(i),1)),...
            zeros([1,size(sortedarr,2)-1])];...
            [sortedarr(indgap(i)+1,1)-eps(sortedarr(indgap(i)+1,1)),...
            zeros([1,size(sortedarr,2)-1])];...
            sortedarr((indgap(i)+1):end,:)];
        indgap = indgap+2;
    end
end

newarray = sortedarr;

end
```

ptsintrack

```
%% ptsintrack

function [ npts ] = ptsintrack( totaldist,stepsize )

npts=round(totaldist/stepsize);

end
```

E.2.5 plotabsdistance

```
%% ptsintrack

function [ npts ] = ptsintrack( totaldist,stepsize )

npts=round(totaldist/stepsize);

end
```

E.2.6 disttopath

```
%% disttopath
%
% PURPOSE: Determine distance between observed footprint oval and
% calculated footprints
%
% INPUT ARGUMENTS:
%     * calcpt ... calculated footprints
%     * calcstartR ... radial distance at which the calculation started
%           = orbital distance of moon in RJ
%     * calcstartLon ... longitude at which calculation started (deg, SIII)
%     * obspath ... observed footprint oval
%     * JupiterSpheroid ... ellipsoid describing Jupiter's shape
%     * satellite ... moon for which to do the analysis
%
% OUTPUT ARGUMENTS:
%     * distabs ... absolute distance to corresponding oval point
%     * distalong ... distance to corresponding oval point parallel to oval
%     * distnormal ... distance to corresponding oval point normal to oval
%     * pathpttrue ... oval points corresponding to satellite longitudes
%     * pathptcalc ... oval points closest to modeled footprints


function [ distabs,distalong,distnormal,pathpttrue,pathptcalc ] = ...
    disttopath( calcpt,calcstartR,calcstartLon,obspath,...
    JupiterSpheroid,satellite )

%change left-handed SIII longitude to right-handed
calcpt(:,3) = 360-calcpt(:,3);
calcstartLon = 360-calcstartLon;
obspath(:,1:2)=360-obspath(:,1:2);

diffpath = abs(diff(obspath(:,1)));
indgap = find(diffpath>1);
if length(indgap)==1
    obspath = [obspath(indgap+1:end,:);obspath(1:indgap,:)];
    disp([satellite,': restructured obspath'])
elseif length(indgap)>1
    error('more than 1 gap in obspath')
end


satellite = validatestring(satellite,{'Europa','Ganymede'});
```

```
if strcmp(satellite,'Ganymede')
    calcstartLon=calcstartLon(calcstartR>10);
    calcpt=calcpt(calcstartR>10,:);
else
    calcstartLon=calcstartLon(calcstartR<10);
    calcpt=calcpt(calcstartR<10,:);
end


pathpttrue = zeros(length(calcstartLon),2);
pathptcalc = zeros(length(calcstartLon),2);
distalong = zeros(length(calcstartLon),1);


for ind=1:length(calcstartLon)
    pathpttrue_ind = find(abs(obspath(:,1)-calcstartLon(ind))==...
        min(abs(obspath(:,1)-calcstartLon(ind))));
    if length(pathpttrue_ind)>1
        warning(['WARNING: ',...
            'Two path points at same distance from calc point, ',...
            'taking first one\nsatellite: %s\n',...
            'path indices: %g, %g\ncalc index: %g\n'],...
            satellite,pathpttrue_ind,ind)
        pathpttrue_ind=pathpttrue_ind(1);
    end

    pathptcalc_ind = find(distance(calcpt(ind,2:3),obspath(:,3:-1:2),...
        JupiterSpheroid)==...
        min(distance(calcpt(ind,2:3),obspath(:,3:-1:2),JupiterSpheroid)));

    if isequal(obspath(pathptcalc_ind,[3,2]),obspath(1,[3,2])) || ...
            isequal(obspath(pathptcalc_ind,[3,2]),obspath(end,[3,2]))
        pathptcalc(ind,:) = NaN(1,2);
    else
        pathptcalc(ind,:) = obspath(pathptcalc_ind,[3,2]);
    end

    if isequal(obspath(pathpttrue_ind,[3,2]),obspath(1,[3,2])) || ...
            isequal(obspath(pathpttrue_ind,[3,2]),obspath(end,[3,2]))
        pathpttrue(ind,:) = NaN(1,2);
        distalong(ind) = NaN;
    else
        pathpttrue(ind,:) = obspath(pathpttrue_ind,[3,2]);

        if pathpttrue_ind<=pathptcalc_ind
            pathsegment = obspath(pathpttrue_ind:pathptcalc_ind,[3,2]);
            signum = 1;
        else
            pathsegment = obspath(pathptcalc_ind:pathpttrue_ind,[3,2]);
            signum = -1;
        end
        segmentlengths = ...
            distance(pathsegment(1:end-1,:),pathsegment(2:end,:),...
            JupiterSpheroid);
        distalong(ind) = sum(segmentlengths)*signum;
    end
```

```
end
distnormal = distance(calcpt(:,2:3),pathptcalc,JupiterSpheroid);
distabs = distance(calcpt(:,2:3),pathpttrue,JupiterSpheroid);

distabs(isnan(distnormal))=NaN;
distalong(isnan(distnormal))=NaN;

%change output back to SIII longitude
pathpttrue(:,2) = 360-pathpttrue(:,2);
pathptcalc(:,2) = 360-pathptcalc(:,2);

end
```

E.2.7 plotdisttopath

```
%% ReadJRM09data
%
% PURPOSE: plot distance between oval and calculated footprints
%
% INPUT ARGUMENTS:
%     * startR ...  radial distance at which the calculation started
%               = orbital distance of moon in RJ
%     * startLon ... longitude at which calculation started (deg, SIII)
%     * calclon ... longitudinal position of calculated footprint (deg, SIII)
%     * distalong ... distance parallel to oval
%     * distnormal ... distance normal to oval
%     * satellite ... moon for which to do the analysis
%     * hemisphere ... Jovian hemisphere for which to do the analysis
%     * model ... magnetic field model to use
%     * PlotFontSize ... font size for plot annotations
%     * xiscalc ... =1 if calculated footprint longitude is to be the x-axis
%
% OUTPUT ARGUMENTS:
%     * fig_disttopath ... figure handle to plot


function [ fig_disttopath ] = ...
    plotdisttopath( startR,startLon,calclon,...
    distalong,distnormal,satellite,hemisphere,model,PlotFontSize,xiscalc )

fig_disttopath = figure;
hold on

validateattributes(xiscalc,{'numeric'},{'scalar'})
if xiscalc~=0 && xiscalc~=1
    error('ERROR\n"xiscalc" has to be 0 or 1.\nxiscalc = %g',xiscalc)
end
satellite = validatestring(satellite,{'Europa','Ganymede'});

if strcmp(satellite,'Ganymede')
    calclon=calclon(startR>10);
    startLon=startLon(startR>10);
    coloralong=[0,0,1];
    colornormal=[0,.6,1];
else
```

```
        calclon=calclon(startR<10);
        startLon=startLon(startR<10);
        coloralong=[1,0,0];
        colornormal=[1,.5,0];
    end

    distalong = distalong/1E6;
    distnormal = distnormal/1E6;

    if xiscalc==1
        xvalues = calclon;
        xlabelstring = 'Calculated Footprint Longitude (SIII) [deg]';
    else
        xvalues = startLon;
        xlabelstring = 'Satellite Longitude (SIII) [deg]';
    end

    plot(xvalues,distalong,'LineStyle','none','Color',coloralong,...
        'Marker','x','MarkerFaceColor',coloralong,'MarkerSize',7,'LineWidth',1);
    plot(xvalues,distnormal,'LineStyle','none','Color',colornormal,...
        'Marker','s','MarkerFaceColor','none','MarkerSize',7);
    plot([0,360],[0,0],'LineStyle','--','Color',[.4,.4,.4],'LineWidth',1)

    ylim([-6,15])
    xlim([0,360])
    set(gca,'FontSize',PlotFontSize)
    xlabel(xlabelstring)
    ylabel('Distance [1000 km]')
    title('Distances Between Calculated Footprints and Observed Oval',...
        'FontSize',PlotFontSize+2)
    legend({'Distance along oval','Distance normal to oval'});
    text(10,14.5,{[hemisphere,'ern hemisphere'];model;satellite},...
        'FontSize',PlotFontSize,'EdgeColor',[0 0 0],'VerticalAlignment','cap');

    hold off


    end
```

E.3 FootprintComparison_PolarPlots

```
%% FootprintComparison_PolarPlots
%
% PURPOSE:
% Plot polar projections of footprint data:
%     * modeled footprints
%     * observed footprints, with or without error bars
%     * footprint ovals
%     * connectors between sets of corresponding footprint points
%
% AUTHOR: Nina Sejkora
% DATE OF LAST REVISION: 26-Apr-2018
%
% INPUT ARGUMENTS:
%     * plotFPcalc ... =1 if calculated footprints shall be plotted
```

```
%     * plotFPobs ...  =1 if observed footprints shall be plotted
%     * plotobsErr ...  =1 if observational errorbars shall be plotted
%     * plotFPconnect ...  =1 if connections between calculated and observed
%           footprints shall be plotted
%     * plotobsOval ...  =1 if observed reference oval shall be plotted
%     * plotovalconnect_abs ...  =1 if connections between calculated
%           footprints and corresponding point on oval shall be plotted
%     * plotovalconnect_normal ... =1 if connections between calculated
%           footprints and closest point on oval shall be plotted
%     * imgprefix ... prefix of file name with which to save the image
%     * configstructfile ... .mat-file containing the config information
%           where to find files, plot setup etc.
%     * hemisphere ... hemisphere of Jupiter for which to do the analysis.
%           Possible options: 'North', 'South'
%     * model ... magnetic field model for which to do the analysis.
%           Possible options: 'VIP4','VIPAL','JRM09'
%
% OUTPUT ARGUMENTS: -


function [  ] = ...
    FootprintComparison_PolarPlots( plotFPcalc,plotFPobs,plotobsErr,...
    plotFPconnect,plotobsOval,plotovalconnect_abs,plotovalconnect_normal,...
    imgprefix,configstructfile,hemisphere,model )

global JupiterRadius ;
JupiterRadius=71492000; %Jupiter equatorial radius in m
JupiterFlattening = 0.064935;

%ellipsoid describing Jupiter's shape
JupiterSpheroid = oblateSpheroid;
JupiterSpheroid.SemimajorAxis=JupiterRadius;
JupiterSpheroid.InverseFlattening=1/JupiterFlattening;

%% Test of input arguments
%check if correct number of input arguments are specified
minargs = 10;
maxargs = 11;
narginchk(minargs,maxargs)
%check if input arguments are of the correct data type (and size)
validateattributes(plotFPcalc,{'numeric'},{'scalar'})
validateattributes(plotFPobs,{'numeric'},{'scalar'})
validateattributes(plotobsErr,{'numeric'},{'scalar'})
validateattributes(plotFPconnect,{'numeric'},{'scalar'})
validateattributes(plotobsOval,{'numeric'},{'scalar'})
validateattributes(plotovalconnect_abs,{'numeric'},{'scalar'})
validateattributes(plotovalconnect_normal,{'numeric'},{'scalar'})
validateattributes(imgprefix,{'char'},{})
validateattributes(configstructfile,{'char'},{})
validateattributes(hemisphere,{'char'},{})
validateattributes(model,{'char'},{})
%check if plotFPcalc,plotFPobs,plotobsErr,plotFPconnect,
%plotobsOval,plotovalconnect_abs,plotovalconnect_normal are boolean (0 or 1)
if plotFPcalc~=0 && plotFPcalc~=1
    error(['ERROR\n',...
        '"plotFPcalc" has to be 0 or 1.\nplotFPcalc = %g'],plotFPcalc)
```

```
end
if plotFPobs~=0 && plotFPobs~=1
    error(['ERROR\n',...
        '"plotFPobs" has to be 0 or 1.\nplotFPobs = %g'],plotFPobs)
end
if plotobsErr~=0 && plotobsErr~=1
    error(['ERROR\n',...
        '"plotobsErr" has to be 0 or 1.\nplotobsErr = %g'],plotobsErr)
end
if plotFPconnect~=0 && plotFPconnect~=1
    error(['ERROR\n',...
        '"plotFPconnect" has to be 0 or 1.\nplotFPconnect = %g'],...
        plotFPconnect)
end
if plotobsOval~=0 && plotobsOval~=1
    error(['ERROR\n',...
        '"plotobsOval" has to be 0 or 1.\nplotobsOval = %g'],plotobsOval)
end
if plotovalconnect_abs~=0 && plotovalconnect_abs~=1
    error(['ERROR\n',...
        '"plotovalconnect_along" has to be 0 or 1.\n',...
        'plotovalconnect_along = %g'],plotovalconnect_abs)
end
if plotovalconnect_normal~=0 && plotovalconnect_normal~=1
    error(['ERROR\n',...
        '"plotovalconnect_normal" has to be 0 or 1.\n',...
        'plotovalconnect_normal = %g'],plotovalconnect_normal)
end
%check if the string specified for 'hemisphere' is valid
hemisphere = validatestring(hemisphere,{'North','South'});

% check if model for calculated footprints is necessary (if plotFPcalc is 1)
if plotFPcalc==1
    %check if model is given
    if nargin==minargs
        %model is not given -> ERROR (it is necessary here, as plotFPcalc==1)
        error(['ERROR\n',...
            'If calculated footprints are to be plotted, ',...
            '"model" needs to be specified'])
    else
        %model is given -> validate if it is the proper string
        model = validatestring(model,{'VIP4','VIPAL','JRM09'});
    end
else
    %model not necessary here (plotFPcalc==0) -> set to empty
    model = [];
end


%abbreviation for hemisphere (used in file names)
if strcmp(hemisphere,'North')
    hemshort='n';
else
    hemshort='s';
end

```

```
%% load config file

configdata = load(configstructfile);
fn = fieldnames(configdata);
configdata=configdata.(fn{1});

%% in- & output file name

%current directory = where the program is located
programfolder = pwd;

%input: get absolute path of input folder (not all MATLAB functions take
%relative paths)
cd(configdata.FPDataFolder)
FPdatafolder = pwd;
cd(programfolder)

%input: get absolute path of input folder (not all MATLAB functions take
%relative paths)
cd(configdata.JRM09datafolder)
JRM09datafolder = pwd;
cd(programfolder)

%input: get absolute path of input folder (not all MATLAB functions take
%relative paths)
cd(configdata.FPpathFolder)
FPpathfolder = pwd;
cd(programfolder)

%output: get absolute path of output folder (not all MATLAB functions take
%relative paths)
cd(configdata.ImageFolder)
imgfolder = pwd;
cd(programfolder)

if plotFPcalc == 1
    imagename = [imgfolder,'\',imgprefix,'_',hemshort,'_',model,'.png'];
else
    imagename = [imgfolder,'\',imgprefix,'_',hemshort,'.png'];
end

%% read footprint data

if ~strcmp(model,'JRM09')
    [ ~,~,~,...
        startpos,startpos(:,2),startpos(:,3),...
        FPcalc,FPcalc(:,2),FPcalc(:,3),...
        FPobs,FPobsErr,FPobsErr(:,2),...
        FPobs(:,2),FPobsErr(:,3),FPobsErr(:,4),...
        ~ ] = ReadFPdata( FPdatafolder,hemshort,model,0 );
else
    [ startpos,startpos(:,2),FPcalc,FPcalc(:,2) ] = ...
        ReadJRM09data( JRM09datafolder,configdata.JRM09names,hemisphere );
    startpos = [startpos(:,1),zeros(size(startpos,1),1),startpos(:,2)];
    FPcalc = [zeros(size(FPcalc,1),1),FPcalc(:,1),FPcalc(:,2)];
end
```

```
%% Set up polar plots
PlotFontSize = configdata.PlotFontSize;
plotradius = configdata.PlotRadius;
plotcenter = configdata.PlotCenter; %center of the plot
OutermostLat = configdata.OutermostLatitude;
LatCircDist = configdata.LatitudeCircleDistance;
NLatCirc = (90-OutermostLat)/LatCircDist;

PolarPlotSetup( ...
    hemisphere,plotradius,plotcenter,LatCircDist,NLatCirc,PlotFontSize )

[ centerLat,projectionradius ] = ...
    ProjectionParameters( hemisphere,plotradius,LatCircDist,NLatCirc );

plothandles = [];
legendstrings = {};

%% plot oval fitted through observations by Bonfond e.a.

if plotobsOval==1
    [ plotpathEu,plotpathGa ] = ...
        PlotFPpath( FPpathfolder,configdata.FPpathFilenames,hemisphere,...
        centerLat,plotcenter,projectionradius );
    plothandles = [plothandles,plotpathEu,plotpathGa];
    legendstrings = [legendstrings,'Europa FP oval','Ganymede FP oval'];
end

%% determine distance along and normal to path

if (plotovalconnect_abs==1 || plotovalconnect_normal==1)
    [Eupath,Gapath] = ...
        ReadFPpath(FPpathfolder,configdata.FPpathFilenames,hemisphere);

    [ ~,~,~,pathpttrueGa,pathptcalcGa ] = ...
        disttopath( FPcalc,startpos(:,1),startpos(:,3),...
        Gapath,JupiterSpheroid,'Ganymede' );
    [ ~,~,~,pathpttrueEu,pathptcalcEu ] = ...
        disttopath( FPcalc,startpos(:,1),startpos(:,3),...
        Eupath,JupiterSpheroid,'Europa' );

    pathpttrue = [pathpttrueEu;pathpttrueGa];
    pathptcalc = [pathptcalcEu;pathptcalcGa];
end


%% plot connections calc-oval

if plotovalconnect_abs==1
    [ plotEu_connect,plotGa_connect ] = ...
        PlotFootprintConnections( pathpttrue(:,1),pathpttrue(:,2),...
        FPcalc(:,2),FPcalc(:,3),...
        startpos(:,1),centerLat,plotcenter,projectionradius );
```

```
        legendstrings = ...
            [legendstrings,'Europa connections','Ganymede connections'];
    plothandles = [plothandles,plotEu_connect,plotGa_connect];
end
if plotovalconnect_normal==1
    [ plotEu_connect,plotGa_connect ] = ...
        PlotFootprintConnections( pathptcalc(:,1),pathptcalc(:,2),...
        FPcalc(:,2),FPcalc(:,3),...
        startpos(:,1),centerLat,plotcenter,projectionradius );
    legendstrings = ...
        [legendstrings,'Europa connections','Ganymede connections'];
    plothandles = [plothandles,plotEu_connect,plotGa_connect];
end


%% plot observed footprints

if plotFPobs==1
    [ plotEu_obs,plotGa_obs ] = ...
        PolarPlotFootprints( FPobs(:,1),FPobs(:,2),...
        startpos(:,1),centerLat,plotcenter,projectionradius,...
        'obs',0);
    plothandles = [plothandles,plotEu_obs,plotGa_obs];
    legendstrings = [legendstrings,'Europa observed','Ganymede observed'];
end

%% plot error bars

if plotobsErr==1
    [ plotEu_Err,plotGa_Err ] = ...
        PolarPlotFootprints( FPobs(:,1),FPobs(:,2),...
        startpos(:,1),centerLat,plotcenter,projectionradius,...
        'obs',1,[FPobsErr(:,1),FPobsErr(:,2)],[FPobsErr(:,3),FPobsErr(:,4)]);
    plothandles = [plothandles,plotEu_Err,plotGa_Err];
    legendstrings = [legendstrings,'Europa errorbars','Ganymede errorbars'];
end

%% plot connections (if desired)

if plotFPconnect==1
    [ plotEu_connect,plotGa_connect ] = ...
        PlotFootprintConnections( FPobs(:,1),FPobs(:,2),...
        FPcalc(:,2),FPcalc(:,3),...
        startpos(:,1),centerLat,plotcenter,projectionradius );
    plothandles = [plothandles,plotEu_connect,plotGa_connect];
    legendstrings = ...
        [legendstrings,'Europa connections','Ganymede connections'];
end

%% plot calculated footprints

if plotFPcalc==1
    [ plotEu_calc,plotGa_calc ] = ...
        PolarPlotFootprints( FPcalc(:,2),FPcalc(:,3),...
        startpos(:,1),centerLat,plotcenter,projectionradius,...
        'calc');
```

```
    plothandles = [plothandles,plotEu_calc,plotGa_calc];
    legendstrings = ...
        [legendstrings,'Europa calculated','Ganymede calculated'];
end

%% plot annotations

if ~isempty(model)
    title({[model,', ',hemisphere,'ern hemisphere'];''},...
        'FontSize',PlotFontSize+2);
else
    title({[hemisphere,'ern hemisphere'];''},'FontSize',PlotFontSize+2);
end
legend(plothandles,legendstrings,'Location','SouthEastOutside',...
    'FontSize',PlotFontSize+2);

%% save image

%set paper size & position
set(gcf,'PaperUnits','centimeters');
set(gcf,'Units','centimeters');
set(gcf,'PaperPositionMode','manual');
set(gcf,'PaperPosition',[0,0,30,18]);
%print image to png-file
print(gcf,imagename,'-dpng');

%reset paper size and position to default values
set(gcf,'PaperUnits','default');
set(gcf,'Units','default');
set(gcf,'PaperPositionMode','default');
set(gcf,'PaperPosition','default');

end
```

E.3.1 PolarPlotSetup

```
%% PolarPlotSetup
%
% PURPOSE: setup of polar plots (plot and annotate lat/lon grid)
%
% INPUT ARGUMENTS:
%     * hemisphere ... hemisphere for which to plot the grid ('North', 'South')
%     * plotradius ... radius of plot
%     * plotcenter ...  center of plot
%     * LatCircDist ... distance between latitude circles
%     * NLatCirc ... number of latitude circles to draw
%     * font ... font size for plot annotations
%
% OUTPUT ARGUMENTS: -


function [  ] = PolarPlotSetup( hemisphere,plotradius,plotcenter,...
    LatCircDist,NLatCirc,font )
%% plot setup
greycolor = [.3,.3,.3];
```

```
figure;
hold on;
set(gca,'DataAspectRatioMode','manual')
%set(gca,'XTick',[],'XColor',greycolor,'YTick',[],'YColor',greycolor)
set(gca,'XTick',[],'YTick',[])
set(gca,'Box','on')
if strcmp(hemisphere,'North')
    Lat0 = 80;
    Lat90 = 60;
    Lat180 = 50;
    Lat270 = 70;
    Lattop = Lat0;
    Latbottom = Lat180;
else
    Lat0 = 60;
    Lat90 = 60;
    Lat180 = 70;
    Lat270 = 70;
    Lattop = Lat180;
    Latbottom = Lat0;
end
imgsize = (90-[Lat270,Lat90;Latbottom,Lattop])/...
    LatCircDist/NLatCirc*.55*plotradius;
imgsize = imgsize.*[-1,1;-1,1];
imgsize = imgsize+[plotcenter(1),plotcenter(1);plotcenter(2),plotcenter(2)];

% imgsize = [-1,1;-1,1]*.5*plotradius;
set(gca,'XLim',imgsize(1,:),'YLim',imgsize(2,:))


%% plot constant latitude circles
%plot 4 latitude circles (for latitudes from 80 deg to 50 deg)
for i=1:NLatCirc
    radius=i*.5*plotradius/NLatCirc;
    rectangle('Position',[plotcenter-radius,2*radius,2*radius],...
        'Curvature',[1 1],'EdgeColor',greycolor,'LineStyle','--')
end

%% plot longitude grid
%(a line every 15 deg)
%the lines are described by arrays containg the coordinates of the start
%and end point of each line. The array "lines_x" contains the x- and
%"lines_y" the y-coordinates of those points. In the arrays, every third
%value is NaN. I.e. "lines_x" is
%[x_l1_start,x_l1_end,NaN,x_l2_start,x_l2_end,NaN,...], where l1,l2,...
%stand for the 1st,2nd,... line to be drawn. The arrays are specified in
%this manner, because without the NaN values inbetween, the program
%would plot one continuous polyline, instead of a set of disjoined lines.
lines_phi=repmat([1,1,nan],1,12);
counter=repmat(0:11,3,1);
counter=counter(:)';
%the lines are first specified in polar coordinates (points lying on a
%circle, i.e. constant r, and spaced constant angle intervals apart
lines_phi=lines_phi.*counter;
lines_phi=lines_phi+repmat([0,12,nan],1,12);
lines_phi=lines_phi*pi/12;
```

```
lines_r=repmat([1,1,nan],1,12)*plotradius*.5;
%transformation of start/end points to cartesian coordinates for plotting
[lines_x,lines_y]=pol2cart(lines_phi,lines_r);
lines_x=lines_x+plotcenter(1);
lines_y=lines_y+plotcenter(2);
%plot the lines on top of the image
plot(lines_x,lines_y,'Color',greycolor,'Linestyle','--')

%% mark coordinate grid lines

if strcmp(hemisphere,'North')
    hemsign = 1;
else
    hemsign = -1;
end

% mark latitude lines with 80,70,...,50 deg
for i=1:(90-Latbottom)/LatCircDist
    text(plotcenter(1),plotcenter(2)-.5*plotradius*i/NLatCirc,...
        strcat(num2str((90-i*LatCircDist)*hemsign),'\circ'),...
        'color',greycolor,'Fontsize',font,'HorizontalAlignment','center',...
        'VerticalAlignment','middle','BackGroundColor','w')
end


%mark longitudes 0, 90, 180, 270 deg
label_right = '90\circ';
label_left = '270\circ';

if strcmp(hemisphere,'North')
    label_top = '0\circ';
    label_bottom = '180\circ';
else
    label_top = '180\circ';
    label_bottom = '0\circ';
end

text(plotcenter(1),plotcenter(2)+imgsize(2,2),label_top,'Fontsize',font,...
    'HorizontalAlignment','center','VerticalAlignment','bottom',...
    'color',greycolor)
text(plotcenter(1)+imgsize(1,2),plotcenter(2),label_right,'Fontsize',font,...
    'HorizontalAlignment','center','Rotation',-90,...
    'VerticalAlignment','bottom','color',greycolor)
text(plotcenter(1),plotcenter(2)+imgsize(2,1),label_bottom,'Fontsize',font,...
    'HorizontalAlignment','center','VerticalAlignment','top',...
    'color',greycolor)
text(plotcenter(1)+imgsize(1,1),plotcenter(2),label_left,'Fontsize',font,...
    'HorizontalAlignment','center','Rotation',90,...
    'VerticalAlignment','bottom','color',greycolor)



end
```

E.3.2 ProjectionParameters

```
%% ProjectionParameters
%
% PURPOSE: determine parameters for polar projection based on
% hemisphere and desired plot setup
%
% INPUT ARGUMENTS:
%     * hemisphere ... hemisphere onto which to project ('North', 'South')
%     * plotradius ... radius of plot
%     * LatCircDist ... distance between latitude circles
%     * NLatCirc ... number of latitude circles
%
% OUTPUT ARGUMENTS:
%     * centerLat ... central latitude of projection
%     * projectionradius ... radius of projection


function [ centerLat,projectionradius ] = ...
    ProjectionParameters( hemisphere,plotradius,LatCircDist,NLatCirc )

minargs = 4;
maxargs = 4;
narginchk(minargs,maxargs)
validateattributes(hemisphere,{'char'},{})
validateattributes(plotradius,{'numeric'},{'scalar'})
validateattributes(LatCircDist,{'numeric'},{'scalar'})
validateattributes(NLatCirc,{'numeric'},{'scalar'})

% polar projection of footprint positions
if strcmp(hemisphere,'North')
    centerLat = 90;
else
    centerLat = -90;
end
projectionradius = .5*plotradius*180/LatCircDist/NLatCirc;


end
```

E.3.3 PlotFPpath

```
%% PlotFPpath
%
% PURPOSE: plot polar projection of observed footprint oval
%
% INPUT ARGUMENTS:
%     * datafolder ... directory where data files are located
%     * filenames ... filenames of data files
%     * hemisphere ... hemisphere for which to plot the data ('North', 'South')
%     * centerLat ... central latitude of projection
%     * plotcenter ...  center of plot
%     * projectionradius ... radius of projection
%
% OUTPUT ARGUMENTS:
%     * plotpathEu ... plot handle for Europa data
%     * plotpathGa ... plot handle for Ganymede data
```

```
17
function [ plotpathEu,plotpathGa ] = ...
    PlotFPpath( datafolder,filenames,hemisphere,...
    centerLat,plotcenter,projectionradius )

22 [Eupath,Gapath] = ReadFPpath(datafolder,filenames,hemisphere);

[XEupath,YEupath] = PolarProjection(Eupath(:,3),Eupath(:,2),...
    centerLat,plotcenter,projectionradius );
[XGapath,YGapath] = PolarProjection(Gapath(:,3),Gapath(:,2),...
27     centerLat,plotcenter,projectionradius );

diffEu = diff(Eupath(:,1));
diffGa = diff(Gapath(:,1));
indEu = find(diffEu>1);
32 indGa = find(diffGa>1);

for i=1:length(indEu)
    XEupath = [XEupath(1:indEu(i));NaN;XEupath((indEu(i)+1):end)];
    YEupath = [YEupath(1:indEu(i));NaN;YEupath((indEu(i)+1):end)];
37     indEu = indEu+1;
end
for i=1:length(indGa)
    XGapath = [XGapath(1:indGa(i));NaN;XGapath((indGa(i)+1):end)];
    YGapath = [YGapath(1:indGa(i));NaN;YGapath((indGa(i)+1):end)];
42     indGa = indGa+1;
end
plotpathEu = plot(XEupath,YEupath,'Color',[1,.4,0],'LineStyle','--',...
    'LineWidth',2);
plotpathGa = plot(XGapath,YGapath,'Color',[0,.4,1],'LineStyle','--',...
47     'LineWidth',2);

end
```

PolarProjection

```
%% PolarProjection
%
% PURPOSE: polar projection of latitude/longitude data
%
5 % INPUT ARGUMENTS:
%     * Lat ... latitude of points to project
%     * Lon ... longitude of points to project
%     * centerLat ... central latitude of projection
%     * plotcenter ...  center of plot
10 %     * projectionradius ... radius of projection
%
% OUTPUT ARGUMENTS:
%     * X ... x-coordinate of projected data
%     * Y ... y-coordinate of projected data
15

function [ X,Y ] = ...
    PolarProjection( Lat,Lon,centerLat,plotcenter,projectionradius )
```

```
minargs = 5;
maxargs = 5;
narginchk(minargs,maxargs)
validateattributes(Lat,{'numeric'},{'vector'})
validateattributes(Lon,{'numeric'},{'vector'})
validateattributes(centerLat,{'numeric'},{'scalar'})
validateattributes(plotcenter,{'numeric'},{'vector'})
validateattributes(projectionradius,{'numeric'},{'scalar'})

if centerLat~=90 && centerLat~=-90
    error('ERROR\n"centerLat" has to be +90 or -90.\ncenterLat = %g',...
        centerLat)
end

% polar projection of footprint positions
[X, Y] = Spherical2AzimuthalEquidistant(...
    Lat,360-Lon+180,centerLat,0,plotcenter(1),plotcenter(2),projectionradius);

X(isnan(Lat))=NaN;
X(isnan(Lon))=NaN;
Y(isnan(Lat))=NaN;
Y(isnan(Lon))=NaN;

end
```

E.3.4 PlotFootprintConnections

```
%% PlotFootprintConnections
%
% PURPOSE: plot connections between corresponding footprints
%
% INPUT ARGUMENTS:
%     * Latobs ... latitudinal position of observed footprint (deg)
%     * Lonobs ... longitudinal position of observed footprint (deg, SIII)
%     * Latcalc ... latitudinal position of calculated footprint (deg)
%     * Loncalc ... longitudinal position of calculated footprint (deg, SIII)
%     * startR ... radial distance at which the calculation started
%           = orbital distance of moon in RJ
%     * centerLat ... central latitude of projection
%     * plotcenter ... center of plot
%     * projectionradius ... radius of projection
%
% OUTPUT ARGUMENTS:
%     * plot_connectEu ... plot handle for Europa data
%     * plot_connectGa ... plot handle for Ganymede data


function [ plot_connectEu,plot_connectGa ] = ...
    PlotFootprintConnections( Latobs,Lonobs,Latcalc,Loncalc,startR,...
    centerLat,plotcenter,projectionradius )

% project footprint positions
[ Xobs,Yobs ] = ...
    PolarProjection( Latobs,Lonobs,centerLat,plotcenter,projectionradius );
[ Xcalc,Ycalc ] = ...
```

```
    PolarProjection( Latcalc,Loncalc,centerLat,plotcenter,projectionradius );

31
% plot connections between observed and calculated positions
connectionsX = zeros (1,3*length(Xcalc));
connectionsY = zeros (1,3*length(Ycalc));
startRlong = zeros (1,3*length(Ycalc));
36
for i=1:length(Xcalc);
    connectionsX(3*i-2) = Xobs(i);
    connectionsX(3*i-1) = Xcalc(i);
    connectionsX(3*i) = NaN;
41  connectionsY(3*i-2) = Yobs(i);
    connectionsY(3*i-1) = Ycalc(i);
    connectionsY(3*i) = NaN;
    startRlong(3*i-2) = startR(i);
    startRlong(3*i-1) = startR(i);
46  startRlong(3*i) = startR(i);
end

plot_connectEu = ...
    plot(connectionsX(startRlong<10),connectionsY(startRlong<10),...
51  'Color',[1,.4,0]);
plot_connectGa = ...
    plot(connectionsX(startRlong>10),connectionsY(startRlong>10),...
    'Color',[0,.4,1]);


56
end
```

E.3.5 PolarPlotFootprints

```
%% PolarPlotFootprints
2 %
% PURPOSE: plot polar projection of observed footprint oval
%
% INPUT ARGUMENTS:
%     * LatFP ... latitudinal position of  footprint (deg)
7 %     * LonFP ... longitudinal position of footprint (deg, SIII)
%     * startR ... radial distance at which the calculation started
%                = orbital distance of moon in RJ
%     * centerLat ... central latitude of projection
%     * plotcenter ... center of plot
12 %     * projectionradius ... radius of projection
%     * ObsOrCalc ... are footprints to plot observed or calculated ('obs',
%           'calc')
%     * ploterrors ... =1 if error bars are to be plotted
%     * LatErr ... latitudinal uncertainties
17 %     * LonErr ... longitudinal uncertainties
%
% OUTPUT ARGUMENTS:
%     * plotEu ... plot handle for Europa data
%     * plotGa ... plot handle for Ganymede data
22
```

```
function [ plotEu,plotGa ] = PolarPlotFootprints( LatFP,LonFP,startR,...
    centerLat,plotcenter,projectionradius,ObsOrCalc,...
    ploterrors,LatErr,LonErr)

minargs = 7;
maxargs = 10;
narginchk(minargs,maxargs)
%check if input arguments are of the correct data type (and size)
validateattributes(LatFP,{'numeric'},{'vector'})
validateattributes(LonFP,{'numeric'},{'vector'})
validateattributes(startR,{'numeric'},{'vector'})
validateattributes(centerLat,{'numeric'},{'scalar'})
validateattributes(plotcenter,{'numeric'},{'vector'})
validateattributes(projectionradius,{'numeric'},{'scalar'})
validateattributes(ObsOrCalc,{'char'},{})

ObsOrCalc = validatestring(ObsOrCalc,{'obs','calc'});


if strcmp(ObsOrCalc,'obs')
    if nargin<minargs+1
        error(['ERROR\n',...
            'Observed␣footprints␣shall␣be␣plotted,␣but␣it␣is␣not␣',...
            'specified␣if␣error␣bars␣should␣be␣plotted␣or␣not.'])
    else
        validateattributes(ploterrors,{'numeric'},{'scalar'})
        if ploterrors~=0 && ploterrors~=1
            error(['ERROR\n',...
                '"ploterrors"␣has␣to␣be␣0␣or␣1.\nploterrors␣=␣%g'],...
                ploterrors)
        elseif ploterrors==1
            if nargin<maxargs
            error(['ERROR\n',...
                'Error␣bars␣shall␣be␣plotted,␣but␣the␣errors␣are␣not␣',...
                'specified.'])
            else
            validateattributes(LatErr,{'numeric'},{'2d'})
            validateattributes(LonErr,{'numeric'},{'2d'})
            end
        end
    end
elseif strcmp(ObsOrCalc,'calc') && nargin>minargs
    warning(['WARNING\nCalculated␣footprints␣will␣be␣plotted,␣',...
        'additional␣error␣bar␣data␣is␣given,␣but␣will␣be␣ignored.'])
end


%% polar projection of footprint positions

[Xfp, Yfp] = ...
    PolarProjection( LatFP,LonFP,centerLat,plotcenter,projectionradius );


%% plot footprints

if strcmp(ObsOrCalc,'calc')
```

```
        plotEu = plot(Xfp(startR<10), Yfp(startR<10),'LineStyle','none',...
            'Color','r','Marker','o','MarkerFaceColor','r','MarkerSize',2);
        plotGa = plot(Xfp(startR>10), Yfp(startR>10),'LineStyle','none',...
            'Color','b','Marker','o','MarkerFaceColor','b','MarkerSize',2);
    else
        if ploterrors==1
            NErrbarpoints = 10;
            [LatErrbarsEu,LonErrbarsEu] = ...
                LatLonErrorbars(LatFP(startR<10),LonFP(startR<10),...
                LatErr(startR<10,:),LonErr(startR<10,:),NErrbarpoints,...
                centerLat,plotcenter,projectionradius);
            [LatErrbarsGa,LonErrbarsGa] = ...
                LatLonErrorbars(LatFP(startR>10),LonFP(startR>10),...
                LatErr(startR>10,:),LonErr(startR>10,:),NErrbarpoints,...
                centerLat,plotcenter,projectionradius);

            plotEu = plot(LatErrbarsEu(1,:),LatErrbarsEu(2,:),'Color','r');
            plot(LonErrbarsEu(1,:),LonErrbarsEu(2,:),'Color','r');
            plotGa = plot(LatErrbarsGa(1,:),LatErrbarsGa(2,:),'Color','b');
            plot(LonErrbarsGa(1,:),LonErrbarsGa(2,:),'Color','b');
        else
            plotEu = plot(Xfp(startR<10), Yfp(startR<10),'LineStyle','none',...
                'Color','r','Marker','o','MarkerSize',2);
            plotGa = plot(Xfp(startR>10), Yfp(startR>10),'LineStyle','none',...
                'Color','b','Marker','o','MarkerSize',2);
        end
    end

    end
```

LatLonErrorbars

```
%% LatLonErrorbars
%
% PURPOSE: construct (curved) error bars for correct plotting of
%   lon/lat uncertainties
%
% INPUT ARGUMENTS:
%     * Lats ... latitudinal position of footprint (deg)
%     * Lons ... longitudinal position of footprint (deg, SIII)
%     * LatErr ... latitudinal uncertainties
%     * LonErr ... longitudinal uncertainties
%     * Npoints ... number of points per (curved) error bar
%     * centerLat ... central latitude of projection
%     * centerXY ... center of plot
%     * projectionradius ... radius of projection
%
% OUTPUT ARGUMENTS:
%     * plotpathEu ...
%     * plotpathGa ... plot handle for Ganymede data


function [ LatErrbars,LonErrbars ] = LatLonErrorbars( Lats,Lons,...
    LatErr,LonErr,Npoints,centerLat,centerXY,projectionradius )

if centerLat~=90 && centerLat~=-90
```

```
        error('ERROR\n"centerLat" has to be +90 or -90.\ncenterLat = %g',...
            centerLat)
    end

    LatErrbars = zeros(2,3*length(Lats));
    LonErrbars = zeros(2,(Npoints+1)*length(Lons));

    [LatErrposX, LatErrposY] = Spherical2AzimuthalEquidistant(LatErr(:,1),...
        360-Lons+180,centerLat,0,centerXY(1),centerXY(2),projectionradius);
    [LatErrnegX, LatErrnegY] = Spherical2AzimuthalEquidistant(LatErr(:,2),...
        360-Lons+180,centerLat,0,centerXY(1),centerXY(2),projectionradius);

    for i=1:length(Lats)
        LatErrbars(1,3*i-2) = LatErrposX(i);
        LatErrbars(1,3*i-1) = LatErrnegX(i);
        LatErrbars(1,3*i) = NaN;
        LatErrbars(2,3*i-2) = LatErrposY(i);
        LatErrbars(2,3*i-1) = LatErrnegY(i);
        LatErrbars(2,3*i) = NaN;
    end

    [positionX, positionY] = Spherical2AzimuthalEquidistant(Lats,Lons,...
        centerLat,0,centerXY(1),centerXY(2),projectionradius);
    radii = sqrt(positionX.^2+positionY.^2);

    if centerLat==90
        LonErrproj = 360-LonErr+90;
    else
        LonErrproj = LonErr-90;
    end

    for i=1:length(Lons)
        [X,Y] = circleArcToPolyline([centerXY(1),centerXY(2),radii(i),...
            LonErrproj(i,2),LonErrproj(i,1)-LonErrproj(i,2)],Npoints);

        LonErrbars(1,((Npoints+1)*i-Npoints):((Npoints+1)*i-1)) = X.';
        LonErrbars(1,(Npoints+1)*i) = NaN;
        LonErrbars(2,((Npoints+1)*i-Npoints):((Npoints+1)*i-1)) = Y.';
        LonErrbars(2,(Npoints+1)*i) = NaN;
    end

    end
```

E.4 FootprintComparison_v2

```
%% FootprintComparison_v2
%
% PURPOSE:
% Calculate satellite footprints for observation times using a specified
% magnetic field model. Save results together with observed footprints to a
% text file.
%
% AUTHOR: Nina Sejkora
% DATE OF LAST REVISION: 27-Apr-2018
```

```
clear

global JupiterRadius JupiterFlattening;
JupiterRadius=71492000; %Jupiter equatorial radius in m
JupiterFlattening = 0.064935;

% orbital parameters of Eu and Ga
aEu = 670900000/JupiterRadius; %mean orbital radius of Europa in RJ
aGa = 1070400000/JupiterRadius; %mean orbital radius of Ganymede in RJ

%observed footprint data
fpfile_Eu = './FP_Bonfond/FP_Eu.mat';
fpfile_Ga = './FP_Bonfond/FP_Ga.mat';
load(fpfile_Eu);
load(fpfile_Ga);

% line tracing parameters
SchmidtCoefficientsCell = './SchmidtCoefficients/SchmCoCellVIPAL2.mat';
FieldModel = 'VIPAL';
hemisphere = input('Specify␣hemisphere␣(North␣or␣South):\n');
hemisphere = validatestring(hemisphere,{'North','South'});
hline = 0.01;
plotlines = 0;
linesout = 0;

% file names for image and text output

programfolder = pwd;
outputfolder = '..\Data\fpdistance';
cd(outputfolder)
outputfolder = pwd;
cd(programfolder)

if strcmp(hemisphere,'North')
    fpoutname = [outputfolder,'\fpcomp_n_',FieldModel,'.txt'];
    imagename = [outputfolder,'\fpcomp_n_',FieldModel,'.png'];
else
    fpoutname = [outputfolder,'\fpcomp_s_',FieldModel,'.txt'];
    imagename = [outputfolder,'\fpcomp_s_',FieldModel,'.png'];
end

%% satellite longitudes

if strcmp(hemisphere,'North')
    FPobs_Eu = FPobs_Eu_n;
    FPobs_Ga = FPobs_Ga_n;
else
    FPobs_Eu = FPobs_Eu_s;
    FPobs_Ga = FPobs_Ga_s;
end

LonEu = cell2mat(FPobs_Eu(:,4)).';
LonGa = cell2mat(FPobs_Ga(:,4)).';

%% calculate satellite footprints
```

```
StartTime = datestr(now);
disp(['start time: ',StartTime])

%calculate the footprints from the satellite positions; the past positions
%are calculated based on the satellite orbital period (assuming a circular
%orbit, coplanar with the Jovian equatorial plane)
fpall_Eu = TraceFieldLines_fct_v3( SchmidtCoefficientsCell,FieldModel,...
    hline,'Eu',aEu*ones(1,length(LonEu)),zeros(1,length(LonEu)),LonEu,...
    hemisphere,plotlines,linesout);
fpall_Ga = TraceFieldLines_fct_v3( SchmidtCoefficientsCell,FieldModel,...
    hline,'Ga',aGa*ones(1,length(LonGa)),zeros(1,length(LonGa)),LonGa,...
    hemisphere,plotlines,linesout);

%convert cell array to numeric
fp_Eu=cell2mat(fpall_Eu);
fp_Ga=cell2mat(fpall_Ga);

%convert to spherical coordinates
[Lonfp_Eu,Latfp_Eu,rfp_Eu] = cart2sph(fp_Eu(:,4),fp_Eu(:,5),fp_Eu(:,6));
[Lonfp_Ga,Latfp_Ga,rfp_Ga] = cart2sph(fp_Ga(:,4),fp_Ga(:,5),fp_Ga(:,6));
Lonfp_Eu = 360-Lonfp_Eu*180/pi;
Lonfp_Eu(Lonfp_Eu<0) = ...
    Lonfp_Eu(Lonfp_Eu<0)-floor(Lonfp_Eu(Lonfp_Eu<0)/360)*360;
Lonfp_Eu(Lonfp_Eu/360>=1) = ...
    Lonfp_Eu(Lonfp_Eu/360>=1)-floor(Lonfp_Eu(Lonfp_Eu/360>=1)/360)*360;
Lonfp_Ga = 360-Lonfp_Ga*180/pi;
Lonfp_Ga(Lonfp_Ga<0) = ...
    Lonfp_Ga(Lonfp_Ga<0)-floor(Lonfp_Ga(Lonfp_Ga<0)/360)*360;
Lonfp_Ga(Lonfp_Ga/360>=1) = ...
    Lonfp_Ga(Lonfp_Ga/360>=1)-floor(Lonfp_Ga(Lonfp_Ga/360>=1)/360)*360;
Latfp_Eu = Latfp_Eu*180/pi;
Latfp_Ga = Latfp_Ga*180/pi;


%% determine distance between calculated and observed footprints
JupiterSpheroid = oblateSpheroid;
JupiterSpheroid.SemimajorAxis=JupiterRadius;
JupiterSpheroid.InverseFlattening=1/JupiterFlattening;

%observed footprint latitudes and longitudes
Lonobs_Eu = cell2mat(FPobs_Eu(:,5)).';
Latobs_Eu = cell2mat(FPobs_Eu(:,6)).';
Lonobs_Ga = cell2mat(FPobs_Ga(:,5)).';
Latobs_Ga = cell2mat(FPobs_Ga(:,6)).';
%errors of observation
Lonerr_Eu = cell2mat(FPobs_Eu(:,7:8));
Laterr_Eu = cell2mat(FPobs_Eu(:,9:10));
Lonerr_Ga = cell2mat(FPobs_Ga(:,7:8));
Laterr_Ga = cell2mat(FPobs_Ga(:,9:10));
%calculate distance obs-calc
arcdist_Eu = distance(Latfp_Eu.',Lonfp_Eu.',Latobs_Eu,Lonobs_Eu,...
    JupiterSpheroid);
arcdist_Ga = distance(Latfp_Ga.',Lonfp_Ga.',Latobs_Ga,Lonobs_Ga,...
    JupiterSpheroid);
```

```
%% save footprint position and distance data

%starting position (r[RJ], lat[deg], lon[deg])
fpmat = [fp_Eu(:,1)/JupiterRadius,fp_Eu(:,2:3);...
    fp_Ga(:,1)/JupiterRadius,fp_Ga(:,2:3)];
%calculated footprint (r[RJ], lat[deg], lon[deg])
fpmat(:,4:6) = [rfp_Eu/JupiterRadius,Latfp_Eu,Lonfp_Eu;...
    rfp_Ga/JupiterRadius,Latfp_Ga,Lonfp_Ga];
%observed footprint (lat[deg])
fpmat(:,7) = [Latobs_Eu.';Latobs_Ga.'];
%error lat (err+[deg], err-[deg])
fpmat(:,8:9) = [Laterr_Eu;Laterr_Ga];
%error lon (err+[deg], err-[deg])
fpmat(:,10:11) = [Lonerr_Eu;Lonerr_Ga];
%observed footprint (lon[deg])
fpmat(:,12) = [Lonobs_Eu.';Lonobs_Ga.'];
%distance between calc and obs footprint [km]
fpmat(:,13) = [arcdist_Eu.';arcdist_Ga.']/1000;

fpall = mat2cell(fpmat,ones(1,size(fpmat,1)),[3,3,1,2,1,2,1]);
%obs ID, date and time
obsinfo = [FPobs_Eu(:,1:3);FPobs_Ga(:,1:3)];
fpall = [obsinfo,fpall];

fp_table = cell2table(fpall,'VariableNames',...
    {'ObsID','ObsDate','ObsTime','StartRLatLon','FPcalcRLatLon',...
    'FPobsLat','FPobsLatErr','FPobsLon','FPobsLonErr','Distance_km'});
writetable(fp_table,fpoutname);
TableContents = fileread(fpoutname);
TableHeader = [...
    'hemisphere: ',hemisphere,char(10),...
    'field model: ',FieldModel,char(10),...
    'stepsize: ',hline,char(10),...
    'calc start time: ',StartTime,char(10),...
    'file creation time: ',datestr(now),char(10),...
    '--------------------',char(10)];
TableWithHeader = [TableHeader,TableContents];
fid=fopen(fpoutname,'w');
fwrite(fid, TableWithHeader, 'char');
fclose(fid);
```

E.4.1 TraceFieldLines_fct_v3

```
%% TraceFieldLines_fct_v3
%
% PURPOSE: Follow magnetic field lines from a point in the equatorial
% plane to the Jovian polar regions.
%
% DESCRIPTION: The calculations start in the equatorial plane at the radial
% orbital positions of Europa and Ganymede. The field line is calculated
% iteratively by following the local magnetic field directions. The
% magnetic field at any given position is determined from a set of Schmidt
% coefficients. The field line is traced towards the planetary hemisphere
% specified. The planetary body is assumed to be an ellipsoid.
%
```

```
% INPUT ARGUMENTS:
%     SchmidtCoefficientsCell ... path to cell array containing the
%         Schmidt coefficients of the respective field model
%     model ... string containing the name of the field model, possible
%         model names are: 'VIP4', 'VIT4', 'VIPAL' or 'Dipole' (not case
%         sensitive)
%     hline ... step size for integration along the magnetic
%         field line in Jovian radii (e.g. if hline should be
%         0.005*JupiterRadius, the input argument must state "0.005")
%     satellite ... string containing the name of the satellite for which
%         to calculate the field line, i.e. 'Europa' or 'Ganymede' (not
%         case sensitive, also unambiguous abbreviations accepted, e.g.
%         'eu' for 'Europa')
%     start_r,start_latitude,start_longitude ... starting position for
%         the field line calculation in System III (1965); vectors
%         containing multiple positions may be given if more than one
%         field line should be calculated. In that case all all vectors
%         need to have the same dimensions. r shall be given in RJ,
%         latitude and longitude in degrees.
%     hemisphere ... string containing the planetary hemisphere towards
%         which the field line is to be calculated, i.e. 'North' or
%         'South' (not case sensitive, also unambiguous abbreviations
%         accepted, e.g. 'n' for 'North')
%     plotlines ... 0 or 1: if plotlines=1 a 3D plot of the calculated
%         field lines is produced, if plotlines=0 or left unspecified not
%     linesout ... 0 or 1: if linesout=1 the arrays containing the entire
%         field lines are given in the output, if linesout=0 or left
%         unspecified, only the footprints and the errors in the
%         equatorial plane and the polar regions are given
%
%   OUTPUT ARGUMENTS:
%     footprints ... cell array containing the starting positions,
%         footprints and used stepsize of every field line.
%         Col1 = [start_r,start_latitude,start_longitude] of the
%           respective line
%         Col2 = footpoint in the hemisphere specified (cartesian
%           coordinates, format [x,y,z])
%     varargout ... cell array containing containing the entire field
%         lines, one cell per array. The lines are ordered the same way
%         as in "footprints", i.e. the starting position in row x
%         corresponds to the line in cell x here.
%
% AUTHOR: Nina Sejkora
% DATE OF LAST REVISION: 30-Aug-2017

function [ footprints,varargout ] = ...
    TraceFieldLines_fct_v3( SchmidtCoefficientsCell,model,hline,...
    satellite,start_r,start_latitude,start_longitude,hemisphere,...
    plotlines,linesout )

%% Test of input arguments
%check if correct number of input arguments are specified
narginchk(8,10)
%check if input arguments are of the correct data type (and size)
validateattributes(SchmidtCoefficientsCell,{'char'},{})
validateattributes(model,{'char'},{})
```

```
validateattributes(hline,{'numeric'},{'scalar'})
validateattributes(satellite,{'char'},{})
validateattributes(start_r,{'numeric'},{'vector'})
validateattributes(start_latitude,{'numeric'},{'vector'})
validateattributes(start_longitude,{'numeric'},{'vector'})
validateattributes(hemisphere,{'char'},{})
validateattributes(plotlines,{'numeric'},{'scalar'})
validateattributes(linesout,{'numeric'},{'scalar'})
%check if the strings specified for 'model' and 'satellite' are valid
model = validatestring(model,{'VIP4','VIT4','VIPAL','Dipole'});
disp(['Calculating␣field␣lines␣using␣the␣"',model,'"␣model.'])
satellite = validatestring(satellite,{'Europa','Ganymede'});
disp(['Calculating␣field␣lines␣starting␣at␣the␣satellite␣',satellite,'.'])
hemisphere = validatestring(hemisphere,{'North','South'});
disp(['Calculating␣field␣lines␣towards␣the␣',hemisphere,'ern␣hemisphere.'])
%
if ~isequal(length(start_r),length(start_latitude),length(start_longitude))
    error(['ERROR\nThe␣dimensions␣of␣"start_r","start_latitude"␣',...
        'and␣"start_longitude"␣have␣to␣be␣equal:\nlength(start_r)␣=␣',...
        '%g\nlength(start_latitude)␣=␣%g\nlength(start_longitude)␣=␣%g'],...
        length(start_r),length(start_latitude),length(start_longitude))
end
if plotlines~=0 && plotlines~=1
    error('ERROR\n"plotlines"␣has␣to␣be␣0␣or␣1.\nplotlines␣=␣%g',plotlines)
end
if linesout~=0 && linesout~=1
    error('ERROR\n"linesout"␣has␣to␣be␣0␣or␣1.\nlinesout␣=␣%g',linesout)
end
%--------------------------------------------------------------------------
%% Settings and global variables
format long;

global JupiterRadius Mu0;
Mu0=4*pi*1e-7;

%EuropaRadius=1560000;
%GanymedeRadius=2634000;

hline = hline*JupiterRadius;
start_r = start_r*JupiterRadius;
start_latitude = start_latitude*pi/180;
start_longitude = 2*pi-start_longitude*pi/180;
%--------------------------------------------------------------------------
%% Load Schmidt coefficients
%load cell arrays containing the Schmidt coefficients for different
%magnetic field models into the workspace
% cell array structure: col1 = l, col2 = all m to that l, col3 = all g_l^m
% to that l, col4 = all h_l^m to that l (h_l^0 is always 0)
% Schmidt coefficients given in Jupiter System III (1965) coordinate system

SchmCoCell = load(SchmidtCoefficientsCell);
if strcmp(model,'VIP4')
    SchmCoCell = SchmCoCell.SchmCoCellVIP4;
elseif strcmp(model,'VIT4')
    SchmCoCell = SchmCoCell.SchmCoCellVIT4;
elseif strcmp(model,'VIPAL')
```

```
    SchmCoCell = SchmCoCell.SchmCoCellVIPAL2;
elseif strcmp(model,'Dipole')
    SchmCoCell = SchmCoCell.SchmCoCellDipole;
end

%-------------------------------------------------------------------------
%% Conversion of starting position to cartesian coordinates

NLines = length(start_r);%number of field lines to be determined

%starting position(s) in cartesian coordinates
[start_x,start_y,start_z] = ...
    sph2cart(start_longitude,start_latitude,start_r);

%-------------------------------------------------------------------------
%% Determine direction of field line calculation

if strcmp(hemisphere,'North')
    direction = -1;
else
    direction = 1;
end

%-------------------------------------------------------------------------
%% Calculate magnetic field lines from equatorial plane to polar regions
FieldLines = cell(NLines,1);

for ind_pos=1:NLines %loop over all starting positions

    %field line segment from satellite to specified hemisphere with
    %stepsize = hline
    FieldLines{ind_pos} = ...
        CalcFieldLines_ell( [start_x(ind_pos),start_y(ind_pos),...
        start_z(ind_pos)],direction,SchmCoCell,hline );

end

%-------------------------------------------------------------------------
%% Output: footprints & errors, optional whole field lines

footprints = cell(NLines,2);

for ind=1:NLines
    footprints{ind,1}=...
        [start_r(ind),start_latitude(ind)*180/pi,...
        360-start_longitude(ind)*180/pi];
    footprints{ind,2}=FieldLines{ind}(end,:);
end

if nargout==2 && linesout==1
    varargout{1}=FieldLines;
end

%-------------------------------------------------------------------------
%% Plot magnetic field lines + planet

```

```
if plotlines==1
    % plot a sphere with 1 RJ radius = planet Jupiter
    sphere_phi=linspace(0,pi,30);
    sphere_theta=linspace(0,2*pi,40);
    [sphere_phi,sphere_theta]=meshgrid(sphere_phi,sphere_theta);
    r=1;%distance unit for plot = 1 RJ -> radius of the sphere is 1 RJ
    sphere_x=r*sin(sphere_phi).*cos(sphere_theta);
    sphere_y=r*sin(sphere_phi).*sin(sphere_theta);
    sphere_z=r*cos(sphere_phi);
    %hold off
    mesh(sphere_x,sphere_y,sphere_z)
    colormap copper
    hold on
    % plot magetic field lines on top
    for ind=1:NLines
        FieldLineplot=FieldLines{ind}/JupiterRadius; %distance unit = 1 RJ
        plot3(FieldLineplot(:,1),FieldLineplot(:,2),FieldLineplot(:,3))
    end
    axis equal
    title(['Jovian Magnetic Field Lines - ',model],'FontWeight','bold',...
        'FontSize',12);
    xlabel('$x ~ (R_\mathrm{J})$','Interpreter','latex','FontSize',12);
    ylabel('$y ~ (R_\mathrm{J})$','Interpreter','latex','FontSize',12);
    zlabel('$z ~ (R_\mathrm{J})$','Interpreter','latex','FontSize',12);
end

end
```

CalcFieldLines_ell

```
%% CalcFieldLines
%
% PURPOSE: Calculate the magnetic field lines from a point P0 to the next
% point where the line impinges Jupiter (assumed as an ellipsoid), using an
% Euler integration method.
%
% INPUT ARGUMENTS:
%     P0 ... starting point for tracing of field line as a row vector of
%         cartesian coordinates (x,y,z); starting point has to be on or
%         above the planetary surface
%         direction ... direction of integration (in or against direction of
%         magnetic field, i.e. whether towards Northern or Southern
%         hemisphere; -1 = towards N, +1 towards S
%     SchmCo ... set of Schmidt coefficients; required format: cell array
%         with: col1 = degree l, col2 = all orders m to that l,
%         col3 = all g_l^m coefficients to that l, col4 = all h_l^m
%         coefficients to that l (h_l^0 is always 0)
%     hline ... step size for integration along the magnetic field line
%
%   OUTPUT ARGUMENTS:
%     FieldLine ... array containing a sequence of points that form
%         the field line; the array has 3 columns: col1=x, col2=y,col3=z
%
%   AUTHOR: Nina Sejkora
%   DATE OF LAST REVISION: 29-Oct-2017
```

```
function [ FieldLine ] = CalcFieldLines_ell( P0,direction,SchmCo,hline )

global JupiterRadius JupiterFlattening;


% array allocated for the field line. The length of the line is not yet
% known. But a dipole field line with a distance of 15 RJ (~ orbit of
% Ganymede) has a length of approx. 40 RJ. Therefore an array with
% 50 RJ/hline (rounded to the next integer) rows is initialised. In case
% this is too long, the rows which are not needed will be cut in the end.
FieldLine = zeros(round(50*JupiterRadius/hline),3);

surface_distance = srfdist_ell(JupiterRadius,JupiterFlattening,P0);

FieldLine(1,:) = P0;
k=1;

%if the starting point for the calculation is slightly below the surface
%(e.g. due to rounding errors), the main loop for the calculation would not
%be entered. Therefore if the surface distance is <0, first the tracing is
%done until the position lies above the surface, then that loop is
%terminated and the main loop (which is calculating until the surface of
%the hemisphere in question is reached)
if surface_distance < 0
    %     [phi,elev,r,]=cart2sph(P0(1),P0(2),P0(3));
    %     r=r+.0001*hline;
    %     [P0(1),P0(2),P0(3)]=sph2cart(phi,elev,r);
    %     surface_distance = srfdist_ell(JupiterRadius,JupiterFlattening,P0);
    while ~(surface_distance>0)
        %the current position = the entry for FieldLine calculated in the
        %last loop iteration:
        pos_curr=FieldLine(k,:);
        %magnetic field at that position:
        B_pos = MagneticField(pos_curr,hline,SchmCo);
        %the function MagneticField returns the field components as a column
        %vector, the position is given as a row vector -> B needs to be
        %transposed for summation:
        B_pos = B_pos.';
        %next point of the field line determined by adding with the
        %orientation of +/- (determined by direction) B_pos and the
        %magnitude hline to the current position:
        pos_new = pos_curr + direction*hline*B_pos/norm(B_pos);
        FieldLine(k+1,:) = pos_new;

        k=k+1;
        %current distance from the planet's surface:
        surface_distance = ...
            srfdist_ell(JupiterRadius,JupiterFlattening,pos_curr);
    end

end


%iterative calculation of the field line. the calculation is stopped once
%the distance from the planet's surface is smaller than 0, i.e. the
```

```
%field line has entered the planet
while ~(surface_distance<0)
    %the current position = the entry for FieldLine calculated in the last
    %loop iteration:
    pos_curr=FieldLine(k,:);
    %magnetic field at that position:
    B_pos = MagneticField(pos_curr,hline,SchmCo);
    %the function MagneticField returns the field components as a column
    %vector, the position is given as a row vector -> B needs to be
    %transposed for summation:
    B_pos = B_pos.';
    %next point of the field line determined by adding with the orientation
    %of +/- (determined by direction) B_pos and the magnitude hline to the
    %current position:
    pos_new = pos_curr + direction*hline*B_pos/norm(B_pos);
    FieldLine(k+1,:) = pos_new;

    k=k+1;
    %current distance from the planet's surface:
    surface_distance = srfdist_ell(JupiterRadius,JupiterFlattening,pos_curr);
end

%In case less steps are required to reach the planet's surface than the
%array had been allocated for (i.e. 50 RJ/hline), the array elements that
%were not needed will contain 0. Those elements are cut from the FieldLine
%array by determining the index of the last row where the radius of the
%point (i.e. the norm of a row of the array FieldLines) is non-zero. Only
%the rows from 1 to this index are kept.
Radii = sqrt(sum(abs(FieldLine).^2,2));
FieldLine=FieldLine(1:find(Radii,1,'last'),:);

end
```

srfdist_ell

```
%% srfdist_ell
%
% PURPOSE: Determine the distance of the current position from an ellipsoid
% (or rather a spheroid) of given flattening
%
% INPUT ARGUMENTS:
%     radius_eq ... equatorial radius R of the spheroid
%     flattening ... flattening f of the spheroid; f = (R-c)/R where R is
%         the equatorial and c the polar radius
%     pos_curr ... current position as a row vector of cartesian
%         coordinates (x,y,z)
%
% OUTPUT ARGUMENTS:
%     distance ... distance of the current point from the spheroids
%         surface
%
%   AUTHOR: Nina Sejkora
%   DATE OF LAST REVISION: 30-Aug-2017

function [ distance ] = srfdist_ell( radius_eq,flattening,pos_curr )
```

```
% transform current position to spherical coorinates (only r and theta
% relevant)
[~,elev_curr,r_curr]=cart2sph(pos_curr(1),pos_curr(2),pos_curr(3));
theta_curr = .5*pi-elev_curr;

% radius of the ellipsoid at theta_curr
r_ell = 1/sqrt(1+flattening*(2-flattening)/(1-flattening)^2*...
    (cos(theta_curr))^2)*radius_eq;
% distance from surface
distance=r_curr-r_ell;

end
```

MagneticField

```
%% MagneticField
%
% PURPOSE: Calculate the magnetic field at a given position from a set of
% Schmidt Coefficients and a given step size in space.
%
% INPUT ARGUMENTS:
%     position ... position at which to calculate the magnetic field
%         given as a row vector of cartesian coordinates (x,y,z)
%     SchmCo ... set of Schmidt coefficients; required format: cell array
%         with: col1 = degree l, col2 = all orders m to that l,
%         col3 = all g_l^m coefficients to that l, col4 = all h_l^m
%         coefficients to that l (h_l^0 is always 0)
%     stepsize ... spatial size of the micro-grid on which the magnetic
%         potential, from which the magnetic field is derived via
%         differentiation, is to be calculated
%
% OUTPUT ARGUMENTS:
%     MagField ... column vector containing the three components of the
%         local magnetic field in cartesian coordinates; the 3 rows
%         contain: row1=B_x, row2=B_y,row3=B_z
%         unit: depending on the unit of the input Schmidt coefficients,
%         the unit of the output magnetic field will be either Gauss or
%         Tesla
%
%   AUTHOR: Nina Sejkora
%   DATE OF LAST REVISION: 31-Aug-2017

function [ MagField ] = MagneticField( position,stepsize,SchmCo )

global JupiterRadius
%dimensions of the current sheet; the first entry is the radius of the
%inner edge R0, the second entry is the radius of the outer edge R1, the
%thrid entry is the half-thickness; all in RJ
currsheet_dim = [5,50,2.5];
%I(r) = I0/r is the surface-current density in the central plane of the
%current sheet; mu0I0half = mu0*I0/2
mu0I0half = 225;
%matrix to change from cartesian coordinates aligned to SIII into the tilted
%coordinate system of the current sheet (the sheet lies in the z=0 plane in
%that system)
currsheet_orientation=...
```

```
    [-0.914200,-0.374606,-0.154625;...
    0.369361,-0.927184,0.0624727;...
    -0.166769,0.,0.985996];

% spatial grid on which the potential will be calculated. It contains in
% each direction (x,y,z) a point 0.5*stepsize ahead of and behind position
% The indices (i,j,k) of grid stand for: i ... axis(x->1,y->2,z->3),
% j ... behind(1) or ahead (2), k ... vector components (x->1,y->2,z->3)
grid = zeros(3,2,3);
for k=1:3
    grid(:,:,k)=position(k);
    grid(k,:,k) = [position(k)-.5*stepsize,position(k)+.5*stepsize];
end

% potential_grid contains the calculated potential on each of the points of
% the grid. The indices (i,j) of potential_grid stand for:
% i ... axis(x->1,y->2,z->3), j ... behind(1) or ahead (2)
potential_grid = zeros(3,2);
grid_pos = zeros(1,3);
%loops over all 6 positions, determining the magnetic potential in each of
%the points
for i=1:3
    for j=1:2
        grid_pos(:)=grid(i,j,:); %current position vector
        potential_grid(i,j) = MagneticPotential(grid_pos,SchmCo);
    end
end

%calculate magnetic field from the potential (equation B = -grad(psi)) by
%numeric differentiation
MagField = -diff(potential_grid,1,2)/stepsize;

Bsheet = currentsheet( position/JupiterRadius,...
    currsheet_dim(1),currsheet_dim(2),currsheet_dim(3),...
    mu0I0half,currsheet_orientation );
%transpose Bsheet (row vector) as MagField is a column vector
Bsheet = Bsheet.';

MagField = MagField+Bsheet*1e-5;

end
```

MagneticPotential

```
%% MagneticPotential
%
% PURPOSE: Calculate the magnetic potential at a given position from a set
% of Schmidt Coefficients.
%
% INPUT ARGUMENTS:
%     position ... position at which to calculate the magnetic field
%         given as a row vector of cartesian coordinates (x,y,z)
%     SchmCo ... set of Schmidt coefficients; required format: cell array
%         with: col1 = degree l, col2 = all orders m to that l,
%         col3 = all g_l^m coefficients to that l, col4 = all h_l^m
%         coefficients to that l (h_l^0 is always 0)
```

```
%
% OUTPUT ARGUMENTS:
%     MagPot ... magnetic potential at the given position;
%              unit: depending on the unit of the input Schmidt coefficients,
%              the unit of the output magnetic potential will be either
%              Gauss*metre or Tesla*metre
%
%   AUTHOR: Nina Sejkora
%   DATE OF LAST REVISION: 02-Aug-2017


function [ MagPot ] = MagneticPotential( position,SchmCo )

global JupiterRadius;

%convert the position, given in cartesian coordinates, to sphericaal
%coordinates (azimuth,elevation,radius):
[phi,elev,radius]=cart2sph(position(1),position(2),position(3));
%elevation is counted from the equatorial plane, but the following
%calculations require theta, counted from the positive z-axis:
theta=.5*pi-elev;

lmax=double(max([SchmCo{:,1}]));

%calculate the Schmidt Seminormalized Associated Legendre Functions at
%given theta for all degrees l up to lmax, the maximum l present in the
%tabulated Schmidt coefficients
LegendrePols=cell(1,lmax);
for i=1:lmax
    LegendrePols{i}=legendre(i,cos(theta),'sch');
end

%equation for the magnetic potential, which is implemented below:
% psi(r,theta,phi) = R/mu_0 sum_{l=1}^{inf} sum_{m=0}^{inf} (R/r)^(l+1)
% P_l^m(cos(theta))(g_l^m cos(m*phi)+h_l^m sin(m*phi))
pot_tmp = 0;
for l=1:lmax %loop over l (outer sum)
    for m=1:l+1 %loop over m (inner sum)
        % it's (m-1) in the cos, as m=1:l+1, other than the order of the
        % Legendre polinomial, which is m=0:l
        new_term=JupiterRadius*(JupiterRadius/radius)^(l+1)*...
            LegendrePols{l}(m)*...
            (SchmCo{l,3}(m)*cos(double((m-1)*phi))+...
            SchmCo{l,4}(m)*sin(double((m-1)*phi)));

        pot_tmp=pot_tmp+new_term;
    end %m
end %l


MagPot=pot_tmp;


end
```

currentsheet

```
%%currentsheet
%
% PURPOSE: calculate the magnetic field generated by the current sheet
%
% INPUT ARGUMENTS:
%     position ... position at which to calculate the magnetic field
%         given as a row vector of cartesian coordinates (x,y,z) in RJ
%     R0 ... radius of inner edge of current sheet in RJ
%     R1 ... radius of outer edge of current sheet in RJ
%     D ... half-thivkness of the current sheet in RJ
%     mu0I0half ... I(r) = I0/r is the surface-current density in the
%         z = 0 plane; mu0I0half = mu0*I0/2
%     orientation ... matrix to change from cartesian coordinates aligned
%         to SIII into the tilted coordinate system of the current sheet
%         (the sheet lies in the z=0 plane in that system)
% OUTPUT ARGUMENTS:
%     B_sheet ... magnetic field generated by the current sheet in
%         cartesian coordinates, the unit of the output magnetic field
%         will be nT if mu0I0half is 255 (as suggested by
%         Connerney e.a. 1981)
%
% AUTHOR: Nina Sejkora (based on VIPAL IDL code by Hess(?))
% DATE OF LAST REVISION: 31-Aug-2017


function [ B_sheet ] = currentsheet( position,R0,R1,D,mu0I0half,orientation )

%transform into cylindrical coordinate system in which current sheet lies
%in the z=0 plane (= tilted to original (SIII) system due to tilt of dipole
%axis)
pos_tilted=position*orientation;
radius=sqrt(pos_tilted(1)^2+pos_tilted(2)^2);
z = pos_tilted(3);

%calculate the Br and Bz compunents for a semi-infinite sheet extending
%from R1 to infinity; this part will later be subtracted from the field of
%a sheet from R0(<R1) to infinity to obtain the field of a finite sheet
F1_R1 = sqrt((z-D)^2+R1^2);
F2_R1 = sqrt((z+D)^2+R1^2);
Br_R1 = radius/2*(1/F1_R1-1/F2_R1);
Bz_R1 = (2*D/sqrt(z^2+R1^2)-radius^2/4*((z-D)/F1_R1^3-(z+D)/F2_R1^3));

%calculate the field for a sheet from R0 - the implemented analystic
%approximation is split into three different cases/regions
%Region I: for radii smaller R0 (i.e. closer to the planet than the sheet's
%inner edge)
if radius<R0
    F1=sqrt((z-D)^2+R0^2);
    F2=sqrt((z+D)^2+R0^2);
    Br=mu0I0half*(radius/2*(1/F1-1/F2)-Br_R1);
    Bz=mu0I0half*(2*D/sqrt(z^2+R0^2)...
        - radius^2/4*((z-D)/F1^3-(z+D)/F2^3)-Bz_R1);
    %Region II: r>R0, above or below the sheet (i.e. |z|>D)
elseif abs(z)>D
    F1=sqrt((z-D)^2+radius^2);
    F2=sqrt((z+D)^2+radius^2);
```

```
        Br=mu0I0half*((F1-F2+abs(z)/z*2*D)/radius...
58          -R0^2*radius/4*(1/F1^3-1/F2^3)-Br_R1);
        Bz=mu0I0half*(2*D/sqrt(z^2+radius^2)...
            -R0^2/4*((z-D)/F1^3-(z+D)/F2^3)-Bz_R1);
        %Region III: r>R0, within the sheet (i.e. |z|<D)
    else
63      F1=sqrt((z-D)^2+radius^2);
        F2=sqrt((z+D)^2+radius^2);
        Br=mu0I0half*(((F1-F2+2*z)/radius...
            -R0^2*radius/4*(1/F1^3-1/F2^3))-Br_R1);
        Bz=mu0I0half*(2*D/sqrt(z^2+radius^2)...
68          -R0^2/4*((z-D)/F1^3-(z+D)/F2^3)-Bz_R1);
    end

    %transform the obtained field components back to cartesian coordinates in
    %the SIII system (z parallel rotational axis)
73  B_sheet = [Br*pos_tilted(1)/radius,Br*pos_tilted(2)/radius,Bz]/orientation;


    end
```